D 2015

U.PORTO

FMUP FACULDADE DE MEDICINA
UNIVERSIDADE DO PORTO

UTERINE ARTERIAL IMPEDANCE IN THE REPRODUCTIVE LIFE AS MODULATED BY LOCAL REDOX BALANCE

LUÍS GUEDES-MARTINS

TESE DE DOUTORAMENTO APRESENTADA
À FACULDADE DE MEDICINA DA UNIVERSIDADE DO PORTO EM
MEDICINA E ONCOLOGIA MOLECULAR

Uterine arterial impedance in the reproductive life as modulated by local redox balance

Luís Guedes-Martins

Porto, 2015

Uterine arterial impedance in the reproductive life as modulated by local redox balance

Impedância arterial uterina na vida reprodutiva, modulada pelo balanço redox local

Luís Guedes-Martins

Porto, 2015

Dissertação de candidatura ao grau de Doutor em Medicina e Oncologia Molecular apresentada à Faculdade de Medicina da Universidade do Porto.

Art.º, 48º, §3º - "A Faculdade não responde pelas doutrinas expendidas na dissertação." (Regulamento da Faculdade de Medicina da Universidade do Porto – Decreto-Lei nº19337 de 29 de Janeiro de 1931).

Júri

Júri de Doutoramento em Medicina e Oncologia Molecular, do licenciado Luís Guedes Martins, nomeado por despacho vice-reitoral de 18 de setembro de 2015, com a tese 'Uterine arterial impedance in the reproductive life as modulated by local redox balance':

Presidente:
Reitor da Universidade do Porto.

Vogais:
Doutor João Francisco Montenegro de Andrade Lima Bernardes, professor catedrático da Faculdade de Medicina da Universidade do Porto;

Doutor Luís Fernando Pacheco Mendes da Graça, professor catedrático da Faculdade de Medicina da Universidade de Lisboa;

Doutor Henrique Manuel Nunes de Almeida, professor associado da Faculdade de Medicina da Universidade do Porto e orientador da tese;

Doutora Alexandra Matias Pereira da Cunha Coelho de Macedo, professora associada convidada da Faculdade de Medicina da Universidade do Porto;

Doutor António Tomé Costa Pereira, professor associado convidado do Instituto de Ciências Biomédicas Abel Salazar;

Doutor Lino Manuel Martins Gonçalves, professor associado da Faculdade de Medicina da Universidade de Coimbra.

Investigação realizada no Departamento de Biologia Experimental da Faculdade de Medicina da Universidade do Porto e na Unidade Maternidade Júlio Dinis do Centro Hospitalar do Porto.

Orientador: Doutor Henrique Manuel Nunes de Almeida

Co-orientador: Doutor Luís Filipe Vilela Pereira Macedo

Corpo Catedrático da Faculdade de Medicina da Universidade do Porto

Professores Catedráticos Efetivos

Doutor Manuel Alberto Coimbra Sobrinho Simões
Doutora Maria Amélia Duarte Ferreira
Doutor José Agostinho Marques Lopes
Doutor Patrício Manuel Vieira Araújo Soares da Silva
Doutor Daniel Filipe de Lima Moura
Doutor Alberto Manuel Barros da Silva
Doutor José Manuel Lopes Teixeira Amarante
Doutor José Henrique Dias Pinto de Barros
Doutora Maria Fátima Machado Henriques Carneiro
Doutora Isabel Maria Amorim Pereira Ramos
Doutora Deolinda Maria Valente Alves Lima Teixeira
Doutora Maria Dulce Cordeiro Madeira
Doutor Altamiro Manuel Rodrigues Costa Pereira
Doutor Rui Manuel Almeida Mota Cardoso
Doutor José Carlos Neves da Cunha Areias
Doutor Manuel Jesus Falcão Pestana Vasconcelos
Doutor João Francisco Montenegro Andrade Lima Bernardes
Doutora Maria Leonor Martins Soares David
Doutor Rui Manuel Lopes Nunes
Doutor José Eduardo Torres Eckenroth Guimarães
Doutor Francisco Fernando Rocha Gonçalves
Doutor José Manuel Pereira Dias de Castro Lopes
Doutor António Albino Coelho Marques Abrantes Teixeira
Doutor Joaquim Adelino Correia Ferreira Leite Moreira
Doutora Raquel Ângela Silva Soares Lino

Professores Catedráticos Jubilados ou Aposentados

Doutor Abel Vitorino Trigo Cabral
Doutor Alexandre Alberto Guerra Sousa Pinto
Doutor Álvaro Jerónimo Leal Machado de Aguiar
Doutor Amândio Gomes Sampaio Tavares
Doutor António Augusto Lopes Vaz
Doutor António Carlos de Freitas Ribeiro Saraiva
Doutor António Carvalho Almeida Coimbra
Doutor António Fernandes Oliveira Barbosa Ribeiro Braga
Doutor António José Pacheco Palha
Doutor António Manuel Sampaio de Araújo Teixeira
Doutor Belmiro dos Santos Patrício
Doutor Cândido Alves Hipólito Reis
Doutor Carlos Rodrigo Magalhães Ramalhão
Doutor Cassiano Pena de Abreu e Lima
Doutor Daniel Santos Pinto Serrão
Doutor Eduardo Jorge Cunha Rodrigues Pereira
Doutor Fernando Tavarela Veloso
Doutor Henrique José Ferreira Gonçalves Lecour de Menezes
Doutor Jorge Manuel Mergulhão Castro Tavares
Doutor José Carvalho de Oliveira
Doutor José Fernando Barros Castro Correia
Doutor José Luís Medina Vieira
Doutor José Manuel Costa Mesquita Guimarães
Doutor Levi Eugénio Ribeiro Guerra
Doutor Luís Alberto Martins Gomes de Almeida
Doutor Manuel António Caldeira Pais Clemente
Doutor Manuel Augusto Cardoso de Oliveira
Doutor Manuel Machado Rodrigues Gomes
Doutor Manuel Maria Paula Barbosa
Doutora Maria da Conceição Fernandes Marques Magalhães
Doutora Maria Isabel Amorim Azevedo
Doutor Mário José Cerqueira Gomes Braga
Doutor Serafim Correia Pinto Magalhães
Doutor Valdemar Miguel Botelho dos Santos Cardoso
Doutor Walter Friedrich Alfred Osswald

"O sonho é ver as formas invisíveis
Da distância imprecisa, e, com sensíveis
Movimentos da esp'rança e da vontade,
Buscar na linha fria do horizonte
A árvore, a praia, a flor, a ave, a fonte –
Os beijos merecidos da Verdade."

Fernando Pessoa

Aos meus pais

À minha mulher, Mª Luísa

Aos nossos filhos, Maria, Luís e Luísa

Aos meus irmãos

Agradecimentos

A realização deste trabalho foi possível graças à colaboração de muitos a quem agradeço o companheirismo e dedicação. A todos, a minha sincera gratidão.

Ao Professor Doutor Henrique Almeida agradeço a disponibilidade permanente, a persistência, o rigor e a afabilidade constantes. Jamais esquecerei as 'aulas de ciência', o treino do espírito crítico, da paciência, da 'procura da pergunta certa' e da mestria na análise dos dados, revisão dos manuscritos e compilação da tese.

Ao Professor Doutor Filipe Macedo agradeço o acolhimento, cordialidade, apreço, estímulo positivo e interesse demonstrados ao longo destes anos.

Ao Professor Doutor Manuel Sobrinho Simões agradeço a inspiração e interdisciplinaridade proporcionadas no programa doutoral.

Ao Dr. Joaquim Saraiva, pela amizade, partilha de ideias, companheirismo e disponibilidade. A minha gratidão pela motivação permanente e pelos primeiros passos na ecografia obstétrica.

À Dra. Ana Cunha agradeço o entusiasmo, a audácia e a capacidade de organização transmitidos, fundamentais para a colheita dos dados.

À Professora Doutora Rita Gaio, pela paciência, simpatia e profissionalismo na elaboração da análise estatística.

À Dra. Helena Graça, agradeço a participação na realização dos estudos no Bloco de Urgência e ao Dr. Hermano Rodrigues, Dra. Delfina Leite, Dra. Cristina Soares e Dra. Elisabete Luzeiro por terem assumido a supervisão da colheita das biópsias.

À Doutora Elisabete Silva e Dra. Liliana Matos agradeço o empenho e profissionalismo na realização dos trabalhos laboratoriais.

Ao Departamento de Biologia Experimental e aos elementos da direcção da Unidade Maternidade Júlio Dinis / Centro Materno Infantil do Norte agradeço a confiança e a criação das condições necessárias para a concretização das investigações. A todos os médicos, enfermeiros, funcionários administrativos e assistentes operacionais agradeço a colaboração constante e acolhimento proporcionados. Às grávidas, puérperas e a todas as pacientes estudadas agradeço a generosidade inestimável.

Por fim, aos meus pais, à minha mulher, aos meus filhos e aos meus irmãos, agradeço a compreensão, apoio incondicional, o carinho e a intensa felicidade que alimentaram a perseverança necessária para a realização desta tese.

Ao abrigo do Art.º 8º do Decreto-Lei nº388/70 fazem parte desta dissertação as seguintes publicações:

Guedes-Martins L, Silva E, Gaio AR, Saraiva J, Soares AI, Afonso J, Macedo F, Almeida H. Fetal-maternal interface impedance parallels local NADPH oxidase related superoxide production. *Redox Biol.* 2015; 5:114-123.

Guedes-Martins L, Saraiva JP, Gaio AR, Reynolds A, Macedo F, Almeida H. Uterine artery Doppler in the management of early pregnancy loss: a prospective, longitudinal study. *BMC Pregnancy Childbirth.* 2015; 15:28.

Guedes-Martins L, Gaio R, Saraiva J, Cerdeira S, Matos L, Silva E, Macedo F, Almeida H. Reference ranges for uterine artery pulsatility index during the menstrual cycle: a cross-sectional study. *PLoS One*. 2015; 10:e0119103.

Guedes-Martins L, Gaio AR, Saraiva J, Cunha A, Macedo F, Almeida H. Uterine artery impedance during the first eight postpartum weeks. *Sci Rep*. 2015; 5:8786.

Guedes-Martins L, Saraiva J, Felgueiras Ó, Carvalho M, Cerdeira A, Macedo F, Gaio R, Almeida H. Uterine artery impedance during puerperium in normotensive and chronic hypertensive pregnant women. *Arch Gynecol Obstet.* 2015; 291:1237-46.

Guedes-Martins L, Graça H, Saraiva JP, Guedes L, Gaio R, Cerdeira AS, Macedo F, Almeida H. The effects of spinal anaesthesia for elective caesarean section on uterine and umbilical arterial pulsatility indexes in normotensive and chronic hypertensive pregnant women: a prospective, longitudinal study. *BMC Pregnancy Childbirth.* 2014; 14:291.

Guedes-Martins L, Cunha A, Saraiva J, Gaio R, Macedo F, Almeida H. Internal iliac and uterine arteries Doppler ultrasound in the assessment of normotensive and chronic hypertensive pregnant women. *Sci Rep*. 2014; 4:3785.

Guedes-Martins L, Saraiva J, Gaio R, Macedo F, Almeida H. Uterine artery impedance at very early clinical pregnancy. *Prenat Diagn.* 2014; 34:719-25.

Abbreviations

BH_4	Tetrahydrobiopterin
DUOX	Dual oxidase
eNOS	Endothelial nitric oxide synthase
ERK	Extracellular-signal-regulated kinases
EVTs	Extravillous trophoblasts
FAD	Flavin adenine dinucleotide
H_2O_2	Hydrogen peroxide
IIA	Internal iliac artery
IUGR	Intra-uterine growth restriction
MAP	Mean arterial pressure
MAPK	Mitogen-activated protein kinase
NADPH	Nicotinamide adenine dinucleotide phosphate
NF-κB	Nuclear factor kappa-light-chain-enhancer of activated B cells
NH_2	Amino
NMC	Normal menstrual cycle
NO	Nitric oxide
NOX	NADPH oxidase
$O_2^{\bullet-}$	Superoxide
$ONOO^-$	Peroxynitrite
PE	Preeclampsia
PI	Pulsatility index
PIGF	Placental growth factor
RI	Resistance index
ROS	Reactive oxygen species
sFlt-1	Soluble fms-like tyrosine kinase 1
SOD	Superoxide dismutase
UtA	Uterine artery
VEGF	Vascular endothelial growth factor

Abstract

Adequate uterine artery (UtA) blood flow during pregnancy is essential for the development of the fetus. UtA final divisions, the spiral arteries, undergo well known structural changes that associate to UtA impedance reduction. Uterine arterial impedance variation is an important issue in obstetrics, because of the continued changes in fetal needs, and is currently studied employing Doppler frequency shift waveform analysis. Less well known are additional local or systemic contributing factors that influence UtA artery Doppler waveforms and thus modulate the pelvic circulation. To their approach, the current research focused on the UtA impedance in reproductive-age women before pregnancy, during pregnancy, at delivery, and during the puerperium. Additional information on artery performance in the pregnancy and postpartum periods combined the performance of the UtA predecessor, the internal iliac artery (IIA), and a parallel study in women with long-term, stable, essential hypertension. This is a prevalent condition, and also a known risk factor for serious disorders of pregnancy. The study evidenced a decrement in UtA impedance from the first day of menstruation to delivery; a reduction was also noticed in incomplete miscarriage and, in contrast, its reversion was verified several weeks following delivery and the removal of the placenta. The comparison of IIA and UtA hemodynamic properties evidenced a peculiar impedance character. In fact, IIA hemodynamics paralleled the iliac artery, thus exhibiting a pregnancy-related enhanced resistance and promoted the enormous influx of blood that is delivered distally. Insights regarding the molecular mechanisms underlying the changes at the placental bed, as the imbalance of redox mechanisms, were also investigated. Although the findings did not identify placental bed NADPH oxidase (NOX) as a disorder biomarker, they provided strong evidence that, in both the uterus and the placenta, NOX is a redox balance intervenient at the human fetal-maternal interface and, therefore, a modulator of uterine vascular resistance.

Resumo

Durante a gravidez, um fluxo de sangue adequado na artéria uterina (UtA) é essencial para o desenvolvimento do feto. Os ramos terminais da UtA, as artérias espiraladas, passam por mudanças estruturais bem conhecidas que se associam à redução da impedância na UtA. Esta variação é uma questão importante em obstetrícia devido às contínuas mudanças nas necessidades nutricionais fetais e é atualmente estudada recorrendo à análise da frequência Doppler. Menos conhecidos são os fatores contribuintes locais ou sistémicos que influenciam a forma de onda Doppler da UtA e, assim, modulam a circulação pélvica. Para a sua abordagem, a atual investigação centrou-se na impedância da UtA de mulheres em idade reprodutiva antes da gravidez, durante a gravidez, no parto e no puerpério. Informações adicionais sobre o desempenho da UtA nos períodos de gravidez e pós-parto combinaram a performance do seu precursor, a artéria ilíaca interna (IIA), e a variação na UtA de mulheres com hipertensão essencial estável. Esta é uma entidade frequente e um fator de risco conhecido para a ocorrência de distúrbios sérios durante a gravidez. O estudo evidenciou um decréscimo na impedância da UtA a partir do primeiro dia da menstruação até ao parto; uma redução também foi notada em casos de abortamento incompleto e, em contrapartida, a sua reversão foi verificada apenas várias semanas após o parto e remoção da placenta. A comparação das propriedades hemodinâmicas da IIA e UtA evidenciaram um caráter peculiar em termos de impedância. De facto, o comportamento hemodinâmico da IIA acompanhou o da artéria ilíaca, exibindo, assim, uma resistência crescente ao longo da gravidez, promovendo o enorme fluxo de sangue entregue distalmente. Os mecanismos moleculares subjacentes às alterações no leito placentar, como o desequilíbrio de mecanismos redox, também foram investigados. Embora os resultados não tenham mostrado que a expressão de NADPH-oxidase (NOX) no leito placentar é um biomarcador de doença, trouxeram forte evidência de que, tanto no útero como na placenta, a NOX é um interveniente do equilíbrio redox na interface materno-fetal e, por conseguinte, um modulador da resistência vascular uterina.

Contents

1. INTRODUCTION

Generation of the ultrasonic Doppler image and Doppler indices

The Doppler effect is named after the physicist Christian Johann Doppler (1803-1853) who proposed a physical explanation and mathematical expression for the natural occurrence of wave frequency reduction when it recedes from the source. In recent decades, the principle has been applied in Medicine to assess blood movement inside vessels and quantitate its velocity. In obstetrics, this approach was first reported in 1983 for the assessment of the uteroplacental circulation (Campbell *et al.*, 1983).

When sound waves strike a moving target (for instance, red blood cells), the frequency reduction of the waves reflected back is proportional to the velocity and direction of the red blood cells – a phenomenon known as the *Doppler frequency shift*. Because the magnitude and direction of the frequency shift depend on the relative motion of the moving target, Doppler can thus be used to evaluate flow within blood vessels (O'Leary, 1985; Yoganathan *et al.*, 1988; Taylor & Hollands, 1990; Amador, 1994). In clinical practice, this evaluation has been accomplished by using continuous wave spectral Doppler, pulsed wave spectral Doppler, and Doppler color flow imaging modes of operation.

Continuous wave Doppler employs two separate types of crystals: one transmits high-frequency sound waves and another continuously captures signals; although M-mode imaging uses continuous wave Doppler to evaluate motion through time, it cannot image individual vessels. Pulsed-wave Doppler uses one crystal that transmits the signal and then waits until the returning signal is received before transmitting another one (Cunningham *et al*., 2014).

By placing multiple gates (sample volumes), across an entire area in the gray-scale image and separately processing the Doppler shift signals in each of these gates, a two-dimensional distribution of Doppler shift signals can be obtained (O'Leary, 1985; Yoganathan *et al.*, 1988; Kossoff, 2000; McVeigh, 2006). In *color velocity imaging* mode, based in a color scale, a real-time image representing blood flow velocities is displayed as an overlay on top of the gray-scale two-dimensional image. Additionally, the spectral density function at each velocity is proportional to the number of blood cells moving at that velocity, reflecting a sound wave with the corresponding frequency

shift (Campbell *et al.,* 1987; Kurjak *et al.,* 1993; Aldrich, 2007; Abramowicz & Sheiner, 2008; Evans, 2010); this approach is referred as *spectral analysis* (Figure 1). Extensive information is obtained from each spectrum because the spectral density function at each velocity is proportional to the number of blood cells (moving target) at that velocity, reflecting a sound wave to a crystal with the corresponding frequency shift (Cunningham *et al*., 2014).

Through the combined use of continuous wave and pulsed Doppler, a spectrum of Doppler frequency shifts is obtained from the systolic/diastolic cycle. Upon their analysis, the arterial blood velocity is estimated and the collected data are integrated in a quantitative determination of vessel impedance parameters such as the pulsatility (PI) and the resistance (RI) indices (Figure 1). It is thus understandable the breakthrough character of the first report (Campbell et al., 1983) in obstetrics assessment because, rather than the simple uterine wall, arcuate vessel blood flow, it was the uterine artery resistance properties that were measured.

Due to the relative operating simplicity of the currently used devices and the non-invasive nature of the procedure, pulsed wave Doppler ultrasound became a necessary tool in modern clinical obstetrics. Although different impedance parameters may be employed, the emphasis has been put on PI because of its ability to more accurately describe the arterial velocity waveform variation (Gómez *et al.*, 2008), quite distinct from the flat, constant velocity waveform usually found in veins. Furthermore, while the term ‘resistance’ is often used in the context of UtA Doppler determination, it is impedance the measured parameter, that results from the combination of forward and reflected blood flow (Everett & Lees, 2012). Generally, a low impedance waveform is indicative of low distal resistance, whereas high impedance waveforms occur in high resistance vascular beds (Everett & Lees, 2012).

Doppler effect development application in obstetrics revealed to be paramount for the assessment of the uteroplacental interface, where the fetal and maternal circulations meet. In this setting, although Doppler research in obstetrics has devoted much effort into the fetal circulation, it also showed the value of addressing the mother side. In particular, it focused on the maternal uterine artery (UtA), critical to the entire female reproductive physiology and pathology. Interestingly, there is a lack in the study of the internal iliac artery (IIA), a thick, 3–4 cm long division of the common iliac

artery and the main artery entering the pelvis, whose anterior division gives off the uterine artery.

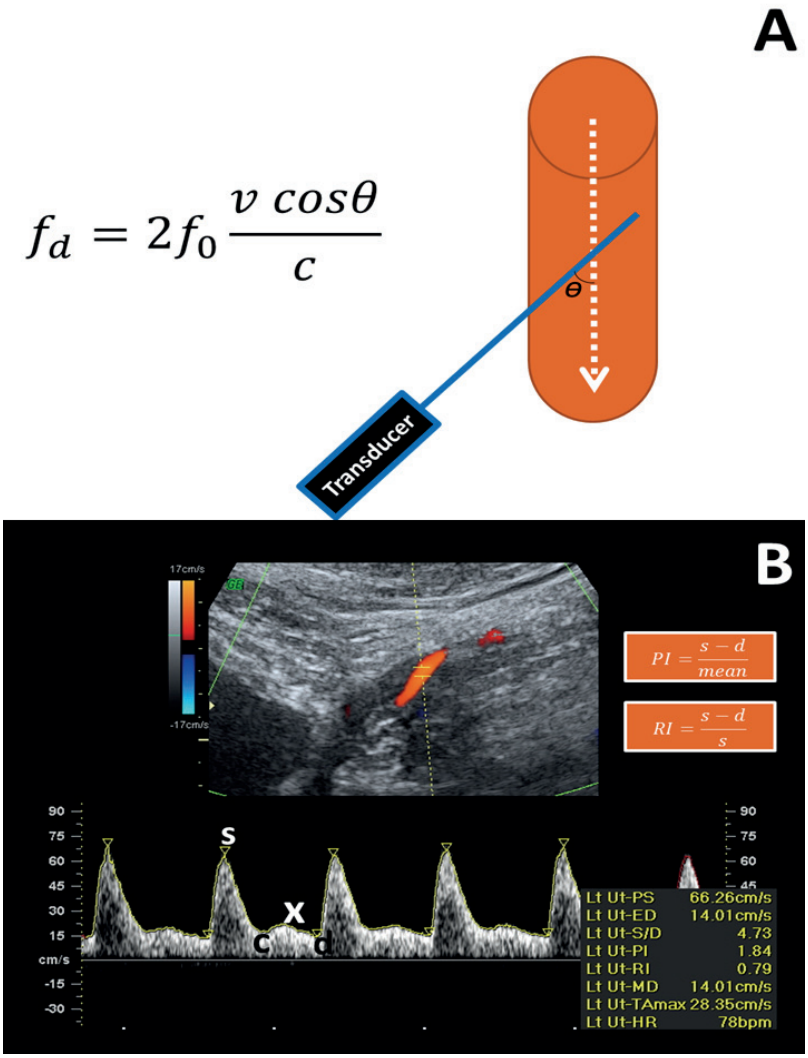

Figure 1. Panel A: Doppler equation. Ultrasound emanating from the transducer with initial frequency f_0 strikes blood moving at velocity v. Reflected frequency f_d is dependent on the angle θ between the beam of sound and the vessel. Measurement error becomes large when θ is not close zero. Panel B: Doppler spectra of UtA flow. Vascular impedance, which is inversely proportional to volume flow, can be indirectly evaluated via indices obtained from the Doppler spectrum. These indices are dimensionless relations of flow velocities, which are therefore independent of the Doppler angle θ correction. The pulsatility index (PI) is used as a measure of impedance of the flow of blood distal to the sampling point and is automatically calculated according to the formula $PI = \frac{(s-d)}{mean}$, where s is the peak, d is the minimum, and the average is the *mean* maximum Doppler shift frequency over the cardiac cycle. The resistance index (RI) is automatically calculated using the formula $RI = \frac{(s-d)}{s}$, where s is the peak systolic, d is the end-diastolic, c is the early diastolic, and x is the maximum diastolic frequency.

Uteroplacental blood flow

During the course of pregnancy, remarkable circulatory changes take place in the pelvis; on one side is the developing fetus with enhanced nutritional demands, and on the other side, the uterine circulation that perfuses the placental bed and must adapt continuously to cope with such demands. These distinct features make the uteroplacental interface a critical circulatory site, requiring a dual approach: the fetal, umbilical or aortic artery parameters, and, on the maternal side, the total uterine blood flow. However, currently, the simultaneous measurement of uterine, ovarian, and collateral vessels is not possible because the ovarian vessels are not consistently visualized even when magnetic resonance angiography is used (Pates *et al.*, 2010). Therefore, Doppler ultrasonography of major vessels remains the best approach to estimate uterine blood flow properties in pregnancy.

Cardiovascular changes related to normal pregnancy begin early, prior to full placentation (Chapman *et al*., 1998). They include an increase in cardiac output, blood volume expansion, peripheral vasodilation and blood pressure reduction. One-half of the cardiac output increase occurs by 8 weeks of gestation and continues in the succeeding weeks to reach 30-50% (1.8 L/min) above the typical baseline of the non-pregnant state (Katz *et al*., 1978; Capeless & Clapp, 1989; van Oppen, *et al.,* 1996). In early pregnancy, the uterus receives 3 to 6% of the cardiac output, whereas by 37-41 weeks, this proportion is approximately 12% (Flo *et al*., 2010). On account of the increase in cardiac output and the UtA diameter increase (Figure 2), that doubles after 20 weeks of pregnancy (Konje *et al.,* 2001), there is a significant enhancement of UtA blood flow capacity (Palmer *et al*., 1992; Mandala & Osol, 2012) and a concomitant Doppler velocity increment. In fact, blood flow within the vessels increases in the proportion of the fourth power of the radius, resulting in a UtA blood flow increase from 50 to 60 mL/min in the late first trimester, to 185 mL/min at 28 weeks, and to 450 to 750 mL/min at term (Assali *et al*., 1960; Flo *et al*., 2010) (Figure 2).

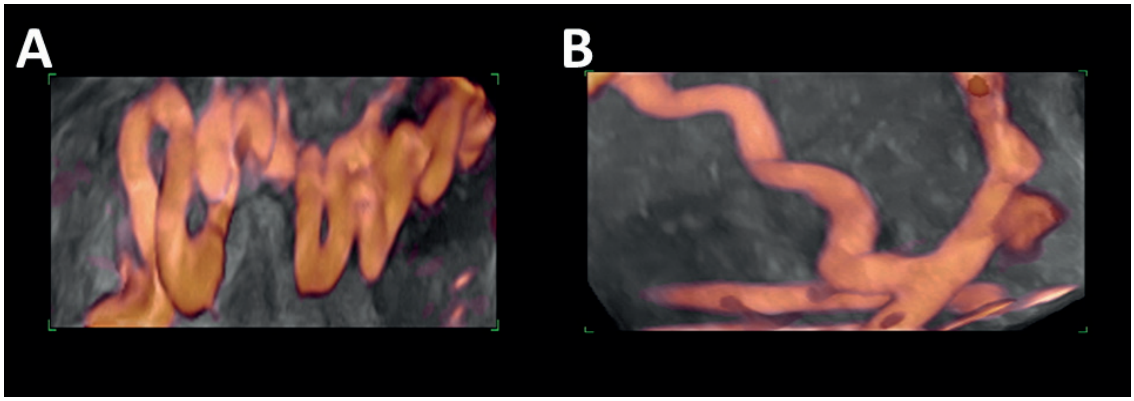

Figure 2. 3D *Color Power Angio* imaging of the right UtA in the same pregnant woman at 7 weeks (A) and 36 weeks (B) of pregnancy. UtA diameter increases with advancing gestation. Simultaneously, the loss of tortuosity on the artery route can be observed. The vessels that supply the uterine corpus widen and elongate while preserving contractile function. In contrast, the spiral arteries, which directly supply the placenta, widen but completely lose contractility.

This progression, in the maternal-placental blood flow during gestation is mainly due to vasodilation, in part related to increased levels of 17β-estradiol, progesterone, and relaxin (Sprague *et al.*, 2009; Vodstrcil *et al*., 2012). Additionally, the downstream fall in vascular resistance and growth of vessel circumference, appears to result from nitric oxide (NO) regulatory involvement. NO is generated by the endothelial cell nitric oxide synthase (eNOS) and is essential for proper endothelium function and vascular tone regulation (McCarthy *et al*., 1993). The enzyme itself, and consequent NO production, are regulated by vasoactive compounds as estrogen, placental growth factor (PIGF), and vascular endothelial growth factor (VEGF) (Grummer *et al*., 2009; Sprague *et al*., 2010; Mandala & Osol, 2012). In addition, another regulator, as soluble fms-like tyrosine kinase 1 (sFlt-1), was found to inactivate and decrease circulating PIGF and VEGF concentrations and was recognized as an important factor in preeclampsia (PE) pathogenesis. In turn, the relative vascular insensitivity to infused angiotensin II and norepinephrine (Rosenfeld *et al.*, 2012) also serves to increase the uteroplacental blood supply.

It is agreed that the increased blood flow to the uterus during pregnancy is accommodated through a close relationship between maternal and fetal circulations. This point was supported by previous studies showing that failure of the normal physiological conversion from a high-resistance/low-flow to a low-resistance/high-flow

uteroplacental circulation enhances the risk for poor fetal and neonatal outcomes (Trudinger *et al*., 1985; Harrington *et al*., 2004; Gómez *et al*., 2006).

Theoretically, as a pathological increment in placental vascular resistance should be detectable as an abnormal Doppler flow measurement of the maternal UtA impedance, this finding would offer the potential to detect women at risk for perinatal mortality, PE and intra-uterine growth restriction (Sciscione *et al*., 2009). In fact, when micro-beads were injected to embolize ovine spiral arteries, uterine vascular impedance increase was found, thereby providing *in vivo* validation for the models of resistance and flow classically described for the UtA (Ochi *et al*., 1995).

Application of UtA Doppler for reproductive assessment

In the non-pregnant state, the UtA Doppler waveform exhibits a rapid rise and fall in systolic flow velocity (Figure 3) that is followed by a notch in the early diastole (Steer *et al.*, 1995). The monthly genital tract cyclic changes in the non-pregnant condition also suggest that regulated changes occur in the uterine blood supply to endow the endometrium with the ability to receive the ovum, should fertilization occur. Indeed, such cyclic changes were the subject of a number of hemodynamic studies on the UtA and its distal branches, the radial and spiral arteries. Such studies, reported complex temporal relationships and sometimes conflicting results that ranged from the existence of UtA impedance changes to their absence (Ziegler *et al.*, 1999). Interestingly, UtA distal branches indicated low impedance to flow during the late follicular and midluteal phases (Sladkevicius *et al.*, 1993, Dal *et al*., 2005), when the endometrial thickness and vascularity increased (Jokubkiene *et al.*, 2006). Moreover decreased luteal phase UtA-PI emphasized the importance of enhanced local blood perfusion for implantation to occur (Sladkevicius *et al.*, 1993; Tan *et al.*, 1996). In fact, low PI of the UtA (Ivanovski *et al*., 2012; Wang *et al*., 2010) and endometrial flow (Wang *et al*., 2010) are associated with improved implantation rates, further supporting the view that increased local perfusion favors successful pregnancy establishment.

The peculiar UtA notching feature typically fades during pregnancy; the prevalence of bilateral notching is 46.3% between 11 and 14 weeks, 16.5% between 15 and 24 weeks, and 5% between 25 and 41 weeks (Gómez *et al.*, 2008). As consequence

of notch disappearance, the mean diastolic velocity rises, which results in PI value reduction (Figure 3).

Due to the value of UtA impedance assessment employing Doppler ultrasound, the reference ranges for the mean PI from 11 to 41 weeks in uneventful pregnancies were established and clearly revealed a general progressive gestational age-related decrement (Gómez *et al.,* 2008). This trend has been attributed to the major structural changes in the placental bed that modify the properties of the UtA from a resistance vessel into a capacitance vessel (Osol & Mandala, 2009).

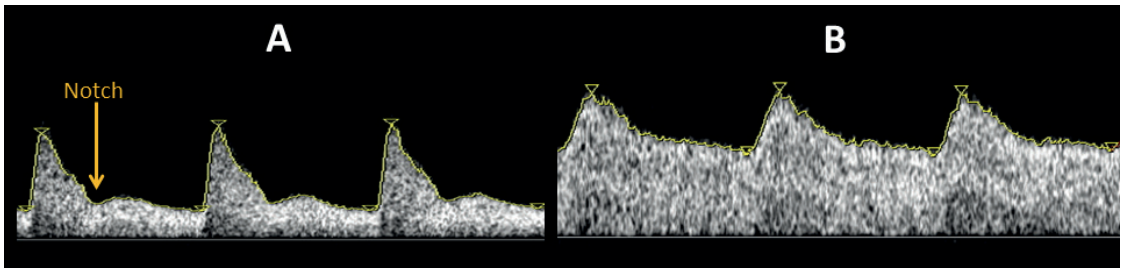

Figure 3. UtA waveforms. Spectral analysis of normal blood flow velocity waveforms obtained from the same UtA at 6 weeks (A) and 21 weeks (B) of gestation. In non-pregnant women and during the first half of a normal pregnancy, the flow velocity waveforms from the main UtA are characterized by a well-defined protodiastolic notch (A). End-diastolic flow increases in the main UtA and their branches during the second half of the menstrual cycle, and this increase continues as pregnancy advances. The presence of early diastolic notches remains relevant, particularly if bilateral, to adverse pregnancy outcome, even with normal UtA resistance values (Albaiges *et al*., 2003).

Beyond the reference ranges for an uneventful pregnancy, a number of studies at different gestational ages have shown that UtA impedance is able to provide important predictive information on serious obstetrical disorders. Notably, in women with gestational hypertension just before term, the incidence of elevated UtA impedance was found to be as high as 68% and to rise to 89% when associated with PE (Frusca *et al.*, 2003). Other studies also reported a high incidence of abnormal UtA-PI, although at lower values, likely reflecting the different criteria for inclusion (Li H *et al*., 2005; Meler *et al.*, 2010).

In a group of unselected pregnant women at 22-24 weeks of gestation (Papageorghiou *et al.*, 2001), enhanced UtA-PI was reported to show 69% sensitivity for the appearance of PE with intra-uterine growth restriction (IUGR) in subsequent

weeks, a value that increased to 83% when the criteria included protodiastolic notch persistence. However, although the detection rate of PE as a result of enhanced UtA-PI had already been shown to be superior to the patient´s epidemiological data detection rate (Papageorghiou *et al.*, 2005), additional conditions had to be met. In fact, other reports indicated that the correlation between abnormal UtA impedance at 22 weeks and the establishment of PE was significant only when the fetal outcome was poor, including IUGR and preterm birth (van den Elzen *et al*., 1995; Aardema *et al.*, 2004). More recently, top-decile PI values and the presence of bilateral notching were considered to have good predictive value for an enhanced risk of stillbirth resulting from placental causes (Smith *et al*., 2007). As a corollary of these studies, an extensive systematic review of 74 studies including 79.547 women (Cnossen *et al.,* 2008), with the intended purpose of evaluating the use of UtA Doppler velocimetry for the prediction of PE, concluded that UtA Doppler ultrasonography was more accurate for the prediction of PE when performed in the second trimester rather than in the first trimester. In addition, the prediction of the overall risk of PE and the risk of severe PE is significantly different in pregnant women with a low risk than in those with a high risk of developing the disease. In the group of low-risk patients, the overall risk of PE was best predicted by the presence of a second-trimester elevation of PI accompanied by UtA notching [sensitivity 23%, specificity 99%, positive likelihood ratio (+ve LR) 7.5, -ve LR 0.59]. In addition, in this low-risk group, the risk of severe PE was best predicted by either the second trimester PI (sensitivity 78%, specificity 95%, +ve LR 15.6, -ve LR 0.23) or bilateral notching (sensitivity 65%, specificity 95%, +ve LR 13.4, -ve LR 0.37). In contrast, in women at a high risk of developing PE, the overall risk of PE was best predicted by the presence of a second-trimester elevation of PI accompanied by UtA notching (sensitivity 19%, specificity 99%, +ve LR 21, -ve LR 0.82). Furthermore, the risk of severe PE in high-risk patients was best predicted by second-trimester elevated RI (sensitivity 80%, specificity 78%, + ve LR 3.7, -ve LR 0.26). These findings supported the recommendation to employ PI and notching assessment in daily clinical practice (Cnossen *et al.*, 2008).

Few studies have focused at an earlier gestational age, in the range of 11-16 weeks, although higher PIs were shown to correlate with pregnancy complications too, such as PE and IUGR (van den Elzen *et al.*, 1995; Harrington *et al.*, 1996; Harrington *et*

al., 1997; Gómez *et al.*, 2005) and premature delivery (Harrington *et al*., 1997). Nevertheless, the ability of UtA impedance to identify pregnancy complications as PE and IUGR at this younger gestational age was considered less accurate (Cnossen *et al.,* 2008) and the predictability was only comparable if a large set of parameters was employed (Harrington *et al.*, 1997). In summary, UtA impedance assessment at early pregnancy was shown to be of limited clinical value in an unselected population, although its potential usefulness, when combined with other biochemical and clinical data, was recognized (Gómez *et al.*, 2005). In fact, at this extreme gestational ages as less than 11 weeks, PI studies on the UtA are scarce and addressed a smaller number of cases (Jauniaux *et al.*, 1991; Jurkovic *et al.*, 1991; Arduini *et al.*, 1991; Valentin *et al.*, 1996; Mäkikallio *et al.*, 2004) confirming that an extensive evaluation of uterine circulation was lacking.

Similarly, in contrast to the extensive literature available throughout the pregnancy, Doppler research on the uterine artery impedance during the postpartum period is also scarce. Such insufficiency is disappointing because UtA impedance is likely to be affected by puerperal conditions that might be predicted employing Doppler ultrasound measurement (Mulic-Lutvica *et al.*, 2007). Among the potential complications, preeclampsia, postpartum haemorrhage, retained placental tissue, and infection are particularly relevant.

Regulation at the maternal-fetal interface

Hypertension is a serious human disorder that, if left untreated, can lead to dire consequences, most often affecting target organs such as the heart, brain, kidney and retina (Edwards *et al*., 2014; Leow, 2015). Not unexpectedly, when a woman is diagnosed with hypertension and becomes pregnant, greater care is taken due to the additional effect of hypertension on the placenta and the fetus (Bramham *et al.*, 2014; Seely & Ecker, 2014).

According to the Report of the Working Group on Research on Hypertension During Pregnancy, from the 2001 Meeting at the National Heart, Lung, and Blood Institute, “hypertension during pregnancy is categorized as: preeclampsia/eclampsia, gestational hypertension, the continued presence of chronic hypertension, and preeclampsia superimposed upon chronic hypertension” (National Heart, Lung and

Blood Institute, 2001). The report further defines and emphasizes the relevance of these entities, in particular the previous existence of hypertension and the precise point that women suffering from hypertension have a significant risk "of superimposed PE (25% risk), preterm delivery, fetal growth restriction or demise, abruptio placentae, congestive heart failure and renal failure". In addition, the outcome for mother and infant is worse than for de novo PE (National Heart, Lung and Blood Institute, 2001; Report of the ACOG' Task Force on Hypertension in Pregnancy, 2013).

Hypertension is defined as systolic blood pressure of at least 140 mmHg and diastolic blood pressure of 90 mmHg on at least 2 occasions; these measurements should be at least 4 hours (but not more than 7 days) apart. The situation is considered severe if the systolic blood pressure is at least 160 mmHg and/or the diastolic pressure is at least 110 mm Hg on 2 occasions at least 4 hours apart (Sibai *et al*., 2009).

As hypertension affects 5-15% of pregnancies (Lain & Roberts, 2002; Anumba *et al.,* 2010), it is a matter of concern particularly because of the increased risk of worsening and appearance of superimposed PE. Compared to severe hypertension, the likelihood of preterm delivery and abruptio placenta in severe PE may increase to 50% and fetal death may supervene (Sibai *et al*., 2009). Understandably, the search for factors that underlie or promote the development of this disorder have been the subject of intense research, although, despite the wealth of knowledge, the cause or causes remain to be determined (Karumanchi *et al*. 2005).

A personal history of PE, the presence of hypertension, parity, obesity, black ancestry, insulin-dependent diabetes, collagen disorder, thrombotic abnormalities, twin pregnancy, hydatidiform molar disease and extremes of reproductive age, all are factors that increase the risk for PE (Karumanchi *et al*., 2005; Lain & Roberts, 2002). This last point, older maternal age, became an important issue in western societies where the age at which women deliver their first child has steadily increased (Istance *et al*., 2008; Mathews *et al.,* 2009). Indeed, pregnancy in older women carries the enhanced risk for the occurrence of the most serious pregnancy disorders or complications (Oyelese *et al*., 2006; Balasch *et al*., 2011). Moreover, when compared to pregnant younger women, older women are more prone to suffer from previous illnesses, including hypertension (Hajjar *et al.,* 2006), that further enhance the risks.

All these maternal conditions substantiate the view that much of the obstetric outcome has indeed a maternal origin and that fetal structures are a target. Therefore, notwithstanding the much effort devoted to the fetal side, efforts aiming at understanding the ordered or the disordered progress of the pregnancy should emphasize the maternal side. In this context, UtA impedance assessment in pregnancy, as predictor of pregnancy complications, was discussed in the previous section. More than the provision of information, is their value in support of preventive actions aiming at ensuring a successful final outcome. In addition, the assessment is likely to reveal important data on pelvic circulation along a normal pregnancy course, when maternal normotensive or even stable hypertensive conditions are present. In fact, not all pregnant women with chronic hypertension are adversely affected and indeed, their study is likely to uncover important mechanisms of pelvic circulation adjustments. Therefore, we reasoned that additional information on the UtA performance during pregnancy could be provided by a parallel study in women with chronic stable hypertension because it is a prevalent condition and a known risk factor for serious pregnancy disorders.

It is also important that such clinical problems be studied in a biomedical approach. In fact, they reflect disordered local gene expression that may be unveiled through the application of molecular biology techniques.

Most of the above mentioned pregnancy complications are recognized to result from abnormalities in the uterine placental bed transformation (Brosens *et al*., 2011). Yet, despite the amount of reports on the structural changes observed in the myometrium, decidua and spiral arteries, the local regulation that leads to normal placentation or its derangement is still unknown.

One biological process that appears to be involved in disorders of pregnancy is the cell redox status, namely its imbalance consequent to local, enhanced production or reduced scavenging of reactive oxygen species (ROS). Interestingly, such imbalance was long ago proposed to underlie the ageing process (Harman, 1956). Free radicals are defined as species containing one or more unpaired electrons, and it is this incomplete electron shell that confers their high reactivity. In fact, there is evidence in support of redox process intervenients, including ROS and antioxidant enzymes, as important human placentation players and pointing their imbalance to placental bed apoptosis or

necrosis. As a consequence, loss of placenta function (Burton, 2009; Burton *et al*., 2010; Burton *et al*., 2011) or the establishment of serious pregnancy complications (Burton *et al*., 2011; Bedard *et al*., 2007; Myatt, 2010; Guedes-Martins *et al.*, 2013) may ensue.

There are many potential sources of ROS, and the relative contribution of these will depend on the prevailing environmental circumstances. Thus, it is plausible that the uterine placental site of aged and hypertensive females is susceptible to mild moderate oxidative stress that enhances the risk for pregnancy morbidity (Guedes-Martins *et al*., 2013). However, at present, the specific contribution of the redox players at the fetal-maternal interface is unknown. To fill this knowledge gap, the study of likely contributors is indicated. In this context, the effects of ROS generated by nicotinamide adenine dinucleotide phosphate (NADPH)-oxidase (NOX) activity appear to be important for redox signaling (Burton, 2009; Myatt, 2010). In recent years, six homologs of the cytochrome subunit of the phagocyte NADPH oxidase were found (Suh *et al.,* 1999; Bánfi *et al.,* 2000; Babior *et al*., 2002; Lambeth *et al.,* 2007): NOX1, NOX2, NOX3, NOX4, NOX5, and DUOX1/2. These homologs are generally referred to as the NOX family of NADPH oxidases.

The NOX family members are transmembrane proteins that transport electrons to reduce oxygen to superoxide ($O_2^{\bullet-}$). To ensure this role, there are conserved structural properties of NOX enzymes common to all members of the family (Figure 4). These conserved features include an NADPH-binding site at the carboxyl (COOH)-terminus, a flavin adenine dinucleotide (FAD)-binding region in proximity to the COOH-terminal transmembrane domain, six conserved transmembrane domains, and four heme-binding histidines, two in the third and two in the fifth transmembrane domain. In addition to a NOX1–4 homology domain and an EF-hand region, dual oxidase (DUOX) proteins contain a seventh transmembrane domain at the amino (NH_2) terminus with a peroxidase-like domain (Suh *et al.,* 1999; Bánfi *et al.,* 2000; Babior *et al*., 2002; Lambeth *et al.,* 2007).

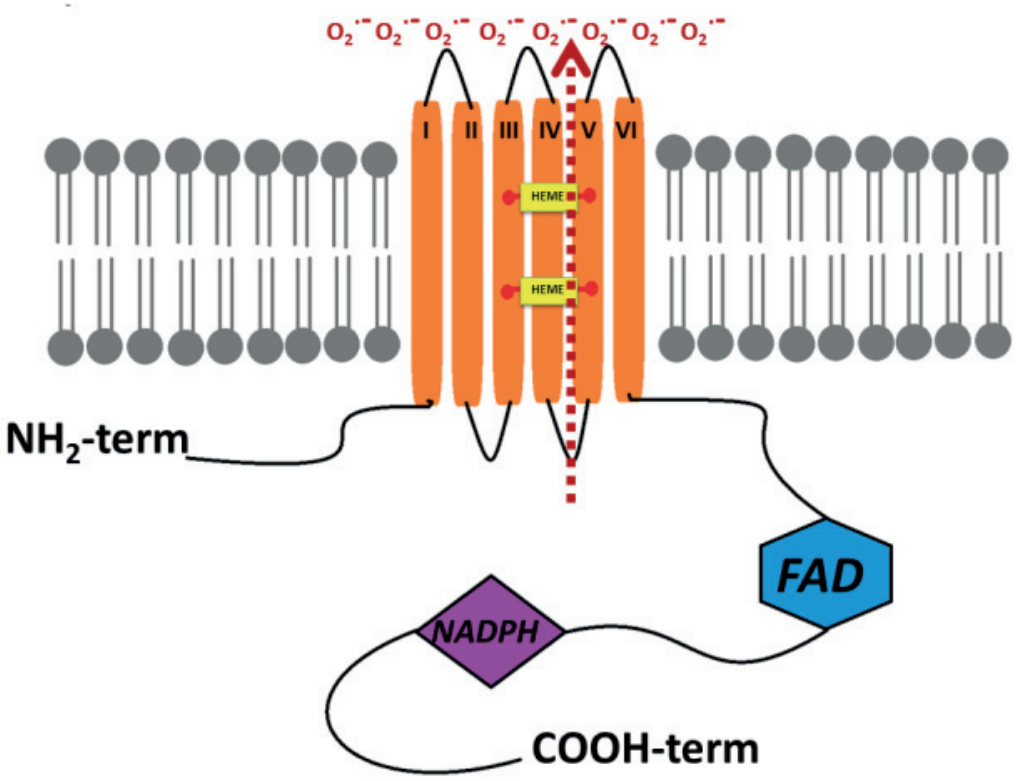

Figure 4. Conserved structure of all NADPH oxidase (NOX) enzymes. The biological function of the NOX family of NADPH oxidases is the generation of reactive oxygen species (ROS). All NOX family members are transmembrane proteins with conserved structural properties. They include a NADPH-binding site at the COOH terminus, a flavin adenine dinucleotide (FAD)-binding region in proximity of the COOH-terminal transmembrane domain, six conserved transmembrane domains, and four preserved heme-binding histidines.

Despite their similar structure and enzymatic function, NOX family enzymes differ in their pattern of expression and the need for cytosolic subunits to form a functionally active NADPH oxidase complex (Figure 5).

In the uterus, NOX-derived ROS were found to activate the nuclear factor kappa-light-chain-enhancer of activated B cells (NF-κB) and regulate angiogenesis (Bedard K *et al.*, 2007; Davis & Auten 2010), which has a determinant role in normal placental bed transformation. The activity of superoxide dismutase (SOD), the main $O_2^{\bullet-}$ scavenger and protector against redox imbalance, was observed in areas of the female reproductive tract and correlated with a successful pregnancy outcome (Matos *et al.*, 2009). It is conceivable that this effect extends to the uterus and its placental site, where it may exert specific regulatory effects upon local ROS generation.

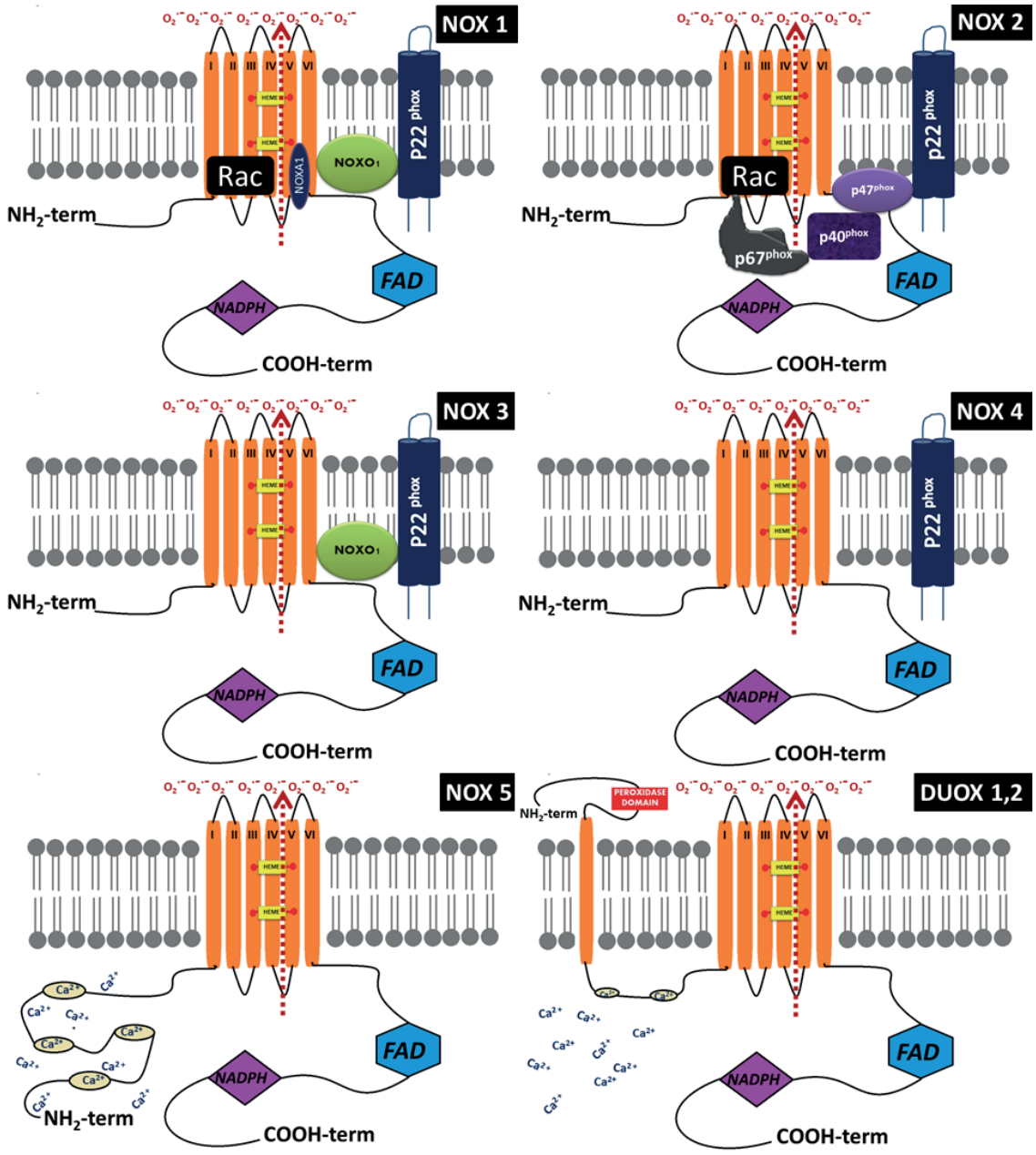

Figure 5. Mechanism of activation of the NADPH oxidase isoforms. NOX1 activity requires p22phox, NOXO1 and NOXA1, and Rac (GTPase); NOX2 requires p22phox, p47phox, p67phox, and Rac; NOX3 requires p22phox and NOXO1; NOX4 requires p22phox, but it is constitutively active without the requirement for other subunits; NOX5, DUOX1, and DUOX2 are activated by Ca^{2+} and do not require subunits.

Although knowledge of the uterine actions of these enzymes is still limited, they are likely to have relevant local roles. In fact, the expression of NOX1, NOX5 and all

SOD isoforms was demonstrated in the uterus (Bedard K *et al*., 2007; Valko *et al*., 2007), and both NOX-derived $O2^{\bullet-}$ and SOD-derived hydrogen peroxide (H_2O_2) have been shown to regulate cell signal transduction. Mitogen-activated protein kinase (MAPK) is one such signaling pathway that is activated by ROS in various cells (Moon *et al*., 2008). Moreover, mutations in genes coding for MAPKs resulted in deficient placental development in mice, and the involvement of signal-regulated kinase (ERK1/2) and p38 MAPK in the differentiation and invasion of trophoblasts was demonstrated (Allen *et al*., 2000; Mudgett *et al*., 2000; Webster *et al*., 2008).

In addition, the endothelial regulation of vascular tone is correlated with the production of NO by eNOS. This regulation is sensitive to any alterations in local stimuli, such as shear stress, or the presence of vasodilators (Amanso *et al.*, 2012). In response to these stimuli, increases and redistribution of blood flow occur in specific vascular networks (Palmer *et al*., 1988; Hwang *et al*., 2003; Price *et al*., 2000). The presence of $O_2^{\cdot-}$ in this environment plays an important role in NO action because $O_2^{\cdot-}$ rapidly interacts with NO to form peroxynitrite ($ONOO^-$). Consequently, the bioavailability of NO is reduced and other reactive species are generated. $ONOO^-$ uncouples eNOS by oxidizing tetrahydrobiopterin (BH_4), thus leading to reduce NO and increased $O_2^{\cdot-}$, inactivation of prostacyclin synthase (an important source of endothelium-derived relaxing factor), inhibition of superoxide dismutases and the onset of oxidative stress (Zou *et al.,* 2002).

Therefore, redox imbalance at the placental bed may be consequent to the disordered activity of molecules having signaling properties. Disruption of fetal/placental interactions can thus lead and promote the serious complications observed in normotensive and hypertensive pregnant women.

2 . AIMS

The previous review indicates that in the setting of reproduction, the wealth of the studies concerning the woman´s pelvic circulation has addressed mostly the uterine artery and emphasis has been put on the second trimester of pregnancy. While this period of time provides important information regarding the prognosis of pregnancy, we are convinced that the assessment of such an important artery and its filling predecessor, the internal iliac artery, is inestimable and extends beyond mid pregnancy.

Such extension includes early pregnancy and even before, when the uterus is organizing structurally and functionally to reproduction; in addition, it is also likely to be so upon delivery when pelvic circulation changes return to pre-pregnancy settings. We are thus convinced that an extended uterine artery hemodynamic assessment will provide valuable insights regarding the uterine involvement in the whole reproductive physiology.

On account of this view we engaged in a study with the following essential aims:

1. To analyze the UtA impedance profile in reproductive-age women before pregnancy, during pregnancy, at delivery, and in puerperium;
2. To search for insights on the pelvic circulation regulation by comparing uterine arteries impedance in normotensive and stage-1 essential hypertensive women who had normal course of their pregnancies;
3. To verify whether the redox status, measured as the NOX activity at the placental bed and in the placenta, is related to fetal-maternal interface blood flow impedance.

3 . PUBLICATIONS

Article 1. Reference ranges for uterine artery pulsatility index during the menstrual cycle: a cross-sectional study.
Where it is evidenced the uterine artery impedance decrease during the first third of the menstrual cycle to recover the initial values along the last two thirds of the cycle.

Article 2. Uterine artery impedance at very early clinical pregnancy.
Where evidence of progressive reduction of uterine vascular impedance in a very early stage of pregnancy is presented.

Article 3. Uterine artery Doppler in the management of early pregnancy loss: a prospective, longitudinal study.
Where it is suggested that retained ovular products are likely to modulate uterine artery blood flow.

Article 4. Internal iliac and uterine arteries Doppler ultrasound in the assessment of normotensive and chronic hypertensive pregnant women.
Where it is evidenced that internal iliac artery impedance in normotensive and chronic hypertensive women increases progressively along the pregnancy, which contrasts notably with the decreasing trend of the uterine artery.

Article 5. The effects of spinal anaesthesia for elective caesarean section on uterine and umbilical arterial pulsatility indexes in normotensive and chronic hypertensive pregnant women: a prospective, longitudinal study.
Where evidence is provided that in chronic hypertensive pregnant women at term, the sympathetic tonus loss reduces uterine artery impedance but not umbilical artery impedance.

Article 6. Fetal-maternal interface impedance parallels local NADPH oxidase related superoxide production.
Where it is shown that a placental bed redox intervenient, the NADPH oxidase activity, parallels uterine artery pulsatility index, suggesting that redox imbalance underlies the development of pregnancy disorders coursing with enhanced uterine artery impedance.

Article 7. Uterine artery impedance during puerperium in normotensive and chronic hypertensive pregnant women.
Where it is evidenced that postpartum recovery of UtA impedance is similar in normotensive and hypertensive women, albeit following peculiar trends.

Article 8. Uterine artery impedance during the first eight postpartum weeks.
Where it is reported that by 8 weeks postpartum, the uterine artery impedance had not yet actively recovered to the non-pregnant state.

Article 1

Guedes-Martins L, Gaio R, Saraiva J, Cerdeira S, Matos L, Silva E, Macedo F, Almeida H. Reference ranges for uterine artery pulsatility index during the menstrual cycle: a cross-sectional study. *PLoS One*. 2015; 10:e0119103.

PLOS | ONE

RESEARCH ARTICLE

Reference Ranges for Uterine Artery Pulsatility Index during the Menstrual Cycle: A Cross-Sectional Study

Luís Guedes-Martins[1,2,3]*, Rita Gaio[4,5], Joaquim Saraiva[1,3,6], Sofia Cerdeira[7,8], Liliana Matos[1,2,9], Elisabete Silva[1,2], Filipe Macedo[10], Henrique Almeida[1,2,11]

1 Department of Experimental Biology, Faculty of Medicine, University of Porto, 4200–319 Porto, Portugal, **2** IBMC-Instituto de Biologia Molecular e Celular, 4150–180 Porto, Portugal, **3** Centro Hospitalar do Porto EPE, Departamento da Mulher e da Medicina Reprodutiva, Largo Prof. Abel Salazar, 4099–001 Porto, Portugal, **4** Department of Mathematics, Faculty of Sciences, University of Porto, Rua do Campo Alegre, 4169–007 Porto, Portugal, **5** CMUP-Centre of Mathematics, University of Porto, Rua do Campo Alegre, 4169–007 Porto, Portugal, **6** Obstetrics-Gynecology, Private Hospital Trofa, 4785–409 Trofa, Portugal, **7** Gulbenkian Program for Advanced Medical Education, 1067–001 Lisbon, Portugal, **8** Department of Medicine, Beth Israel Deaconess Medical Center, Harvard Medical School, Boston, Massachusetts, United States of America, **9** Faculty of Nutrition and Food Sciences, University of Porto, Rua Dr. Roberto Frias, 4200–465 Porto, Portugal, **10** Department of Cardiology, Faculty of Medicine, University of Porto, 4200–319 Porto, Portugal, **11** Obstetrics-Gynecology, Hospital-CUF Porto, 4100–180 Porto, Portugal

* luis.guedes.martins@gmail.com

OPEN ACCESS

Citation: Guedes-Martins L, Gaio R, Saraiva J, Cerdeira S, Matos L, Silva E, et al. (2015) Reference Ranges for Uterine Artery Pulsatility Index during the Menstrual Cycle: A Cross-Sectional Study. PLoS ONE 10(3): e0119103. doi:10.1371/journal.pone.0119103

Academic Editor: Fatima Crispi-Brillas, University of Barcelona, SPAIN

Received: September 26, 2014

Accepted: January 28, 2015

Published: March 5, 2015

Data Availability Statement: All relevant data are within the paper and its Supporting Information file.

Funding: The authors have no support or funding to report.

Competing Interests: The authors have declared that no competing interests exist.

Abstract

Background

Cyclic endometrial neoangiogenesis contributes to changes in local vascular patterns and is amenable to non-invasive assessment with Doppler sonography. We hypothesize that the uterine artery (UtA) impedance, measured by its pulsatility index (PI), exhibits a regular pattern during the normal menstrual cycle. Therefore, the main study objective was to derive normative new day-cycle-based reference ranges for the UtA-PI during the entire cycle from days 1 to 34 according to the isolated time effect and potential confounders such as age and parity.

Methods

From January 2009 to December 2012, a cross-sectional study of 1,821 healthy women undergoing routine gynaecological ultrasound was performed. The Doppler flow of the right and left UtA-PI was studied transvaginally by colour and pulsed Doppler imaging. The mean right and left values and the presence or absence of a bilateral protodiastolic notch were recorded. Reference intervals for the PI according to the cycle day were generated by classical linear regression.

Results

The majority of patients (97.5%) presented unilateral or bilateral UtA notches. The crude 5th, 50th, and 95th reference percentile curves of the UtA-PI at 1–34 days of the normal

menstrual cycle were derived. In all curves, a progressive significant decrease occurred during the first 13 days, followed by an increase and recovery in the UtA-PI. The adjusted 5th, 50th, and 95th reference percentile curves for the effects of age and parity were also obtained. These two conditions generated an approximately identical UtA-PI pattern during the cycle, except with small but significant reductions at the temporal extremes.

Conclusions

The median, 5th, and the 95th percentiles of the UtA-PI decrease during the first third of the menstrual cycle and recover to their initial values during the last two thirds of the cycle. The rates of decrease and recovery depend significantly on age and parity.

Introduction

The uterus requires an adequate blood supply to fulfil its essential role in human reproduction. As the uterine artery (UtA) provides most of the perfusion, assessment of its vascular properties is expected to provide important information on the uterine ability to allow the fertilized ovum to implant and pregnancy to progress. Doppler ultrasound has become a mainstay in the assessment of such properties because of the development of adequate, non-invasive procedures and easy-to-use equipment. Using Doppler ultrasound, a variety of circulatory data can be estimated and integrated into a quantitative determination of different impedance parameters. Of these, major importance has been attributed to the pulsatility index (PI) because it appears to more appropriately describe the blood velocity waveform [1].

Pregnancy is the most impressive change that occurs in the uterus. The nutritionally demanding growing foetus necessitates a large and progressive adaptation in the pelvic circulation, which includes the UtA and the internal iliac artery, from where it is derived [2]. In the non-pregnant condition, the UtA Doppler waveform velocity shows a systolic flow rapid rise and sudden fall that is immediately followed by a notch during early diastole [3]; however, this high impedance feature progressively disappears during pregnancy and is present in only 5% of women from 25 weeks onwards [1]. In this context, the most important change in the UtA-PI is its progressive decrement [1,4]. This change is related to major changes at the placental bed and in the uterine artery itself, which shifts from a resistance vessel to a capacitance vessel to cope with the foetal demands. Such change is so important that, during the second trimester, the uterine artery PI increases rather than decreases, and combined with the notch presence, is considered a good predictor of preeclampsia and severe intra-uterine growth restriction [5].

The monthly cyclic changes in the non-pregnant genital tract also suggest that regulated changes occur in the uterine blood supply to endow the endometrium with the ability to receive the ovum, should fertilization occur. Indeed, such cyclic changes were the subject of a number of studies measuring circulatory data in the UtA and its distal branches such as the radial and spiral arteries. The reports, however, evidenced complex temporal relationships and sometimes conflicting results.

Both a lack of significant UtA impedance changes during the cycle [6] and higher UtA-PI early and late in the cycle, with a comparatively lower level during the mid-cycle period or luteal phase, were reported [7,8]. In addition, other reports have found small peaks at mid-cycle just before ovulation [9] that appeared to interrupt the seeming regularity of UtA-PI trends. Interestingly, studies of the UtA distal branches indicated low impedance to flow during the late follicular and midluteal phases [8,10], times when the endometrial thickness and vascularity

increased [11]. The decreased UtA-PI, particularly during the luteal phase, together with the increased blood velocity in the UtA and its vascular network, indicated increased uterine perfusion in preparation for implantation [8,9]. In fact, low PI of the uterine artery [12] and endometrial flow [13] were associated with improved implantation rates, further supporting the view that increased local perfusion favours successful establishment of pregnancy.

It should be emphasized that, in contrast to the UtA distal branches, the data for the UtA itself have been less consistent. While some studies failed to evidence any association [13–15], others reported an association between the lower UtA-PI at mid-cycle, higher pregnancy rates [12,16,17], and fewer miscarriage events [18]. These findings indicate that a more in-depth knowledge of the uterine circulation during the normal menstrual cycle (NMC) will provide relevant insights on reproductive physiological changes and allow the recognition of abnormal patterns; in turn, these data would prove useful in the management of reproductive disorders such as polycystic ovary syndrome, miscarriage, and repeated abortion.

Notwithstanding the gains afforded by previous investigations in unveiling UtA impedance variations during the menstrual cycle, these studies were limited by the number of women enrolled and the duration that each cycle was evaluated. In addition, day-cycle-based reference ranges for the mean UtA-PI have not been established using well-established methodological guidelines [19–21], which would prove helpful in the management of fertility disorders such as those mentioned above.

These shortcomings led us to determine normative new reference ranges for the UtA-PI based on the day-cycle from days 1 to 34 of the NMC, while also isolating the time effect and adjusting the findings for potential confounders such as age and parity.

Materials and Methods

Subjects

The research protocol was approved by the ethics committee (IRB protocol number: 150–13 [096-DEFI/122-CES]) of Centro Hospitalar do Porto, Unidade Maternidade Júlio Dinis (CHP-MJD), and all subjects provided written informed consent.

A cross-sectional study of 1821 healthy women undergoing routine gynaecological ultrasound examination was performed from January 2009 to December 2012. During the first appointment that coincided with the ultrasound evaluation, subjects were examined by a senior specialist who reviewed the patient's history, and verified the absence of previous hypertension, structural heart disease, diabetes and other endocrine disorders, immune disease, renal and haematological conditions, and chronic infections. A detailed gynaecological examination ruled out the presence of any pelvic or gynaecological abnormality. Inclusion criteria were: identification of the first day of the most recent menstrual period (day 1); regular menstrual cycles; absence of gynaecological disorders, menorrhagia, and established pelvic pathology on transvaginal ultrasound examination (including fibroids, abnormal sizes or clusters of ovarian cysts, and tubal disease); no chronic medication, including hormonal contraception, for the preceding 4 months; and absence of pregnancy as confirmed by ultrasound.

On the day of ultrasound examination, a menstrual calendar was handed to the patient, and a subsequent clinical appointment was scheduled 60–90 days later. The date and duration of the most recent menstruation and the date of the ultrasound evaluation were recorded on the menstrual calendar. Additionally, patients were instructed to write the dates of subsequent menstruation. Patients failing to complete the menstrual calendar or those becoming pregnant during follow-up were excluded.

Doppler flow assessment

The ultrasound examination was performed with the woman in the lithotomy position and at any time of day. Uterine artery Doppler evaluation was performed using a Voluson 730 Pro (GE Healthcare Technologies, Milwaukee, WI, USA) ultrasound unit containing multifrequency transvaginal and transabdominal transducers. Assessments were performed by a single operator with vast experience in Doppler ultrasound to avoid inter-observer variability using a transvaginal transducer. A sagittal image of the uterus that included the cervical canal and internal cervical os was obtained. The transducer was then gently tilted from side to side, and colour flow mapping was used to identify each uterine artery at the level of the internal os. Pulsed wave Doppler was used with a sampling gate set at 2 mm to image the entire vessel and ensure that the angle of insonation was less than 30°. UtA-PIs were measured automatically as follows:

$$PI = \frac{\text{systolic peak velocity} - \text{end diastolic velocity}}{\text{mean velocity during cardiac cycle}}$$

Three similar consecutive waveforms were obtained, and the mean PI of the left and right arteries was calculated. The presence or absence of a bilateral early protodiastolic notch in UtA was evaluated. A positive notch was defined as a persistent decrease in the blood flow velocity during early diastole that was less than the diastolic peak velocity in at least one UtA Doppler ultrasound spectrum. Absence of the notch was defined by its bilateral absence.

Intraobserver reliability was obtained from two readings performed at the beginning and end of the examination during the first 100 recordings of pulsatility indices in the uterine arteries.

Statistical analysis

The Chi-squared test assessed the homogeneity of proportions for categorical variables. The population reference intervals for PI were derived by regression modelling of the PI values over time during the menstrual cycle. The response was log-transformed because of the positive skewness observed in the empirical distribution (Fig. 1). Age group, Body Mass Index (BMI), parity status (primiparous vs multiparous), and smoking were considered potential time-effect confounders. However, adequate adjustment for these variables identified age and parity as the only statistically significant confounders. The crude and adjusted (for age group and parity) trends of the PI during the menstrual cycle were identified.

To study the crude effect of the menstrual cycle progression on the UtA-PI, a cubic polynomial fit the data significantly better than did a quadratic. No polynomial of a degree higher than three was considered, as those curves may exhibit unrealistic features such as waviness or sharp deviation at extreme values of the days [19]. Each day of the menstrual cycle was denoted as d, and a fitted model was generated as follows:

$$\mathbb{E}(\log(PI) \mid d) = \beta_0 + \beta_1 \frac{d}{10} + \beta_2 \left(\frac{d}{10}\right)^2 + \beta_3 \left(\frac{d}{10}\right)^3 \quad (1)$$

with constants $\beta_0\beta_1\beta_2\beta_3$ and a rescaling in the variable d to avoid very small regression coefficients. This equation was rewritten using multiplicative effects as follows:

$$\mathbb{E}(PI \mid d) = Ce^{\gamma_1 d + \gamma_2 d^2 + \gamma_3 d^3}$$

with $C = e^{\beta_0}$, $\gamma_1 = \frac{\beta_1}{10}$, $\gamma_2 = \frac{\beta_2}{10^2}$ and $\gamma_3 = \frac{\beta_3}{10^3}$. The letter $\mathbb{E}$ in both equations denoted the conditional expected value.

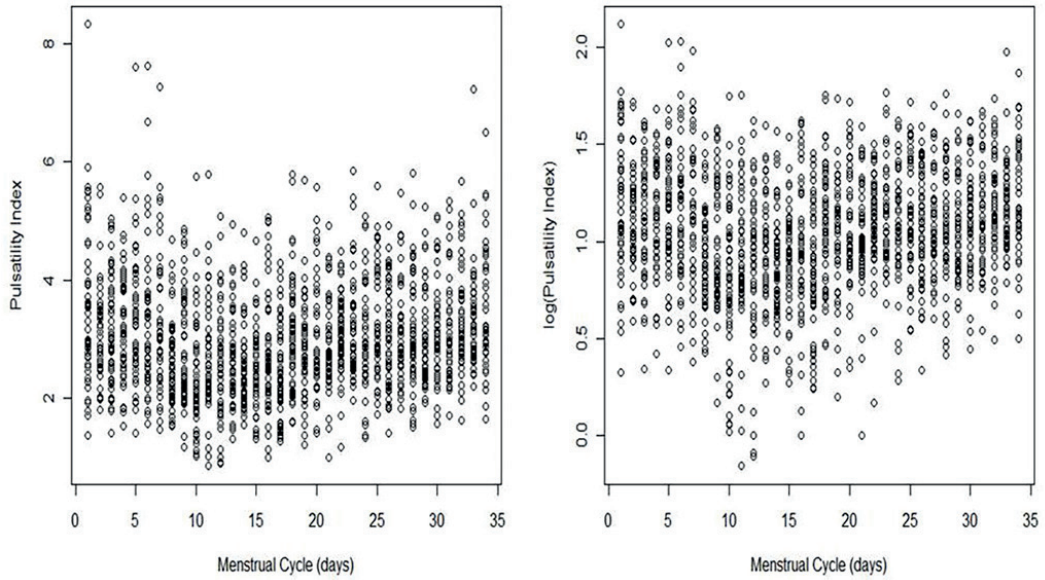

Fig 1. Plot of PI (left panel) and the log(PI) (right panel) measured in the uterine artery during the menstrual cycle. PI, pulsatility index.

doi:10.1371/journal.pone.0119103.g001

Every centile curve for PI was then estimated by the following equation:

$$centile(d) \;=\; \exp[\widehat{log(PI)}(d) + K \times \widehat{sd})].$$

Here,$\widehat{\log(\mathrm{PI})}(\mathrm{d})$ is the predicted response at day d of model (1), K is the corresponding centile of the standard Gaussian distribution, and $\widehat{sd}$ is the standard deviation of the unscaled residuals of model (1).

To obtain centile curves stratified by age group (group 1, 18–26 years; group 2, 27–35 years; group 3, 36–50 years) and parity (nulliparous *vs* parous), the above regression procedure was refined. For age group a and parity status p, the best fitted model was as follows:

$$\mathbb{E}(\log(PI)|(d,\ a,\ p)) \;=\; \beta_0(a,p) + \beta_1(a)\frac{d}{10} + \beta_2(a)\left(\frac{d}{10}\right)^2 + \beta_3\left(\frac{d}{10}\right)^3 \qquad (2)$$

with β_0 depending on the two considered factors, β_1 and β_2 depending only on the age group, and β_3 designated as a constant. The reference categories corresponded to the youngest and the nulliparous classes.

Intraclass correlation coefficients (ICC) and 95% confidence intervals were calculated using a two-way mixed-effects model with absolute agreement. The reliability coefficient, which is the difference value exceeded by only 5% of pairs of measurements in a single subject, was calculated as 1.96 times the standard deviation of the difference between pairs of repeated measurements [22].

All statistical analyses were carried out using the R language and software environment for statistical computation, version 2.12.1 [23]. The significance level was fixed at 0.05.

The study adhered to the STROBE (Strengthening the Reporting of Observational studies in Epidemiology) guidelines for observational studies, and all recommendations were included in the study [S1 Table].

Results

A total of 1821 healthy women were considered eligible for this study. Of these, 153 were excluded (8.4%); 128 women did not have clinical records in the menstrual calendar according to the study protocol; 11 women were pregnant at the time of ultrasound assessment; in 10 cases, the pulsatility index in the uterine arteries could not be measured because of technical difficulties; and four women refused to participate in the study.

The demographic characteristics of the 1668 women included in the study are summarized in Table 1. Their ages ranged from 18 to 50 years old, and 41.4% were older than 35 years. Additionally, 39.1% were nulliparous, and the majority of the patients (97.5%) exhibited a notch in the uterine arteries (unilaterally or bilaterally).

UtA-PI during the normal menstrual cycle

The reliability coefficient for the UtA-PI was 0.434. The ICC for the intraobserver reliability of the UtA-PI measurements was 0.984, with a 95% confidence interval ranging from 0.976 to 0.989.

Table 1. Demographic characteristics of the 1668 women included in the study.

		n(%)
Age (intervals in years)	Group 1. 18–26	251 (15.0)
	Group 2. 27–35	727 (43.6)
	Group 3. 36–50	690 (41.4)
Body Mass Index[a] (Kg/m^2)	16–24	1032 (61.9)
	25–29	480 (28.8)
	30–39	156 (9.3)
Parity	0	653 (39.1)
	≥1	1015 (60.9)
Age at menarche, years (mean±SD)	12.1 (1.17)	-
Age at first sexual intercourse (years±SD)	17.9 (2.33)	-
History of miscarriage	No	1479 (88.7)
	Yes	188 (11.3)
History of preeclampsia	No	1644 (98.6)
	Yes	24 (1.4)
Smoking	No	1380 (82.7)
	Yes	288 (17.3)
Presence of bilateral notching	No	100 (6.0)
	Yes	1568 (94.0)
Presence of unilateral notching	No	42(2.5)
	Yes	1626 (97.5)
Menstrual cycle length, days (mean±SD)	28.8(4.2)	-
Menstrual period length, days (mean±SD)	5.0(1.7)	-

SD, standard deviation

[a]Body Mass Index (BMI) was measured immediately before Doppler assessment.

doi:10.1371/journal.pone.0119103.t001

The days evaluated in the menstrual cycle varied from 1 to 34, and the collected data were slightly unbalanced. The least frequently assessed point was day 34 (39 patients), and the most frequently assessed were days 22 and 26 (54 patients each) (Table 2). However, the empirical distribution for the day number was essentially uniform, with a sample mean ± standard deviation of 17.3 ± 9.7 compared with 17.0 ± 9.8 expected in a uniform distribution.

Concerning the fitting of model (1), visual inspection of the normality and homoscedasticity of the residuals was performed (Fig. 2, Panel A). There were no serious departures from normality except at a few extreme points, mostly located on the left tail. Data with an absolute value of the standardized residuals greater than three were removed. A total of 11 data points were removed (eight on the left tail), corresponding to less than 1% of the total sample size. The highest and lowest cutoff values for PI in these women were 7.26 and 1.03, respectively.

All parameter estimates of the final fitted model were statistically significant (Table 3). Standard errors of the estimates were up to 3% smaller than the errors in the model using the total data. Residual plots exhibited reasonable properties for normality adherence (Fig. 2, Panel B): 89% of the standardized residuals lay between-1.645 and 1.645; the boxplot revealed an approximately symmetric distribution with the median line at approximately the centre of the box and symmetric whiskers; and the quantile-quantile (Q-Q) plot of the studentized residuals showed little departure from the confidence band for the correspondent *t* distribution. In addition, the Lilliefors-corrected Kolmogorov-Smirnov normality test provided a p-value of 0.002; this statistical significance was overlooked because of the large sample size (n = 1657). The outliers were again removed, but the results were no better.

The plot of the logarithmized UtA-PI values against the days of the cycle did not show any substantive changes in the standard deviations of the values along the menstrual cycle (Fig. 1); however, a formal statistical model for this relationship was applied. The linear regression of the scaled absolute residuals (SARs), defined as the product of $\sqrt{\pi/2}$ by the absolute residuals, on a polynomial of degree 1 in the variable *Day* was statistically significant ($p < 0.001$), and no higher-order terms were identified. As this regression only explained approximately 1% of the SARs' total variability, it was considered redundant, and therefore the residual homoscedasticity of model (1) did not appear violated.

The predicted 5th, 50th, and 95th percentile regression curves are presented in Table 2 and plotted in Fig. 3. The expected ovulation date (EOD) was calculated in each patient assuming that the luteal phase lasted approximately 2 weeks (*i.e.*, *EOD* = *menstrual cycle length*−14). Accordingly, the 50th centile curve for PI, which under the normality assumption coincides with the mean curve, began at day 1 at its maximum value (3.40) and decreased until reaching its minimum value at day 12–13. From this day onwards, the curve increased until reaching 3.20 (50th centile) at the end of the menstrual cycle (day 34). If the curve failed to stop at day 34, it continued to decrease afterwards. Day 34 corresponded to the local maximum of the defined function.

As the 5th and the 95th centile curves were simply the product of the 50th percentile and a constant value, they showed the same monotonicity behaviour as the 50th centile curve, with maximum and minimum values attained on the same days (Table 2). The 5th centile curve began at 2.08, ended at a similar PI value of 1.96, and had a minimum PI value of 1.60. The 95th centile curve began at 5.55, ended at 5.23, and had a minimum PI value of 4.27. The steepest decrease in the PI during the first 12–13 days of the menstrual cycle occurred in the 95th centile curve, and the smallest decrease occurred in the 5th centile curve (Fig. 3).

Table 2. Observed and predicted percentiles of the uterine artery pulsatility index on each cycle day.

			Observed			Predicted		
Cycle (days)	n	EOD[a] (n)	5th centile	50th centile	95th centile	5th centile	50th centile	95th centile
1	50	0	1.74	3.37	5.55	2.08	3.40	5.55
2	50	0	2.00	3.04	4.59	1.99	3.24	5.29
3	49	0	1.88	3.02	4.90	1.90	3.11	5.07
4	48	0	1.83	3.17	4.60	1.83	2.99	4.89
5	51	0	1.94	3.25	5.00	1.78	2.90	4.73
6	52	1	1.88	3.15	5.77	1.73	2.82	4.60
7	46	20	1.80	3.12	5.37	1.69	2.76	4.50
8	52	46	1.59	2.41	4.03	1.66	2.71	4.42
9	50	107	1.83	2.48	4.64	1.63	2.67	4.36
10	52	110	1.09	2.21	3.93	1.62	2.64	4.31
11	49	136	1.24	2.40	4.48	1.61	2.62	4.28
12	48	131	1.05	2.60	4.10	1.60	2.61	4.27
13	49	103	1.52	2.62	4.18	1.60	2.61	4.26
14	53	209	1.81	2.33	4.09	1.60	2.62	4.27
15	46	160	1.42	2.56	3.66	1.61	2.63	4.29
16	50	71	1.43	2.60	4.87	1.62	2.65	4.32
17	52	104	1.36	2.33	3.93	1.63	2.67	4.36
18	52	103	1.93	2.99	4.66	1.65	2.70	4.40
19	49	67	1.62	2.88	3.96	1.67	2.73	4.45
20	49	99	1.89	2.74	4.78	1.69	2.76	4.51
21	50	96	1.85	2.72	4.31	1.72	2.80	4.57
22	54	61	2.14	3.01	4.18	1.74	2.84	4.64
23	48	19	2.30	2.86	5.03	1.77	2.88	4.70
24	45	21	1.56	2.91	4.81	1.79	2.92	4.77
25	51	4	1.81	3.07	4.73	1.82	2.97	4.84
26	54	0	1.87	2.96	4.30	1.84	3.01	4.91
27	46	0	2.08	2.86	4.71	1.87	3.05	4.98
28	47	0	1.67	2.94	4.52	1.89	3.09	5.04
29	47	0	2.16	2.90	4.58	1.91	3.12	5.09
30	50	0	1.97	3.00	4.61	1.93	3.15	5.14
31	43	0	2.19	2.94	4.90	1.94	3.17	5.18
32	49	0	2.16	3.25	4.95	1.95	3.19	5.21
33	48	0	2.41	3.14	4.29	1.96	3.20	5.23
34	39	0	2.11	3.21	5.42	1.96	3.20	5.23

[a]For each patient, the expected ovulation date (EOD) was calculated assuming that the luteal phase exhibited a consistent duration of approximately 2 weeks, i.e., *E0D = menstrual cycle length*—14.

doi:10.1371/journal.pone.0119103.t002

Effect of maternal age and parity on UtA-PI during normal menstrual cycle

To obtain centile curves stratified by age group and parity status, the regression procedure was refined taking these factors into consideration, while also excluding the same 11 data points as previously. The best fitted model is described in model (2), and the estimated regression coefficients and corresponding 95% confidence intervals are summarized in Table 4. All estimates

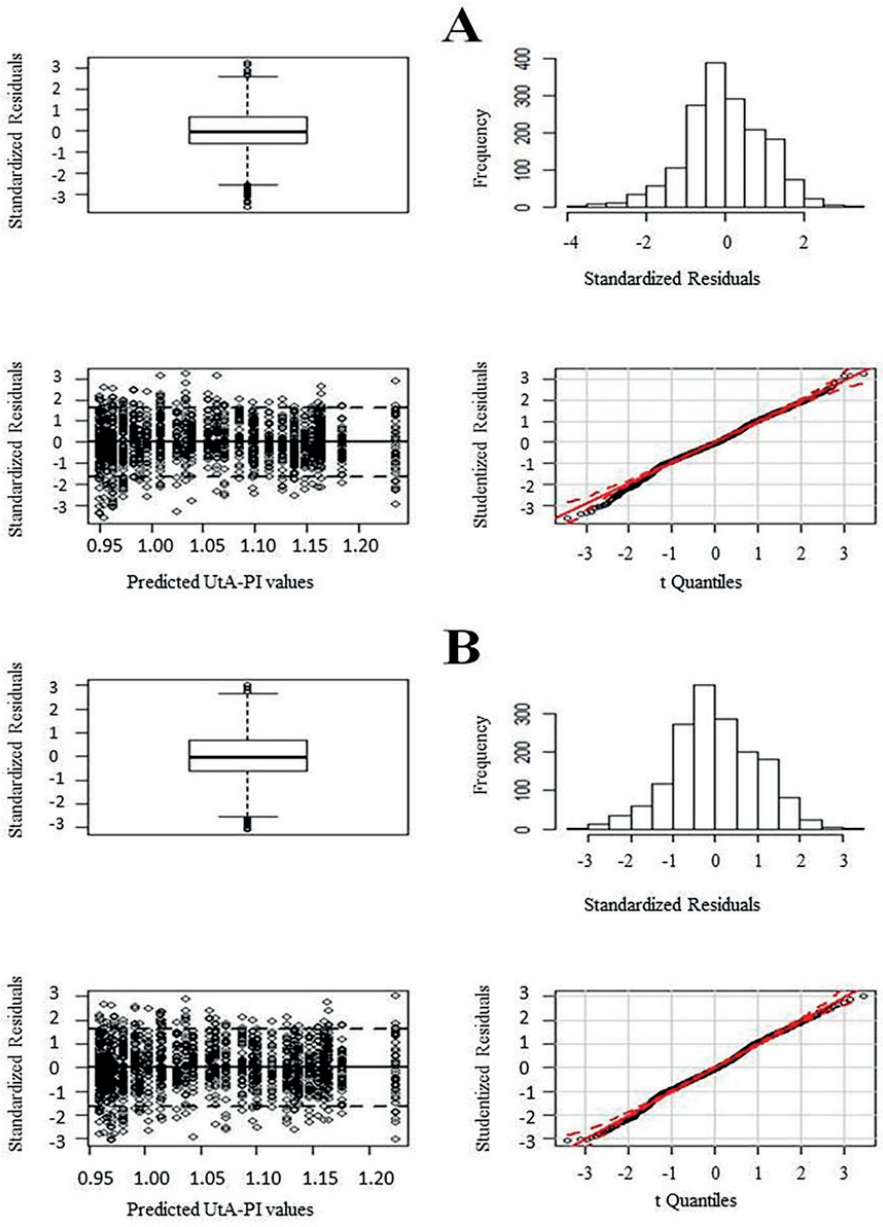

Fig 2. Residual plots for the fitted models; from top to bottom and from left to right: boxplot of the standardized residuals, histogram of the standardized residuals, plot of the standardized residuals against the predicted values, and QQ-plot of the studentized residuals. Panel A employs the entire dataset; Panel B eliminates data from 11 outliers.

doi:10.1371/journal.pone.0119103.g002

Table 3. Estimates of the regression coefficients and corresponding 95% confidence intervals (CI) of model (1) fitted without the 11 identified outliers.

Variables	Regression Coefficients	95% CI
Intercept	1.279	(1.214, 1.344)*
Day/10	-0.573	(-0.730, -0.416)*
$(Day/10)^2$	0.310	(0.206, 0.414)*
$(Day/10)^2$	-0.044	(-0.064, -0.024)*

*Significant at the 0.05 level.

doi:10.1371/journal.pone.0119103.t003

but one (a quadratic term on days of the menstrual cycle for women aged 27–35 years, p = 0.089) were statistically significant.

No significant interaction effects involving parity were identified. No serious outliers or evidence of violations in normality and homoscedasticity assumptions were detected within each age-parity sub-model (Figs. 4 and 5). The residual regression on the explanatory variables, with a linear dependence on the cycle days, presented a value for the coefficient of determination (R^2) of approximately 1% and did not identify the effect of age group as statistically significant. As before, the residual homoscedasticity of the model did not appear compromised. The residual normality could only be rejected for nulliparous women aged 27–35 years (Fig. 4).

The standard deviation of the residuals of model (2) did not significantly change during the menstrual cycle; therefore, the coefficient significance in Table 4 remained true for all centile curves.

For any fixed age group and centile curve, a significant difference between the intercepts of the curves for nulliparous and parous women was identified, with the menstrual cycle in nulliparous women beginning at higher UtA-PI values. Similarly, for any fixed parity status and centile curve, there were significant differences between the intercept of the age group 2 (or 3) curve and that of age group 1 (Fig. 5).

Overall, the PI values exhibited a soft wave-like trend during the menstrual cycle within each maternal age and parity group. The values decreased until approximately the first third of the menstrual cycle and then increased to approximately the original value over the remainder of the cycle. This trend was independent from the parity status but was significantly dependent on the maternal age at the linear and quadratic levels. As the age increased, the minimum UtA-PI was reached more quickly, the range of the PI values decreased, and the curves became flatter (Fig. 5).

Discussion

Transvaginal assessment of UtA perfusion employing Doppler ultrasound offers several advantages over the transabdominal route [24]. The vessel is easily identified and located at close proximity, thus yielding clearer waveforms, and the insonation angle is near 0°, which results in high reproducibility [24,25]. Despite the diversity of features that may be determined through arterial resistance, it is impedance, the combination of forward and reflected blood flow, that is measured [26]. This is accomplished by indirectly measuring the UtA-PI, a technique that has gained popularity in recent studies compared with other Doppler indices such as resistance index [1,27] and other scoring systems [28,29].

These principles were applied in the current study to generate Doppler colour-based reference ranges for the mean UtA-PI between days 1 and 34 of the NMC in an appropriately large

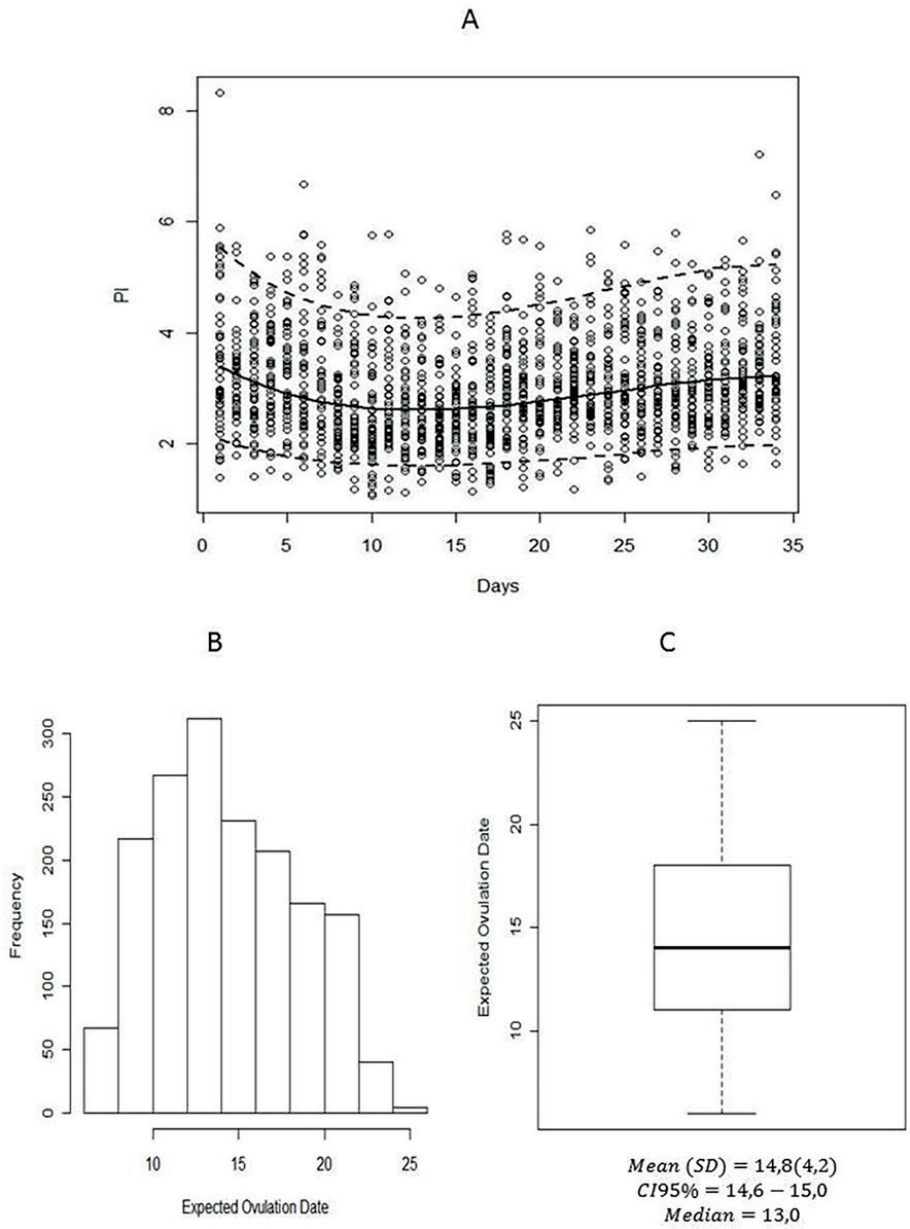

Fig 3. (A) Observed (circles) and predicted 5th, 50th, and 95th percentile regression curves for the pulsatility index during the menstrual cycle. Histogram (B) and boxplot (C) of the expected ovulation date (EOD). For each patient, the EOD was calculated assuming that the luteal phase exhibited a consistent duration of approximately 2 weeks, i.e., *EOD = menstrual cycle length* − 14.

doi:10.1371/journal.pone.0119103.g003

Table 4. Estimates of the regression coefficients and corresponding 95% confidence intervals (CI) for the model stratified by age and parity.

Variables	Regression Coefficients	95% CI
Intercept	1.546	(1.438, 1.654)*
Age Group 2	-0.236	(-0.361, -0.110)*
Age Group 3	-0.335	(-0.463, -0.206)*
Parous	-0.066	(-0.098, -0.034)*
Day/10	-0.792	(-0.992, -0.592)*
$(Day/10)^2$	0.353	(0.244, 0.461)*
$(Day/10)^3$	-0.042	(-0.062, -0.023)*
(Age Group 2):(Day/10)	0.216	(0.041, 0.391)*
(Age Group 3):(Day/10)	0.365	(0.188, 0.543)*
(Age Group 2):$(Day/10)^2$	-0.044	(-0.044, 0.026)
(Age Group 3):$(Day/10)^2$	-0.091	(-0.142, -0.039)*

*Significant at the 0.05 level.

doi:10.1371/journal.pone.0119103.t004

sample of healthy women. In addition, the effects of age and parity were assessed for each day during the NMC.

Statistics

The reliability evaluation demonstrated that UtA-PI measurement was highly repeatable as indicated by the ICC. There is sufficient scientific consensus that an ICC > 0.7 reflects very low measurement error [22,30].

Stringer and validated methodological guidelines were used to construct the reference curves from the collected data [19–21,31]; a cross-sectional design was used as such studies are easier to perform and combine with clinical practice; and finally, the good intraobserver reproducibility in our study suggests that the mean UtA-PI is a reliable parameter in a clinical setting. The overarching principle is that a reference interval is the range of values encompassed by a pair of symmetrically placed extreme centiles, such as the 2.5^{th} and 97.5^{th} centiles for a 95% interval [19]. Values lying outside the reference limits are considered unusual or extreme.

Several statistical methods have been used to generate reference intervals: linear regression (if necessary with modelling of the residual standard deviation), the LMS method [32], the non-parametric method of Healy, Rabash, and Young (HRY), and non-parametric quantile regression [21]. Each method has its advantages and limitations; however, the method that is most desired is the one allowing identification of the population centile of a given observation. Linear regression has that property and is simple and easily implemented by basic statistical software packages.

Perfusion changes during the normal menstrual cycle

The current study revealed a cyclic variation in the UtA impedance during the NMC; the UtA-PI was high during the temporal extremes and showed a mid-cycle depression, with the minimal values occurring between days 13 and 17. Independent assessment of the effects of age and parity also revealed that both conditions were associated with a significant decrease in the UtA impedance at the extremes of the cycle, but not during the mid-cycle, when the uterus undergoes impressive structural changes. These circulatory variations include the median, 5^{th}, and 95^{th} percentiles of the UtA-PI regression curves from the initial through to the final third of

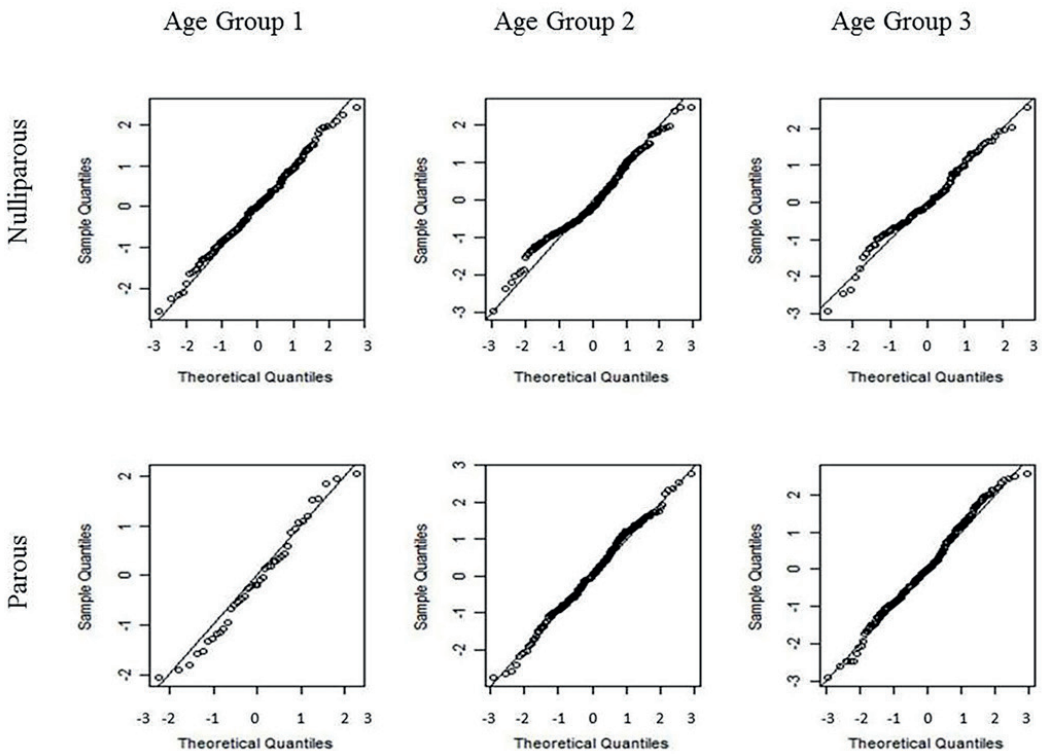

Fig 4. Quantile-quantile (Q-Q) plots of the standardized residuals of model (2) for each combination of age and parity groups. Nulliparous women are presented in the first row, and parous women are presented in the second row. The age group increases from the left to right columns. From left to right and from top to bottom, the Lilliefors-corrected Kolmogorov-Smirnov normality test calculated p-values of 0.738, <0.001, 0.111, 0.954, 0.082, and 0.373, respectively.

doi:10.1371/journal.pone.0119103.g004

the menstrual cycle. The mechanism underlying such impedance variation is unknown, but it likely reflects regulatory factors affecting the local vasculature and myometrium function.

Early during the cycle, increased myometrial tone is required to expel the remains of the sloughing endometrium; for this purpose, the smooth muscle cells contract, which has a negative effect on uterine perfusion and generates high impedance to UtA blood flow. We suspect that a similar muscular change underlies the UtA-PI rise near the end of the cycle.

There is evidence that variations in muscular tone reflect circulating levels of female steroid hormones, particularly oestrogen, which is low early in the cycle but increases later during the follicular phase. Oestrogen promotes vascular smooth muscle relaxation and reduces sensitivity to adrenergic stimulation [33]; moreover, in experimental conditions, it was found to depress uterine contractility both *in vivo* [34] and in freshly isolated rat uterine specimens [35]. This decrease in myometrial tone and increasingly thickened endometrium during the proliferative phase, together with the development of an extensive small vessel network, is the likely cause for the downward trend in impedance that reaches a minimum near day 13. After ovulation, progesterone concentration rises through the mid-secretory phase, promoting endometrium decidualization. Oestrogen decrement [36] and the ability of progesterone to overcome the

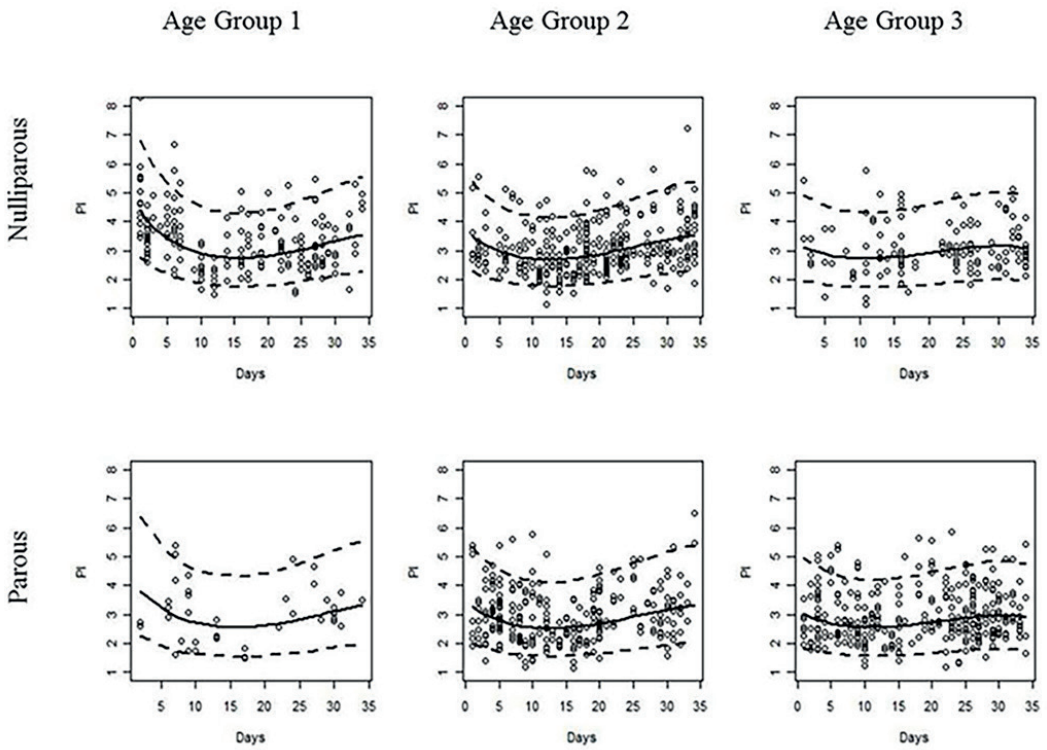

Fig 5. Observed (points) and estimated 5th, 50th, and 95th percentile regression curves of the pulsatility index during the menstrual cycle for each combination of age and parity groups. Nulliparous and parous women are presented in the first and second rows, respectively. The age group increases from the left to right columns.

doi:10.1371/journal.pone.0119103.g005

inhibitory action of 17β-oestradiol on smooth muscle contractility [34,35] favour the rise in UtA-PI.

Other important molecules, acting independently or under the effect of sex steroids, may contribute to the circulatory changes. Prostanoids such as prostaglandin $F_{2\alpha}$ and latanoprost promote murine [35,36] and human [35] myometrial contractility, but their blood concentration variation during the cycle is uncertain. In addition, vasopressin and oxytocin stimulate uterine contraction via myometrial vasopressin V_{1a} and oxytocin receptors [37]. Near the end of the cycle, although circulating at a lower concentration [38], vasopressin exerts a stronger effect than oxytocin [37]. Therefore, although the known actions of these compounds on the myometrium and its perfusion are appealing, their role during the cycle remains to be established.

Effect of parity and age on uterine flow impedance

In the current study, in non-pregnant women, the UtA-PI early and late in the cycle was significantly lower in parous women than in nulliparous women. This point has not been examined in any known reports previously.

UtA-PI reduction is important because it is accompanied by improved myometrium perfusion, which provides local benefits. Indeed, it has been suggested that impaired uterine perfusion is a cause for unexplained infertility [39] and is reportedly a predictive indicator for the implantation and pregnancy outcomes [40–42]. Moreover, upon pregnancy establishment, parous women appear to have improved perfusion. In fact, as early as the first trimester, parous women exhibited lower UtA-PI and total peripheral resistance compared with those in nulliparous women [43], a finding that was also described in twin pregnancies compared between parous and nulliparous women [44]. Furthermore, all reports indicate that parous women have a lower prevalence of protodiastolic notching [45,46], a feature whose persistence is associated with a poor prognosis [5].

The enhanced perfusion in parous women likely results from vascular structural features that persist after the first pregnancy. Shortly after implantation, the spiral arteries undergo remarkable structural remodelling, which is necessary to accommodate the increased uteroplacental perfusion [47]. At the end of pregnancy, these largely regress, but not entirely; in contrast to nulliparous women, spiral artery internal elastic lamina duplication or fragmentation has been observed at the endometrial/myometrial junction of parous women [48]. Such permanent structural changes endow spiral arteries with reduced impedance that supports the parity-related UtA-PI reduction here reported.

Similar to parous women, the UtA-PI decreased at the extremes of the cycle in older women when compared with younger women. Interestingly, uterine stripes from aged non-pregnant women exhibited reduced contractility either spontaneously or upon exposure to oxytocin [49], suggesting that reduced uterine muscular tone underlies the lessened UtA impedance. The cause for this sluggish response in unknown but may be consequent to an age-related change in local regulation. For example, in the pregnant uterus, the UtA-PI shows a general decreasing trend starting at the first trimester [1,2,4]; yet, when the UtA is measured at specific pregnancy time-points, a slight age-related increase may be observed [50,51]. Degenerative changes in the UtA wall, present even before menopause [52], or other local factors are the likely contributors to this particular observation.

Therefore, both age and parity similarly affect the UtA-PI of non-pregnant women during the NMC. Interestingly, the downward trend favours perfusion, which appears to bear reproductive benefits. Infants born to parous women tend to have increased birth weight [43], while older pregnant women tend to have increased placental weights [53], but the significance of these trends remains undefined.

Study limitations and future research

(1) The study was conducted in a sample of healthy women. (2) Further studies are necessary to assess abnormal uterine artery PI as a diagnostic or prognostic tool of reproductive disorders as the ovulation day was not identified, and the endometrial structure was not examined. (3) Our data were collected by a single, experienced operator, which could compromise the external validity of his results. Because the usefulness of a screening test depends not only on its predictive ability but also on its reproducibility, future studies are needed to demonstrate the usefulness of these reference ranges, as well as their applicability.

Conclusions

This cross-sectional study employing a large set of women evidences a clear decrement in the UtA impedance during the middle of the menstrual cycle compared with its extremities. For unknown reasons, age and parity do not change this trend; they instead flatten the extremes

while leaving the mid-cycle unchanged, suggesting that local mechanisms regulate an adequate uterine perfusion in preparation for implantation.

To the well-known cyclic structural features occurring in the uterus, the current study adds another cyclic circulatory event. The elucidation of the mechanisms underlying these changes, apart from providing new insights into the fascinating implantation process, may improve prediction of reproductive and pregnancy disorders, thus enhancing the importance of UtA assessment.

Supporting Information

S1 Table. STROBE Statement—checklist of items that should be included in reports of observational studies.
(DOCX)

Acknowledgments

We thank the staff at the Department of Gynaecology of Centro Hospitalar do Porto for their kind contribution to this work.

Author Contributions

Conceived and designed the experiments: LG-M FM. Performed the experiments: LG-M HA. Analyzed the data: LG-M RG SC LM ES HA. Contributed reagents/materials/analysis tools: LG-M JS. Wrote the paper: LG-M HA FM SC. Critical revision of the manuscript: JS SC LM ES.

References

1. Gómez O, Figueras F, Fernández S, Bennasar M, Martínez JM, Puerto B, et al. (2008) Reference ranges for uterine artery mean pulsatility index at 11–41 weeks of gestation. Ultrasound Obstet Gynecol. 32:128–32. doi: 10.1002/uog.5315 PMID: 18457355
2. Guedes-Martins L, Cunha A, Saraiva J, Gaio R, Macedo F, Almeida H (2014) Internal iliac and uterine arteries Doppler ultrasound in the assessment of normotensive and chronic hypertensive pregnant women. Sci Rep. 4:3785. doi: 10.1038/srep03785 PMID: 24445576
3. Schulman H, Fleischer A, Farmakides G, Bracero L, Rochelson B, Grunfeld L (1986) Development of uterine artery compliance in pregnancy as detected by Doppler ultrasound. Am J Obstet Gynecol. 155:1031–6. PMID: 2946229
4. Guedes-Martins L, Saraiva J, Gaio R, Macedo F, Almeida H (2014) Uterine artery impedance at very early clinical pregnancy. Prenat Diagn. 34:719–25. doi: 10.1002/pd.4325 PMID: 24431243
5. Cnossen JS, Morris RK, ter Riet G, Mol BW, van der Post JA, Coomarasamy A, et al. (2008) Use of uterine artery Doppler ultrasonography to predict pre eclampsia and intrauterine growth restriction: a systematic review and bivariable meta-analysis. CMAJ. 178:701–11. doi: 10.1503/cmaj.070430 PMID: 18332385
6. Ziegler WF, Bernstein I, Badger G, Leavitt T, Cerrero ML (1999) Regional hemodynamic adaptation during the menstrual cycle. Obstet Gynecol. 94:695–9. PMID: 10546712
7. Steer CV, Campbell S, Pampiglione JS, Kingsland CR, Mason BA, Collins WP (1990) Transvaginal colour flow imaging of the uterine arteries during the ovarian and menstrual cycles. Hum Reprod. 5:391–5. PMID: 2193940
8. Sladkevicius P, Valentin L, Marsál K (1993) Blood flow velocity in the uterine and ovarian arteries during the normal menstrual cycle. Ultrasound Obstet Gynecol. 3:199–208. PMID: 12797290
9. Tan SL, Zaidi J, Campbell S, Doyle P, Collins W (1996) Blood flow changes in the ovarian and uterine arteries during the normal menstrual cycle. Am J Obstet Gynecol. 175:625–31. PMID: 8828425
10. Dal J, Vural B, Caliskan E, Ozkan S, Yucesoy I (2005) Power Doppler ultrasound studies of ovarian, uterine, and endometrial blood flow in regularly menstruating women with respect to luteal phase defects. Fertil Steril. 84:224–7. PMID: 16009189

11. Jokubkiene L, Sladkevicius P, Rovas L, Valentin L (2006) Assessment of changes in endometrial and subendometrial volume and vascularity during the normal menstrual cycle using three-dimensional power Doppler ultrasound. Ultrasound Obstet Gynecol. 27:672–9. PMID: 16676367

12. Ivanovski M, Damcevski N, Radevska B, Doicev G (2012) Assessment of uterine artery and arcuate artery blood flow by transvaginal color Doppler ultrasound on the day of human chorionic gonadotropin administration as predictors of pregnancy in an in vitro fertilization program. Akush Ginekol (Sofiia). 51:55–60.

13. Wang L, Qiao J, Li R, Zhen X, Liu Z (2010) Role of endometrial blood flow assessment with color Doppler energy in predicting pregnancy outcome of IVF-ET cycles. Reprod Biol Endocrinol. 8:122. doi: 10.1186/1477-7827-8-122 PMID: 20955593

14. Wakeman S, Benny P (2009) Is it possible to predict a fertile cycle? Uteroovarian blood flow parameters in conception versus nonconception cycles. Fertil Steril. 91:2726–31. doi: 10.1016/j.fertnstert.2008.03.069 PMID: 18672235

15. Yildiz G, Yavuzcan A, Yildiz P, Göynümer G, Yücel N (2012) Effect of uterine artery blood flow on recurrent pregnancy loss. Clin Exp Obstet Gynecol. 39:326–9. PMID: 23157035

16. Steer CV, Williams J, Zaidi J, Campbell S, Tan SL (1995) Intra-observer, interobserver, interultrasound transducer and intercycle variation in colour Doppler assessment of uterine artery impedance. Hum Reprod. 10:479–81. PMID: 7769083

17. Chien LW, Lee WS, Au HK, Tzeng CR (2004) Assessment of changes in utero-ovarian arterial impedance during the peri-implantation period by Doppler sonography in women undergoing assisted reproduction. Ultrasound Obstet Gynecol. 23:496–500. PMID: 15133803

18. Wahab H, El-Din D, Zain E, Abdelgany M, Youssef M (2001) Uterine artery Doppler and subendometrial blood flow in patients with unexplained recurrent miscarriage. Middle East Fertility Society Journal. 16:209–214.

19. Royston P, Wright EM (1998) How to construct 'normal ranges' for fetal variables. Ultrasound Obstet Gynecol. 11:30–8. PMID: 9511193

20. Silverwood RJ, Cole TJ (2007) Statistical methods for constructing gestational age-related reference intervals and centile charts for fetal size. Ultrasound Obstet Gynecol. 29:6–13. PMID: 17200989

21. Hynek M (2010) Approaches for Constructing Age-Related Reference Intervals and Centile Charts for Fetal Size. Eur J Biomed Inform. 6:43–52.

22. Bland JM, Altman DG (2003) Applying the right statistics: analyses of measurement studies. Ultrasound Obstet Gynecol. 22:85–93. PMID: 12858311

23. R Development Core Team. R: A Language and Environment for Statistical Computing. R Foundation for Statistical Computing, Vienna, Austria, 2008. Available at http://www.R-project.org. Accessed October 10, 2013.

24. Papageorghiou AT, To MS, Yu CK, Nicolaides KH (2001) Repeatability of measurement of uterine artery pulsatility index using transvaginal color Doppler. Ultrasound Obstet Gynecol. 18:456–9. PMID: 11844164

25. Jaffa AJ, Weissman A, Har-Toov J, Shoham Z, Peyser RM (1995) Flow velocity waveforms of the uterine artery in pregnancy: transvaginal versus transabdominal approach. Gynecol Obstet Invest. 40:80–3. PMID: 8575696

26. Everett TR, Lees CC (2012) Beyond the placental bed: placental and systemic determinants of the uterine artery Doppler waveform. Placenta. 33:893–901. doi: 10.1016/j.placenta.2012.07.011 PMID: 22902007

27. Harrington K, Goldfrad C, Carpenter RG, Campbell S (1997) Transvaginal uterine and umbilical artery Doppler examination of 12–16 weeks and the subsequente development of pre-eclampsia and intrauterine growth retardation. Ultrasound Obstet Gynecol. 9:94–100. PMID: 9132263

28. Park YW, Cho JS, Choi HM, Kim TY, Lee SH, Yu JK, et al. (2000) Clinical significance of early diastolic notch depth: uterine artery Doppler velocimetry in the third trimester. Am J Obstet Gynecol. 182:1204–9. PMID: 10819859

29. Hernandez-Andrade E, Brodszki J, Lingman G, Gudmundsson S, Molin J (2002) Uterine artery score and perinatal outcome. Ultrasound Obstet Gynecol. 19:438–42. PMID: 11982974

30. Walter SD, Eliasziw M, Donner A (1998) Sample size and optimal designs for reliability studies. Stat Med 17:101–10. PMID: 9463853

31. Altman DG (1993) Construction of age-related reference centiles using absolute residuals. Stat Med. 12: 917–924. PMID: 8337548

32. Cole TJ, Green PJ (1992) Smoothing reference centile curves: the LMS method and penalized likelihood. Stat Med. 11:1305–19. PMID: 1518992

33. Meyer MC, Cummings K, Osol G (1997) Estrogen replacement attenuates resistance artery adrenergic sensitivity via endothelial vasodilators. Am J Physiol. 272:2264–70.

34. Downing SJ, Porter DG, Redstone CD (1981) Myometrial activity in rats during the oestrous cycle and pseudopregnancy: interaction of oestradiol and progesterone. J Physiol. 317: 425–433. PMID: 7198147

35. Vedernikov YP, Hartke JR, De Long MA, Saade GR, Garfield RE (2003) Sex hormone effects in non-pregnant rat and human myometrium. Eur J Obstet Gynecol Reprod Biol. 108:59–66. PMID: 12694972

36. Gordan PL, Jenkins SL, Wentworth RA, Nathanielsz PW (1997) Effect of in vivo estradiol administration to bilaterally ovariectomized rats on in vitro myometrial responsiveness to prostaglandin F2alpha and oxytocin. Biol Reprod. 57:597–601. PMID: 9282996

37. Bossmar T, Akerlund M, Szamatowicz J, Laudanski T, Fantoni G, Maggi M (1995) Receptor-mediated uterine effects of vasopressin and oxytocin in nonpregnant women. Br J Obstet Gynaecol. 102:907–12. PMID: 8534628

38. Liedman R, Hansson SR, Howe D, Igidbashian S, Russell RJ, Akerlund M (2008) Endometrial expression of vasopressin, oxytocin and their receptors in patients with primary dysmenorrhoea and healthy volunteers at ovulation. Eur J Obstet Gynecol Reprod Biol 137:189–92. PMID: 18082926

39. Groutz A, Wolman I, Jaffa AJ, Lessing JB, Yovel I, Amit A (1997) Influence of ovulation induction with human menopausal gonadotropin on uterine blood flow: comparison of unexplained and mechanical infertility. J Ultrasound Med. 16:455–8. PMID: 9315195

40. Serafini P, Batzofin J, Nelson J, Olive D (1994) Sonographic uterine predictors of pregnancy in women undergoing ovulation induction for assisted reproductive treatments. Fertil Steril. 62:815–22. PMID: 7926093

41. Ferreira AM, Pires CR, Moron AF, Araujo Júnior E, Traina E, Mattar R (2007) Doppler assessment of uterine blood flow in recurrent pregnancy loss. Int J Gynaecol Obstet. 98:115–9. PMID: 17588574

42. Dechaud H, Bessueille E, Bousquet PJ, Reyftmann L, Hamamah S, Hedon B (2008) Optimal timing of ultrasonographic and Doppler evaluation of uterine receptivity to implantation. Reprod Biomed Online. 16:368–75. PMID: 18339259

43. Turan OM, De Paco C, Kametas N, Khaw A, Nicolaides KH (2008) Effect of parity on maternal cardiac function during the first trimester of pregnancy. Ultrasound Obstet Gynecol. 32:849–54. doi: 10.1002/uog.5354 PMID: 18536067

44. Suzuki S (2006) Influence of parity on second-trimester uterine artery Doppler waveforms in twin pregnancy. J Matern Fetal Neonatal Med. 19:193–4. PMID: 16690514

45. Hafner E, Schuchter K, Metzenbauer M, Philipp K (2000) Uterine artery Doppler perfusion in the first and second pregnancies. Ultrasound Obstet Gynecol. 16:625–9. PMID: 11169368

46. Prefumo F, Bhide A, Sairam S, Penna L, Hollis B, Thilaganathan B (2004) Effect of parity on second-trimester uterine artery Doppler flow velocity and waveforms. Ultrasound Obstet Gynecol. 23:46–9. PMID: 14970999

47. Brosens JJ, Parker MG, McIndoe A, Pijnenborg R, Brosens IA (2009) A role for menstruation in preconditioning the uterus for successful pregnancy. Am J Obstet Gynecol. 200:615. doi: 10.1016/j.ajog.2008.11.037 PMID: 19136085

48. Khong TY, Adema ED, Erwich JJ (2003) On an anatomical basis for the increase in birth weight in second and subsequent born children. Placenta. 24:348–53. PMID: 12657508

49. Arrowsmith S, Robinson H, Noble K, Wray S (2012) What do we know about what happens to myometrial function as women age? J Muscle Res Cell Motil. 33:209–17. doi: 10.1007/s10974-012-9300-2 PMID: 22644420

50. Pirhonen J, Bergersen TK, Abdlenoor M, Dubiel M, Gudmundsson S (2005) Effect of maternal age on uterine flow impedance. J Clin Ultrasound. 33:14–7. PMID: 15690442

51. Oloyede OA, Iketubosin F (2013) Uterine artery Doppler study in second trimester of pregnancy. Pan Afr Med J. 15:87. doi: 10.11604/pamj.2013.15.87.2321 PMID: 24198883

52. Crawford BS, Davis J, Harrigill K (1997) Uterine artery atherosclerotic disease: histologic features and clinical correlation. Obstet Gynecol. 90:210–5. PMID: 9241295

53. Haavaldsen C, Samuelsen SO, Eskild A (2011) The association of maternal age with placental weight: a population-based study of 536,954 pregnancies. BJOG. 118:1470–6. doi: 10.1111/j.1471-0528.2011.03053.x PMID: 21749632

Article 2

Guedes-Martins L, Saraiva J, Gaio R, Macedo F, Almeida H. Uterine artery impedance at very early clinical pregnancy. *Prenat Diagn.* 2014; 34:719-25.

DOI: 10.1002/pd.4325 PRENATAL **DIAGNOSIS**

ORIGINAL ARTICLE

Uterine artery impedance at very early clinical pregnancy

Luís Guedes-Martins[1,2]*, Joaquim Saraiva[2,3], Rita Gaio[4,5], Filipe Macedo[6,7] and Henrique Almeida[1,8]

[1]Department of Experimental Biology, Faculty of Medicine, University of Porto, 4200-319 Porto, Portugal
[2]Departamento da Mulher e da Medicina Reprodutiva, Centro Hospitalar do Porto EPE, Largo Prof. Abel Salazar, 4099-001 Porto, Portugal
[3]Obstetrics-Gynecology, Private Hospital Trofa, 4785-409 Trofa, Portugal
[4]Department of Mathematics, Faculty of Sciences, University of Porto, 4169-007 Porto, Portugal
[5]CMUP-Centre of Mathematics, University of Porto, 4169-007 Porto, Portugal
[6]Department of Medicine, Faculty of Medicine, University of Porto, 4200-319 Porto, Portugal
[7]Centro Hospitalar S. João, 4200-319 Porto, Portugal
[8]Obstetrics-Gynecology, Hospital-CUF Porto, 4100-180 Porto, Portugal
*Correspondence to: L. Guedes-Martins. E-mail: luis.guedes.martins@gmail.com

ABSTRACT

Objective The aim of the study was to construct gestational age-based reference ranges for the uterine artery (UtA) mean pulsatility (PI) and resistance (RI) indices from 6 to 10 weeks of pregnancy.

Method A prospective, cross-sectional, observational study was carried out in 312 singleton pregnancies with gestational age ranging from 6 to 10 weeks. UtAs were examined transvaginally by color and pulsed Doppler imaging, and the mean of the right and left values of PI and RI, as well as the presence or absence of a bilateral protodiastolic notch, was recorded. UtA-PI and UtA-RI reference percentiles were derived through time-conditional quantile regression.

Results The authors derived the 10th, 50th, and 90th reference percentile curves and correspondent 95% confidence intervals, for the evolution of the UtA mean PI and RI from week 6 to week 10 of gestation. The prevalence of bilateral notching absence was 8.1% (6/74) at 6 weeks and 28.8% (15/52) at 10 weeks.

Conclusion The authors present evidence of progressive reduction of uterine vascular impedance in a very early stage of pregnancy and provide new, averaged UtA-PI and UtA-RI charts between 6 and 10 weeks of gestation. © 2014 John Wiley & Sons, Ltd.

Funding sources: None
Conflicts of interest: None declared

INTRODUCTION

The use of Doppler ultrasound has become a fundamental tool to assess blood circulation. Essentially, along the systolic/diastolic cycle, the arterial blood velocity is estimated, and the collected data are integrated in a quantitative determination of impedance parameters such as the pulsatility (PI) and the resistance (RI) indices; however, emphasis was put on PI because of its ability to better describe the velocity waveform.[1]

In the nonpregnant state, uterine artery (UtA) Doppler waveform exhibits a rapid rise and fall in systolic flow velocity that is followed by a notch in the early diastole.[2] This peculiar feature usually fades along the pregnancy: The prevalence of bilateral notching is 46.3% between 11 and 14 weeks, 16.5% between 15 and 24 weeks, and 5% between 25 and 41 weeks.[1] As consequence of notch disappearance, the mean diastolic velocity rises, which results in PI value reduction.

Because of the value of the UtA impedance assessment employing Doppler ultrasound, reference ranges of its mean PI from 11 to 41 weeks in uneventful pregnancies were established and clearly evidenced a general progressive gestational age-related decrement.[1] This trend has been attributed to major changes in the placental bed that modify the UtA properties from a resistance vessel into a capacitance vessel.

The incidence of elevated UtA impedance just before term was found to be as high as 68% and to mount to 89% when associated to preeclampsia (PE).[3] Other studies also found high incidence of abnormal UtA-PI, although at lower values, probably reflecting different criteria for inclusion.[4,5]

In the second trimester, after analyzing a large number of studies,[6–10] an extensive meta-analysis of UtA Doppler impedance[11] concluded that enhanced PI combined with notch presence was a good predictor of preeclampsia in low and high risk patients and of severe intrauterine growth restriction (IUGR) in low risk patients. The findings supported the recommendation to employ PI and notching assessment in daily clinical practice.[11]

Studies focusing at an earlier gestational age, 11 to 16 weeks, are less frequent. However, higher PIs were found to correlate with pregnancy complications as PE and IUGR[8,12–14] as well as premature delivery.[15] Similar to 20-week to 24-week studies, the inclusion of bilateral notching persistence in the criteria also increased the predictive value,[16] mainly by improving the specificity.[13] Nevertheless, the ability of UtA impedance to identify pregnancy complications as PE and IUGR at this younger gestational age was considered less accurate[11] unless, perhaps, a large set of parameters were employed, in which case the predictability would be comparable.[13] In summary, UtA impedance assessment at early pregnancy ages was considered of limited clinical value in an unselected population, but the possibility of its usefulness in the future when combined with other biochemical and clinical data was recognized.[14]

At more extreme gestational ages, less than 11 weeks, PI studies on the UtA are scarce and addressed a smaller number of cases.[17–21] We thus hypothesized that even at such early gestational ages, UtA-PI would follow regular trends in normal conditions, whose deviation might indicate the appearance of pregnancy disorders. This led us to measure the UtA-PI at 6 to 10 weeks of pregnancy in an unselected population with the purpose to derive normative[22] gestational age-based reference ranges.

METHODS

Subjects

The research protocol was approved by the ethics committee [Ref. 133/10(086-DEFI/126-CES)] of Centro Hospitalar do Porto, Unidade Maternidade Júlio Dinis (CHP-MJD), and all subjects gave their informed consent particularly, upon adequate explanation of the study safety.

From January 2010 to December 2012, a prospective cross-sectional observational study was carried out in 455 singleton pregnancies with gestational age ranging from 6 to 10 completed weeks. In the first appointment, coincident with the first ultrasound evaluation, their history was reviewed by a senior specialist who verified the absence of hypertension, diabetes, and other endocrine disorders, immune diseases, renal and structural heart diseases, hematological conditions, and chronic infections; acceptable medication was folic acid, vitamin, and iron supplements. A transvaginal transducer was employed thereafter to determine the gestational age by crown-rump length measurement[23] and to collect the Doppler flow study data. The surveillance of the pregnant women enrolled in the study was performed in accordance with the hospital protocols.

Along the follow-up made at the same hospital unit, abnormal conditions in the mother and fetus were closely monitored. They included fetal abnormal Doppler ultrasound indices in the umbilical and middle cerebral arteries and fetal growth <10th and >90th percentiles[24,25] in subsequent sonographic observations. Moreover, as all women delivered at CHP-MJD, the healthy condition of the infant was verified by a neonatologist at birth and 1 month later.

In the follow-up, 49 (10.7%) women failed one or more sonograms or delivery at CHP-MJD. In addition, maternal or fetal complications were recorded in 94 (20.7%) pregnancies, including gestational diabetes mellitus/endocrine/immune diseases ($n = 37$), gestational hypertension ($n = 31$), miscarriage ($n = 14$), and fetal/newborn pathology ($n = 12$). Therefore, at the end, 312 women were enrolled in the study.

Doppler flow study

Uterine artery Doppler examinations were performed using a Voluson 730 Pro (GE Healthcare Technologies, USA) ultrasound machine equipped with multifrequency transvaginal and transabdominal transducers. All measurements were performed by a single experienced operator in order to minimize inter-observer variability, and all examinations were carried out employing a transvaginal transducer. Intra-observer reliability was obtained from two consecutive readings, on the first 33 recordings of RI and PI in the UtAs. This concept concerns the degree to which measurements taken by the observer are consistent. In the present context, there was only one observer, and he was totally unaware of any of the results (see Section on Statistical Analysis).

Smokers were required to abstain from smoking for at least 2 h prior to examination. Sagittal section of the uterus was obtained, and the cervical canal and internal cervical ostium were identified. Subsequently, the transducer was gently tilted from side to side, and then color flow mapping was used to identify each UtA along the side of the cervix and uterus at the level of the internal ostium. Pulsed wave Doppler was used with the sampling gate set at 2 mm to cover the whole vessel and ensuring that the angle of insonation was less than 30°. The PI and RI were measured when three similar consecutive waveforms were obtained and then the mean PI and RI of the left and right arteries were calculated (Figure 1). In general, no more than 1 min was necessary to assess both arteries, and the embryo was not directly insonated.

Note was taken of the presence or absence of a bilateral early protodiastolic notch, which was defined as a persistent decrease in blood flow velocity in early diastole, below the diastolic peak velocity.

Statistical analysis

The chi-squared test was used to evaluate adherence to a uniform distribution for categorical variables. PI and RI reference ranges over gestational ages were constructed using quantile regression analysis, a form of nonparametric regression in which a specified conditional quantile of the response variable is expressed as a function of a set of explanatory variables. The model was estimated for the 10th, 50th, and 90th percentiles, independently, and polynomial functions (linear or quadratic) of the gestational age were fitted. Confidence intervals (CIs) for the estimated parameters were obtained by the rank score test inversion method. Quantile regression estimators were preferred over least squares estimators because of the presence of non-normal error terms in the latter process that could not be corrected by numeric transformations, and the existence of different profile curves along gestational time, especially for low quantiles. Comparisons amongst the estimated curves, and in particular of their decreasing rates, were performed using basic methods from differential calculus.

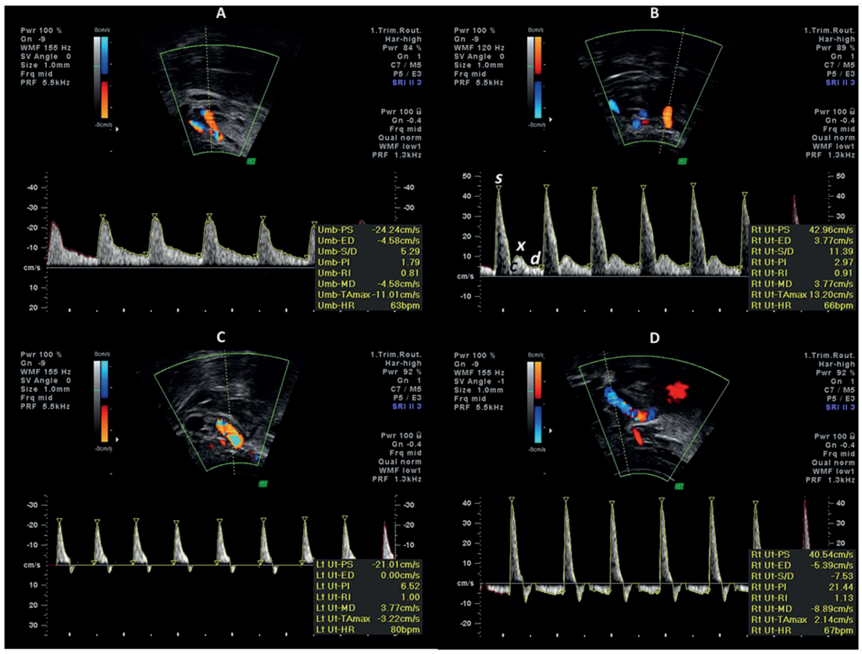

Figure 1 Different types of Doppler shift spectra recorded from the uterine arteries at 6 to 10 weeks of gestation. (A) Waveforms with velocities gradually decreasing from the systolic peak and with continuous forward flow in diastole; (B) waveforms with a notch and with continuous forward flow in diastole; (C) waveforms with absent diastolic flow; and (D) waveforms with reversed diastolic flow. Pulsatility index (PI) is used as a measure of impedance of the flow of blood distal to the sampling point and is automatically calculated according to the formula $PI = \frac{(s-d)}{mean}$ where *s* is the peak, *d* is the minimum, and the average is the *mean* maximum Doppler shift frequency over the cardiac cycle. Resistance index (RI) is automatically calculated using the formula $RI = \frac{(s-d)}{s}$. where *s* is the peak systolic, *d* is the end diastolic, *c* is the early diastolic, and *x* is the maximum diastolic frequency

Intraclass correlation coefficients (ICCs) and 95% CIs were calculated using a two-way mixed-effects model with absolute agreement. We used the ICC to assess repeatability because there is sufficient consensus in the scientific literature to consider that values for ICC > 0.7 reflect very low measurement error.[26,27] The reliability coefficient, which is the difference value that will be exceed by only 5% of pairs of measurements on the same subject, was calculated as 1.96 times the standard deviation of the difference between pairs of repeated measurements.

All statistical analyses were carried out using the R language and software environment for statistical computation, version 2.12.1.[28] For quantile regression analysis, the package *quantreg* contributed by Koenker was used. The significance level was fixed at 0.05.

RESULTS

The main characteristics and pregnancy outcomes of the 312 women are depicted in Table 1.

Gestational age ranged from 6.29 to 10.86 weeks, with an average of 8.27 weeks and a standard deviation of 1.37 weeks. No significant differences were identified regarding the number of pregnant women assessed within each gestational age. This legitimates the inclusion of all collected data, even if having different sample sizes for each gestational week.

The reliability coefficient was 0.127 (resp. 0.024) for the pulsatility (resp. resistance) index. The ICC for the evaluation of intra-observer reliability concerning the PI (resp. RI) measurements was very high, 0.999 (resp. 0.996), with ICC values ranging from 0.998 to 1.000 (resp. from 0.991 to 0.998). The main reason for the high repeatability of the UtA-PI and UtA-RI was the short time between measurements (a few seconds or minutes).

Figure 1 shows different types of Doppler shift spectra that may be obtained from the UtAs at 6 to 10 weeks of gestation. Such types were employed to categorize our findings as follows: Type A showed a gradual diastolic decline following the systolic peak, did not evidence a clear notch, but did show continuous forward flow; type B was similar to type A but exhibited a notch; type C waveform did not evidence a forward flow, and type D waveform showed a reverse diastolic flow.

By analyzing the images, one can see a gradual increase in RI and PI from A to D while the diastolic flow becomes null or reversed. Table 2 confirms that type B was the most frequent

Table 1 **Main characteristics and pregnancy outcomes of the 312 women included in the study**

		n (%)
Gestational age (weeks)	6	74 (24)
	7	69 (24)
	8	64 (20)
	9	53 (17)
	10	52 (17)
Age (intervals in years)	17–24	64 (20)
	25–34	171 (55)
	35–43	77 (25)
Parity	0	134 (43)
	≥1	178 (57)
History of early pregnancy loss (≤12 weeks)	No	275 (88)
	Yes	37 (12)
Body mass index[a] (kg/m^2)	16–24	177 (57)
	25–29	99 (32)
	30–44	36 (11)
Smoking	No	253 (81)
	Yes	59 (19)
Bilateral notching	No	48 (15)
	Yes	264 (85)
Age at menarche (years ± SD)	12.2 (1.6)	—
Age at first sexual intercourse (years ± SD)	18.0 (2.4)	—
GA at delivery (weeks ± SD)	39.3 (1.1)	—
Apgar index 5′	<7	0 (0)
Birth weight at delivery (g ± SD)	3162.5 (377.2)	—
Birth weight at delivery < 10th centile[b]		31(10)

GA, gestational age; SD, standard deviation.
[a]BMI: measurement in the moment of the Doppler flow acquisition.
[b]Birth weight in the sample performed at the tenth percentile was 2690 g.

Doppler shift spectra at any gestational age. Additionally, 9% of the Doppler shift spectra recorded (59/624) were characterized by the presence of null diastolic flow (8%, 51/624) or inverted (1%, 8/624). The majority of these morphological types of waveforms were recognized only at 6 and 7 weeks of pregnancy.

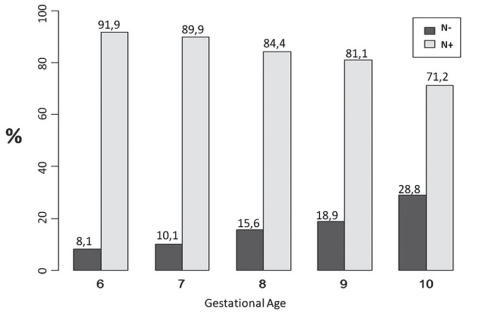

Figure 2 **Sampling relative frequencies (%) of bilateral notching throughout gestation at 6 to 10 weeks of pregnancy. N− is the absence of bilateral notching and N+ is the presence of bilateral notching**

The prevalence of bilateral notching absence was 8.1% (6/74) at 6 weeks, 10.1% (7/69) at 7 weeks, 15.6% (10/64) at 8 weeks, 18.9% (10/53) at 9 weeks, and 28.8% (15/52) at 10 weeks (Figure 2).

Table 3 presents sample percentiles of the PI and RI for the observed gestational weeks.

Quantile regression analysis was applied to UtA-PI and UtA-RI values, independently, in order to express the 10th, 50th, and 90th percentiles of the response as a function of the gestational weeks. Results from the fitting of the models are presented in Table 4.

The median UtA-PI was modeled as a linear function of the gestational age while for the 10th and 90th percentiles of UtA-PI, a quadratic gestational time dependence was estimated. While the 90th and 50th percentile regression models predicted a significant decrease in UtA-PI values throughout the considered gestational age, the tenth percentile model decreased only until 9.6 weeks, starting then a soft but significant increasing tendency (Figure 3). The highest decrease was predicted to happen for the 90th percentile curve until 9.5 weeks of gestation, when the curve slope became smaller than that of the median regression line.

As for UtA-RI values, the median and 90th percentile regression models were linearly dependent on the gestational

Table 2 **Different types of Doppler shift spectra recorded from the right (R) and left (L) uterine arteries at 6 to 10 weeks of gestation**

		Types												
		A			B			C			D			Partial total (t)
		R	L	*n* (%)	R	L	*n* (%)	R	L	*n* (%)	R	L	*n* (%)	
Weeks	6	8	8	16 (11)	48	47	95 (64)	14	17	31 (21)	4	2	6 (4)	148
	7	9	9	18 (13)	50	52	102 (74)	10	7	17 (12)	0	1	1 (1)	138
	8	10	10	20 (16)	52	52	104 (81)	2	1	3 (2)	0	1	1 (1)	128
	9	12	10	22 (21)	41	43	84 (79)	0	0	0 (0)	0	0	0 (0)	106
	10	18	16	34 (33)	34	36	70 (67)	0	0	0 (0)	0	0	0 (0)	104
Total (T) *n* (%)		110 (18)				455 (73)			51 (8)			8 (1)		624 (100)

Table 3 Sample percentiles of the pulsatility and resistance indices at the observed gestational weeks

		PI			RI		
		10th	50th	90th	10th	50th	90th
Gestational age (weeks)	6	1.768	2.933	4.040	0.776	0.915	1.000
	7	1.391	2.660	3.374	0.729	0.890	0.977
	8	1.085	2.167	3.150	0.688	0.832	0.914
	9	1.069	1.945	2.486	0.612	0.810	0.864
	10	1.060	1.770	2.307	0.620	0.700	0.803

PI, pulsatility index; RI, resistance index.

Table 4 Results from the fitting of the models

PI			RI		
Covariates	Coefficient	95% CI	Covariates	Coefficient	95% CI
0.10th quantile					
Intercept	9.281	(6.928, 10.936)	Intercept	2.153	(1.086, 2,624)
GA	−1.729	(−2.115, −1.267)	GA	−0.307	(−0.417, −0.049)
GA^2	0.090	(0.063, 0.114)	GA^2	0.015	(0.001, 0.022)
0.50th quantile					
Intercept	5.083	(4.387, 5.437)	Intercept	1.246	(1.156, 1.313)
GA	−0.330	(−0.376, −0.252)	GA	−0.049	(−0.057, −0.038)
0.90th quantile					
Intercept	13.590	(7.181, 16.016)	Intercept	1.309	(1.280, 1.349)
GA	−2.036	(−2.658, −0.507)	GA	−0.047	(−0.053, −0.042)
GA^2	0.092	(0.003, 0.121)	GA^2[a]		

GA, gestational age; PI, pulsatility index; RI, resistance index; CI, confidence interval.
[a]This variable did not make part of the regression model.

time while the tenth percentile model exhibited a quadratic dependence with time, with positive curvature. For the 90th and 50th percentile regression lines, very similar negative estimates of the slopes were obtained (Figure 3). The highest decrease was estimated to happen on the tenth percentile curve, from week 6 to week 8.7. The monotonicity of this curve changed from 10.3 weeks onwards, although in a nonsignificant way.

DISCUSSION

Adequate UtA blood flow during pregnancy is an essential condition for the healthy development of the fetus. For its assessment, increasing attention has been given to the UtA waveform and its PI measurement.[29,30]

The study by Gómez *et al*,[1] starting at week 11 and continuing until the end of the term, evidenced that UtA-PI declines progressively along the pregnancy. In agreement with previous concepts,[17] it was stated that the trend would result from the characteristic vascular structural changes that take place at the decidua and the myometrium.

This process starts by 8 weeks of gestations with early invasion of extravillous trophoblasts but attains major expression by 14 weeks onwards, when the involvement extends to the myometrium layer.[31–33] The set of events there occurring is designated deep placentation, in contrast with defective deep placentation, the condition of abnormal or absent myometrium spiral artery remodeling.[34]

A most important consequence of deep placentation is the vessel loss of smooth muscle cells, the acquisition of capacitance properties and consequent PI reduction in local vessels and the UtA. However, in the case of defective spiral arteries remodeling, there is increased UtA impedance, findings associated to PE, and other obstetrical disorders.[35–39]

Much of the data on UtA-PI levels so far collected has focused on the early second trimester onwards. In contrast, hemodynamic assessment in the first trimester has received much less attention, although structural changes are already evidenced. In the current investigation, from 6 weeks to the end of the tenth week, we noticed a gestational age-related progressive decrement of UtA-RI and PI. Previous UtA-RI assessment at this early gestational age range[40] produced a trend similar to ours, but our view is that the use of UtA-RI in the study of impedance has important limitations at very early stages of pregnancy. Indeed, RI cannot distinguish levels of high resistance when the flow in diastole is absent or negative.

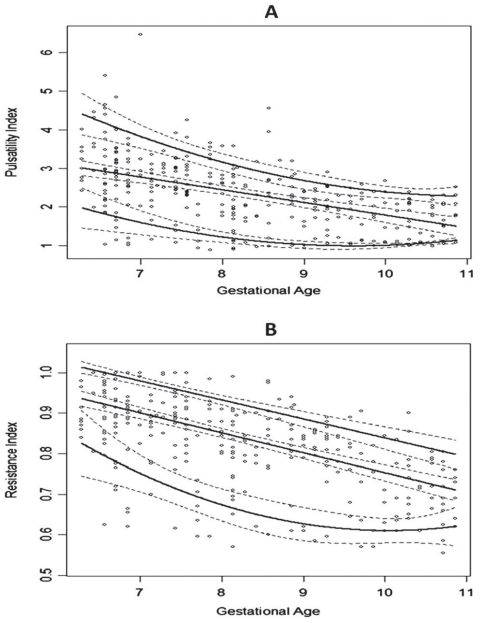

Figure 3 Estimated 10th, 50th, and 90th percentile regression curves of the pulsatility index (A) and of the resistance index (B) with respect to gestational age, and respective 95% confidence bands

In the present study, the flow in the UtA between 6 and 10 weeks was null in 9% of the population, in which cases the RI was invariably equal to 1.

In previous PI studies at the same early age range, although employing a rather limited number of patients, a declining trend was noticed as well.[18,20,21,40] In the current study, involving more than 300 women, median PI exhibited a progressive linear reduction from 2.99 at 6 weeks to 1.77 at 10 weeks, which fits rather well to 1.79 found at 11 weeks[1] and is thus pointing to a continuous PI decrement throughout the entire pregnancy. Moreover, the velocity waveform of the UtA also included a protodiastolic notch in a considerable number of cases; it was present in 91.9% of women at 6 weeks and in 71.2% of them at 10 weeks, a progressive drop that was found to continue from 11 weeks onwards.[1]

Both cross-sectional and longitudinal study designs are suitable for the construction of standard curves.[22] Notwithstanding, a cross-sectional design was used because it is easier to perform and to combine with clinical practice. The study of reliability demonstrated that a Doppler blood flow measurement of the UtA-PI and UtA-RI was found highly repeatable,[26,41] especially when carried out by well-trained operators.[6,20] Additionally, transvaginal assessment offers a number of advantages over the transabdominal route as the vessel is identified more easily,[6] more closely, which favors impedance variability reduction,[6,42] and the insonation angle to the UtA is close to the optimal 0°.[2,6]

The downward trend from 6 to 10 weeks, accompanied by relevant CIs at the 10th, 50th, and 90th percentiles, provides statistically robust data on the UtA reference UtA-PI along a normal course pregnancy. Just as PIs from midtrimester pregnancies appear to yield consistent predictive data regarding near term pregnancy disorders, it is possible that later pregnancy disorders may also be anticipated by the detection of high or abnormal UtA-PI patterns at these early gestational ages. Future studies in this setting will provide answers to this point.

This finding of vascular resistance decrement at such early gestational age indicates that local mechanisms of vascular impedance reduction are in progress well before the deep placentation is established. Previous studies of spiral and radial arteries employing power Doppler transvaginal ultrasound support this view. In fact, a reduction of spiral artery PI from 5 weeks onwards[20,21,43] or radial artery RI from 6 weeks onwards[40] was noticed. The failure to do so and consequent impairment of local vascular relaxation were associated with pregnancy loss.[40]

The question still remains as to what underlies such vascular changes. There is evidence for additional decidual contribution unrelated to endovascular colonization by trophoblasts. Indeed, decidual modifications similar to normal remodeling were reported in the absence of trophoblast invasion[44] and, when interstitial extravillous trophoblasts were present in the vicinity of altered vessels, only rarely they were intimately associated to them[45]; as a matter of fact, when remarkable vascular modifications were taking place in the decidua, the most impressive cellular feature was the large quantities of leukocytes, uterine natural killer cells, and macrophages. These are important producers of vasoactive, extracellular matrix, and angiogenic compounds whose role in the spiral artery remodeling process was amply recognized.[45–47]

We are convinced that the elucidation of the mechanisms of the involvement of such cells, apart from providing new insights on the fascinating implantation process, is likely to provide new molecular diagnostic tools that, combined with impedance assessment at early gestational ages, will improve the ability to predict pregnancy disorders.

CONCLUSIONS

The median, 10th, and 90th percentile regression curves of the PI and RI of the UtA essentially decrease from the sixth to the tenth week of gestation.

WHAT'S ALREADY KNOWN ABOUT THIS TOPIC?

- There is a consistent, progressive reduction on uterine artery impedance along the pregnancy from 11 weeks onwards, with predictive value for preeclampsia in selected groups of patients.

WHAT DOES THIS STUDY ADD?

- The median, 10th, and 90th percentile regression curves of the pulsatility and resistance indices of the uterine artery decrease from the sixth to the tenth week of gestation.

REFERENCES

1. Gómez O, Figueras F, Fernández S, *et al.* Reference ranges for uterine artery mean pulsatility index at 11–41 weeks of gestation. Ultrasound Obstet Gynecol 2008;32:128–32.
2. Steer CV, Williams J, Zaidi J, *et al.* Intra-observer, interobserver, interultrasound transducer and intercycle variation in colour Doppler assessment of uterine artery impedance. Hum Reprod 1995;10:479–81.
3. Frusca T, Soregaroli M, Platto C, *et al.* Uterine artery velocimetry in patients with gestational hypertension. Obstet Gynecol 2003;102:136–40.
4. Li H, Gudnason H, Olofsson P, *et al.* Increased uterine artery vascular impedance is related to adverse outcome of pregnancy but is present in only one-third of late third-trimester pre-eclamptic women. Ultrasound Obstet Gynecol 2005;25:459–63.
5. Meler E, Figueras F, Mula R, *et al.* Prognostic role of uterine artery Doppler in patients with preeclampsia. Fetal Diagn Ther 2010;27:8–13
6. Papageorghiou AT, Yu CK, Bindra R, *et al.* Multicenter screening for pre-eclampsia and fetal growth restriction by transvaginal uterine artery Doppler at 23 weeks of gestation. Ultrasound Obstet Gynecol 2001;18:441–9.
7. Papageorghiou AT, Yu CK, Erasmus IE, *et al.* Assessment of risk for the development of pre-eclampsia by maternal characteristics and uterine artery Doppler. BJOG 2005;112:703–9.
8. van den Elzen HJ, Cohen-Overbeek TE, Grobbee DE, *et al.* Early uterine artery Doppler velocimetry and the outcome of pregnancy in women aged 35 years and older. Ultrasound Obstet Gynecol 1995;5:328–33.
9. Aardema MW, Saro MC, Lander M, *et al.* Second trimester Doppler ultrasound screening of the uterine arteries differentiates between subsequent normal and poor outcomes of hypertensive pregnancy: two different pathophysiological entities? Clin Sci (Lond) 2004;106:377–82.
10. Smith GC, Yu CK, Papageorghiou AT, *et al.* Maternal uterine artery Doppler flow velocimetry and the risk of stillbirth. Obstet Gynecol 2007;109:144–51.
11. Cnossen JS, Morris RK, ter Riet G, *et al.* Use of uterine artery Doppler ultrasonography to predict pre-eclampsia and intrauterine growth restriction: a systematic review and bivariable meta-analysis. CMAJ 2008;178:701–11.
12. Harrington K, Cooper D, Lees C, *et al.* Doppler ultrasound of the uterine arteries: the importance of bilateral notching in the prediction of pre-eclampsia, placental abruption or delivery of a small-for-gestational-age baby. Ultrasound Obstet Gynecol 1996;7:182–8.
13. Harrington K, Carpenter RG, Goldfrad C, Campbell S. Transvaginal Doppler ultrasound of the uteroplacental circulation in the early prediction of pre-eclampsia and intrauterine growth retardation. Br J Obstet Gynaecol 1997;104:674–81.
14. Gómez O, Martínez JM, Figueras F, *et al.* Uterine artery Doppler at 11–14 weeks of gestation to screen for hypertensive disorders and associated complications in an unselected population. Ultrasound Obstet Gynecol 2005;26:490–4.
15. Harrington K, Goldfrad C, Carpenter RG, Campbell S. Transvaginal uterine and umbilical artery Doppler examination of 12–16 weeks and the subsequent development of pre-eclampsia and intrauterine growth retardation. Ultrasound Obstet Gynecol 1997;9:94–100.
16. Bower S, Bewley S, Campbell S. Improved prediction of preeclampsia by two stage screening of uterine arteries using the early diastolic notch and color Doppler imaging. Obstet Gynecol 1993;82:78–83.
17. Jauniaux E, Jurkovic D, Campbell S. *In vivo* investigations of the anatomy and the physiology of early human placental circulations. Ultrasound Obstet Gynecol 1991;1:435–45.
18. Jurkovic D, Jauniaux E, Kurjak A, *et al.* Transvaginal color Doppler assessment of the uteroplacental circulation in early pregnancy. Obstet Gynecol 1991;77:365–9.
19. Arduini D, Rizzo G, Romanini C. Doppler ultrasonography in early pregnancy does not predict adverse pregnancy outcome. Ultrasound Obstet Gynecol 1991;1:180–5.
20. Valentin L, Sladkevicius P, Laurini R, *et al.* Uteroplacental and luteal circulation in normal first-trimester pregnancies: Doppler ultrasonographic and morphologic study. Am J Obstet Gynecol 1996;174:768–75.
21. Mäkikallio K, Jouppila P, Tekay A. First trimester uterine, placental and yolk sac haemodynamics in pre-eclampsia and preterm labour. Hum Reprod 2004;19:729–33.
22. Royston P, Wright EM. How to construct 'normal ranges' for fetal variables. Ultrasound Obstet Gynecol 1998;11:30–8.
23. Robinson HP. Sonar measurement of fetal crown-rump length as means of assessing maturity in first trimester of pregnancy. Br Med J 1973;4:28–31.
24. Snijders RJ, Nicolaides KH. Fetal biometry at 14–40 weeks' gestation. Ultrasound Obstet Gynecol 1994;4:34–48.
25. Yudkin PL, Aboualfa M, Eyre JA, *et al.* New birthweight and head circumference centiles for gestational ages 24 to 42 weeks. Early Hum Dev 1987;15:45–52.
26. Bland JM, Altman DG. Applying the right statistics: analyses of measurement studies. Ultrasound Obstet Gynecol 2003;22:85–93.
27. Walter SD, Eliasziw M, Donner A. Sample size and optimal designs for reliability studies. Stat Med 1998;17:101–10.
28. R Development Core Team. R: A Language and Environment for Statistical Computing. R Foundation for Statistical Computing, Vienna, Austria, 2008. Available at http://www.R-project.org. Accessed October 30, 2012.
29. Everett TR, Lees CC. Beyond the placental bed: placental and systemic determinants of the uterine artery Doppler waveform. Placenta 2012;33:893–901.
30. McLeod L. How useful is uterine artery Doppler ultrasonography in predicting pre-eclampsia and intrauterine growth restriction? CMAJ 2008;178:727–9.
31. Pijnenborg R, Vercruysse L, Hanssens M. The uterine spiral arteries in human pregnancy: facts and controversies. Placenta 2006;27:939–58.
32. Pijnenborg R, Vercruysse L, Brosens I. Deep placentation. Best Pract Res Clin Obstet Gynaecol 2011;25:273–85.
33. Lyall F. The human placental bed revisited. Placenta 2002;23:555–62.
34. Brosens I, Pijnenborg R, Vercruysse L, Romero R. The 'Great Obstetrical Syndromes' are associated with disorders of deep placentation. Am J Obstet Gynecol 2011;204:193–201.
35. Olofsson P, Laurini RN, Marsál K. A high uterine artery pulsatility índex reflects a defective development of placental bed spiral arteries in pregnancies complicated by hypertension and fetal growth retardation. Eur J Obstet Gynecol Reprod Biol 1993;49:161–8.
36. Sağol S, Ozkinay E, Oztekin K, Ozdemir N. The comparison of uterine artery Doppler velocimetry with the histopathology of the placental bed. Aust N Z J Obstet Gynaecol 1999;39:324–9.
37. Hafner E, Metzenbauer M, Höfinger D, *et al.* Comparison between three-dimensional placental volume at 12 weeks and uterine artery impedance/notching at 22 weeks in screening for pregnancy-induced hypertension, pre-eclampsia and fetal growth restriction in a low-risk population. Ultrasound Obstet Gynecol 2006;27:652–7.
38. Madazli R, Somunkiran A, Calay Z, *et al.* Histomorphology of the placenta and the placental bed of growth restricted foetuses and correlation with the Doppler velocimetries of the uterine and umbilical arteries. Placenta 2003;24:510–6.
39. Naicker T, Khedun SM, Moodley J, Pijnenborg R. Quantitative analysis of trophoblast invasion in preeclampsia. Acta Obstet Gynecol Scand 2003;82:722–9.
40. Tamura H, Miwa I, Taniguchi K, *et al.* Different changes in resistance index between uterine artery and uterine radial artery during early pregnancy. Hum Reprod 2008;23:285–9.
41. Tekay A, Jouppila P. Intraobserver reproducibility of transvaginal Doppler measurements in uterine and intraovarian arteries in regularly menstruating women. Ultrasound Obstet Gynecol 1996;7:129–34.
42. Weissman A, Jaffa AJ, Lurie S, *et al.* Continuous wave Doppler velocimetry of the main-stem uterine arteries: the transvaginal approach. Ultrasound Obstet Gynecol 1995;5:38–43.
43. Mercé LT, Barco MJ, Bau S. Color Doppler sonographic assessment of placental circulation in the first trimester of normal pregnancy. J Ultrasound Med 1996;15:135–42.
44. Craven CM, Morgan T, Ward K. Decidual spiral artery remodelling begins before cellular interaction with cytotrophoblasts. Placenta 1998;19:241–52.
45. Smith SD, Dunk CE, Aplin JD, *et al.* Evidence for immune cell involvement in decidual spiral arteriole remodeling in early human pregnancy. Am J Pathol 2009;174:1959–71.
46. Lash GE, Otun HA, Innes BA, *et al.* Low oxygen concentrations inhibit trophoblast cell invasion from early gestation placental explants via alterations in levels of the urokinase plasminogen activator system. Biol Reprod 2006;74:403–9.
47. Hazan AD, Smith SD, Jones RL, *et al.* Vascular-leukocyte interactions: mechanisms of human decidual spiral artery remodeling *in vitro*. Am J Pathol 2010;177:1017–30.

Article 3

Guedes-Martins L, Saraiva JP, Gaio AR, Reynolds A, Macedo F, Almeida H. Uterine artery Doppler in the management of early pregnancy loss: a prospective, longitudinal study. *BMC Pregnancy Childbirth.* 2015; 15:28.

Guedes-Martins et al. BMC Pregnancy and Childbirth (2015) 15:28
DOI 10.1186/s12884-015-0464-9

BMC Pregnancy & Childbirth

RESEARCH ARTICLE Open Access

Uterine artery Doppler in the management of early pregnancy loss: a prospective, longitudinal study

Luís Guedes-Martins[1,2*], Joaquim P Saraiva[2,3], Ana R Gaio[4,5], Ana Reynolds[6], Filipe Macedo[7,8] and Henrique Almeida[1,9]

Abstract

Background: The pharmacological management of early pregnancy loss reduced substantially the need for dilation and curettage. However, prognostic markers of successful outcome were not established. Thus the major purpose of this study was to determine the sensitivity and specificity of the uterine artery pulsatility (PI) and resistance (RI) indices to detect early pregnancy loss patients requiring dilation and curettage after unsuccessful management.

Methods: A cohort prospective observational study was undertaken to include women with early pregnancy loss, ≤ 12 weeks of gestation, managed with mifepristone (200 mg) and misoprostol (1600 μg) followed by PI and RI evaluation of both uterine arteries 2 weeks after. At this time, in 173/315 patients, incomplete miscarriage was diagnosed. Among them, 32 underwent uterine dilatation and curettage at 8 weeks of follow-up.

Results: The cut-off points for the uterine artery PI and RI, leading to the maximum values of sensitivity (69.5%, $CI_{95\%}$: 61.5%-76.5% and 75.0%, $CI_{95\%}$: 57.9%-86.8%, respectively) and specificity (75.0%, $CI_{95\%}$: 57.9%-86.8% and 65.6%, $CI_{95\%}$: 48.3%-79.6%, respectively), for the discrimination between the women who needed curettage from those who resolved spontaneously were 2.8 and 1, respectively.

Conclusions: The potential usefulness of uterine artery Doppler evaluation to predict the need for uterine curettage in patients submitted to medical treatment for early pregnancy loss was demonstrated.

Keywords: Early pregnancy loss, Incomplete miscarriage, Uterine artery Doppler

Background

Spontaneous abortion, or miscarriage, has been defined as clinically recognized pregnancy loss before the 20th week of gestation [1], and 80% of these events occur in the first 12 weeks [2].

Although medical management with misoprostol, as an alternative to uterine dilation and curettage (D&C), has been associated with very high success rates of up to 99% in cases of early pregnancy loss [3-6], expectant management has also been indicated as a safe option for women with a first-trimester miscarriage [7-9]. The clear benefits of each of these approaches compared to the others have not been demonstrated [4,8], and management decisions have been adapted to the local circumstances and characteristics of patients.

The lack of consensus on the criteria for the success or failure of medical management in early miscarriage [4,7-10] precludes comprehensive conclusions regarding the obtained results. In the clinical setting, this lack of comparative data hinders a timely decision regarding whether to proceed with a uterine D&C, which, although it is a simple procedure, could result in serious complications. Clinical markers are thus needed to reliably support conservative management of early pregnancy loss [8,9,11].

Although uterine sonographic assessment in incomplete miscarriages might estimate the amount of ovular tissue remaining in the uterine cavity and the decidua thickness, the data fail to accurately predict the outcome when conservative management is an option [7]. More

* Correspondence: luis.guedes.martins@gmail.com
[1]Department of Experimental Biology, Faculty of Medicine, University of Porto, 4200-319 Porto, Portugal
[2]Hospital Centre of Porto EPE, Department of Women and Reproductive Medicine, Largo Prof. Abel Salazar, 4099-001 Porto, Portugal
Full list of author information is available at the end of the article

recently, a color Doppler evaluation of the uterine cavity contents was proposed to explore persistent communication between the residual trophoblasts and maternal circulation [11]; in contrast to the simple assessment of retained material volume, the presence or absence of flow were able to provide a quantitative estimate of the success of conservative management. Based on these findings, we reasoned that the extension of communication to the uterine artery would produce additional measurable Doppler changes in its impedance. In this case, the changes would enhance the predictability of successful conservative management and decrease the need for D&C.

The main purpose of this study was to determine the sensitivity and specificity of the uterine artery pulsatility (PI) and resistance (RI) indices, aiming to detect the patients with early pregnancy loss requiring D&C after unsuccessful conservative management using mifepristone *plus* misoprostol.

Methods

Study population and design

The research protocol was approved by the local ethics committee [IRB protocol number: 150/13(096-DEFI/122-CES)] of Hospital Center of Porto (CHP). All of the subjects gave their informed consent.

This is a cohort prospective observational study including women with early pregnancy loss (≤12 weeks gestation), as determined by the last menstrual period, attended at the emergency department of a tertiary university hospital center (CHP), from January 2011 to March 2013.

The diagnosis of early pregnancy loss was confirmed by vaginal ultrasound based on the guidelines of the Royal College of Obstetricians and Gynaecologists in the UK.[12] The vaginal ultrasound criteria for early miscarriage-empty sac are an intra-uterine image consistent with a gestational sac with a mean diameter > 20 mm with no detectable embryonic pole or if the diameter is ≤ 20 mm with no change on rescan at 7 days. The criteria for early miscarriage-missed miscarriage are the visualization of a gestational sac with an embryo/fetus with a crown-rump length (CRL) > 6 mm with no heart activity or ≤ 6 mm with no change on rescan 7 days later [12]. Criteria for complete miscarriage included no evidence of retained products of conception in the uterine cavity and endometrial thickness (ET) < 12 mm (previous work [7] used ET < 15 mm). The sonographic criteria for incomplete miscarriage were: presence of heterogeneous features in the uterine cavity (without gestational sac) and endometrial midline echo distortion (at any endometrial thickness).

The inclusion criteria were cases of early pregnancy loss, defined as intrauterine pregnancy with reproducible evidence of lost fetal heart activity and/or the lack of increased crown–rump length over one week or the persisting presence of an empty sac at less than 12 weeks of gestation [10] (empty sac or missed miscarriage) in

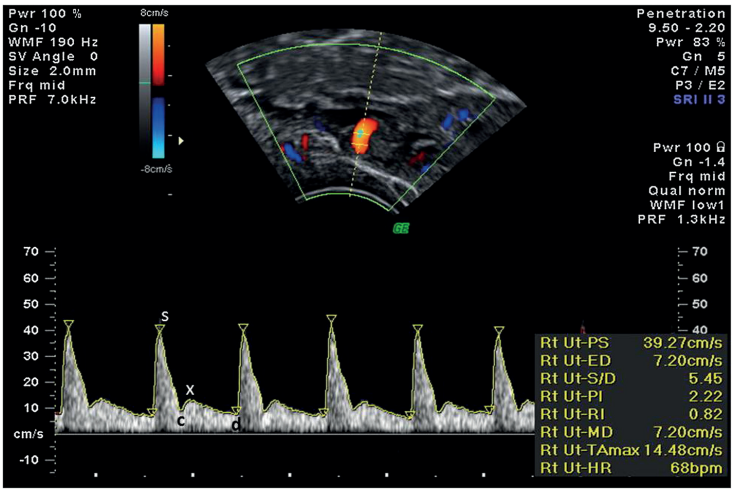

Figure 1 Doppler spectra of uterine artery flow. Pulsatility index (PI) is used as a measure of impedance of the flow of blood distal to the sampling point and is automatically calculated according to the formula $PI = \frac{(s-d)}{mean}$ where *s* is the peak *d* is the minimum and the average is the *mean* maximum Doppler shift frequency over the cardiac cycle. Resistance index (RI) is automatically calculated using the formula $RI = \frac{(s-d)}{s}$ *s*, peak systolic; *d*, end-diastolic; *c*, early diastolic; *x*, maximum diastolic frequency.

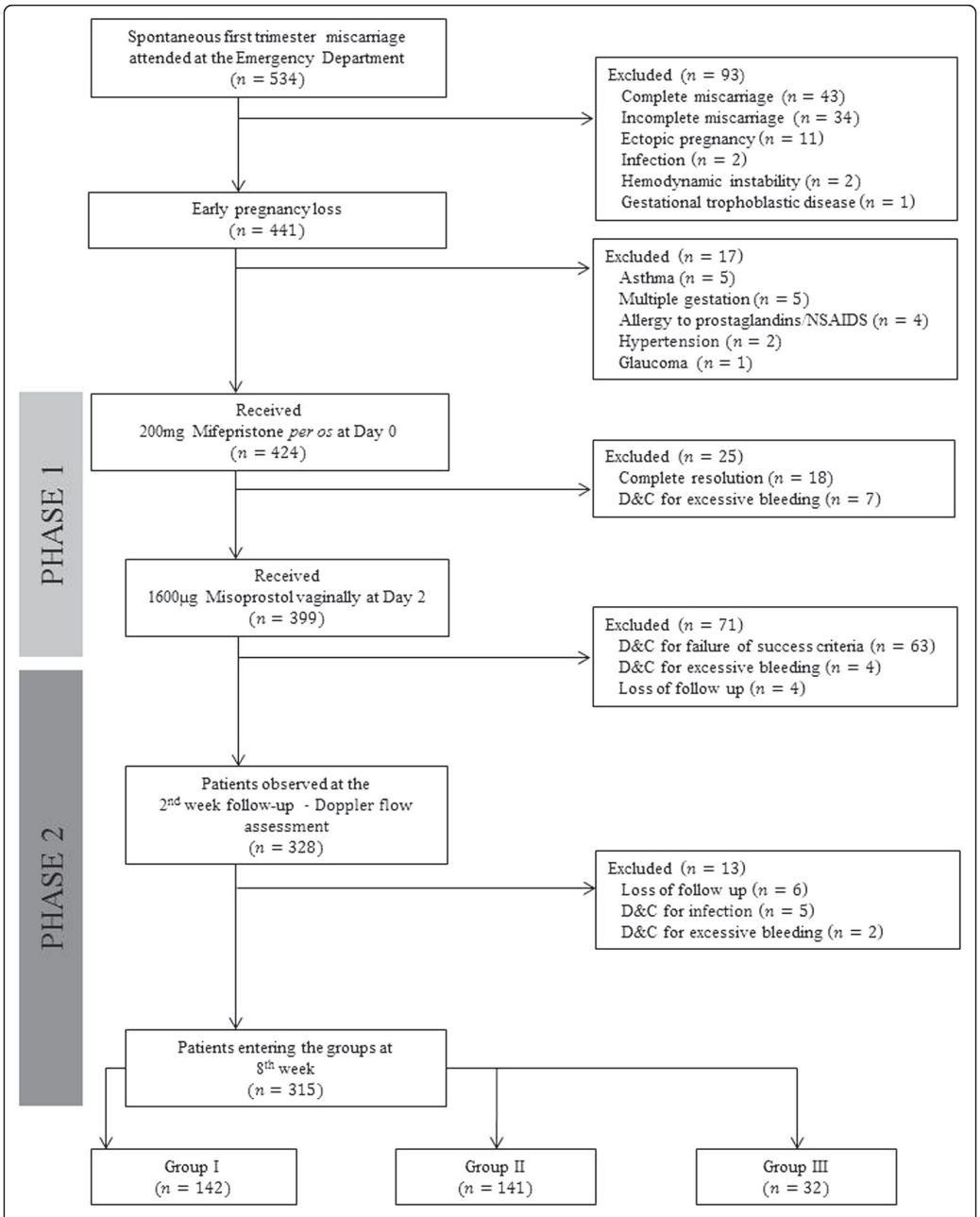

Figure 2 Study flowchart: number of patients (n), follow-up, Doppler assessment and grouping. Group I – complete miscarriage at the 2nd week. Group II – incomplete miscarriage at the 2nd week and complete miscarriage at the 8th week. Group III – incomplete miscarriage at 2nd and 8th week of follow-up, submitted to D&C. D&C, dilation and curettage.

Table 1 The demographic data, uterine content thickness and Doppler assessment in all groups and in each group (I, II and III) of the included patients

		All n(%) 315(100)	p-value[1]	Group I n(%) 142(45)	p-value[1]	Group II n(%) 141(45)	p-value[1]	Group III n(%) 32(10)	p-value[1]
Age (in years)	20-24	36(12)	**<0.001**	18(13)	**<0.001**	14(10)	**<0.001**	4(12)	0.030
	25-34	159(50)		67(47)		76(54)		16(50)	
	35-46	120(38)		57(40)		51(36)		12(38)	
Education level (in years)	≤9	115(37)	**<0.001**	55(39)	**<0.001**	48(34)	**<0.001**	12(38)	0.197
	10-12	146(46)		60(42)		72(51)		14(44)	
	>12	54(17)		27(19)		21(15)		6(19)	
Parity	0	171(54)	0.128	64(45)	0.240	49(49)	0.842	25(78)	**0.001**
	≥1	144(46)		78(55)		51(51)		7(22)	
Previous spontaneous first trimester miscarriage (≤12 weeks)	1	277(88)	**<0.001**	125(88)	**<0.001**	124(88)	**<0.001**	28(88)	**<0.001**
	>1	38(12)		17(12)		17(12)		4(12)	
Body Mass Index (Kg/m^2)	16-24	142(45)	**<0.001**	72(51)	**<0.001**	53(38)	**0.001**	17(53)	**0.001**
	25-29	134(43)		58(41)		62(44)		14(44)	
	30-44	39(12)		12(8)		26(18)		1(3)	
Smoking	No	243(77)	**<0.001**	103(39)	**<0.001**	115(82)	**<0.001**	25(78)	**0.001**
	Yes	72(23)		73(27)		26(18)		7(22)	
GA at early pregnancy loss diagnosis [weeks (SD)]		8.0(1.3)		7.6(1.0)		8.2(1.3)		9.1(1.3)	
Uterine arteries Doppler assessment [days (SD)]		18.2(2.8)		18.0(2.4)		18.3(3.2)		18.9(2.6)	
Intra-uterine content thickness [mm (SD)]		11.8(5.8)		6.1(2.5)		15.8(2.3)		19.6(2.3)	
Uterine content thickness at 2nd week follow-up visit	<12 mm	148(0.53)	0.328	142(100)	0	7(5)	0	0	0
	≥12 mm	167(0.47)		0		141(100)		32(100)	
Uterine artery Doppler - Bilateral notching	No	3(1)	**<0.001**	0	**<0.001**	1(1)	**<0.001**	2(6)	**<0.001**
	Yes	312(99)		142(100)		140(99)		30(94)	
Decision for D&C at 8th week follow-up visit	No	283(90)	**<0.001**	142(100)	0	141(100)	0	0	0
	Yes	32(10)		0		0		32(100)	

Legend: GA-gestational age; D&C - Dilation and Curettage; [1]Chi-square test or Fisher's test, as adequate; Statistical analysis (p) was obtained to evaluate the differences within each demographic and clinical characteristics.

Table 2 Comparison of the average (min-max) pulsatility (PI) and resistance (RI) indices in the uterine arteries between groups (I + II) and III

	Group I + II (*n = 283*)	Group III (*n = 32*)	p-value[1]
PI	3.55(1.17-8.01)	2.57(1.16-3.97)	<0.001
RI	1.00(0.66-1.00)	0.90(0.75-1.00)	<0.001

[1]Wilcoxon rank sum test with corrections for multiple testing following the Holm's method.

clinically stable women. The exclusion criteria included ectopic pregnancy, complete or incomplete miscarriage, known allergy to prostaglandins or NSAIDS, multiple gestation, heavy vaginal bleeding or hemodynamic instability, blood clotting problems or current treatment with anticoagulants, hemoglobin < 10 g/dL, body temperature > 38°C, CRL larger than 12 weeks of gestation and prostaglandin contraindications, including uncontrolled blood pressure, mitral stenosis, severe asthma or glaucoma.

Management protocol, data collection and follow-up

Phase 1 Management

For each patient, the last menstrual period, age, parity, educational level, previous history of spontaneous first trimester miscarriage, body mass index, history of smoking, and previous uterine curettage were recorded.

Upon diagnosis of early pregnancy loss, confirmed by an experienced sonographer, a management protocol adopted in the department was employed. Patients with no or light vaginal bleeding were medicated with 200 mg of mifepristone [13] orally and followed-up as outpatients. They were instructed to make an additional appointment 48 h later or earlier in case of severe pain, bleeding or fever. At this time, unless the uterus was empty, the patients were admitted to the hospital and treated with 1600 μg of vaginal misoprostol divided into two doses, administered 4 hours apart. Eight hours after starting the procedure, a uterine ultrasound exam was performed followed by D&C in the cases in which the gestational sac was evident. The stable patients without evidence of a gestational sac were discharged and enrolled in Phase 2.

Phase 2 Management

At the end of the second week following the completed diagnosis, the patients visited the hospital for a review of the symptoms and a pelvic sonogram, including a uterine artery Doppler study. The patients were divided into three groups (I, II and III). When the condition was considered resolved (complete miscarriage), the patients were assigned to group I. In the cases of incomplete miscarriage, the patients were required to revisit the hospital 6 weeks later (8 weeks after the initial diagnosis). At this time, if resolution had been achieved (complete miscarriage), the patients were assigned to group II, whereas patients with a persistence of an incomplete miscarriage, were assigned to group III and submitted to D&C.

Table 3 The average (min-max) pulsatility (PI) and resistance (RI) indices of the uterine arteries in groups I, II and III

	Group I (*n = 142*)	Group II (*n = 141*)	Group III (*n = 32*)
PI	3.84 (1.17-8.01)	3.35 (1.43-7.70)	2.57 (1.16-3.97)
RI	1.00 (0.66-1.00)	1.00 (0.74-1.00)	0.90 (0.75-1.00)

Doppler flow assessment

At the 2nd week of follow-up uterine artery (UtA) Doppler assessment was performed by a single, experienced operator (L.G-M, 6 years of experience in obstetric and gynaecologic ultrasound) to avoid inter-observer variability. A Voluson 730 Pro (GE Healthcare Technologies, Milwaukee, WI, USA) multifrequency transvaginal and transabdominal ultrasound device equipped with a 5 MHz transvaginal transducer was employed. A sagittal plane of the uterus including the viewing of the cervical canal and internal cervical os was obtained. Subsequently, the transducer was gently tilted from side to side and each uterine artery was identified at the level of the internal os with the aid of a color flow mapping. Pulsed wave Doppler was used with a sampling gate set at 2 mm to cover the entire vessel, ensuring that the angle of insonation was less than 30°. When three similar consecutive waveforms were obtained - Figure 1 - mean PI and RI of the left and right arteries were calculated. The presence or absence of a bilateral early protodiastolic notch in the UtA was noticed. A positive notch was defined as a persistent decrease in the blood flow velocity in the early diastole, below the diastolic peak velocity in at least one UtA Doppler ultrasound spectrum. Notch absence was defined by its bilateral absence.

The intra-observer reliability was obtained from two readings, at the beginning and the end of the scan, on the first 33 recordings of the resistance and pulsatility indices in the uterine arteries. The intraclass correlation coefficients (ICC) and 95% confidence intervals were calculated using a two-way mixed-effects model with absolute agreement. The reliability coefficient, which is the difference value that will be exceed by only 5% of the pairs of measurements in the identical subject, was calculated as 1.96 times the standard deviation of the difference between the pairs of repeated measurements.

Statistical analysis

The statistical inference from the descriptive measures comprised the chi-squared test or Fisher's test (as adequate) to evaluate the fitting of a categorical variable distribution to the uniform distribution, and the

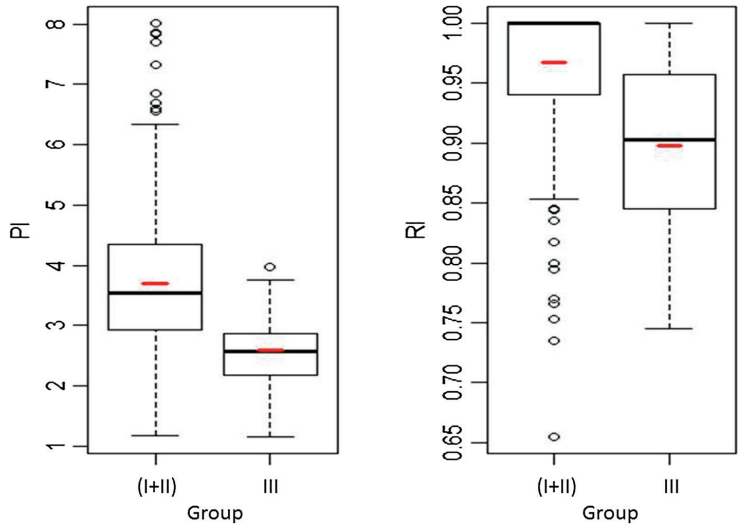

Figure 3 The boxplot of the pulsatility (PI) and resistance (RI) indices for the patients in groups I + II (n = 283) and III (n = 32). The mean of each boxplot is marked with a small horizontal line.

Wilcoxon rank sum test to compare the medians from two independent populations. The Kruskal-Wallis test (or ANOVA on ranks) was used to assess whether samples from different groups originate from the same population. The pairwise comparisons between the group levels used the Wilcoxon rank sum test with corrections for multiple testing following Holm's method [14]. Non-parametric techniques were applied once the normality and homoscedasticity of the residuals from parametric models were not satisfied.

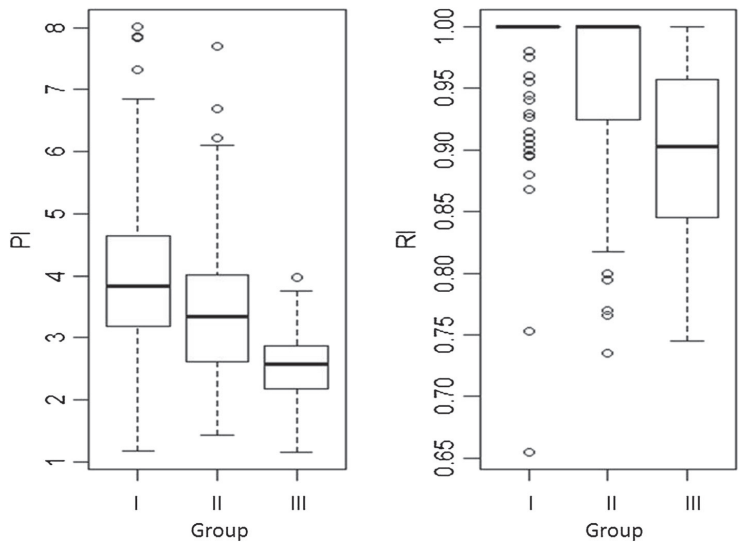

Figure 4 The boxplot for pulsatility (PI) and resistance (RI) indices according to each studied group.

Receiver-operating characteristic (ROC) curves evaluated the discrimination ability of the RI and PI, independently and between the women who underwent curettage and those who had a spontaneous resolution of the clinical condition. These curves plot the true positive rate (Sensitivity) against the false positive rate (1-Specificity) at various discrimination threshold settings. The closer the ROC curve is to the upper left corner, the higher the overall accuracy of the test, and this criterion was used to identify the optimal thresholds [15]. At these cut-off points, the likelihood ratios (LRs) for the positive and negative tests (the LR (+ve test) and the LR (–ve test), respectively) and the positive and negative predicted values were computed. In particular, the pretest odds for D&C multiplied by the LR (+ve test) or the LR (–ve test) determines the post- (+ve test) or post- (–ve test) odds, respectively. The positive tests are associated with D&C if the LR (+ve test) is greater than 1, and the negative tests are associated with no D&C if the LR (–ve test) is smaller than 1. The further away the values are from 1, the stronger the evidence [16].

All of the statistical analyses were carried out using the R language and software environment for statistical computation, version 2.12.1. The significance level was fixed at 0.05.

Results

Of the 534 consecutive cases with spontaneous first trimester miscarriages who were attended at the emergency department during the study period, 315 (59%) patients entered the final groups, as shown in the flowchart in Figure 2.

Table 1 describes the patient demographic data and variables considered in the study, with the statistical analysis. As previously defined, groups I, II and III included 142

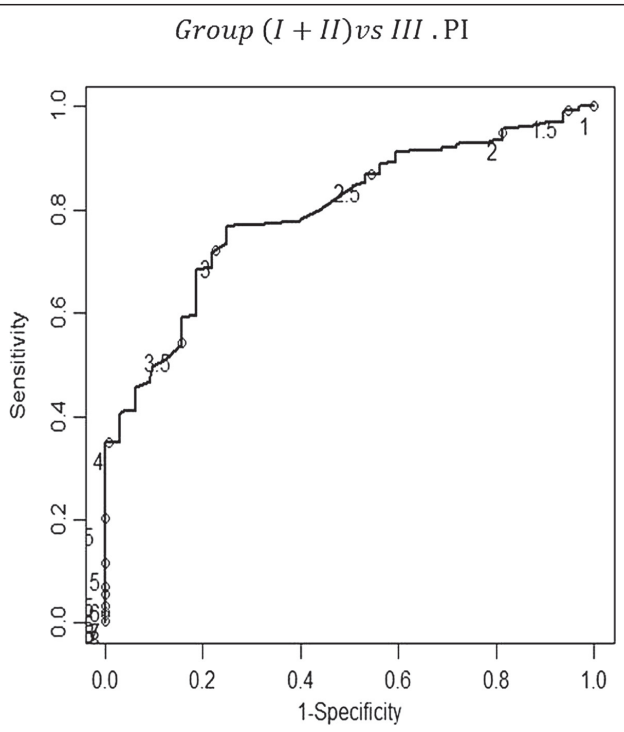

Figure 5 Receiver-operator characteristic (ROC) curve for the different values of the pulsatility index concerning the discrimination between groups (I + II) and III. The curve describes the association between sensitivity and specificity at different cut-offs of the pulsatility index. Values from 1 to 8 in intervals of 0.5 are identified with a circle. The point in the curve that is closer to the upper-left corner of the plot corresponds to the value 2.78 of the pulsatility index. At that cut-off point, the sensitivity and specificity values of the pulsatility index in the uterine artery were 77.0% (CI $_{95\%}$: 71.8%-81.6%) and 75.0% (CI $_{95\%}$: 57.9%-86.8%), respectively; the area under the curve (AUC) was 0.796 (0.727-0.865). The correspondent positive and negative predictive values were 96.5% and 27.0%, respectively. The likelihood ratio (LR) for a positive or negative test was 3.08 (CI $_{95\%}$: 1.68%-5.63%) or 0.31 (CI $_{95\%}$: 0.23%-0.41%), respectively.

(45%), 141 (45%) and 32 (10%) patients, respectively. The histological examination of the intra-uterine contents after D&C in the group III patients (n = 32) revealed conception debris/ovular tissue in all cases. Only 1% of all the included cases showed an absence of bilateral notching on the Doppler evaluation of the uterine artery blood flow.

For the Doppler indices (PI and RI), the null hypothesis that samples from each group of patients (I, II and III) originate from an identical population could be rejected (Table 2).

The reliability coefficients were 0.127 and 0.024 for the PI and RI, respectively. The ICC values for the evaluation of the intraobserver reliability concerning the PI and RI measurements were very high, at 0.999 (range: 0.998 to 1.000) and 0.996 (range: 0.991 to 0.998), respectively.

Table 3 presents the average and the variation (minimum – maximum) of the Doppler indices obtained in each studied group. The non-parametric Kruskal-Wallis test (ANOVA on ranks; IR: chi-squared = 60.331, df = 2, p-value < 0.001; IP: chi-squared = 50.610, df = 2, p-value < 0.001) was used, followed by Holm's method for multiple comparisons. Within each index, all three pairwise comparisons were statistically significant ($p < 0.001$) – Figures 3 and 4.

The Doppler of the uterine arteries was first used to discriminate the women in group III from those in groups I + II. The cut-off points for the uterine artery pulsatility (PI) and resistance (RI) indices, providing the maximum values of sensitivity (77.0%, $CI_{95\%}$: 71.8%-81.6% and 65.0%, $CI_{95\%}$: 59.3%-70.3%, respectively) and specificity (75.0%, $CI_{95\%}$:57.9%-86.8% and 87.5%, $CI_{95\%}$: 71.9%-95.0%, respectively) were 2.78 and 1, respectively, for distinguishing the women in group III from those in groups I + II. A test was considered positive if the PI or RI was less than 2.78 or 1, respectively. The positive predictive values were 96.5% and 97.9% for the PI and RI, respectively. The negative predictive values were 27.0% and 22.0% for the PI and the RI, respectively. The LR for a positive or negative test was 3.08 (CI $_{95\%}$: 1.68%-5.63%) or 0.31 (CI $_{95\%}$: 0.23%-0.41%), respectively, for the PI. Similarly, the LR for a positive or negative test was 5.20 (CI $_{95\%}$: 2.07%-13.06%) or 0.40 (CI $_{95\%}$: 0.33%-0.49%), respectively, for the RI – Figures 5 and 6.

Additionally, uterine artery Doppler was used to discriminate between the women in group III and those in

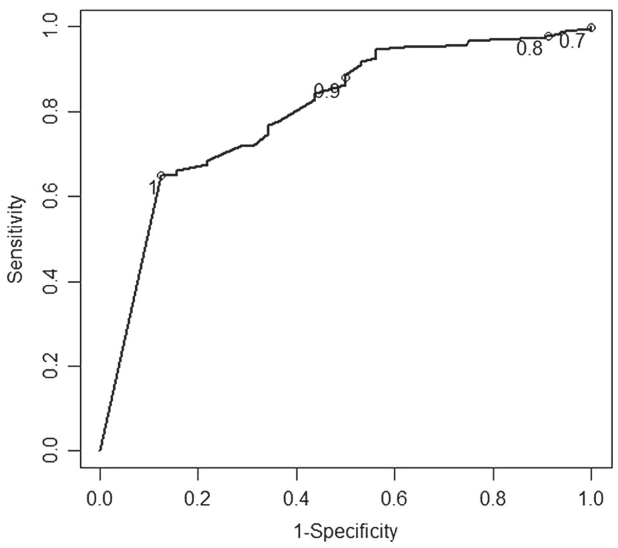

Figure 6 The receiver-operator characteristic (ROC) curve for the different values of the resistance index concerning the discrimination between groups (I + II) and III. The values 0.7, 0.8, 0.9 and 1.0 are identified in the curve with a circle. The point in the curve that is closer to the upper-left corner of the plot corresponds to value 1 for the resistance index. At that cut-off point, the sensitivity and specificity values of the resistance index in the uterine artery were of 65.0% (CI $_{95\%}$: 59.3%-70.3%) and 87.5% (CI $_{95\%}$: 71.9%-95.0%), respectively; the area under the curve (AUC) was 0.798 (0.754-0.843). The correspondent positive and negative predictive values were 97.9% and 22.0%, respectively. The likelihood ratio (LR) for a positive or negative test was 5.20 (CI $_{95\%}$: 2.07%-13.06%) or 0.40 (CI $_{95\%}$: 0.33%-0.49%), respectively.

group II. This discrimination was the main goal of the study. The cut-off points for the uterine artery pulsatility (PI) and resistance (RI) indices, with maximum values of sensitivity (69.5%, $CI_{95\%}$: 61.5%-76.5% and 75.0%, $CI_{95\%}$: 57.9%-86.8%, respectively) and specificity (75.0%, $CI_{95\%}$: 57.9%-86.8% and 65.6%, $CI_{95\%}$: 48.3%-79.6%, respectively) were 2.80 and 1, respectively, for distinguishing the women in group III from those in group II. A test was considered positive if the PI or RI was less than 2.8 or 1, respectively, and negative otherwise. The positive predictive values were 92.5% and 89.9% for the PI and the RI, respectively. The negative predictive values were 35.8 and 32.8% for the PI and the RI, respectively. The LR for a positive or negative test was 2.78 (CI $_{95\%}$: 1.51%-5.12%) or 0.41 (CI $_{95\%}$: 0.30%-0.56%), respectively, for the PI. Similarly, the LR for a positive or negative test was 2.18 (CI $_{95\%}$: 1.34%-3.55%) or 0.38 (CI $_{95\%}$: 0.26%-0.56%), respectively, for the RI – Figures 7, 8.

Discussion

In recent decades, the need for uterine evacuation in cases of early pregnancy loss (delayed miscarriages or incomplete miscarriages) has been a matter of debate. Because surgical procedures have potential risk and might result in complications, including infection, hemorrhage and uterine perforation, the decision to employ drugs or to adopt an expectant attitude are considered acceptable, safe and efficient. The success rate measured within a reasonable period of time, such as 2 weeks [9], did preclude the use of D&C. Success rates of 71% to 84% were reported for expectant attitudes [7,9,17], and, in cases in which misoprostol was administered, complete miscarriage was found in 83 to 86% of the patients for periods of follow up that spanned from 1 week up to 4 weeks [6,17-19]. The data indicate that within a reasonable period of time, the success rate is similar when the option is for the expectant attitude or the use of pharmacological means. However, a significant number of patients will have an unplanned admission to the hospital for surgery [8,17], and some patients will require an emergency D&C [9].

As accurate predictive criteria for successful conservative management of early pregnancy loss have not been established, new clinical indicators are necessary, particularly those that might predict the need for uterine surgical evacuation [8,11,18]. Considering that sonographic assessment of the uterine content volume in incomplete miscarriages did not accurately predict this need [7], other approaches must be devised.

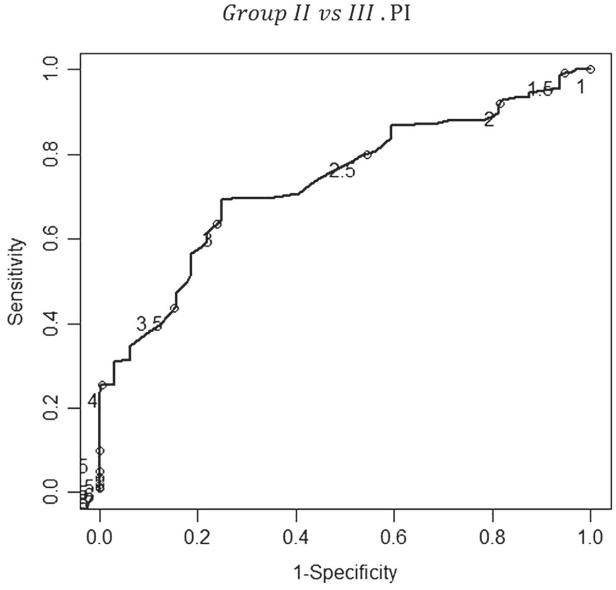

Figure 7 The receiver-operator characteristic (ROC) curve for the different values of the pulsatility index concerning the discrimination between groups II and III. All the values from 1 to 8 in increments of 0.5 are identified in the curve with a circle. The point in the curve that is closer to the upper-left corner of the plot corresponds to the value 2.808 of the pulsatility index. At that cut-off point, the sensitivity and specificity values of the pulsatility index in the uterine artery were of 69.5%(CI $_{95\%}$: 61.5%-76.5%) and 75.0%(CI $_{95\%}$: 57.9%-86.8%), respectively; the area under the curve (AUC) was 0.734 (0.648-0.819). The correspondent positive and negative predictive values were 92.5% and 35.8%, respectively. The likelihood ratio (LR) for a positive or negative test was 2.78 (CI $_{95\%}$: 1.51%-5.12%) or 0.41 (CI $_{95\%}$: 0.30%-0.56%), respectively.

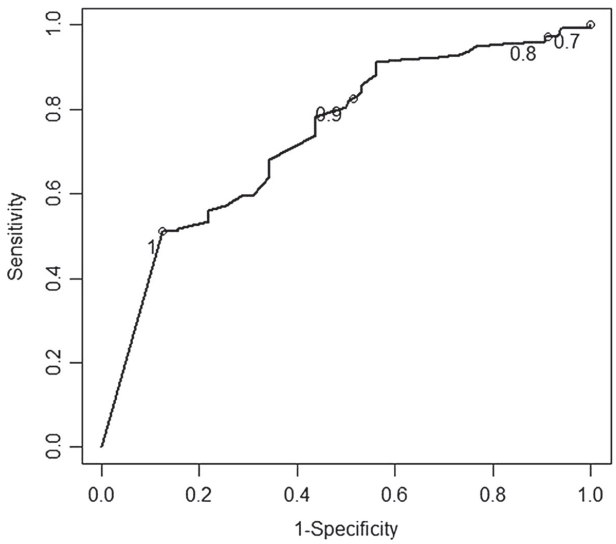

Figure 8 The receiver-operator characteristic (ROC) curve for the different values of the resistance index concerning the discrimination between groups II and III. The values 0.7, 0.8, 0.9 and 1.0 are identified in the curve with a circle. The point in the curve that is closer to the upper-left corner of the plot corresponds to a value of 1 for the resistance index. At that cut-off point, the sensitivity and specificity values of the resistance index in the uterine artery were of 75% (CI $_{95\%}$: 57.9%-86.8%) and 65.6% (48.3%-79.6%), respectively; the area under the curve (AUC) was 0.738 (0.676-0.799). The correspondent positive and negative predictive values were 89.9% and 32.8%, respectively. The likelihood ratio (LR) for a positive or negative test was 2.18 (CI $_{95\%}$: 1.34%-3.55%) or 0.38 (CI $_{95\%}$: 0.26%-0.56%), respectively.

Regarding the fundamental role of maternal-fetal circulation, a maternal pelvic blood flow study using Doppler ultrasound technology is useful in pregnancy follow-up [20,21]. As a consequence of the widespread availability of equipment, several studies have analyzed the uterine artery blood flow patterns in pregnant women, emphasizing the PI and RI. Both indices provide quantitative data on end-arteriolar impedance [22] and, therefore, on local vascular resistance and blood flow velocity.

The application of Doppler ultrasound in the study of the retained products of conception after miscarriage or delivery had been proposed [23,24], and its use in the assessment of incomplete early miscarriage was recently reported for a large number of patients [11]. It was demonstrated that the absence of blood flow in the remaining intra-uterine trophoblastic tissue is associated with a significantly higher success rate of expectant management when compared to the presence of flow [9,11].

In this investigation, we explored the likelihood that intra-uterine retained ovular products could modulate uterine artery blood flow and change the PI and RI. Our results indicate that this modulation does occur. Additionally, the data indicate that uterine artery low PI and RI persistence associates to a considerable risk [16] for uterine curettage 8 weeks after an incomplete early miscarriage diagnosis, a time when a spontaneous resolution is unlikely. At 2 weeks after the decision for expectant management, the indices were significantly lower in the cases of incomplete miscarriage, compared to those of complete miscarriage. At the first follow-up visit, Doppler findings allowed us to distinguish women who would achieve complete resolution (group I) from those who should remain under surveillance (group II + III). The UtA-RI and PI at 2 weeks showed a reasonable sensitivity, specificity and positive predictive value for the identification of those patients who would need a D&C 8 weeks after starting the treatment. The obtained LR values showed only a moderate usefulness of the UtA Doppler evaluation on the prediction of the need for D&C (due to incomplete miscarriage) in patients submitted to medical management for early pregnancy loss [16].

Finally, the reliability study demonstrated that the Doppler blood flow measurement of the PI-UtA and RI-

UtA was highly repeatable by our sonographer [25]. We used the ICC to assess the repeatability because there is sufficient consensus in the scientific literature to consider that values for ICC > 0.7 reflect a very low measurement error [25,26].

Study limitations and future research

The absolute values of the uterine artery PI and RI have not been validated for uneventful early pregnancy, representing a limitation of the study. Although the reference ranges for the uterine artery mean PI are well known, covering pregnancy from 6 to 41 weeks of gestation [21,27], further studies are required to establish the identical curves of normality in women with spontaneous abortion and managed expectantly. This reference range will be helpful for validating the use of uterine artery Doppler in the management of cases of early pregnancy loss.

Conclusions

This is the first prospective study providing evidence that uterine artery Doppler evaluation can predict the need for D&C due to incomplete miscarriage, after management of early pregnancy loss using mifepristone plus misoprostol.

Abbreviations

CHP: Hospital Center of Porto; CRL: Crown-rump length; D&C: Dilation and curettage; ET: Endometrial thickness; ICC: Intraclass correlation coefficients; LR: Likelihood ratio; PI: Pulsatility index; RI: Resistance index; ROC: Receiver-operating characteristic; UtA: Uterine artery; +/− ve: Positive/negative.

Competing interests

The authors declare that they have no competing interests.

Authors' contributions

LG-M designed the study, performed all Doppler measurements, analysed the data, and composed the manuscript. JPS coordinated quality control of the ultrasound data, contributed to the critical revision of the manuscript, coordinated the review of clinical cases and organization of study groups. ARG performed all statistical analyses. AR contributed to the critical revision of the manuscript. FM designed the study, and HA designed the study, analysed the data, and composed the manuscript. All authors contributed to the data interpretation and the final version of the manuscript, which all approved.

Acknowledgements

We thank the staff Department of Obstetrics of Centro Hospitalar do Porto for their kind contributions to this work. A.R.G. was funded in part by the European Regional Development Fund through the COMPETE program and by the Portuguese Government through the FCT - Fundação para a Ciência e a Tecnologia - under the project PEst-C/MAT/UI0144/2013.

Author details

[1]Department of Experimental Biology, Faculty of Medicine, University of Porto, 4200-319 Porto, Portugal. [2]Hospital Centre of Porto EPE, Department of Women and Reproductive Medicine, Largo Prof. Abel Salazar, 4099-001 Porto, Portugal. [3]Obstetrics-Gynecology, Private Hospital Trofa, 4785-409 Trofa, Portugal. [4]Department of Mathematics, Faculty of Sciences, University of Porto, 4169-007 Porto, Portugal. [5]CMUP-Centre of Mathematics, University of Porto, 4169-007 Porto, Portugal. [6]Centro de Simulação Médica do Porto (CESIMED), 4465-024 São Mamede de Infesta, Portugal. [7]Department of Medicine, Faculty of Medicine, University of Porto, 4200-319 Porto, Portugal. [8]Department of Cardiology, S. João Hospital Centre, 4200-319 Porto, Portugal. [9]Obstetrics-Gynecology, CUF-Hospital Porto, 4100 180 Porto, Portugal.

Received: 6 November 2014 Accepted: 30 January 2015
Published online: 13 February 2015

References

1. Regan L, Rai R. Epidemiology and the medical causes of miscarriage. Baillieres Best Pract Res Clin Obstet Gynaecol. 2000;14:839–54.
2. Wang X, Chen C, Wang L, Chen D, Guang W, French J. Conception, early pregnancy loss, and time to clinical pregnancy: a population-based prospective study. Fertil Steril. 2003;79:577–84.
3. Hinshaw K, Cooper K, Henshaw R, el-Refaey H, Rispin R, Smith N, et al. Management of uncomplicated miscarriage. Randomized trials are possible. BMJ. 1993;307:259.
4. Chung TK, Lee DT, Cheung LP, Haines CJ, Chang AM. Spontaneous abortion: a randomized, controlled trial comparing surgical evacuation with conservative management using misoprostol. Fertil Steril. 1999;71:1054–9.
5. Muffley PE, Stitely ML, Gherman RB. Early intrauterine pregnancy failure: a randomized trial of medical versus surgical treatment. Am J Obstet Gynecol. 2002;187:321–5.
6. Graziosi GC, Mol BW, Reuwer PJ, Drogtrop A, Bruinse HW. Misoprostol versus curettage in women with early pregnancy failure after initial expectant management: a randomized trial. Hum Reprod. 2004;19:1894–9.
7. Luise C, Jermy K, May C, Costello G, Collins WP, Bourne TH. Outcome of expectant management of spontaneous first trimester miscarriage: observational study. BMJ. 2002;324:873–5.
8. Trinder J, Brocklehurst P, Porter R, Read M, Vyas S, Smith L. Management of miscarriage: expectant, medical, or surgical? Results of randomised controlled trial (miscarriage treatment (MIST) trial). BMJ. 2006;332:1235–40.
9. Casikar I, Bignardi T, Riemke J, Alhamdan D, Condous G. Expectant management of spontaneous first-trimester miscarriage: prospective validation of the '2-week rule'. Ultrasound Obstet Gynecol. 2010;35:223–7.
10. Farquharson RG, Jauniaux E, Exalto N, ESHRE Special Interest Group for Early Pregnancy (SIGEP). Updated and revised nomenclature for description of early pregnancy events. Hum Reprod. 2005;20:3008–11.
11. Casikar I, Lu C, Oates J, Bignardi T, Alhamdan D, Condous G. The use of power Doppler colour scoring to predict successful expectant management in women with an incomplete miscarriage. Hum Reprod. 2012;27:669–75.
12. Guidelines and Audit Committee of the Royal College of Obstetricians and Gynaecologists. The management of early pregnancy loss. Green-top guideline No. 25. London: RCOG; 2006.
13. Henshaw R, Norman J, Thong KJ, Alzugaray MG, Ho PC, Pretnar-Darovec A, et al. Termination of pregnancy with reduced doses of mifepristone. World Health Organisation Task Force on Post-ovulatory Methods of Fertility Regulation. BMJ. 1993;307:532–7.
14. Shaffer J. Multiple hypothesis testing. Annu Rev Psychol. 1995;46:561–76.
15. Gibbons JD. Nonparametric Statistical Inference. 5th ed. Harcover: Chapman and Hall/CRC; 2010.
16. Deeks JJ, Altman DG. Diagnostic tests 4: likelihood ratios. BMJ. 2004;329:168–9.
17. Pauleta JR, Clode N, Graça LM. Expectant management of incomplete abortion in the first trimester. Int J Gynaecol Obstet. 2009;106:35–8.
18. Zhang J, Gilles JM, Barnhart K, Creinin MD, Westhoff C, Frederick MM. National Institute of Child Health Human Development (NICHD) Management of Early Pregnancy Failure Trial. A comparison of medical management with misoprostol and surgical management for early pregnancy failure. N Engl J Med. 2005;353:761–9.
19. Kollitz KM, Meyn LA, Lohr PA, Creinin MD. Mifepristone and misoprostol for early pregnancy failure: a cohort analysis. Am J Obstet Gynecol. 2011;204:386.
20. Papageorghiou AT, Yu CK, Nicolaides KH. The role of uterine artery Doppler in predicting adverse pregnancy outcome. Best Pract Res Clin Obstet Gynaecol. 2004;18:383–96.
21. Gómez O, Figueras F, Fernández S, Bennasar M, Martínez JM, Puerto B, et al. Reference ranges for uterine artery mean pulsatility index at 11–41 weeks of gestation. Ultrasound Obstet Gynecol. 2008;32:128–32.
22. Browne VA, Toledo-Jaldin L, Davila RD, Lopez LP, Yamashiro H, Cioffi-Ragan D, et al. High-end arteriolar resistance limits uterine artery blood flow and restricts fetal growth in preeclampsia and gestational hypertension at high altitude. Am J Physiol Regul Integr Comp Physiol. 2011;300:R1221–9.

23. Alcázar JL, Ortiz CA. Transvaginal color Doppler ultrasonography in the management of first-trimester spontaneous abortion. Eur J Obstet Gynecol Reprod Biol. 2002;102:83–7.
24. Van den Bosch T, Daemen A, Van Schoubroeck D, Pochet N, De Moor B, Timmerman D. Occurrence and outcome of residual trophoblastic tissue: a prospective study. J Ultrasound Med. 2008;27:357–61.
25. Bland JM, Altman DG. Applying the right statistics: analyses of measurement studies. Ultrasound Obstet Gynecol. 2003;22:85–93.
26. Walter SD, Eliasziw M, Donner A. Sample size and optimal designs for reliability studies. Stat Med. 1998;17:101–10.
27. Guedes-Martins L, Saraiva J, Gaio R, Macedo F, Almeida H. Uterine artery impedance at very early clinical pregnancy. Prenat Diagn. 2014;34:719–25.

Article 4

Guedes-Martins L, Cunha A, Saraiva J, Gaio R, Macedo F, Almeida H. Internal iliac and uterine arteries Doppler ultrasound in the assessment of normotensive and chronic hypertensive pregnant women. *Sci Rep*. 2014; 4:3785.

SCIENTIFIC REPORTS

OPEN

SUBJECT AREAS:
MEDICAL RESEARCH
CARDIOVASCULAR DISEASES

Received
14 November 2013

Accepted
2 January 2014

Published
21 January 2014

Correspondence and requests for materials should be addressed to L.G.-M. (luis.guedes.martins@gmail.com)

Internal iliac and uterine arteries Doppler ultrasound in the assessment of normotensive and chronic hypertensive pregnant women

L. Guedes-Martins[1,2,3], A. Cunha[3], J. Saraiva[3], R. Gaio[4,5], F. Macedo[6,7] & H. Almeida[1,2,8]

[1]Departamento de Biologia Experimental, Faculdade de Medicina da Universidade do Porto, 4200–319 Porto, Portugal, [2]IBMC-Instituto de Biologia Molecular e Celular, 4150–180 Porto, Portugal, [3]Centro Hospitalar do Porto EPE, Departamento da Mulher e da Medicina Reprodutiva, Largo Prof. Abel Salazar, 4099–001 Porto, Portugal, [4]Department of Mathematics, Faculty of Sciences of the University of Porto, [5]CMUP-Centre of Mathematics of the University of Porto, Portugal, [6]Departamento de Medicina, Faculdade de Medicina da Universidade do Porto, 4200–319 Porto, Portugal, [7]Centro Hospitalar S. João, 4200–319 Porto, Portugal, [8]Ginecologia-Obstetrícia, Hospital-CUF Porto, 4100 180 Porto, Portugal.

The objective of this work was to compare Doppler flows pulsatility index (PI) and resistance indexes (RI) of uterine and internal iliac arteries during pregnancy in low risk women and in those with stage-1 essential hypertension. From January 2010 and December 2012, a longitudinal and prospective study was carried out in 103 singleton uneventful pregnancies (72 low-risk pregnancies and 31 with stage 1 essential hypertension)at the 1st, 2nd and 3rd trimesters. Multiple linear regression models, fitted using generalized least squares and whose errors were allowed to be correlated and/or have unequal variances, were employed; a model for the relative differences of both arteries impedance was utilized. In both groups, uterine artery PI and RI exhibited a gestational age related decreasing trend whereas internal iliac artery PI and RI increased. The model testing the hemodynamic adaptation in women with and without hypertension showed similar trend. Irrespective of blood pressure conditions, the internal iliac artery resistance pattern contrasts with the capacitance pattern of its immediate pelvic division, suggesting a pregnancy-related regulatory mechanism in the pelvic circulation.

Shortly after the establishment of pregnancy, the maternal circulation undergoes a substantial change to meet the increasing demands of the growing uterus and foetus.

Noteworthy, there is a decrease in total peripheral resistance until midpregnancy[1,2] and a >40% increase of cardiac output measured at the aortic valve[2] that results from enhanced heart rate, a slight increment in the aortic valve area and an increased blood flow velocity across the valve[1,2]. This change is reflected in the pelvic circulation, where volume flow and mean velocity also increase in common iliac arteries[3]. However, past this point, a notorious difference is noticed.

In fact, while in the external iliac artery, that feeds the lower limb, mean velocity and volume flow are reduced along the pregnancy, in contrast, the uterine artery (UtA) exhibits a progressive and persistent increase in volume flow and mean velocity[3,4]. This pregnancy related redistribution of blood to the pelvis is particularly important as the uterine artery provides most of the blood to the uterus and is thus critical to the continuous and adequate foetal nourishment.

In the mid-1990s, the procedures employed in the acquisition of those data, many of them based in velocity measurement, were replaced in part by indices relying on the computerized analysis of Doppler ultrasound frequency spectrum. Such indices include the pulsatility index (PI) and the resistance index (RI), both derived from blood velocity measurements at specific points of the systolic/diastolic cycle. As they are easy to obtain, do not require cumbersome adjustments and are more objective, they have been widely applied in the assessment of the uteroplacental circulation in normal pregnancies[4] and also when they are complicated by pathological conditions as hypertensive disorders[5–7]. In this setting, the uterine artery became an important target in the application of those procedures[8–15].

The enhanced blood volume that is transported by the uterine arteries along the pregnancy is associated with a reduced impedance of flow consequent to the impressive structural changes that take place at the placental bed. In normal pregnancy, placental trophoblastic cells migrate across the decidua, invade the inner third of the myometrium and replace most of the muscular and endothelial cells of the maternal spiral arteries, rendering them low impedance, high capacitance vessels that optimize the delivery of oxygen and nutrients to the foetus. That change is reflected in the uterine artery flow velocity as measured by Doppler ultrasound spectrum[5,6,13].

It was noticed that in the non-pregnant state there is a rapid rise and sudden fall in flow velocity during systole and a "notch" in early diastole[16], a property that reflects an high impedance vessel. As the pregnancy evolves normally from 8 weeks onwards, a progressive increase in uterine artery compliance is noticed, which continues through 26 weeks' gestation, albeit at a lesser extent[16], during which the «notch» is smoothed and lost.

However, when the trophoblast invasion is defective, an enhanced placental vascular resistance is likely to occur as evidenced in abnormal Doppler ultrasound spectrum of the uterine vessels, indicating women at risk for serious pregnancy disorders like preeclampsia[5,12–14]. In fact, abnormal uterine artery blood flow employing Doppler ultrasound assessment, at both the first and second trimesters, was shown to associate with subsequent perinatal complications[17–21] and some studies even referred the analysis of Doppler wave variations as a means to assess the potential benefits of therapeutic interventions[20–23].

The results of the hemodynamic studies of the UtA made so far are evidence of its close relation to the changes taking place in the growing uterus. Such studies contrast with the scarcity of data concerning other pelvic arteries as was pointed out[24]. In fact, it is noteworthy that, while the UtA has been a subject of extensive research, its predecessor, the internal iliac artery (IIA), has not. This is unexpected because it is an easily accessible artery, both in pregnant and non-pregnant women, and is also the first artery entering the pelvis. Thus, it was hypothesized that such unique property would render the IIA an important means for the understanding of the pelvic circulation along the pregnancy.

For this purpose, the most immediate approach would be a longitudinal study of uneventful pregnancies in healthy women. Yet, it was also reasoned that additional information on artery performance along the pregnancy would be provided by a parallel study in women having long term, stable, essential hypertension, a prevalent condition and also a known risk factor for serious disorders of the pregnancy[25–29].

On account of those considerations, particularly the lack of knowledge on the internal iliac artery hemodynamics, in contrast with the larger knowledge on the uterine artery, it was purposed to compare blood flow of both at several time points throughout the pregnancy, employing Doppler ultrasound spectrum analysis.

Results

The main characteristics and pregnancy outcomes of the 103 women are depicted in Table 1. Their age ranged from 17 to 43 years old, 69% of them were less than 34 years old and a similar proportion (74%) had not been educated beyond the secondary level (12 years at most), perhaps because our hospital covers an area with important socio-economic difficulties. For 52% of the women, this was their first pregnancy. A total of 54% of the population studied had a BMI between 18 and 24 Kg/m^2 at the first appointment. The average time of the ultrasound evaluation for the three trimesters was 13.04 weeks (range: 11.43–14.14), 20.73 weeks (range: 19.14–23.71) and 30.46 weeks (range: 28.71–33). They all delivered at term[30,31] with an average at 38.9 weeks (range: 37.14–41).

Regarding NT and HT groups, statistically significant differences were found for BMI (higher classes predominantly in the HT group) and age (older classes predominantly in the HT group).

The presence of uterine artery notching declined along pregnancy, from 48% to 5%, as expected (Table 2). In the first trimester, significant differences for the presence of bilateral notching were not observed; however, in the second and third trimesters, a clear majority of women did not exhibit bilateral notching (Figure 1).

The means and standard deviations of PIs and RIs for both arteries, according to the different trimesters, the normotensive and the hypertensive groups, are displayed in Table 3.

Multivariate analysis and predictions. The (net) effect of the gestational trimesters on the mean values of the indexes were considered merely indicative; therefore, multivariate analyses had to be performed, by adjusting that effect to potential confounders and

Table 1 | Main characteristics and pregnancy outcomes of 103 women included in the study

		n (%)	p-value[2]	Normotensive (NT, n = 72)	Hypertensive (HT, n = 31)	p-value[3]
Age (intervals in years)	17–24	13 (13%)	<0.001	13 (18%)	0 (0%)	<0.001
	25–34	58 (56%)		46 (64%)	12 (39%)	
	35–43	32 (31%)		13 (18%)	19 (61%)	
Education level (in years)	<7	5 (5%)	<0.001	3 (4%)	2 (6%)	0.579
	7–9	31 (30%)		23 (32%)	8 (26%)	
	10–12	38 (37%)		24 (33%)	14 (45%)	
	>12	29 (28%)		22 (31%)	7 (23%)	
Smoking	No	84 (82%)	<0.001	61 (85%)	23 (74%)	0.308
	Yes	19 (18%)		11 (15%)	8 (26%)	
Parity	0	54 (52%)	0.556	43 (60%)	11 (35%)	0.036
	≥1	49 (48%)		29 (40%)	20 (65%)	
Body Mass Index[1] (Kg/m^2)	18–24	56 (54%)	<0.001	50 (69%)	6 (19%)	<0.001
	25–29	32 (31%)		15 (21%)	17 (55%)	
	30–51	15 (15%)		7 (10%)	8 (26%)	
Age at menarche	12.5 (1.6)		–	12.4 (1.5)	12.8 (1.8)	0.243
Age at first intercourse	18.1 (2.0)		–	17.9 (1.8)	18.5 (2.3)	0.205
Trimestral evaluation (weeks ± SD)	13.04 (0.68)		<0.001	13.13 (0.73)	12.82 (0.51)	0.012
	20.73 (0.78)			20.79 (0.80)	20.59 (0.71)	0.210
	30.46 (1.19)			30.61 (0.74)	30.11 (1.85)	0.158
GA at delivery (weeks ± SD)	38.9 (1.7)		–	38.9 (1.65)	38.9 (1.68)	0.956

[1]BMI: measurement in trimester 1;
[2]p - tests equality of population frequencies amongst the different categories of a variable;
[3]p - tests homogeneity of the proportions between HT (hypertensive) and NT (normotensive). SD: standard deviation.

Table 2 | Absolute (relative, %) frequencies for positive notching of uterine arteries along the pregnancy (n = 103), in normotensive (n = 72) and hypertensive (n = 31) women at each trimester

	n (%)	p-value[1]	Normotensive (n = 72)	Hypertensive (n = 31)	p-value[2]
Trimester 1	49 (48)	0.695	41 (57)	8 (26)	0.006
Trimester 2	16 (16)	<0.001	12 (17)	4 (13)	0.772
Trimester 3	5 (5)	<0.001	5 (7)	0 (0)	0.319

[1]p - tests equality of population frequencies amongst positive and negative notching;
[2]p - tests homogeneity of the proportions between HT and NT.

taking the study design into consideration. As the difference between the average evaluation time in trimester 2 and that in trimester 1 was approximately equal to the difference between the average evaluation time in trimester 3 and that in trimester 2 (more precisely, the latter is 1.3 times the former), the multivariate regression model considered the variable *gestational trimester* as continuous. The correspondent model was described in the *Statistical Analysis* section; estimates of the coefficients and respective 95% confidence intervals are presented in Table 4. Statistically significant time curves were obtained for the different combinations of indexes, vessels, hypertension and presence of notching status. The residual standard error was estimated at 0.066 (degrees of freedom: 1236 total, 1220 residual) and the Bayesian Information Criterion[32] was of −956. The parameter for the first order autoregressive time structure was estimated at 0.350, while the variance of the pulsatility index was estimated to be 6.342 times greater than the variance of the resistance index.

Known confounding variables such as maternal age, smoking habits, body mass index and the parity were also taken into account in the analysis; as they were not shown to be statistically significant, they were not considered in the final model.

For each index, a model for the proportion of uterine artery changes relative to the IIA values was also considered. The significance of the estimated coefficients (Table 5) shows that hypertension alone was not a significant predictor in the regression. Its presence in the model is due to the significant interaction between hypertension status and index. All remaining variables proved to have a significant effect on the response, including interaction effects of gestational time and index, and of gestational time and status for the presence of notching. The residual standard error was estimated at 0.099 (degrees of freedom: 618 total, 610 residual) and the Bayesian Information Criterion was of −978. The parameter for the first order autoregressive time structure was estimated at 0.403, while the variance of the pulsatility index was estimated to be 1.321 times greater than the variance of the resistance index.

Pulsatility and Resistance indices. The predicted mean indexes (PI and RI) and their 95% confidence intervals for IIA and UtA during

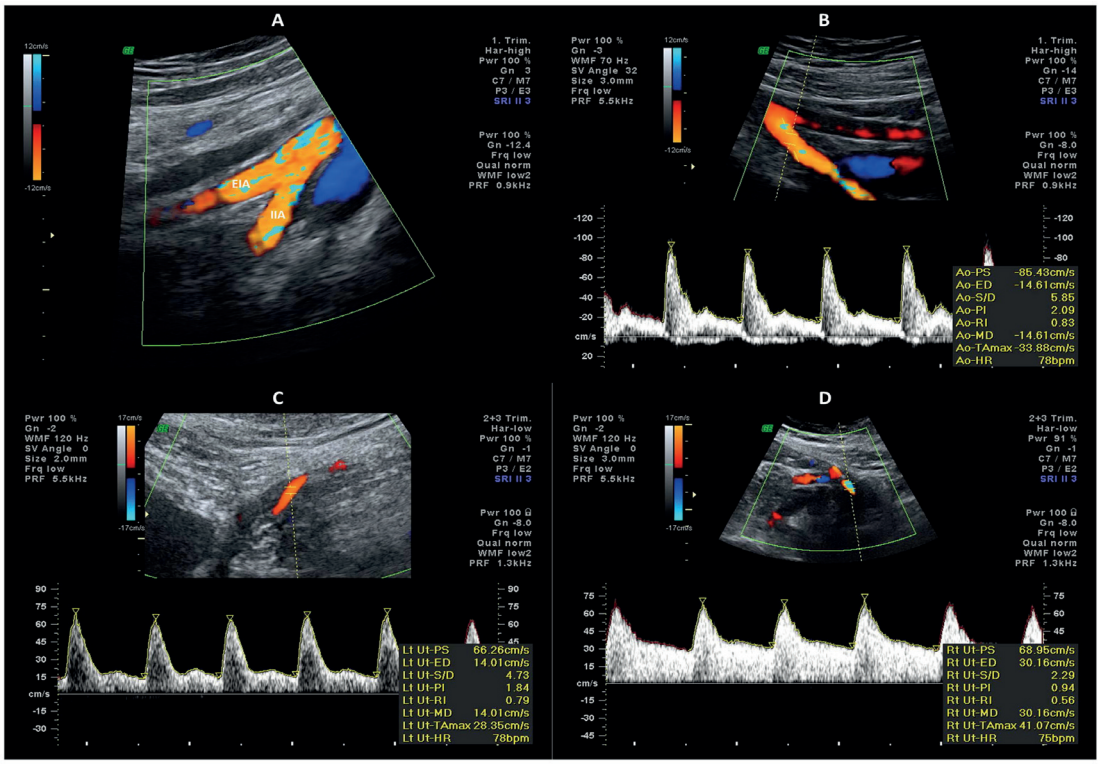

Figure 1 | (A) External iliac (EIA) and internal iliac (IIA) arteries color flow mapping; (B,C,D) Doppler waveform of internal iliac and uterine arteries: notice the biphasic flow of internal iliac artery (B), and uterine artery notch presence (C) or absence (D).

Table 3 | Mean (SD) uterine and internal iliac artery PI and RI indices, measured by transabdominal ultrasound examination at the different trimesters

	IIA			UtA		
	Trimester			Trimester		
	1	2	3	1	2	3
	NT (n = 72)					
PI	2.87 (0.50)	3.16 (0.53)	3.30 (0.63)	1.56 (0.50)	0.99 (0.30)	0.79 (0.18)
RI	0.88 (0.06)	0.90 (0.04)	0.91 (0.05)	0.70 (0.11)	0.57 (0.08)	0.50 (0.07)
	HT (n = 31)					
PI	2.68 (0.40)	2.69 (0.33)	3.08 (0.33)	1.35 (0.41)	1.05 (0.27)	0.84 (0.12)
RI	0.88 (0.04)	0.88 (0.04)	0.93 (0.04)	0.63 (0.07)	0.57 (0.08)	0.48 (0.07)

Abbreviations: IIA, internal iliac artery; UtA, uterine artery; NT, normotensive; HT, hypertensive; PI, pulsatility index; RI, resistance index.

pregnancy in HT and NT pregnant women are on display in Figure 2. In both groups regardless of the absence/presence of notch or hypertension, the simple inspection of the chart shows that UtA-PI and UtA-RI follow a significant downward trend along the gestational age whereas the IIA-PI and IIA-RI show a regular upward tendency.

The PI value of the IIA over time is significantly higher in normotensive women along all trimesters, in contrast with the UtA situation (Figure 2A). The presence of notching does not change the trend and only appears to level the PI up, compared to the condition of absent notch. The PI level at the start is also significantly different when both arteries are compared, as it is higher for the IIA and lower for the UtA, and they diverge progressively along the gestational age.

The inspection of RIs of both IIA and UtA shows that, similarly to the PIs, there is a significant upward and downward trend respectively. Again, notching does not change the trend and only appears to add RI units to the absent notch condition.

In contrast with the PIs, which evidence parallel slopes when NT and HT groups are compared, the RIs of the HT condition point to higher (in the case of the IIA), or smaller (actually convergent in the case of UtA) values at the 3rd trimester when compared to the normotensive condition (Figure 2B). Similarly, the RI at the start (first trimester) is significantly higher for the IIA than for the UtA, and is independent of the hypertensive condition.

Relative change (IIA index value – UtA index value)/(IIA index value). The predicted and observed index proportions (*i.e.*, relative changes) along the pregnancy are depicted in Figure 3. In both indexes, regardless of the state of notch and blood pressure, the proportion undergoes a significant increase over time. The statistical significance of the interaction terms between time and index type, and time and presence/absence of notch, in Table 5, show that the growth rate is significantly influenced by the presence of notch and the type of index. For PI and in women with (+) Notch, the growth rate is the highest. The isolated effect of the hypertensive state on the proportions is not significant but the existence of a significant interaction with the index shows that in the first trimester, mean PI proportion values were lower in hypertensive women compared to normotensive women; the growth rate in the succeeding times was similar. At the beginning of the gestation, the expected relative change for pregnant women with (+) Notch is significantly lower than that in pregnant (−) Notch, for both indices. Over time, mean proportion values in pregnant women with (+) Notch grow faster than on (−) Notch pregnant regardless of the values of other variables – Figure 3.

Table 4 | Estimated coefficients and 95% confidence intervals (CI) of the regression model used to obtain the expected indices at the different covariates combinations

Covariates	Coefficient	95% CI
Intercept	0.860	(0.836, 0.884)
PI	1.705	(1.576, 1.834)
UtA	−0.108	(−0.135, −0.081)
Hypertension	−0.026	(−0.057, 0.005)
Bilateral Notching	0.023	(0.009, 0.037)
PI * UtA	−0.791	(−0.954, −0.628)
Bilateral Notching * PI	0.190	(0.123, 0.257)
Bilateral Notching * UtA	0.036	(0.016, 0.056)
Hypertension * PI	−0.219	(−0.319, −0.119)
Hypertension * UtA	−0.016	(−0.038, 0.006)
Hypertension * PI * UtA	0.287	(0.158, 0.416)
Time	0.012	(0.003, 0.021)
Time * PI	0.197	(0.142, 0.252)
Time * UtA	−0.109	(−0.121, −0.097)
Time * PI * UtA	−0.449	(−0.522, −0.376)
Time * Hypertension	0.015	(0.001, 0.029)

Abbreviations: UtA, uterine artery; NT, normotensive; PI, pulsatility index.

Discussion

The great obstetrical syndromes, as preeclampsia (PE), intra-uterine growth restriction (IUGR), preterm labour and *abruptio placentae* associate to placentation disorders that result from local abnormal vascular remodelling[33]. While effective interventions to prevent such late pregnancy complications are necessary, it is also required that early, reliable, diagnostic or predictive tests become available to support the decisions to undertake such interventions.

On account of the crucial role played by the vascular network, there is currently a wide recognition of Doppler ultrasound studies importance in pregnancy evaluation and, indeed, its application in foetal and mother's pelvic circulation assessment have been of unquestionable interest[13]. Consequent to the widespread availability of equipment, a large number of studies devoted to the analysis of

Table 5 | Estimated coefficients and 95% confidence intervals (CI) of the regression model for the expected relative changes of RI and PI

Covariates	Coefficient	95% CI
Intercept	0.199	(0.156, 0.242)
PI	0.229	(0.196, 0.262)
Hypertension	0.005	(−0.020, 0.030)
Bilateral Notching	−0.176	(−0.227, −0.125)
PI * Hypertension	−0.049	(−0.076, −0.022)
Time	0.087	(0.067, 0.101)
Time * PI	0.029	(0.013, 0.045)
Time * Notching	0.059	(0.035, 0.083)

Abbreviations: PI, pulsatility index; CI, confidence intervals.

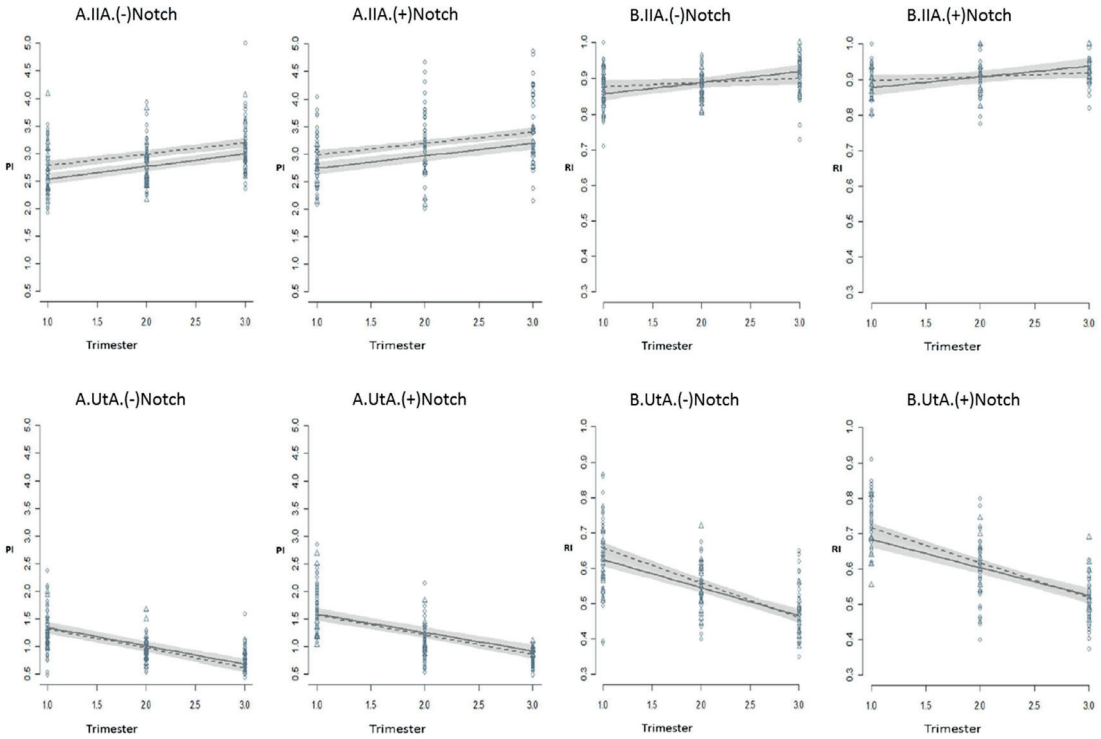

Figure 2 | **Predicted mean PI (A) and RI (B) indices for IIA and UtA during pregnancy in normotensive (dashed line, circles) and hypertensive (solid line, triangles) women in the condition of UtA notch absence (left charts) or presence (right charts).** Gray bars: 95% confidence intervals for the prediction. PI and RI: Pulsatility and resistance indices; IIA and UtA: Internal Iliac and uterine arteries.

uterine artery blood flow patterns were published, employing the resistance index (RI) and the pulsatility index (PI). These are end-arteriolar vascular impedance indices[34] and therefore, provide qualitative and quantitative data pertaining to local blood flow velocity and vascular resistance.

With the purpose to investigate the uteroplacental circulation[19,35], emphasis has been put on the study of uterine arteries in the course of the normal pregnancy or its association with the risk for placentation disorders[20]. There is a general agreement that a progressive decline in uterine artery vascular resistance accompanies the normal pregnancy[5–8,12–14,16,18]. The regularity of the trend led to the establishment of reference ranges for uterine artery mean PI, covering the pregnancy from 11 to 41 weeks of gestation[6]. They show that along the normal course of the pregnancy, there is a regular decrement of PI, indicating that the uterine arteries conversion from resistance vessels (narrow bore) to high capacity vessels (larger bore), is most important to meet the increased demands of blood by the growing foetus[8,11,34]. In contrast, the observation of high resistance patterns in the uterine arteries of pregnant women was associated with local reduction of blood supply, higher incidence of preeclampsia[5,7,8], intrauterine growth retardation[11,19,35] and more unfavourable perinatal outcomes[11,35].

Despite the wealth of data in uterine arteries, there is a lack in the study of other important vessels as the internal iliac artery, a thick, 3–4 cm long division of the common iliac artery and the main artery entering the pelvis, whose anterior division gives off the uterine artery.

As such characteristics are relevant in the context of pelvic circulation assessment, a longitudinal collection of PIs and RIs of IIA and UtA was made in every trimester of uneventful pregnancies of healthy women. As expected, mean UtA-PI and UtA-RI values showed statistically significant progressive decreases from the 1st to the 3rd trimester of pregnancy, a necessary adaptation that is consistent with the foetal trophoblast cell invasion of the walls of spiral arteries (the arteriolar tips of the uterine artery successive branching), the process regarded as underlying the uterine arteries change from resistance into capacitance vessels.

In notorious contrast with the uterine artery, the IIA-PI and IIA-RI evidenced a remarkable increase in the same period. To the best of our knowledge, this is the first time such findings are reported.

This change is quite interesting because, although the internal iliac artery immediately precedes the uterine artery, it exhibits an entirely distinct performance. In fact, instead of becoming a capacitance vessel, the internal iliac arteries behaved much like resistance vessels and their progressive RI and PI increase reflect an enhanced blood velocity, similarly to the previous observation in the common iliac artery[3].

These findings favour the view that along the pregnancy there is an adaptation of the mother circulation to the growing foetus so that the low resistance uterine artery is rapidly filled by the enhanced maternal cardiac output and flow velocity of the internal iliac artery (Figure 4). Moreover, the adaptation is progressive as the trimester-related upward shift of IIA to UtA proportion evidenced. We are convinced that this change provides the local circulation with a reserve capacity that meets the growing foetal needs.

The pregnancy condition also appears to allow the adaptability in another stable, yet different, hemodynamic condition as is the case of long term hypertensive, non-medicated women. They are known to

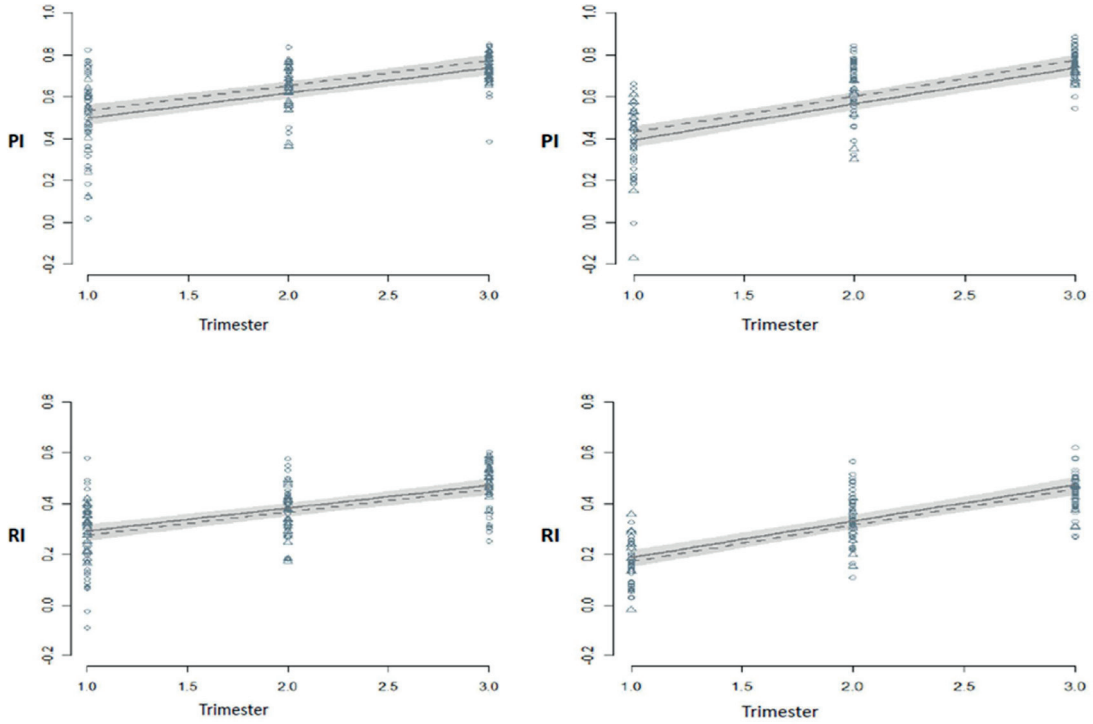

Figure 3 | Relative changes of IIA to UtA PI (top panels) and RI (bottom panels) along the pregnancy in normotensive (dashed line, circles) and hypertensive (solid line, triangles) women in the condition of UtA notch absence (left charts) or presence (right charts). Gray bars: 95% confidence intervals for the prediction. Notice the different y-axis scale for PI and RI. PI and RI: Pulsatility and resistance indices; IIA and UtA: Internal Iliac and uterine arteries.

be at risk for developing preeclampsia and intrauterine growth retardation, but coursed with an uneventful pregnancy and delivered a healthy infant.

The present study showed that the uterine and internal iliac arteries exhibit a performance that parallel the normotensive condition, although at a slightly different level of PI and RI. Therefore, a hemodynamic adaptation is likely to have occurred, probably even before pregnancy, as the 1st trimester PI and RI values of both arteries already evidence. The relative changes established within PIs and RIs, show that in hypertensive pregnant women too, a high velocity flow coming from the internal iliac artery feeds the large capacity uterine arteries and placental intervillous space with nutrient and oxygen rich blood in a progressive, regular pattern.

From this comparison and the elimination of confounding variables, a model emerged indicating that perfusion of the pregnant uterus is not dependent on the mother's age, parity or hypertensive status. Rather, it appears to depend on pelvic circulation regulatory mechanisms that sense the local needs and adapt the arterial flow properties immediately upon entering the pelvis, endowing the internal iliac artery with a determinant role in uterine perfusion.

The specifics of these adaptive hemodynamic mechanisms and how they interact with the structural placental bed changes are unknown. Similarly, it is uncertain whether these findings, collected from stable conditions, are affected by risk factors known to lead to rapidly changing vascular features and pregnancy complications. The fact that the hypertensive condition puts the PIs and RIs of both arteries at different levels, suggests that their evaluation will be beneficial to high risk pregnancy assessment.

In summary, the distinct impedances of internal iliac and uterine here shown in normotensive and chronic hypertensive pregnant women are evidence of a resistance vessel that precedes a typical capacitance vessel. Moreover, apart from the novelty of the IIA data, the results and the developed model suggest a continuous local circulatory adaptation to meet the needs of the growing foetus. They also point to IIA as an accessible, interesting additional target for the prognostic study of obstetrical disorders with major vascular component.

In conclusion, the impedance of the internal iliac artery of normotensive and hypertensive women evidences a progressive increase along the pregnancy, which contrasts notably with the decreasing trend of the uterine artery. This variation adjusts to a model of a continuous filling of the uterine artery by an adaptive internal iliac artery, suggesting a local regulatory mechanism imparted by the pregnancy condition.

Methods

Subjects. The research protocol was approved by the local ethics committee [Ref. 133/10(086-DEFI/126-CES)] of Centro Hospitalar do Porto, Unidade Maternidade Júlio Dinis (CHP-MJD) and all subjects gave their informed consent upon adequate explanation.

From January 2010 and December 2012, a total of 152 pregnant caucasian women were recruited to the study employing as basic criteria to be healthy or to have stable chronic hypertension without known target organ involvement. They had been referred by their family doctors to the CHP-MJD according to local pregnancy health policies.

In the first appointment, that coincided with the first ultrasound evaluation, they were observed by a senior specialist who reviewed the patient's history, verified the absence of diabetes and other endocrine disorders, immune diseases, renal and structural heart diseases, haematological conditions and chronic infections; it was

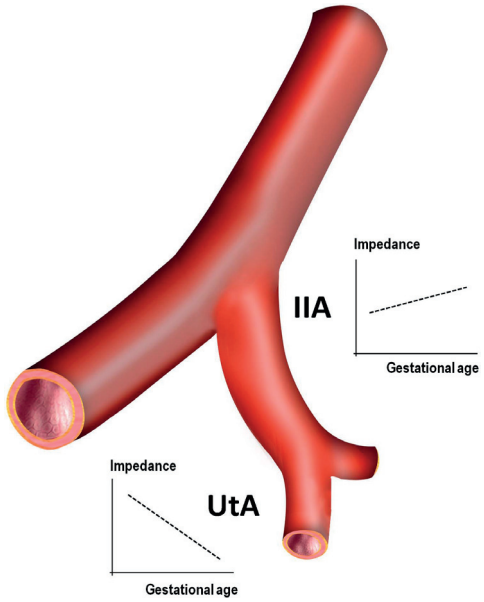

Figure 4 | The internal iliac artery (IIA) precedes the uterine artery (UtA) but has a distinct impedance pattern along the pregnancy. Unlike the capacitance ability of the UtA, whose resistance reduces, the IIA exhibits a progressive increase.

also checked the gestational age (GA) by sonography between 11 and 14 weeks and measured the blood pressure (BP). None of the women had a history of preeclampsia (PE) and only 1 reported having had hypertension during a previous pregnancy. Acceptable medication was folic acid, vitamin and iron supplements and acetylsalicylic acid, 100 mg per day, prescribed to all hypertensive women since the first appointment, until the last Doppler data collection.

Hypertension (HT) was defined as systolic BP ≥140 mmHg and/or diastolic BP ≥90 mmHg, present before pregnancy or the 20th week[26–29]. Mild to moderate hypertension in pregnancy was considered as systolic BP 140 to 159 or diastolic BP of 90 to 109 mm Hg, which corresponds closely to stage 1 of essential hypertension, defined as systolic 140 to 159 mmHg or diastolic 90 to 99 mm Hg[27]. An average of two BP measurements after a 4 hours period of rest was calculated.

All women were then enrolled in a longitudinal prospective study which included a trimestral ultrasound evaluation (centred at 13.04 ± 0.68, 20.73 ± 0.78 and 30.46 ± 1.19 weeks) and the recommended regular blood tests. Body Mass Index (BMI) was determined upon biometrical data collected at the hospital, before the first ultrasound evaluation.

Along the follow-up, a close attention was put on the appearance of abnormal conditions in the mother and foetus. These included foetal abnormal Doppler ultrasound indices in the umbilical and middle cerebral arteries, and foetal growth <10th and >90th percentile[30,31]. Moreover, as all women delivered at CHP-MJD, the healthy condition of the infant was verified by a neonatologist at birth and one month later.

In the follow-up, 49 women (32.2%) were excluded because of events occurring along the pregnancy. These were diabetes (n = 13), psychiatric disorders (n = 8), need of chronic medication beyond the established (n = 4), autoimmune disease (n = 4), later refusal to participate (n = 1), foetal/newborn pathology (n = 4) and failed sonographic evaluation at the defined schedule (n = 15).

Therefore, at the end, among the 103 women who were enrolled in the study, 72 were normotensive (NT) and 31 had chronic hypertension (HT).

Doppler flow study. The Doppler flow study of both right and left internal iliac and uterine arteries was made immediately before the routine trimestral transabdominal obstetrical ultrasound scan employing a Voluson E8 or a Voluson 730 Pro (GE Healthcare Technologies, USA) device, equipped with multifrequency transvaginal and transabdominal transducers.

All measurements were performed by a single investigator with extensive experience in Doppler ultrasound (A.C.), in order to minimize inter-observer variability. Smokers were required to abstain from smoking for at least 2 h prior to examination.

For the exam, the probe was placed on the lower quadrants of the abdomen, angled medially and colour Doppler imaging was used to localize the UtA at its crossing over the external iliac artery. A minor movement of the probe towards the flanks, complemented with a slight medial rotation, evidenced the common iliac artery and its division. As soon as the internal iliac artery was identified, the measurement was made at right and left sides. The procedure became rather easy upon a brief period of training.

In all cases, after an angle less than 30° was assured and pulsed Doppler probe was placed over the whole vessel width, IIA measurements were collected next to the bifurcation of the common iliac artery (Figure 1A). Angle correction was then applied and the signal updated until three similar consecutive waveforms were evidenced, just before calculating left and right uterine arteries PI and RI, using the software of the device (Figure 1B).

The presence or absence of a bilateral early protodiastolic notch in UtA was noted (Figure 1C, D). A positive notch was defined as a persistent decrease in blood flow velocity in early diastole, below the diastolic peak velocity in at least one UtA Doppler ultrasound spectrum. According to the same reasoning, absence of notch was defined by its bilateral absence.

Statistical analysis. Univariate data analysis comprised standard statistical methods: the chi-square test or the Fisher test (as adequate) for the study of independence amongst two factors, and the *t*-test for the assessment of statistically significant differences across means in two independent populations.

Multiple linear regression models with errors that were allowed to be correlated and/or to have unequal variances were fitted using generalized least squares. Multivariate regression had to be considered due to the experiment's nature: two different indexes were read on two different vessels for the same set of individuals, once at each trimester of the pregnancy. We looked for adequate global models and compared the curves (as functions of time but adjusted for potential confounders) instead of only doing comparison of mean indices between different time points.

The response variable read for index d (PI or RI), at vessel v (UtA or IIA), in a subject presenting notching at the first trimester with the status s (present or absent) and hypertension with the status h (hypertensive or normotensive), at (continuous) time t was denoted by $R(d,v,s,h,t)$. Dummy variables had to be considered for the index, vessel, status of notching at the first trimester and status of hypertension; reference categories were taken to be the resistance index, internal iliac artery, the normotensive status and the non-existence of unilateral notching at the first trimester, respectively. The fitted model was

$$R(d,v,s,h,t) = \beta_0(d,v,s,h,d*v,s*d,s*v,h*d,h*v) + \beta_1(d,v,d*v,h)t + \varepsilon$$

with residuals ε following a normal distribution with zero mean and with a variance-covariance matrix that allowed for a time autocorrelation structure of order 1 and for different variances across the indexes. In the above formula, the intercept coefficient β_0 is a function of the index, vessel, hypertensive status, unilateral notching status, and their two-way interactions, while the time-slope coefficient β_1 is a function of the index, vessel, and their interaction.

In order to understand the dynamic transition of each index (PI and RI) from the internal iliac artery to the uterine vessels, a model for the relative change was considered employing the quotient: (IIA index value – UtA index value)/(IIA index value). More precisely, for each of the indexes, the difference between its values on the internal iliac and uterine arteries was divided by the value read at the internal iliac artery for each trimester. Again a multiple regression model with correlated and heteroscedastic errors was adjusted, via generalized least squares.

Similarly to above, the response variable representing the proportion read for fixed index d, hypertensive status h, unilateral notching status s and time t, was denoted by $P(d,h,s,t)$. Dummy variables had to be considered for the index, status of unilateral notching at the first trimester and the status of hypertension; reference categories were taken to be the resistance index, the normotensive status and the non-existence of unilateral notching at the first trimester, respectively. The fitted model was

$$P(d,h,s,t) = \beta_0(d,h,d*h,s) + \beta_1(d,s)t + \varepsilon$$

with an intercept coefficient β_0 depending on d, h, s and the interaction term $d*h$, a time-slope coefficient depending on d and s, and residuals ε following a normal distribution with zero mean and with a variance-covariance matrix that allowed for a time autocorrelation structure of order 1 and for different variances across the indexes.

Final regression models were chosen on the basis of the lowest BIC (Bayesian Information Criterion). All statistical analyses were carried out using the R language and software environment for statistical computation, version 2.12.1[32]. The significance level was fixed at 0.05, as usual.

1. Robson, S. C., Hunter, S., Boys, R. J. & Dunlop, W. Serial study of factors influencing changes in cardiac output during human pregnancy. *Am J Physiol.* **256**, H1060–5 (1989).
2. Mabie, W. C., DiSessa, T. G., Crocker, L. G., Sibai, B. M. & Arheart, K. L. A longitudinal study of cardiac output in normal human pregnancy. *Am J Obstet Gynecol.* **170**, 849–56 (1994).
3. Palmer, S. K. *et al.* Quantitative estimation of human uterine artery blood flow and pelvic blood flow redistribution in pregnancy. *Obstet Gynecol.* **80**, 1000–6 (1992).
4. Konje, J. C., Kaufmann, P., Bell, S. C. & Taylor, D. J. A longitudinal study of quantitative uterine blood flow with the use of color power angiography in

appropriate for gestational age pregnancies. *Am J Obstet Gynecol.* **185**, 608–13 (2001).
5. Gómez, O. *et al.* Uterine artery Doppler at 11–14 weeks of gestation to screen for hypertensive disorders and associated complications in an unselected population. *Ultrasound Obstet Gynecol.* **26**, 490–4 (2005).
6. Gómez, O. *et al.* Reference ranges for uterine artery mean pulsatility index at 11–41 weeks of gestation. *Ultrasound Obstet Gynecol.* **32**, 128–32 (2008).
7. Papageorghiou, A. T., Yu, C. K., Erasmus, I. E., Cuckle, H. S. & Nicolaides, K. H. Assessment of risk for the development of pre-eclampsia by maternal characteristics and uterine artery Doppler. *BJOG.* **112**, 703–9 (2005).
8. Bower, S., Bewley, S. & Campbell, S. Improved prediction of preeclampsia by two-stage screening of uterine arteries using the early diastolic notch and color Doppler imaging. *Obstet Gynecol.* **82**, 78–83 (1993).
9. Veille, J. C., Tatum, K. & Zaccaro, D. Maternal right hypogastric artery blood flow during normal pregnancy and 6 weeks postpartum. *J Soc Gynecol Investig.* **3**, 191–8 (1996).
10. Kurmanavicius, J. *et al.* Reference resistance indices of the umbilical, fetal middle cerebral and uterine arteries at 24–42 weeks of gestation. *Ultrasound Obstet Gynecol.* **10**, 112–120 (1997).
11. Papageorghiou, A. T., Yu, C. K. & Nicolaides, K. H. The role of uterine artery Doppler in predicting adverse pregnancy outcome. *Best Pract Res. Clin Obstet Gynaecol* **18**, 383–96 (2004).
12. Sciscione, A. C. & Hayes, E. J. Society for Maternal-Fetal Medicine. Uterine artery Doppler flow studies in obstetric practice. *Am J Obstet Gynecol.* **201**, 121–6 (2009).
13. Giordano, R. *et al.* Uterine artery Doppler flow studies in obstetric practice. *J Prenat Med.* **4**, 59–62 (2010).
14. Stampalija, T., Gyte, G. M. & Alfirevic, Z. Utero-placental Doppler ultrasound for improving pregnancy outcome. *Cochrane Database Syst Rev.* CD008363. doi: 10.1002/14651858 (2010).
15. Khalil, A., Harrington, K., Muttukrishna, S. & Jauniaux, E. Effect of antihypertensive therapy with alpha-methyldopa on uterine artery Doppler in pregnancies with hypertensive disorders. *Ultrasound Obstet Gynecol.* **35**, 688–94 (2010).
16. Schulman, H., Fleischer, A., Farmakides, G., Bracero, L. & Grunfeld, L. Development of uterine artery compliance in pregnancy as detected by Doppler ultrasound. *Am J Obstet Gynecol.* **155**, 1031–6 (1986).
17. Pijnenborg, R. *et al.* Placental bed spiral arteries in the hypertensive disorders of pregnancy. *Br J Obstet Gynaecol.* **98**, 648–55 (1991).
18. Bower, S., Vyas, S., Campbell, S. & Nicolaides, K. H. Color Doppler imaging of the uterine artery in pregnancy: normal ranges of impedance to blood flow, mean velocity and volume of flow. *Ultrasound Obstet Gynecol.* **2**, 261–265 (1992).
19. Murakoshi, T., Sekizuka, N., Takakuwa, K., Yoshizawa, H. & Tanaka, K. Uterine and spiral artery flow velocity waveforms in pregnancy-induced hypertension and/or intrauterine growth retardation. *Ultrasound Obstet Gynecol.* **7**, 122–128 (1996).
20. Yu, C. K., Papageorghiou, A. T., Parra, M., Palma-Dias, R. & Nicolaides, K. H. Fetal Medicine Foundation Second Trimester Screening Group. Randomized control trial using low-dose asprin in the prevention of preeclampsia in women with abnormal uterine artery Doppler at 23 weeks' gestation. *Ultrasound Obstet Gynecol.* **22**, 233–9 (2003).
21. Poon, L. C., Akolekar, R., Lachmann, R., Beta, J. & Nicolaides, K. H. Hypertensive disorders in pregnancy: screening by biophysical and biochemical markers at 11–13 weeks. *Ultrasound Obstet Gynecol.* **35**, 662–70 (2010).
22. Magee, L. A. *et al.* CHIPS Study Group. How to manage hypertension in pregnancy effectively. *Br J Clin Pharmacol.* **72**, 394–401 (2011).
23. Lawlor, D. A. *et al.* Cardiovascular biomarkers and vascular function during childhood in the offspring of mothers with hypertensive disorders of pregnancy: findings from the Avon Longitudinal Study of Parents and Children. *Eur Heart J.* **33**, 335–45 (2012).
24. Ventura, W. *et al.* Reliability of examining the external iliac artery with Doppler ultrasound in the first trimester and its relationship with maternal blood pressure and uterine artery blood flow. *Eur J Obstet Gynecol Reprod Biol.* **165**, 42–6 (2012).
25. Sibai, B., Dekker, G. & Kupferminc, M. Pre-eclampsia. *Lancet.* **365**, 785–99 (2005).
26. Macdonald-Wallis, C. *et al.* Blood pressure change in normotensive, gestational hypertensive, preeclamptic, and essential hypertensive pregnancies. *Hypertension.* **59**, 1241–8 (2012).
27. NCCWCH, National Collaborating Centre for Women's and Children's Health (UK). Hypertension in Pregnancy: The Management of Hypertensive Disorders During Pregnancy. London: *RCOG Press.* 2010.
28. Romundstad, P. R., Magnussen, E. B., Smith, G. D. & Vatten, L. J. Hypertension in pregnancy and later cardiovascular risk: common antecedents? *Circulation.* **122**, 579–84 (2010).
29. Mustafa, R., Ahmed, S., Gupta, A. & Venuto, R. C. A comprehensive review of hypertension in pregnancy. *J Pregnancy.* doi: 10.1155/2012/105918 (2012).
30. Yudkin, P. L., Aboualfa, M., Eyre, J. A., Redman, C. W. & Wilkinson, A. R. New birthweight and head circumference centiles for gestational ages 24 to 42 weeks. *Early Hum Dev.* **15**, 45–52 (1987).
31. Snijders, R. J. & Nicolaides, K. H. Fetal biometry at 14–40 weeks' gestation. *Ultrasound Obstet Gynecol.* **4**, 34–48 (1994).
32. R Development Core Team. R: A Language and Environment for Statistical Computing. R Foundation for Statistical Computing, Vienna, Austria, 2008. Available at http://www.R-project.org. Accessed October 30, 2012.
33. Brosens, I., Pijnenborg, R., Vercruysse, L. & Romero, R. The "Great Obstetrical Syndromes" are associated with disorders of deep placentation. *Am J Obstet Gynecol.* **204**, 193–201 (2011).
34. Browne, V. A. *et al.* High-end arteriolar resistance limits uterine artery blood flow and restricts fetal growth in preeclampsia and gestational hypertension at high altitude. *Am J Physiol Regul Integr Comp Physiol.* **300**, 1221–9 (2011).
35. Chien, P. F., Arnott, N., Gordon, A., Owen, P. & Khon, K. How useful is uterine artery Doppler flow velcimetry in the prediction of preeclampsia, intrauterine growth retardation and perinatal death? An overview. *BJOG.* **107**, 196–208 (2000).

Acknowledgments

The staff of the Department of Obstetrics of Centro Hospitalar do Porto is acknowledged. We thank Sérgio Evangelista, Laboratório de Iconografia, Faculdade de Medicina da Universidade do Porto, for illustrations. This work was supported in part by «Prémio Crioestaminal» (Federação das Sociedades Portuguesas de Ginecologia e Obstetrícia, Portugal) and FCT project - PEst-C/MAT/UI00144/2011.

Author contributions

L.G.-M. and H.A. designed the study, analyzed the data and wrote the manuscript; A.C. coordinated quality control of ultrasound data; J.S. coordinated review of clinical cases and organization of study groups; R.G. performed all statistical analyses; F.M. designed the study. All authors contributed to the data interpretation and the final version of the manuscript, which they all approve.

Additional information

Competing financial interests: The authors declare no competing financial interests.

How to cite this article: Guedes-Martins, L. *et al.* Internal iliac and uterine arteries Doppler ultrasound in the assessment of normotensive and chronic hypertensive pregnant women. *Sci. Rep.* **4**, 3785; DOI:10.1038/srep03785 (2014).

Article 5

Guedes-Martins L, Graça H, Saraiva JP, Guedes L, Gaio R, Cerdeira AS, Macedo F, Almeida H. The effects of spinal anaesthesia for elective caesarean section on uterine and umbilical arterial pulsatility indexes in normotensive and chronic hypertensive pregnant women: a prospective, longitudinal study. *BMC Pregnancy Childbirth.* 2014; 14:291.

Guedes-Martins et al. BMC Pregnancy and Childbirth 2014, 14:291
http://www.biomedcentral.com/1471-2393/14/291

BMC Pregnancy & Childbirth

RESEARCH ARTICLE Open Access

The effects of spinal anaesthesia for elective caesarean section on uterine and umbilical arterial pulsatility indexes in normotensive and chronic hypertensive pregnant women: a prospective, longitudinal study

Luís Guedes-Martins[1,2*], Helena Graça[3], Joaquim P Saraiva[1,4], Luísa Guedes[5], Rita Gaio[6,7], Ana S Cerdeira[8,9], Filipe Macedo[10,11] and Henrique Almeida[2,12]

Abstract

Background: Despite the known effects of neuraxial blockade on major vessel function and the rapid decrease in uterine vascular impedance, it is unclear how the blockade affects the utero-placental circulation in the near-term. We hypothesize that among women with chronic hypertension, a loss of sympathetic tonus consequent to spinal block may cause significant changes in the utero-placental haemodynamics than the changes typical in normal pregnant women. Therefore, the main study objective was to analyse the effect of spinal anaesthesia for caesarean section on uterine and umbilical arterial impedance in pregnant women at term diagnosed with stage-1 chronic hypertension.

Methods: A prospective, longitudinal study was performed in singleton pregnant women (203 low-risk and 33 with hypertension) scheduled to undergo elective caesarean section. The mean arterial blood pressure and pulsatility indexes for the uterine and umbilical arteries were recorded before and after spinal anaesthesia was performed using 8–9 mg hyperbaric bupivacaine (5 mg/mL) and 2–2.5 μg sufentanil (5 μg/mL). Multiple linear regression models with errors capable of correlation or with unequal variances were fitted using the generalized least squares.

Results: In normotensive women, the mean arterial blood pressure decreased after administering spinal anaesthesia ($p < 0.05$). The pulsatility index of the uterine and umbilical arteries did not change after spinal anaesthesia. In the hypertensive women, the mean arterial blood pressure ($p < 0.05$) and uterine artery pulsatility index ($p < 0.05$) decreased. In both groups, the umbilical artery pulsatility index did not change after spinal anaesthesia.

Conclusions: In stage-1 chronic hypertensive pregnant women at term, spinal anaesthesia for caesarean section reduces uterine artery impedance but not umbilical artery impedance.

Keywords: Spinal anaesthesia, Caesarean section, Blood flow velocity, Hypertension

* Correspondence: luis.guedes.martins@gmail.com
[1]Departamento da Mulher e da Medicina Reprodutiva, Centro Hospitalar do Porto EPE, Largo Prof. Abel Salazar, 4099-001 Porto, Portugal
[2]Department of Experimental Biology, Faculty of Medicine, University of Porto, 4200-319 Porto, Portugal
Full list of author information is available at the end of the article

Background

Hypertension affects 5–15% of pregnancies [1] and creates additional challenges for the mother [2,3] and foetus [4,5]. One major challenge is the increased risk of preeclampsia, eclampsia [6,7], and related conditions, such as preterm delivery [5,6] and intrauterine growth restriction [6,8], that increase morbidity and mortality in the mother [2] and foetus [4,9].

Introduction of a local anaesthetic, such as bupivacaine, into the subarachnoid space to induce anaesthesia and analgesia has long been used during delivery [10] and is advantaged by a short procedure time [11], rapid onset [10], and high success rate [10,12]. However, maternal hypotension may develop soon after anaesthetic administration [13-17] as a consequence of sympathetic blockade, which causes arterial and arteriolar vasodilation [18,19]. Venodilation may also occur, which decreases the cardiac preload and cardiac output, and promotes bradycardia and maternal hypotension. These impacts are further aggravated by aortocaval compression caused by the gravid uterus [15].

Despite the known effects of neuraxial blockade on major vessel function and the rapid decrease in uterine vascular impedance, which can occur in seconds, it is unclear how the blockade affects the utero-placental circulation in the near-term. Furthermore, it is unknown whether hypertension poses additional constraint on local circulatory regulation, because few, if any, studies have evaluated the maternal and foetal haemodynamics in pregnant women with chronic arterial hypertension undergoing spinal anaesthesia.

Many pathophysiologic factors have been implicated in the genesis of chronic arterial hypertension. In most cases, the root cause of the disease remains unknown, but there is mounting evidence that chronic hypertension is initiated and maintained by an elevated sympathetic tone [20]. We hypothesize that among women with chronic hypertension, a loss of sympathetic tonus consequent to spinal block may cause significant changes in the utero-placental haemodynamics than the changes typical in normal pregnant women. Therefore, the current study aimed to compare the effects of spinal anaesthesia comprising hyperbaric bupivacaine for elective caesarean section on uterine and umbilical arteries impedance in normotensive and chronic hypertensive women.

Methods

Subjects

This study was approved by the local ethics committee of Centro Hospitalar do Porto–Unidade Maternidade Júlio Dinis. All subjects provided informed consent (IRB protocol number: 133/10 [086-DEFI/126-CES]).

The study was performed from January 2010 to December 2012. Inclusion criteria were: parturient with singleton term pregnancies and gestational age ≥ 37 weeks, healthy condition or stable chronic arterial hypertension without known target organ involvement, scheduled for elective caesarean section due to foetal breech presentation, suspected cephalopelvic disproportion, or previous caesarean.

Exclusion criteria were: patients in labour or with ruptured membranes; those with multiple gestations, coagulopathy, diabetes, or any pregnancy-induced hypertension including preeclampsia; and those receiving β-tocolytic drugs. Subjects were also excluded from the study as follows: contraindication or impossibility to perform spinal anaesthesia, bilateral sensory block that could not be extended to the T6-T4 level, intravenous drug administration that may alter the haemodynamic state (ex. opioids, propofol), or a history of hypersensitivity to local anaesthetic.

Chronic arterial hypertension was defined as a blood pressure of 140/90 mmHg on more on two occasions before 20 weeks of gestation or after 20 weeks of pregnancy if the findings persist beyond 12 weeks postpartum [21]. However, only women with a history of chronic arterial hypertension prior to pregnancy were enrolled in the study. Acceptable medication was folic acid, vitamin, and iron supplements. All hypertensive pregnant women received acetylsalicylic acid (100 mg daily) and methyldopa (750 mg daily). Gestational age was calculated by the crown-rump length between 11 and 14 weeks [22] by several experienced sonographers from the Prenatal Diagnosis Department of our institution.

On the day of caesarean section, biometrical data was collected and the patients were observed by a senior specialist who reviewed their medical record.

The infant was examined by a neonatologist at birth and 1 month later. The new born physical assessment included: Apgar scoring, birth weight, head circumference, abdominal circumference, length, vital signs (temperature, pulse, and respiratory rate), general appearance, and physical and neuromuscular maturity.

The maternal haemodynamic assessment was performed at two time points: (1) before spinal anaesthesia and (2) immediately after inducing spinal anaesthesia. The upper level of dermatome block between T4-T6 was tested by cold sensation and was deemed adequate for surgical anaesthesia.

Spinal anaesthesia for elective caesarean section

Women were administered intravenous 10 mg metoclopramide and 50 mg ranitidine 2 hours preoperatively. Intravenous cefazoline (2 g) was also administered to all patients 30 minutes before anaesthetic induction. All patients received 500 mL of Lactated Ringer's solution intravenously 15 minutes before receiving anaesthesia and oxygen (3 L/min) through nasal prongs; blood

pressure, electrocardiography, and pulse oximetry were monitored throughout. Patients were placed in a sitting position, the midline approach was used in all women, and the block was performed at the mid-lumbar level. The subarachnoid block was performed in the surgical suite using a combined needle-through-needle spinal-epidural technique (typical for caesarean section at our institution) with an epidural 18-G tuohy needle and 27-G subarachnoid pencil point needle. Spinal anaesthesia comprised 8–9 mg of hyperbaric bupivacaine (5 mg/mL) and 2–2.5 μg sufentanil (5 μg/mL) administered intrathecally, targeting the T4-S4 dermatomes. If the bilateral sensory block could not be extended to the T6-T4 level, then the patient was excluded.

Blood pressure assessment

Blood pressure (BP) was recorded using an automated instrument (GE Healthcare Carescape™ V100 Vital Signs Monitor with DINAMAP Blood Pressure) at 2-min intervals from induction to delivery. Baseline BP was obtained as the mean of three consecutive measurements taken 2 minutes apart before subarachnoid block and insertion of the epidural catheter; a second measurement was recorded immediately after instilling spinal anaesthesia. The blood pressure was expressed as the mean arterial pressure (MAP) employing the formula:

$$MAP = \frac{(2 \times diastolic\ pressure) + systolic\ pressure}{3}$$

Maternal hypotension was treated with ephedrine when necessary. The standard for vasopressor (VP) administration was defined as a 20% decrease from the baseline mean arterial pressure at any time after induction. Cases that were adequately managed by increasing the rate of fluid infusion without need for VP administration at the second blood pressure measurement were included. Cases requiring VP administration before the second Doppler flow assessment were excluded.

Doppler flow assessment

The Doppler flow was evaluated in the right and left uterine and umbilical arteries immediately before (first time point) and after (second time point) spinal anaesthesia using a 4 MHz convex transabdominal probe (GE Healthcare Technologies, GE LOGIC 6, USA). All measurements were made by a single investigator with a high level of expertise in Doppler ultrasound (L.G-M) to minimize inter-observer variability. Intra-observer reliability was estimated from two consecutive readings among the first 30 recordings of the pulsatility indexes in the uterine and umbilical arteries. For uterine artery evaluation, the probe was placed on the lower abdominal quadrants and angled medially, and colour Doppler imaging was used to localize the uterine artery (UtA) as it crossed over the external iliac artery. In all cases, an angle less than 30° was assured before the pulsed Doppler probe was placed over the entire vessel width. Angle correction was then applied, and the signal updated until three similar consecutive waveforms were evidenced to calculate the left and right uterine arteries pulsatility (UtA-PI) indexes as follows:

$$PI = \frac{\text{systolic peak velocity} - \text{end diastolic velocity}}{\text{mean velocity during cardiac cycle}}$$

using the device software (GE Healthcare Technologies, GE LOGIC 6, USA). The mean UtA-PI in the left and right arteries were then determined.

The umbilical artery (U) Doppler flow spectrum was recorded from a free cord loop, and the mean of three consecutive waveforms was analysed to determine the U-PI. Women with absent or reversed diastolic umbilical artery flow before undergoing the subarachnoid block were not included.

No more than 2 minutes were required for the waveform acquisitions. Additionally, the sequence of measurements was extremely accurate and always performed in the same order: (1) right uterine artery, (2) left uterine artery, and finally, (3) the umbilical artery.

Statistical analysis

Univariate data analysis comprised standard statistical methods: Chi-square test or Fisher's test (as appropriate) to compare frequencies within a single categorical variable or to determine independence among two factors; and the *t*-test to assess statistically significant differences between means in two independent populations.

Multiple linear regression models with errors that were correlated or had unequal variances were fitted using the generalized least squares and maximum likelihood estimation. Time was considered a dichotomous variable, reflecting the two evaluation time points.

The PI value at vessel v (UtA or U), time t (before or after spinal anaesthesia), or in a hypertensive patient h (hypertensive or normotensive) was denoted by PI (v, t, h). Dummy variables were considered for the vessels, time, and hypertensive status; the UtA, the time before spinal anaesthesia, and the normotensive status, respectively, were designated as reference categories. The fitted model was as follows:

$$PI(v,t,h) = \beta_0(v,h,v \times h) + \beta_1(v,h,v \times h)t + \varepsilon \quad (1)$$

with errors ε following a normal distribution with a zero mean, a variance-covariance matrix having a correlation structure of compound symmetry at the 2-level grouping structure according to the subject or vessel, and different variances according to the vessel. In the above formula,

Guedes-Martins et al. BMC Pregnancy and Childbirth 2014, 14:291
http://www.biomedcentral.com/1471-2393/14/291

the intercept coefficient β_0 and the time-slope coefficient β_1 are the linear functions of the vessel, the hypertensive status, and their two-way interaction.

For the chosen MAP model, we obtained the following equation:

$$MAP(t,h) = \beta_0(h) + \beta_1(h)t + \varepsilon \quad (2)$$

with errors ε following a normal distribution with a zero mean, a variance-covariance matrix with a correlation structure of compound symmetry for each woman, and different variances according to time. The intercept coefficient β_0 and the time-slope coefficient β_1 were linear functions of the hypertensive status h. Dummy variables for the hypertensive status and time were chosen as in model (1).

Data were plotted to assess the assumptions of normality and heteroscedasticity of the above models. The normal plots of the residuals indicated departures from normality in model (1) and no compromising features in model (2). After removing the observations with standardized residuals in the PI model higher than 3.5 (corresponding to 17 observations from 10 different women, with only one hypertensive), the normality problems seemed to resolve. The outliers corresponded to 17 observations from 10 different women, with only woman hypertensive, and essentially matched the women with PI-values higher than the empirical 98th percentile. Graphical analyses confirmed that the variance function models were successful in accommodating the error heteroscedasticity.

Intraclass correlation coefficients (ICC) and 95% confidence intervals were calculated using a two-way mixed-effects model with absolute agreement. ICC was used to assess repeatability because there is sufficient scientific consensus designating an ICC > 0.7 as reflecting a very low measurement error [23,24]. The reliability coefficient, which is the difference value that will be exceeded by only 5% of measurement pairs on a single subject, was calculated as follows: 1.96 times the standard deviation of the difference between pairs of repeated measurements [23].

Final regression models were chosen based on the lowest Akaike Information Criterion. All statistical analyses were performed using the R language and software environment for statistical computation, version 2.12.1 [25]. The significance level was fixed at 0.05.

Our research has adhered to the Strengthening the Reporting of Observational studies in Epidemiology (STROBE) guidelines for observational studies, and all recommendations were included in the study [Additional file 1].

Results

A total 277 pregnant women at term were considered eligible for this study according to the established inclusion criteria. Forty-one were excluded (13.9%): 11 patients were in early labour; 8 had multiple pregnancies; 7 had diabetes; 5 required bolus administration of VP prior to the Doppler flow assessment; 4 presented technical difficulties in calculating the pulsatility index of the uterine and umbilical arteries; 3 did not have an adequate anaesthetic blockade; 2 had suspected preeclampsia; and 1 refused to participate in the study.

Among the 236 women enrolled in the study, 203 (86%) were normotensive (NT), and 33 (14%) had chronic arterial hypertension stage 1 (HT).

The main characteristics and pregnancy outcomes of the 236 women are depicted in Table 1. Their ages

Table 1 Demographic characteristics and pregnancy outcomes of the 236 included women

		All	Normotensive	Hypertensive	
		n = 236	n = 203	n = 33	p*
Age, mean (SD)		30.0 (6.1)	29.7 (6.0)	31.7 (6.5)	0.110
Parity, median (IQR)		0 (0–1)	0 (0–1)	0 (0–0)	0.047
Education level (in years), n(%)	<7	7 (3%)	4 (2%)	3 (9%)	0.199
	7-9	77 (33%)	66 (33%)	11 (33%)	
	10-12	105 (44%)	92 (45%)	13 (40%)	
	>12	47 (20%)	41 (20%)	6 (18%)	
Body Mass Index[a] (Kg/m), mean (SD)		28.5 (5.6)	27.9 (5.3)	32.5 (5.3)	<0.001
Smoking, n(%)		23 (10%)	19 (9%)	4 (12%)	0.857
Gestational age at delivery (weeks), mean(SD)		40.0 (0.8)	40.1 (0.8)	39.5 (0.8)	<0.001
UtA bilateral notching absence[a]		228 (97%)	196(97%)	32(97%)	1.000
Birth weight at delivery (g), mean (SD)		3140.2 (340.5)	3123.0 (338.8)	3245.9 (337.1)	0.059
Apgar Index 5′	<7	0(0)	0(0)	0(0)	

[a]Body Mass Index and UtA notching were determined before the caesarean section; UtA, uterine artery; SD, standard deviation; IQR, Inter-quartile range. The Chi-square or Fisher's test were used as appropriate to compare frequencies within a single categorical variable or to determine independence when applied to two categorical variables; the *t*-test was used to compare the means between two independent populations. *p, indicates the homogeneity in the proportions between the hypertensive and normotensive groups.

Table 2 Mean (SD) MAP of 236 women before and after bupivacaine anaesthetic blockade

T6-T4 anaesthetic blockade	All (n = 236)	Normotensive (n = 203)	Hypertensive (n = 33)	p
MAP before	86.3 (12.6)	83.1 (10.1)	105.5 (8.9)	<0.001
MAP after	78.8 (8.5)	76.2 (5.7)	94.5 (5.8)	<0.001

SD, standard deviation; MAP, mean arterial pressure.

ranged from 18 to 43 years old; 74% of the subjects were less than 34 years old, and a similar proportion (77%) were not educated beyond the secondary level (maximum of 12 years). For 68% of the women, this was their first pregnancy and most was non-smokers. The mean gestational age at the time of evaluation (caesarean section) was 40.0 weeks (range: 37.0–41.1 weeks). The NT and HT groups (Table 1) showed statistically significant differences in parity (nulliparous predominantly in the HT group), BMI distribution (highest values predominantly in the HT group, $p < 0.001$), and gestational age at delivery (mean gestational age of HT group was slightly but significantly lower than the NT group, 39.5 vs. 40.1 weeks, $p < 0.001$). The mean new born weight was 3140.2 g (±340.5 g), with no significant difference between the NT and HT groups ($p = 0.059$).

In the majority of patients (97%), the uterine artery notch was absent bilaterally.

Blood pressure data are presented in Table 2. Hypertensive pregnant women exhibited a significantly higher MAP at both time points ($p < 0.001$).

The reliability coefficients for the UtA-PI and U-PI indexes were 0.111 and 0.076, respectively. The ICC indicating the intra-observer reliability for the UtA-PI and U-PI measurements were very high at 0.963 and 0.899, respectively; the ICC values ranged from 0.923 to 0.982 and 0.797 to 0.951, respectively.

UtA-PI and U-PI data before and after spinal anaesthesia are presented in Table 3. Before anaesthetic blockade, the UtA-PI was significantly higher in the chronic hypertensive pregnant women than in the normotensive patients ($p = 0.022$).

Multiple analysis

MAP model

Both at the first and second time points, the predicted mean MAP for the HT group was significantly higher than that for the NT group. After blockade, the mean MAP decreased in both groups, with the HT group presenting the highest difference between the two time points (Figure 1). The calculated model for MAP provided expected values for the different combinations of time and hypertensive status (Figure 1 and Table 4) as follows: before anaesthesia, NT group: 83.1 mmHg (95% CI: 81.88–84.5), HT group: 105.5 mmHg (95% CI: 102.2–108.9); and after anaesthesia, NT group: 76.2 mmHg (95% CI: 75.5–77.0), HT group: resp. 94.5 mmHg (95% CI: 92.6–96.5). In particular, the model predicted an 8.3% decrease in the mean MAP in normotensive women and a 10.4% decrease in hypertensive women ($p < 0.05$).

All regression coefficients were statistically significant (Table 4). Moreover, the single correlation parameter (generally referred to as the intra-class correlation coefficient) was estimated at 0.533 (95% CI: 0.436–0.619), and the variance after anaesthetic blockade was predicted at 57.2% (95% CI: 51.3–63.7%) of the variance before blockade. Statistically significant population mean MAP values were estimated for all of the different time and hypertension combinations (Figure 1).

UtA-PI and U-PI model

The model was fitted for both vessels simultaneously. If the process had been done independently for each vessel, the significance level of the conclusions would have been inflated. At the first time point, but not at the second time point, the expected UtA-PI was significantly higher in the HT group than in the NT group. After blockade, there was a statistically significant decrease in the expected UtA-PI only within the HT group (Figure 2). The predicted mean U-PI was not significantly different between the NT and HT groups at any time point, and no significant changes were identified within any of the groups across time (between the first and second time points) (Figure 2). Although all regression coefficients were statistically significant (Table 5) these predictions also accommodated the correlation structure of the model errors. The correlation parameter was estimated at 0.676 (95% CI: 0.623–0.723).

Table 3 Mean (SD) uterine/umbilical artery PI indexes measured by transabdominal ultrasound before and after bupivacaine anaesthesia

T6-T4 anaesthetic blockade	UtA-PI			U-PI		
	Normotensive	Hypertensive	p	Normotensive	Hypertensive	p
Before	0.80 (0.20)	0.87 (0.16)	0.022	0.81 (0.10)	0.82 (0.12)	0.596
After	0.78 (0.19)	0.73 (0.15)	0.068	0.81 (0.08)	0.83 (0.12)	0.299

SD, standard deviation; PI, pulsatility index; UtA, uterine artery; U, umbilical artery.

Guedes-Martins *et al. BMC Pregnancy and Childbirth* 2014, **14**:291
http://www.biomedcentral.com/1471-2393/14/291

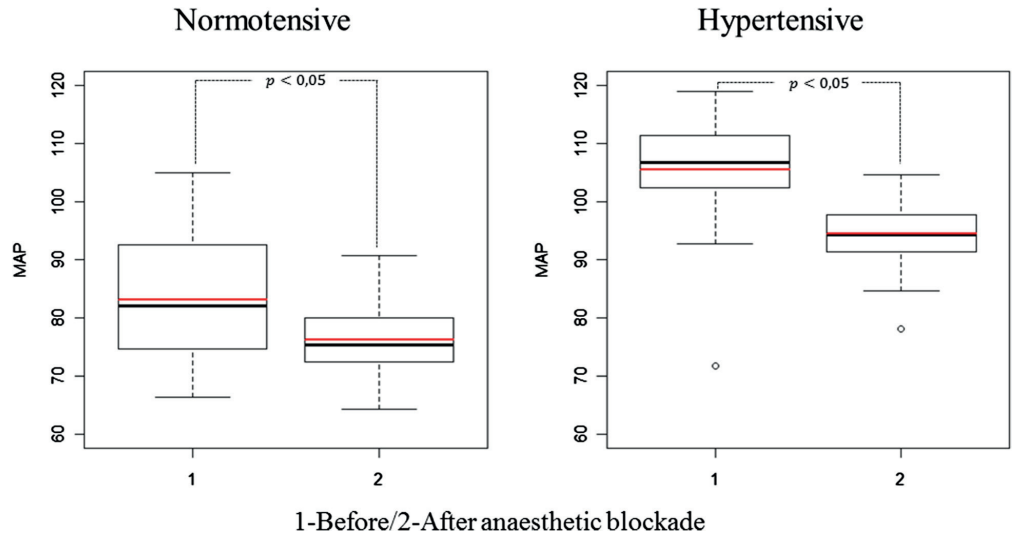

Figure 1 Boxplots of the observed (black) and predicted (red) MAP values before (1) and after (2) the bupivacaine anaesthetic blockade in the normotensive (left) and hypertensive (right) groups. The predicted values were determined using the fitted models. The bold horizontal line represents the median while the bottom and top of the box correspond to the 25th and 75th percentiles, respectively; the height of the box is denoted by interquartile range (IQR); the end of the whiskers represent the lowest datum still within 1.5 IQR of the lower quartile, and the highest datum still within 1.5 IQR of the upper quartile. MAP, mean arterial pressure.

Discussion

Maintenance of normotension requires a number of physiologic mechanisms; derangement in these mechanisms may lead to hypertension [26-29]. Hyperactivity of the sympathetic nervous system is one such derangement that has been shown to contribute to hypertension initiation [26], maintenance [28,29], and progression [27,29].

Hypertension is a major human disorder and an increasingly important public health issue [30] that extends into pregnancy. Although spinal anaesthesia is the most commonly used method of providing surgical anaesthesia for elective caesarean delivery, spinal hypotension can commonly occur in up to 70% of patients [31]. However, the influence of spinal hypotension on uteroplacental perfusion among women with chronic hypertension has been poorly examined.

Table 4 Estimated coefficients and 95% CI of the regression model used to predict the MAP in different variable combinations

Variables	Coefficient	95% CI
Intercept	83.131	(81.765, 84.498)*
After (*vs* before) anaesthetic blockade	−6.900	(−8.057, −5.743)*
Hypertensive (*vs* normotensive) women	22.414	(18.760, 26.069)*
After anaesthetic blockade and Hypertensive women	−4.130	(−7.224, −1.037)*

*Significant designated at p < 0.05.; CI, confidence interval; MAP, mean arterial pressure.

To analyse the effect of anaesthetic spinal blockade on uterine and umbilical circulation, normotensive and stage-1 chronic hypertensive pregnant women at term who were undergoing an elective caesarean section were enrolled. Not unexpectedly, we found a statistically significant decrease in MAP after inducing spinal anaesthesia in both groups, most prominently in the chronic HT group. This finding likely reflects the rapid onset of sympathetic blockade [32,33] and emphasizes the dependence of hypertension on sympathetic intervention, which is distinct from other possible mechanisms such as reduced intravascular volume and left ventricular dysfunction.

It was not our main goal to compare the hypotension incidence between the HT and NT groups, but instead, to study the influence of the decreased MAP during spinal anaesthesia on the uterine artery impedance and to understand the impact on the foetal circulation. Our study is unique as it is the first report evaluating the maternal and foetal circulations in at-term patients with chronic arterial hypertension in the absence of labour, i.e., in the absence of related confounding factors. To that end, Doppler velocimetry was employed because it is a non-invasive tool able to assess the pathophysiological mechanisms underlying foetal [34,35] and maternal [36-39] perfusion changes.

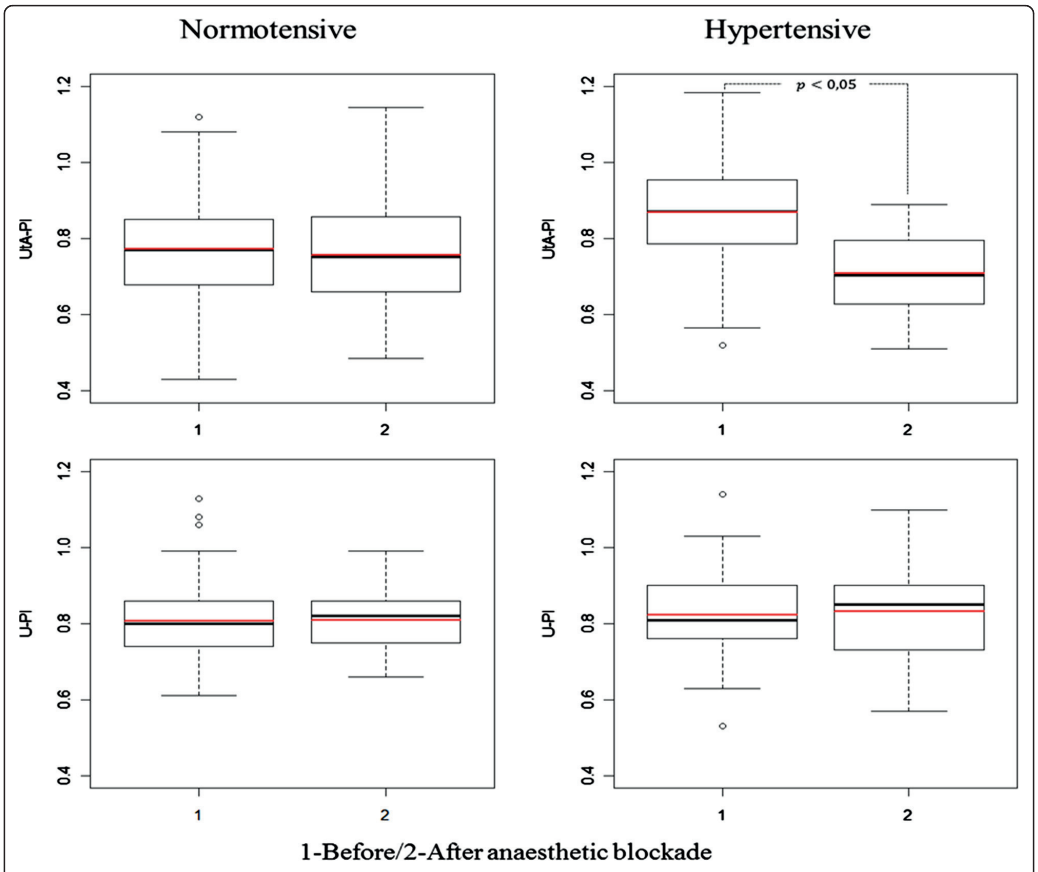

Figure 2 Boxplots of the observed (black) and predicted (red) UtA-PI and U-PI values before (1) and after (2) the bupivacaine anaesthetic blockade in the normotensive (left) and hypertensive (right) groups. The predicted values were determined using the fitted models. PI, pulsatility index; UtA, uterine artery; U, umbilical artery.

Because of the difficulty of performing absolute blood flow measurements, most studies have favoured quantitative analysis of flow-velocity waveform change. The PI is the most commonly used index [36,37] because it describes the shape of the velocity waveform much better than other indexes [36].

There has been concern that during pregnancy, the regulation of pelvic circulation may be disrupted after a sudden decrease in maternal MAP, compromising perfusion to the foetus. This concern was previously addressed in studies performing Doppler velocimetry of umbilical and uterine arteries during epidural analgesia in normal labour patients at term. However, the results were rather conflicting as some authors reported no change in uterine and foetal [40-42] circulations, whereas others found a significant decrease in the resistance of the uterine and umbilical arteries [43]; others even reported an association between the epidural analgesia, maternal hypotension, and increased resistance indexes for the uterine arteries [44,45]. The variations in reported findings are the likely result of substantially different study conditions. In fact, the previous investigations were performed during labour, had small sample sizes, used less capable ultrasonography systems, or employed epidural analgesia, which causes less sympathetic blockade compared with spinal anaesthesia [46-48].

In this study, UtA-PI was significantly higher in the HT group compared with the NT group before spinal anaesthesia. However, upon establishing spinal anaesthesia, both UtA-PI values decreased to a similar mean, demonstrating that UtA-PI decreased significantly in HT women, compared with NT women. This observation is compelling evidence that chronic hypertensive pregnant

Guedes-Martins *et al. BMC Pregnancy and Childbirth* 2014, **14**:291
http://www.biomedcentral.com/1471-2393/14/291

Table 5 Estimated coefficients and correspondent 95% CI of the regression model used to predict the pulsatility index before and after spinal anaesthesia within each artery (UtA or U), adjusted according to the hypertensive status

Variables	Coefficient	95% CI
Intercept	0.773	(0.757, 0.789)*
After (*vs* Before) anaesthetic blockade	−0.016	(−0.030, −0.002)*
U (*vs* UtA)	0.034	(0.012, 0.056)*
Hypertensive (*vs* Non-Hypertensive) women	0.096	(0.053, 0.139)*
U x Hypertensive women	−0.081	(−0.140, −0.022)*
U x After anaesthetic blockade	0.019	(0.001, 0.037)*
After anaesthetic blockade x Hypertensive women	−0.145	(−0.182, −0.108)*
After anaesthetic blockade x Hypertensive women x U	0.153	(0.104, 0.202)*

*Significance designated at $p < 0.05$; CI, confidence interval; UtA, uterine artery; U, umbilical artery; PI, pulsatility index.

women are vulnerable to sympathetic blockade. The findings emphasize the role of the sympathetic nervous system in regulating hypertension and suggest different levels of sympathetic activation in HT patients compared with NT patients [49,50].

Our findings were obtained from linear and parametric models that satisfied the assumption of errors normality. Nevertheless, the difference in sample size between the hypertensive and the normotensive groups is a study limitation, especially in the PI model, which considers a higher number of parameters than does the MAP model. This limitation must be acknowledged when interpreting the regression coefficients [51]. Fortunately, the number of subjects is reasonably large relative to the number of measurement occasions, which strengthens our study and conclusions. Overall, our numbers were in line with the hypertension prevalence within the respective women age group [52].

Study limitations and future research

(1) The study comprises uneventful pregnancies and cannot be extrapolated to patients with other forms of hypertensive disease in pregnancy. (2) From the first trimester onwards, HT patients were medicated with 750 mg methyldopa and low-dose acetylsalicylic acid daily, medications that were previously shown not to affect the uterine and umbilical arteries impedance [53-55]. (3) The second Doppler measurement was made just after blockade was achieved, which introduces light variations in time. The Doppler flow evaluation of the right and left uterine and umbilical arteries was performed immediately before performing spinal anaesthesia (first time point) and after blockade was achieved (second time point). Therefore, the time from the first to the second Doppler acquisition was dependent on the time necessary to achieve anaesthetic blockade (~5 minutes). Although not identical for all the patients, the duration was similar among them because only the procedures considered technically easy and uneventful were eligible for the study. In fact, no more than two minutes was required for to measure the waveforms in both the uterine and umbilical arteries (recorded from a free cord loop). Additionally, the measurement sequence was extremely accurate and always performed in the same order: the right uterine artery, the left uterine artery, and finally, the umbilical artery. (4) Serious hypotension requiring VP were excluded, but additional studies will be needed evaluating this subset of patients. (5) There was a sample size imbalance between the hypertensive and the normotensive groups due to elimination of outliers; 16% of the women that were considered for the fitting of the MAP model were hypertensive, while only 17% were in the PI model. While this is adequate for the MAP model, the results inferred from the PI model must be interpreted cautiously. (6) Because we did not assessed neonatal outcomes in detail, no relationship between the vascular indexes and neonatal outcomes in both groups was explored. Thus, the clinical relevance of our findings remains uncertain. (7) There were additional concerns that in the chronic hypertensive population, the reduction of UtA-PI to values equivalent to those in the normal population might actually indicate uterine hypoperfusion and foetal circulation compromise [42,56], independent of successful compensation against maternal hypotension using VP. This concern is not supported by the current study as there was no change in the U-PI in NT and HT pregnancies, before and after anaesthetic blockade. In contrast, previous studies have shown that in pre-eclamptic women, epidural anaesthesia may help reduce uterine artery vasospasm and may improve intrapartum foetal well-being [18,19]. However, in pregnant women with chronic arterial hypertension, this benefit has not been demonstrated.

Conclusions

In conclusion, our results revealed that in normotensive pregnant women at term, the PI of the uterine artery does not change, before and immediately after administering spinal anaesthesia comprising 8–9 mg of hyperbaric bupivacaine (5 mg/mL) and 2–2.5 μg sufentanil (5 μg/mL) intrathecally. However, in chronically hypertensive women with uncomplicated pregnancies, the mean arterial blood pressure decrease was accompanied by a significant reduction in the UtA-PI. Nevertheless, no change in umbilical artery pulsatility index was found, suggesting that despite the UtA-PI drop, the local circulatory mechanisms are apparently activated prevent adverse foetal effects. More research is needed to assess the relationships between U-PI and UtA-PI values with neonatal outcomes among women with hypertensive disorders undergoing spinal anesthesia.

Additional file

Additional file 1: STROBE Statement—checklist of items that should be included in reports of observational studies. Description of data: Indicates where each of the recommended items is reported in the manuscript.

Abbreviations

BP: Blood pressure; BMI: Body mass index; HT: Hypertensive; ICC: Intraclass correlation coefficients; MAP: Mean arterial pressure; NT: Normotensive; PE: Preeclampsia; PI: Pulsatility index; U: Umbilical artery; UtA: Uterine artery; VP: Vasopressors.

Competing interests

The authors declare that they have no competing interests.

Authors' contributions

LG-M designed the study, performed all Doppler measurements, analysed the data, and composed the manuscript. HG induced anaesthesia, and JPS coordinated quality control of the ultrasound data and contributed to the critical revision of the manuscript. LG coordinated the review of clinical cases and organization of study groups. RG performed all statistical analyses. ASC contributed to the critical revision of the manuscript; FM designed the study, and HA designed the study, analysed the data, and composed the manuscript. All authors contributed to the data interpretation and the final version of the manuscript, which all approved. All authors read and approved the final manuscript.

Acknowledgements

We thank the staff Department of Obstetrics of Centro Hospitalar do Porto for their kind contributions to this work.

Author details

[1]Departamento da Mulher e da Medicina Reprodutiva, Centro Hospitalar do Porto EPE, Largo Prof. Abel Salazar, 4099-001 Porto, Portugal. [2]Department of Experimental Biology, Faculty of Medicine, University of Porto, 4200-319 Porto, Portugal. [3]Department of Anaesthesiology, Centro Hospitalar do Porto EPE, Largo Prof. Abel Salazar, 4099-001 Porto, Portugal. [4]Obstetrics-Gyneacology, Private Hospital Trofa, 4785-409 Trofa, Portugal. [5]Department of Anaesthesiology, Centro Hospitalar S. João, 4200-319 Porto, Portugal. [6]Department of Mathematics, Faculty of Sciences, University of Porto, Porto, Portugal. [7]CMUP-Centre of Mathematics, University of Porto, Porto, Portugal. [8]Gulbenkian Program for Advanced Medical Education, 1067-001 Lisbon, Portugal. [9]Department of Medicine, Beth Israel Deaconess Medical Center, Harvard Medical School, Boston, MA 02215, USA. [10]Department of Medicine, Faculty of Medicine, University of Porto, 4200-319 Porto, Portugal. [11]Serviço de Cardiologia, Centro Hospitalar S. João, 4200-319 Porto, Portugal. [12]Obstetrics-Gynecology, Hospital-CUF Porto, 4100 180 Porto, Portugal.

Received: 20 March 2014 Accepted: 24 August 2014
Published: 28 August 2014

References

1. Lo JO, Mission JF, Caughey AB: **Hypertensive disease of pregnancy and maternal mortality.** *Curr Opin Obstet Gynecol* 2013, **25:**124–132.
2. Moodley J: **Maternal deaths due to hypertensive disorders in pregnancy.** *Best Pract Res Clin Obstet Gynaecol* 2008, **22:**559–567.
3. Lemonnier M, Beucher G, Morello R, Herlicoviez M, Dreyfus M, Benoist G: **Subsequent pregnancy outcomes after first pregnancy with severe preeclampsia and delivery before 34 weeks of gestation.** *J Gynecol Obstet Biol Reprod (Paris)* 2013, **42:**174–183.
4. Ahmad AS, Samuelsen SO: **Hypertensive disorders in pregnancy and fetal death at different gestational lengths: a population study of 2 121 371 pregnancies.** *BJOG* 2012, **119:**1521–1528.
5. Molvarec A, Gullai N, Stenczer B, Fügedi G, Nagy B, Rigó J Jr: **Comparison of placental growth factor and fetal flow doppler ultrasonography to identify fetal adverse outcomes in women with hypertensive disorders of pregnancy: an observational study.** *BMC Pregnancy Childbirth* 2013, **13:**161.
6. Sibai BM, Lindheimer M, Hauth J, Caritis S, VanDorsten P, Klebanoff M, MacPherson C, Landon M, Miodovnik M, Paul R, Meis P, Dombrowski M: **Risk factors for preeclampsia, abruptio placentae, and adverse neonatal outcomes among women with chronic hypertension. National institute of child health and human development network of maternal-fetal medicine units.** *N Engl J Med* 1998, **339:**667–671.
7. Seely EW, Ecker J: **Clinical practice. Chronic hypertension in pregnancy.** *N Engl J Med* 2011, **365:**439–446.
8. van Scheltinga JA T, Krabbendam I, Spaanderman ME: **Differentiating between gestational and chronic hypertension; an explorative study.** *Acta Obstet Gynecol Scand* 2013, **92:**312–317.
9. Lisonkova S, Joseph KS: **Incidence of preeclampsia: risk factors and outcomes associated with early- versus late-onset disease.** *Am J Obstet Gynecol* 2013, **209:**544.
10. Collis RE, Davies DW, Aveling W: **Randomised comparison of combined spinal-epidural and standard epidural analgesia in labour.** *Lancet* 1995, **345:**1413–1416.
11. Niesen AD, Jacob AK: **Combined spinal-epidural versus epidural analgesia for labor and delivery.** *Clin Perinatol* 2013, **40:**373–384.
12. El-Hakeem EE, Kaki AM, Almazrooa AA, Al-Mansouri NM, Alhashemi JA: **Effects of sitting up for five minutes versus immediately lying down after spinal anesthesia for Cesarean delivery on fluid and ephedrine requirement; a randomized trial.** *Can J Anaesth* 2011, **58:**1083–1089.
13. Leo S, Sng BL, Lim Y, Sia AT: **A randomized comparison of low doses of hyperbaric bupivacaine in combined spinal-epidural anesthesia for caesarean delivery.** *Anesth Analg* 2009, **109:**1600–1605.
14. Martínez Navas A, Echevarría Moreno M, Gómez Reja P, Merino Grande S, Caba Barrientos F, Rodríguez Rodríguez R: **Multivariate study of risk factors for arterial hypotension in pregnant patients at term undergoing Caesarean section under subarachnoid anesthesia.** *Rev Esp Anestesiol Reanim* 2000, **47:**189–193.
15. Sharwood-Smith G, Drummond GB: **Hypotension in obstetric spinal anaesthesia: a lesson from pre-eclampsia.** *Br J Anaesth* 2009, **102:**291–294.
16. Dyer RA, Reed AR, van Dyk D, Arcache MJ, Hodges O, Lombard CJ, Greenwood J, James MF: **Hemodynamic effects of ephedrine, phenylephrine, and the coadministration of phenylephrine with oxytocin during spinal anesthesia for elective cesarean delivery.** *Anesthesiology* 2009, **111:**753–765.
17. Langesaeter E, Rosseland LA, Stubhaug A: **Continuous invasive blood pressure and cardiac output monitoring during cesarean delivery: a randomized, double-blind comparison of low-dose versus high-dose spinal anesthesia with intravenous phenylephrine or placebo infusion.** *Anesthesiology* 2008, **109:**856–863.
18. Ramos-Santos E, Devoe LD, Wakefield ML, Sherline DM, Metheny WP: **The effects of epidural anesthesia on the doppler velocimetry of umbilical and uterine arteries in normal and hypertensive patients during active term labor.** *Obstet Gynecol* 1991, **77:**20–26.
19. Ginosar Y, Nadjari M, Hoffman A, Firman N, Davidson EM, Weiniger CF, Rosen L, Weissman C, Elchalal U, ACET study group: **Antepartum continuous epidural ropivacaine therapy reduces uterine artery vascular resistance in pre-eclampsia: a randomized, dose-ranging, placebo-controlled study.** *Br J Anaesth* 2009, **102:**369–378.
20. Guyenet PG: **The sympathetic control of blood pressure.** *Nat Rev Neurosci* 2006, **7:**335–346.
21. **Report of the national high blood pressure education program working group on high blood pressure in pregnancy.** *Am J Obstet Gynecol* 2000, **183**(1):S1–S22.
22. Robinson HP: **Sonar measurement of fetal crown-rump length as means of assessing maturity in first trimester of pregnancy.** *Br Med J* 1973, **4:**28–31.
23. Bland JM, Altman DG: **Applying the right statistics: analyses of measurement studies.** *Ultrasound Obstet Gynecol* 2003, **22:**85–93.
24. Walter SD, Eliasziw M, Donner A: **Sample size and optimal designs for reliability studies.** *Stat Med* 1998, **17:**101–110.
25. **R development core team. R: a language and environment for statistical computing.R foundation for statistical computing.** [http://www.r-project.org]
26. Oparil S, Zaman MA, Calhoun DA: **Pathogenesis of hypertension.** *Ann Intern Med* 2003, **139:**761–776.
27. Grassi G, Cattaneo BM, Seravalle G, Lanfranchi A, Mancia G: **Baroreflex control of sympathetic nerve activity in essential and secondary hypertension.** *Hypertension* 1998, **31:**68–72.

28. Narkiewicz K, Phillips BG, Kato M, Hering D, Bieniaszewski L, Somers VK: **Gender-selective interaction between aging, blood pressure, and sympathetic nerve activity.** *Hypertension* 2005, **45:**522–525.
29. Tsioufis C, Kordalis A, Flessas D, Anastasopoulos I, Tsiachris D, Papademetriou V, Stefanadis C: **Pathophysiology of resistant hypertension: the role of sympathetic nervous system.** *Int J Hypertens* 2011, **2011:**642416.
30. Wolf-Maier K, Cooper RS, Kramer H, Banegas JR, Giampaoli S, Joffres MR, Poulter N, Primatesta P, Stegmayr B, Thamm M: **Hypertension treatment and control in five european countries, Canada, and the united states.** *Hypertension* 2004, **43:**10–17.
31. Klöhr S, Roth R, Hofmann T, Rossaint R, Heesen M: **Definitions of hypotension after spinal anaesthesia for caesarean section: literature search and application to parturients.** *Acta Anaesthesiol Scand* 2010, **54:**909–921.
32. Tarkkila P, Isola J: **A regression model for identifying patients at high risk of hypotension, bradycardia and nausea during spinal anesthesia.** *Acta Anaesthesiol Scand* 1992, **36:**554–558.
33. Carpenter RL, Caplan RA, Brown DL, Stephenson C, Wu R: **Incidence and risk factors for side effects of spinal anesthesia.** *Anesthesiology* 1992, **76:**906–916.
34. Kalache KD, Dückelmann AM: **Doppler in obstetrics: beyond the umbilical artery.** *Clin Obstet Gynecol* 2012, **55:**288–295.
35. Bhide A, Acharya G, Bilardo CM, Brezinka C, Cafici D, Hernandez-Andrade E, Kalache K, Kingdom J, Kiserud T, Lee W, Lees C, Leung KY, Malinger G, Mari G, Prefumo F, Sepulveda W, Trudinger B: **ISUOG practice guidelines: use of doppler ultrasonography in obstetrics.** *Ultrasound Obstet Gynecol* 2013, **41:**233–239.
36. Gómez O, Figueras F, Fernández S, Bennasar M, Martínez JM, Puerto B, Gratacós E: **Reference ranges for uterine artery mean pulsatility index at 11–41 weeks of gestation.** *Ultrasound Obstet Gynecol* 2008, **32:**128–132.
37. Giordano R, Cacciatore A, Romano M, La Rosa B, Fonti I, Vigna R: **Uterine artery doppler flow studies in obstetric practice.** *J Prenat Med* 2010, **4:**59–62.
38. Guedes-Martins L, Cunha A, Saraiva J, Gaio AR, Macedo F, Almeida H: **Internal iliac and uterine arteries doppler ultrasound in the assessment of normotensive and chronic hypertensive pregnant women.** *Sci Rep* 2014, **4:**3785.
39. Guedes-Martins L, Saraiva J, Gaio R, Macedo F, Almeida H: **Uterine artery impedance at very early clinical pregnancy.** *Prenat Diagn* 2014, **34:**719–725. doi:10.1002/pd.4325.
40. Hughes AB, Devoe LD, Wakefield ML, Metheny WP: **The effects of epidural anesthesia on the doppler velocimetry of umbilical and uterine arteries in normal term labor.** *Obstet Gynecol* 1990, **75:**809–812.
41. Morrow RJ, Rolbin SH, Knox Ritchie JW, Haley S: **Epidural anaesthesia and blood flow velocity in mother and foetus.** *Can J Anaesth* 1989, **36:**519–522.
42. Lindblad A, Marsal K, Vernersson E, Renck H: **Foetal circulation during epidural analgesia for cesarean section.** *Br Med J* 1984, **288:**1329–1330.
43. Giles WB, Trudinger BJ, Baird PJ: **Fetal umbilical artery flow velocity waveforms and placental resistance: pathological correlation.** *Br J Obstet Gynaecol* 1985, **92:**31–38.
44. Manninen T, Aantaa R, Salonen M, Pirhonen J, Palo P: **A comparison of the hemodynamic effects of paracervical block and epidural anesthesia for labor analgesia.** *Acta Anaesthesiol Scand* 2000, **44:**441–445.
45. Fratelli N, Prefumo F, Andrico S, Lorandi A, Recupero D, Tomasoni G, Frusca T: **Effects of epidural analgesia on uterine artery doppler in labor.** *Br J Anaesth* 2011, **106:**221–224.
46. Goodarzi M, Narasimhan RR: **The effect of large-dose intrathecal opioids on the autonomic nervous system.** *Anesth Analg* 2001, **93:**456–459.
47. Gautier P, De Kock M, Huberty L, Demir T, Izydorczic M, Vanderick B: **Comparison of the effects of intrathecal ropivacaine, levobupivacaine, and bupivacaine for Caesarean section.** *Br J Anaesth* 2003, **91:**684–689.
48. Gogarten W: **Spinal anaesthesia for obstetrics.** *Best Pract Res Clin Anaesthesiol* 2003, **17:**377–392.
49. Grassi G, Seravalle G, Dell'Oro R, Mancia G: **Sympathetic mechanisms, organ damage, and antihypertensive treatment.** *Curr Hypertens Rep* 2011, **13:**303–308.
50. Mancia G, Grassi G, Giannattasio C, Seravalle G: **Sympathetic activation in the pathogenesis of hypertension and progression of organ damage.** *Hypertension* 1999, **34:**724–728.
51. Fitzmaurice GM, Laird NM, Ware JH: *Applied longitudinal analysis, Wiley series in probability and statistics.* Hoboken, New Jersey: John Wiley & Sons, Inc; 2004.
52. Egan BM, Zhao Y, Axon RN: **US trends in prevalence, awareness, treatment, and control of hypertension, 1988–2008.** *JAMA* 2010, **303:**2043–2050.
53. Grab D, Paulus WE, Erdmann M, Terinde R, Oberhoffer R, Lang D, Muche R, Kreienberg R: **Effects of low-dose aspirin on uterine and fetalblood flow during pregnancy: results of a randomized, placebo-controlled, double-blind trial.** *Ultrasound Obstet Gynecol* 2000, **15:**19–27.
54. Veille JC, Hanson R, Sivakoff M, Swain M, Henderson L: **Effects of maternal ingestion of low-dose aspirin on the fetal cardiovascular system.** *Am J Obstet Gynecol* 1993, **168:**1430–1437.
55. Khalil A, Harrington K, Muttukrishna S, Jauniaux E: **Effect of antihypertensive therapy with alpha-methyldopa on uterine artery doppler in pregnancies with hypertensive disorders.** *Ultrasound Obstet Gynecol* 2010, **35:**688–694.
56. Valli J, Pirhonen J, Aantaa R, Erkkola R, Kanto J: **The effects of regional anaesthesia for caesarean section on maternal and fetal blood flow velocities measured by doppler ultrasound.** *Acta Anaesthesiol Scand* 1994, **38:**165–169.

doi:10.1186/1471-2393-14-291
Cite this article as: Guedes-Martins *et al.*: The effects of spinal anaesthesia for elective caesarean section on uterine and umbilical arterial pulsatility indexes in normotensive and chronic hypertensive pregnant women: a prospective, longitudinal study. *BMC Pregnancy and Childbirth* 2014 **14**:291.

Article 6

Guedes-Martins L, Silva E, Gaio AR, Saraiva J, Soares AI, Afonso J, Macedo F, Almeida H. Fetal-maternal interface impedance parallels local NADPH oxidase related superoxide production. *Redox Biol.* 2015; 5:114-123.

Redox Biology 5 (2015) 114–123

Contents lists available at ScienceDirect

Redox Biology

journal homepage: www.elsevier.com/locate/redox

Research Paper

Fetal–maternal interface impedance parallels local NADPH oxidase related superoxide production

L. Guedes-Martins [a,b,c,d,*], E. Silva [a,b,c], A.R. Gaio [e,f], J. Saraiva [a,b,c,d], A.I. Soares [a,b,c], J. Afonso [g], F. Macedo [h], H. Almeida [a,b,c,i]

[a] Department of Experimental Biology, Faculty of Medicine, University of Porto, 4200-319 Porto, Portugal
[b] IBMC-Instituto de Biologia Molecular e Celular, 4150-180 Porto, Portugal
[c] Instituto de Investigação e Inovação em Saúde, Universidade do Porto, 4200-319 Porto, Portugal
[d] Centro Hospitalar do Porto EPE, Departamento da Mulher e da Medicina Reprodutiva, Centro Hospitalar do Porto EPE, Largo Prof. Abel Salazar, 4099-001 Porto, Portugal
[e] Department of Mathematics, Faculty of Sciences, University of Porto, Rua do Campo Alegre, 4169-007 Porto, Portugal
[f] CMUP-Centre of Mathematics of the University of Porto, Rua do Campo Alegre, 4169-007 Porto, Portugal
[g] Department of Pharmacology, Faculty of Medicine, University of Porto, 4200-319 Porto, Portugal
[h] Department of Cardiology, Faculty of Medicine, University of Porto, 4200-319 Porto, Portugal
[i] Obstetrics-Gynecology, Hospital-CUF Porto, 4100 180 Porto, Portugal

ARTICLE INFO

Article history:
Received 28 March 2015
Received in revised form
14 April 2015
Accepted 17 April 2015
Available online 20 April 2015

Keywords:
Aortic isthmus
Uterine artery
Doppler
Pulsatility index
Oxidative stress
NADPH oxidase

ABSTRACT

Blood flow assessment employing Doppler techniques is a useful procedure in pregnancy evaluation, as it may predict pregnancy disorders coursing with increased uterine vascular impedance, as pre-eclampsia. While the local causes are unknown, emphasis has been put on reactive oxygen species (ROS) excessive production. As NADPH oxidase (NOX) is a ROS generator, it is hypothesized that combining Doppler assessment with NOX activity might provide useful knowledge on placental bed disorders underlying mechanisms.

A prospective longitudinal study was performed in 19 normal course, singleton pregnancies. Fetal aortic isthmus (AoI) and maternal uterine arteries (UtA) pulsatility index (PI) were recorded at two time points: 20–22 and 40–41 weeks, just before elective Cesarean section. In addition, placenta and placental bed biopsies were performed immediately after fetal extraction.

NOX activity was evaluated using a dihydroethidium-based fluorescence method and associations to PI values were studied with Spearman correlations. A clustering of pregnancies coursing with higher and lower PI values was shown, which correlated strongly with placental bed NOX activity, but less consistently with placental tissue.

The study provides evidence favoring that placental bed NOX activity parallels UtA PI enhancement and suggests that an excess in oxidation underlies the development of pregnancy disorders coursing with enhanced UtA impedance.

Introduction

In recent years, the range of ultrasound applications for the study of blood flow has increased remarkably due to device improvements, extensive and reliable data collection, and the non-invasive nature of the procedure. In particular, Doppler effect assessment of the impedance of fetal and placental circulation has become a routine operation during pregnancy evaluation and a necessary tool in screening for impaired utero-placental circulation [1,2].

Over the course of a pregnancy, remarkable circulatory changes occur in the pelvis: on the one side is a developing foetus with

Abbreviations: AoI, aortic isthmus; BMI, body mass index; CI, confidence interval; DHE, dihydroethidium; DPI, diphenyleneiodonium; ICC, intra-class correlation coefficient; IUGR, intra-uterine growth restriction; NADPH, nicotinamide adenine dinucleotide phosphate; NOX, NADPH oxidase; PI, pulsatility index; PE, pre-eclampsia; ROS, reactive oxygen species; SD, standard deviation; UtA, uterine artery.

* Corresponding author at: Centro Hospitalar do Porto EPE, Departamento da Mulher e da Medicina Reprodutiva, Largo Prof. Abel Salazar, 4099-001 Porto, Portugal.

E-mail addresses: luis.guedes.martins@gmail.com (L. Guedes-Martins), elisabetefersilva@gmail.com (E. Silva), argaio@fc.up.pt (A.R. Gaio), saraivajp@hotmail.com (J. Saraiva), anasoares.alv@gmail.com (A.I. Soares), jafonso@med.up.pt (J. Afonso), filipe.macedo@hsjoao.min-saude.pt (F. Macedo), almeidah@med.up.pt (H. Almeida).

http://dx.doi.org/10.1016/j.redox.2015.04.007

enhanced nutritional demands, whereas on the other side, uterine circulation has to adapt continuously to cope with such demands. These distinct features make the uteroplacental interface a crucial site of circulation whose impedance can be assessed by approaching the aortic isthmus (AoI) on the fetal side and the uterine arteries (UtA) on the maternal side. In this respect, although different impedance parameters may be employed, emphasis has been placed on the pulsatility index (PI) because of its ability to better describe the velocity waveform [3,4].

During prenatal life, the parallel position of both cardiac ventricles assigns a special position to the AoI, as it reflects the balance of the functional accomplishments and the individual territorial impedances of the two ventricles [4,5]. Thus, the direction of blood flow in the aortic isthmus will depend on the relative difference between the upper body and the subdiaphragmatic circulation supplying the lower body and placenta [6]. Abnormal flow patterns in the AoI, identified by high impedance values, have been shown to be associated with fetal circulatory redistribution [6–10]; in addition, routine AoI Doppler assessment has been shown to predict perinatal and long-term neurodevelopmental outcomes in placental insufficiency [6,11,12]. Indeed, the value of AoI blood flow assessment has been emphasized as changes in AoI antedate umbilical artery findings [7].

On the mother's side, a normal uterine artery waveform reflects successful vascular remodelling at the uterine placental bed that includes the decidua and part of the myometrium [13,14]. In early pregnancy, the UtA Doppler waveform exhibits a rapid increase and decrease in systolic flow velocity that is followed by a notch in the early diastole [15,16]. This feature, which usually recedes as the pregnancy progresses [3,16] contributes to a mean diastolic velocity rise and a UtA-PI value reduction [3,17]. Interestingly, in a group of unselected pregnant women at 22–24 weeks, enhanced uterine artery PI was reported to have a 69% sensitivity for pre-eclampsia (PE) and the appearance of intra-uterine growth restriction (IUGR) in the following weeks, a value that rose to 83% in cases of protodiastolic notch persistence [18]. Although the detection rate of PE as a result of enhanced UtA-PI was found to be superior to the use of a patient's epidemiological data [19], additional conditions must be met. Other reports have indicated that abnormal UtA impedance at 22 weeks and PE establishment were significantly correlated only in the case of poor fetal outcome, including IUGR and preterm birth [20,21]. More recently, top decile PI values and bilateral notching were considered to have good predictive value for enhanced risk of stillbirth resulting from placental factors [22]. As a corollary favouring the relevance of UtA Doppler impedance, an extensive meta-analysis [23] concluded that an enhanced second trimester PI combined with a notch was a good predictor of PE in low- and high-risk patients and of severe IUGR in low-risk patients. Moreover, the findings supported the recommendation to employ PI and notching uterine artery assessment in daily clinical practice [23]. Most of the referred obstetrical adverse conditions were recognized to result from abnormal placental bed remodelling [14], but despite a wealth of structural information, there is still insufficient knowledge regarding local regulation during placentation.

The involvement of the process of biological oxidation was proposed. The local, continued production of reactive oxygen species (ROS) is a cellular requirement that, in small and balanced amounts, appears to exert a beneficial role on normal pregnancies. This context is relevant to the effect of ROS generated by NADPH oxidase (NOX) activity in the uterus and placenta where, through the activation of NF-κB, they regulate local angiogenesis [24,25] and play a relevant role in normal placental bed establishment.

By contrast, excessive ROS production results in oxidatively stressful conditions, inflammation, circulatory derangement, and placental bed cell apoptosis or necrosis. These events may occur transiently during labour in a fashion consistent with ischaemia-reperfusion injury [26]; when lasting longer, or throughout the pregnancy, they may result in placental function impairment [27,28] and serious pregnancy complications [24,28].

Despite the likelihood of the process of ROS production, the identity and contribution of the redox players involved have remained unknown. To gain a better understanding, it is reasonable to address putative contributors as part of a wider approach. Therefore, we hypothesize that redox status, measured as the NOX activity at the placental bed and in the placenta, relates to blood flow impedance measured at the fetal aortic isthmus and at the maternal uterine arteries.

Materials and methods

Subjects

This study was approved by the local ethics committee of Centro Hospitalar do Porto–Unidade Maternidade Júlio Dinis and all subjects provided written informed consent [IRB protocol number: 133/10 (086-DEFI/126-CES)]. The methods were performed in accordance with the approved guidelines.

The study was performed from January 2010 to December 2013. Inclusion criteria were: healthy normotensive parturient with singleton term pregnancies and gestational age ≥ 40 weeks, scheduled for elective cesarean section under spinal anesthesia due to fetal breech presentation, suspected cephalopelvic disproportion, or previous caesarean. Acceptable medications were folic acid, vitamins, and iron supplements.

Exclusion criteria were: patients in labour or with ruptured membranes; those with multiple gestations, coagulopathy, diabetes, or any pregnancy-induced hypertension including pre-eclampsia; and those receiving β-tocolytic drugs.

Gestational age was calculated by the crown-rump length between 11 and 14 weeks [29] by several experienced sonographers from the Prenatal Diagnosis Department of our institution.

On the day of caesarean section, biometrical data were collected and the patients were observed by a senior specialist who also reviewed their medical records.

The subarachnoid block was performed in the surgical suite using a combined needle-through-needle spinal-epidural technique (typical for caesarean section at our institution) with an epidural 18-G Tuohy needle and 27-G subarachnoid pencil point needle. Spinal anesthesia comprised 8–9 mg of hyperbaric bupivacaine (5 mg/ml) and 2–2.5 μg sufentanil (5 μg/ml) administered intrathecally, targeting the T4-S4 dermatomes.

The healthy condition of the infant was determined through examination by a neonatologist at birth and 1 month after birth.

Doppler flow assessment

Ultrasound examinations were performed using Voluson 730 Pro (GE Healthcare Technologies, Milwaukee, WI, USA) ultrasound equipment containing multifrequency transabdominal transducers (GE Healthcare Probe Type RAB4-8L) at any time of the day, during the second trimester routine scan (first time point), and immediately before the intrathecal blockade (second time point) for caesarean section.

All measurements were performed by a single experienced investigator (L.G-M; 6 years of experience in obstetric and gynaecologic ultrasound) to minimize inter-observer variability. Intra-observer reliability was estimated from two consecutive readings of the pulsatility indexes in the UtA and AoI. Smokers

were required to abstain from smoking for at least 2 h prior to examination.

For uterine artery evaluation, the probe was placed on the lower abdominal quadrants and angled medially, and color Doppler imaging was used to localize the uterine artery as it crossed over the external iliac artery. In all cases, an angle less than 30° was assured before the pulsed Doppler probe was placed over the entire vessel width. Angle correction was then applied, and the signal was updated until three similar consecutive waveforms were found to calculate the left and right uterine artery pulsatility indexes using the device software. The mean UtA-PIs in the left and right arteries were then determined.

For AoI evaluation, all recordings used for measurements were sampled from the longitudinal aortic arch and performed in the absence of fetal movements. The scanning plane was adjusted to obtain an insonation angle $< 30°$. The filter was set at 50 Hz and the energy output levels used were lower than 50 mW/cm^2.

Placenta and placental bed biopsies

Biopsies of the placenta and placental bed were performed by open biopsy during caesarean section immediately after fetal extraction and prior to oxytocin administration. Using tissue scissors, two fragments approximately 10×5 mm^2 (width $\times$ depth) were obtained. The first fragment was collected from the placental bed and the second was obtained from the central area of the placental maternal surface. In individual cases, because of a small uterine bleeding site, we proceeded to haemostasis control using an isolated absorbable synthetic suture (Polyglactin 910, 2/0). After collection under aseptic conditions, the samples were briefly washed in saline solution and immediately frozen in liquid nitrogen before being stored at − 80 °C.

Dihydroethidium conversion

$O_2^{\bullet -}$ production from NADPH oxidase was evaluated using a dihydroethidium (DHE)-based fluorescence method [30,31]. DHE is used in fluorimetric detection assays because upon reaction with superoxide anions, it is converted to 2-hydroxyethidium, following DNA intercalation, emits red fluorescence.

Placenta and placental bed samples were homogenized in a glass-to-glass homogenizer in cold HEPES buffer (25 mM) containing EDTA (1 mM) and phenylmethyl-sulfonyl fluoride (PMSF) (0.1 mM). Protein content was assayed by the Bradford method [32] and 12.5 μg of homogenate were used for the assay. Tissue homogenates were incubated in HEPES/EDTA buffer with DHE (20 μM), salmon testes DNA (0.5 mg/ml), and NADPH (1 mM). Superoxide dismutase (200 U/ml) was used to confirm the specificity of the method. To determine whether NADPH oxidase was the source of $O_2^{\bullet -}$ an inhibitor of NOX (diphenylene iodonium, DPI, 500 μM) was used. The effects of a xanthine oxidase inhibitor (oxipurinol, 500 μM) and a nitric oxide synthase inhibitor (nitro-L-arginine methylester, L-NAME, 500 μM) were also evaluated to exclude other possible contributors for the $O_2^{\bullet -}$ 2-hydroxyethidium mediated fluorescence [Supplementary Fig. S1]. It was thus demonstrated that, under the experimental conditions used, the observed increase in fluorescence is mainly due to NOX activity; as such, DHE conversion will be considered an indicator of NOX activity. The reaction was followed for 15 min at 37 °C. Fluorescence was measured in a final volume reaction of 200 μl at 480 nm-excitation and 580 nm-emission using a fluorescence microplate reader (Spectramax Gemini, Molecular Devices, Sunnyvale, CA, USA). The results were expressed as fluorescence arbitrary units per 15 min per 12.5 μg of protein.

All drugs were purchased from Sigma Aldrich, St. Louis, MO, USA.

Statistical analysis

Intra-class correlation coefficients (ICC) and 95% confidence intervals (CIs) were calculated with a two-way mixed-effects model. The reliability coefficient, which is the difference value that will be exceeded by only 5% of pairs of measurements on the same subject, was calculated as 1.96 times the standard deviation (SD) of the difference between pairs of repeated measurements [33].

All remaining statistical analysis used only non-parametric techniques. Sample correlations were evaluated by the Spearman rank correlation coefficient. The statistical significance of the difference between the medians of a continuous variable in two disjoint groups was assessed by the Mann–Whitney test. Clustering of longitudinal PI data were obtained from the application of the K-means algorithm implemented with the Euclidean distance [34].

The clustering algorithm was run several times considering 40 different starting conditions and varying the number of clusters from 2 to 3. Varying the initial conditions increased the chances of reaching a global maximum whereas varying the number of clusters enabled the selection of the correct number of clusters. The sample size was the main reason for the upper bound of the number of clusters used in this paper. The final clustering structure was chosen based upon the clinical interpretation of the obtained groups and the statistical criteria of Calinsky & Harabatz and Davies & Bouldin [35].

Clustering was performed on the group of PI individual time profiles, and separately for each evaluated artery. The NOX activity within each obtained class was then identified and comparisons across clusters were also considered. This procedure was thought to be more informative than simply studying the correlations between each enzymatic activity and the PI values collected at each of the evaluation periods.

All statistical analyses were performed using the R language and software environment for statistical computation, version 2.12.1 [36]. The significance level was set at 0.05.

Results

A total of 19 pregnant women at term were considered eligible for this study according to the established inclusion/exclusion criteria, and their characteristics and pregnancy outcomes are depicted in Table 1. Their ages ranged from 22 to 41 years old, and this was the first pregnancy for 74% of the women.

The median gestational age at the time of Doppler measurements was 21.0 weeks (range: 20–22 weeks) at the first time point and 40.6 weeks (range: 40–41 weeks) at the second time point.

Table 1
Characteristics and obstetric data of the 19 women included in the study.

		N (%)
Age, years (mean, SD)	31.2 (5.0)	
Parity	0	14 (74%)
	> 0	5 (26%)
Body Mass Index, kg/m^2 (mean, SD)[a]	30.6 (5.9)	
Smoking	No	18 (95%)
	Yes	1 (5%)
GA at delivery (weeks) (mean ± SD)	40.5 (0.3)	
Apgar Index 5′	< 7	0 (0)
Birth weight at delivery (g) (mean ± SD)[b]	3354 (398)	–

GA, gestational age; SD, standard deviation.

[a] BMI: measured at Caesarean section day.

[b] Birth weight in the sample corresponding to the 10th percentile was 2904 g.

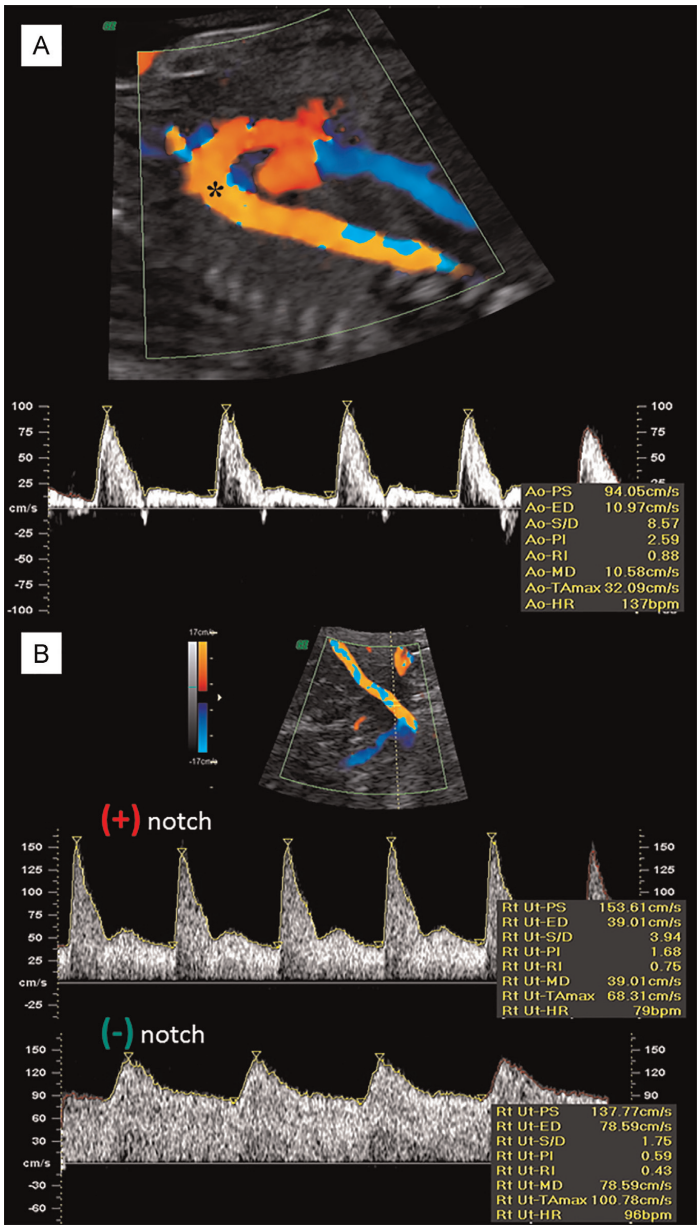

Fig. 1. Doppler flow velocity waveforms obtained from the fetal aortic isthmus (panel A) and maternal uterine artery (panel B). panel A: The aortic Isthmus (AoI) is the segment of the aorta located between the origin of the left subclavian artery and the connection of the ductus arteriosus to the descending aorta (*). Under physiological conditions, the direction of flow in the AoI is forward during the entire cardiac cycle. panel B: With the advent of color Doppler, the precise localization of the uterine arteries became feasible; (+) notch, abnormal waveform demonstrating increased impedance and early diastolic notch; (−) notch, normal pregnant waveform.

Fig. 1 shows the types of AoI and UtA Doppler shift spectra obtained from the fetal aortic isthmus and maternal uterine arteries. The reliability coefficient for the UtA-PI measurements was 0.102. The ICC for absolute agreement among the single observer UtA-PI measurements was 0.990 with a 95% CI ranging from 0.980 to 0.995. Similarly, the reliability coefficient for the AoI-PI measurements was 0.302. The ICC for absolute agreement among the single observer measurements was 0.976 with a 95% CI ranging from 0.954 to 0.987.

Fig. 2 shows how the biopsies in the placenta and placental bed were obtained.

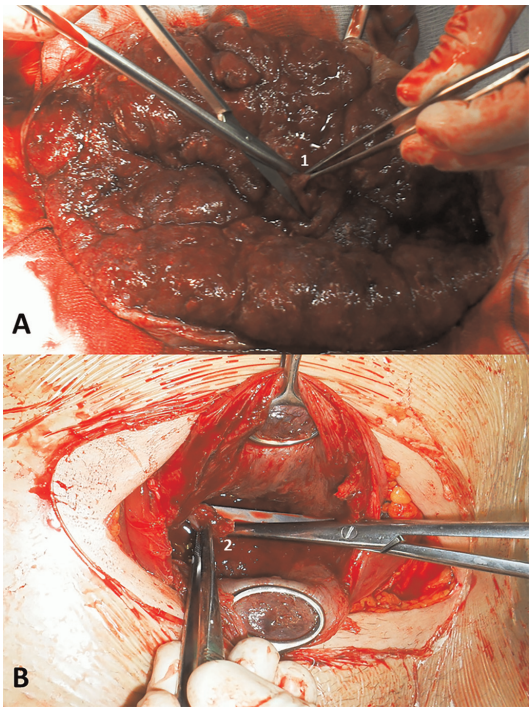

Fig. 2. Placental and placental bed biopsies. (A) Placenta, central maternal surface (1); (B) placental bed (2).

The association between DHE-conversion and PI values (Fig. 3) was first studied using Spearman correlation. From Table 2, AoI-PI and the UtA-PI are positively associated with DHE-conversion (both in the placental bed and in the placenta). In the placental bed, the positive association between DHE-conversion and AoI-PI at the first evaluation period is only statistically significant at the 0.09 level ($p=0.08$), and no significant association exists with AoI-PI at the second evaluation period ($p=0.44$). However, when measured in placental tissue, DHE-conversion showed a significantly positive association with AoI-PI at second time point ($p<0.01$), but not at the first time point ($p=0.164$). There is a significant positive association between DHE-conversion at the placental bed and UtA-PI at the first and second time points, with a stronger association at the first time point. The enzymatic activity of placental DHE-conversion was found to be significantly and positively associated with UtA-PI only at the first time point ($p=0.023$). The positive UtA-PI association with placental bed DHE-conversion at the first time point was 44% higher than the association observed with placental DHE-conversion.

Clustering the individual time profiles to analyze PI values at the AoI and UtA independently allowed for the identification of PI trends. DHE-conversion was then compared across the obtained partition of curves. This was used as a more comprehensive methodology than simply considering correlations with PI values at each of the evaluation time points.

For the AoI-PI measurements, two clusters were identified (Fig. 4A): cluster A comprised 10 (52.6%) pregnant women and cluster B comprised 9 (47.4%). No significant relationship was found between the clustering obtained and the DHE-conversion measured in the placenta and the placental bed (Fig. 4B, Table 3). When examining the UtA-PI values, two clusters were found (Fig. 4C): cluster A comprised 13 (68.4%) individuals and cluster B comprised 6 individuals (31.6%). UtA cluster B contained all those trajectories starting at higher UtA-PI values and is significantly associated with enhanced DHE-conversion in the placental bed (Fig. 4D, Table 3). By contrast, the persistence of a notch in the uterine artery at 20–22 weeks of gestation was significantly associated with high DHE-conversion in the placental bed, but not in the placenta (Table 4).

Finally, we found that elevated DHE-conversion correlated negatively with the Body Mass Index (BMI) of pregnant women (Table 5). No significant relationship was found between age and the enzymatic activity studied.

Discussion

During a pregnancy, both the foetus and the mother experience substantial circulatory changes. Provided that vascular congenital abnormalities are absent, the fetal circulation will follow an intrinsic, species-related developmental programme; on the mother's side, the pregnancy will impart to the placental bed a variety of structural and functional changes that result in important circulatory events.

At approximately 8 weeks of gestation, embryo-derived extravillous trophoblasts (EVTs) tend to surround decidual spiral arteries, invade their walls, and assemble as cell plugs that ultimately fill their lumina from 10 weeks onwards [37]. Upon replacing vessel endothelium and the smooth muscle cells, trophoblasts subsequently extend to the innermost myometrium layers and cluster around the spiral arteries. By 14 weeks, deep myometrium involvement is evidenced by the trophoblast invasion of the spiral arteries of the lumina. In time, this remodelling process, deep placentation, will extend to most spiral arteries [14,37].

An important consequence of the remodelled vessel is its enlargement, implying the acquisition of capacitance properties, reduced impedance to blood flow, and reduced uterine artery PI. However, if spiral artery remodelling is defective, the uterine artery maintains resistance properties and its impedance increases. Such changes were found to associate with PE and other obstetrical disorders with adverse implications for maternal and fetal health [13,38,39].

In this context, it is useful to analyze blood flow waveforms and determine the UtA [3,20] and AoI [40] impedance. Although a high AoI-PI is seen as an indicator of placental insufficiency and fetal cardiac decompensation [41], there is substantial evidence that high UtA impedance measured at 20–22 weeks is a good predictor of serious pregnancy disorders and adverse fetal outcomes arising in the following weeks until term [3,20,23,42].

As none of those adverse conditions affected the outcomes of any of the pregnancies enrolled in the current study, both the first and second time-point measurements reflected a normal pregnancy course; as expected [3,17], UtA-PI decreased from the 20–22 week time point until term.

However, a closer analysis found two different clusters of UtA-PI time trajectories, one (B) having a steeper PI reduction and the other (A) showing a flattened PI reduction. This finding indicates that even in the absence of adverse clinical findings or outcomes, coherent, specific UtA impedance trends exist, suggesting the action of local regulatory mechanisms that are fine-tuned at different levels. When vessel remodelling is deficient or when predisposing conditions exist, UtA-PI is likely to increase and to be accompanied by clinical signs. The reason for this consequence of abnormal remodelling is unknown, but the current study supports the view that continued redox imbalance and established oxidative stress is the underlying process.

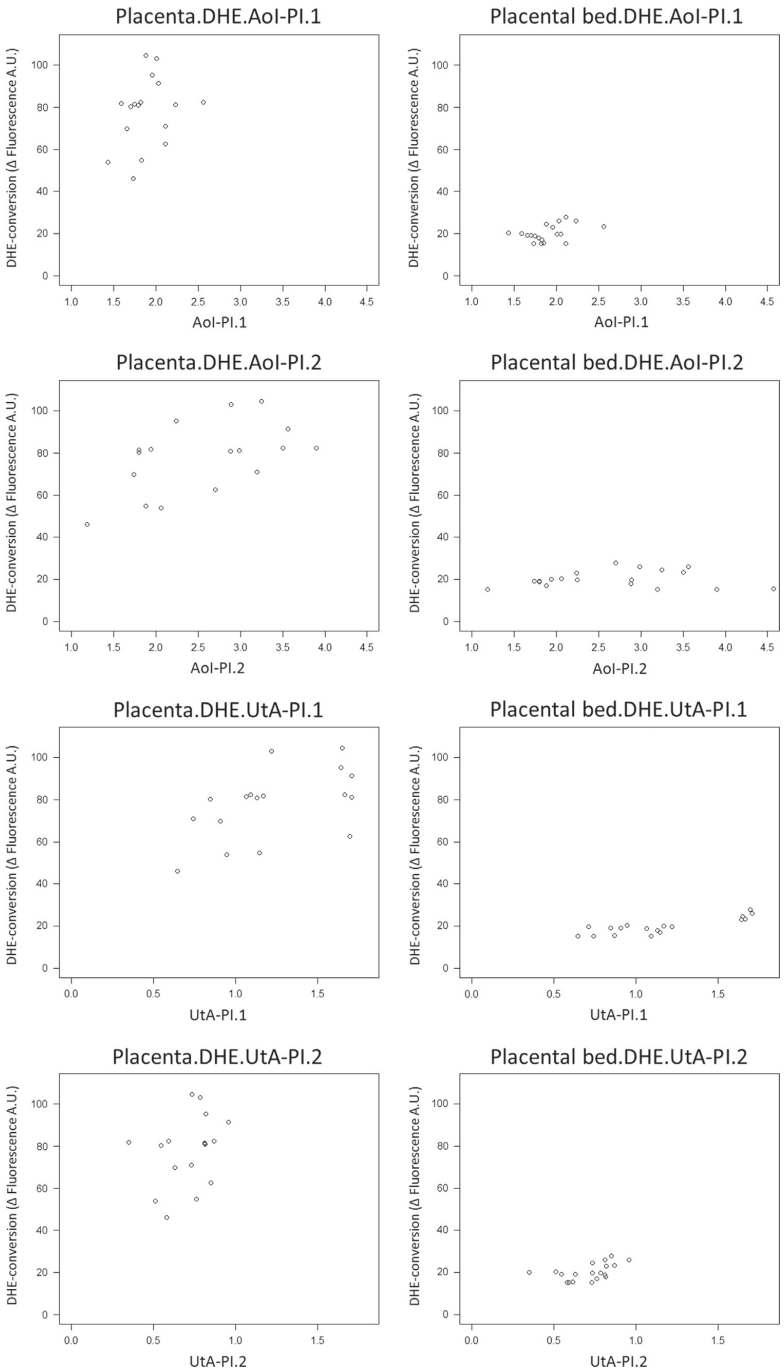

Fig. 3. Plots of the sample values of DHE conversion against AoI-PI and UtA-PI measurements, at the first (1) and second (2) time points, in the placenta and in the placental bed (respectively, left and right columns).

Table 2
Association between DHE-conversion activity and longitudinal AoI-PI and UtA-PI values at the first (1) and second (2) time points.

	AoI-PI.1	AoI-PI.2	UtA-PI.1	UtA-PI.2
DHE-conversion(Δ Fluorescence A.U.)				
Placenta	0.353	**0.612**	**0.548**	0.357
($n=17$)	($p=0.164$)	($p=0.009$)	($p=0.023$)	($p=0.160$)
Placental bed	0.409	0.187	**0.789**	**0.501**
($n=19$)	($p=0.082$)	($p=0.444$)	($p<0.001$)	($p=0.029$)

AoI, aortic isthmus; UtA, uterine artery; PI, pulsatility index; A.U., arbitrary units

Statistics

The high magnitude of the obtained ICC values from AoI and UtA Doppler assessments allowed statistical analysis to ignore one of the two measurements obtained from each woman. Because the sonographer only performed one measurement in day-to-day practice, the first measurements were considered. Both left and right main UtAs were investigated at the same time, as unilateral measurement may provide erroneous results.

Clustering methods besides k-means could have been chosen for the identification of homogeneous classes of individual PI trajectories. More precisely, hierarchical methods, density-based methods, grid-based methods, model-based methods, or other partitioning methods could have been considered [43]. However, the following points illustrate the advantages of the longitudinal k-means algorithm: (1) it does not require any normality or parametric assumptions within clusters; this is particularly important in our study given its sample size and the fact that no prior information was available; (2) it does not require any assumptions regarding the shape of the individual trajectories; and (3) it is independent from the time scaling used. In this study, the clustering of the linear AoI-PI time profiles into 3 classes provided a group consisting of only 2 individuals and that was therefore discarded. Although the 3-cluster solution for UtA-PI longitudinal profiles presented essentially balanced group prevalence (7, 6, and 6 members), it was not favored by the statistical criteria. No significant association was found between the profile partitions obtained for AoI and NOX activity. Although one of the clusters presented a small dispersion of values and seemed to be well-identified from that point of view, the other included a wide range of enzymatic expression values. The 3-cluster solution mentioned above was not capable of solving this lack of correlation.

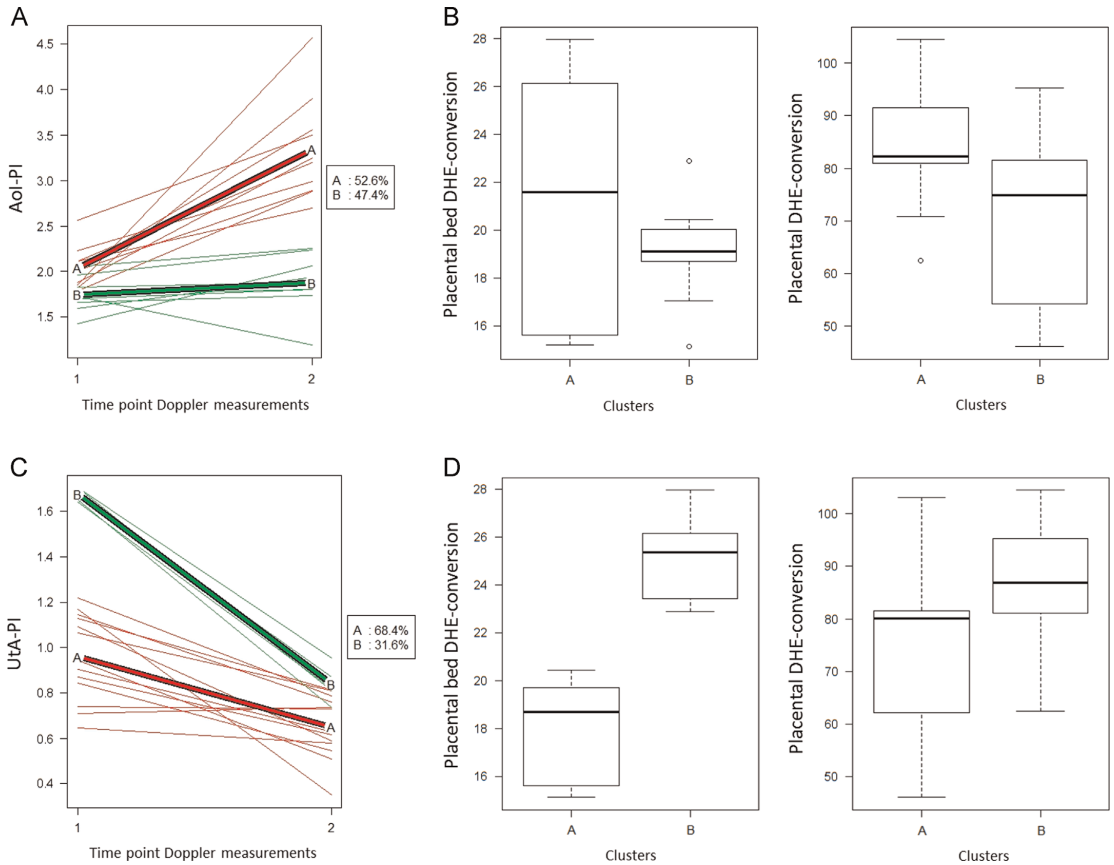

Fig. 4. Panel A+C: individual time profiles of the AoI-PI and UtA-PI (left-hand side) and the two identified clusters, denoted by A and B; all curves in red belong to the A cluster whereas all curves in green belong to the B cluster. Panel B + D: boxplot of placental bed and placental DHE-conversion in each of the clusters found for the AoI-PI and UtA-PI time trajectories.

Table 3
Median (minimum–maximum) placental bed and placental DHE-conversion in each of the clusters (A and B) found for the AoI-PI and UtA-PI time trajectories.

	All	AoI.Cluster A	AoI.Cluster B	*p*	UtA.Cluster A	UtA.Cluster B	*p*
DHE-conversion (Δ Fluorescence A.U.)							
Placenta ($n=17$)	81.08 (46.12–104.52)	82.26 (62.50–104.52)	74.96 (46.12–95.22)	0.093	80.16 (46.12–103.09)	86.89 (62.50–104.52)	0.098
Placental bed ($n=19$)	19.72 (15.14–27.98)	21.59 (15.21–27.98)	19.13 (15.14–22.91)	0.400	18.72 (15.14–20.47)	25.39 (22.91–27.98)	< **0.001**

p-Value from the Mann–Whitney test; AoI, aortic isthmus; UtA, uterine artery

Table 4
Median (minimum–maximum) placental bed and placental DHE-conversion in relation to the presence/absence of UtA notching (at the first time point) and parity.

	All	UtA.Notch (−)	UtA.Notch (+)	*p*	Primiparous	Parous	*p*
DHE- conversion (Δ Fluorescence A.U.)							
Placenta ($n=17$)	81.08 (46.12–104.52)	75.52 (46.12–103.09)	82.26 (62.50–104.52)	0.070	81.41 (46.12–103.09)	74.96 (54.71–104.52)	0.703
Placental bed ($n=19$)	19.72 (15.14–27.98)	18.29 (15.14–20.47)	24.64 (20.05–27.98)	< **0.001**	19.89 (15.14–27.98)	19.01 (15.63–24.64)	0.500

p-Value from the Mann–Whitney test, UtA, uterine artery.

Table 5
Spearman rank correlation coefficient (*p*-value) between age/BMI and DHE-conversion in the placental bed and in the placenta.

	Age	BMI[1]
DHE-conversion (Δ Fluorescence A.U.)		
Placenta ($n=17$)	0.081 (0.757)	−0.277 (0.281)
Placental bed ($n=19$)	0.158 (0.519)	−**0.465 (0.047)**

[a] Measured at the second time point; BMI, Body Mass Index.

NOX activity at the placental bed and Doppler flow study

The structural and functional integrity of the vascular system of the placental bed is controlled by the endothelium [44]. Endothelial cells produce a vast number of circulation regulators that modulate signalling pathways whose activation requires balanced ROS action [45]. In the uterus and placenta, substantial ROS production is the result of NOX activity through its NOX1, NOX2, NOX4, and NOX5 isoforms present in the endothelium, the myometrium smooth muscle cells, the decidualized stromal cells, and the syncytiotrophoblasts, where they generate H_2O_2 and superoxide anions [24,46,47].

The balanced production of ROS has local signalling properties through the synthesis of nitric oxide, NO [48], a primary endothelial cell vasodilator that is critical for endothelium transformation during pregnancy [49].

However, the balance may be disrupted when local conditions enhance NOX activity and ROS production and lead to vessel disorders. In human vascular samples, NOX-dependent superoxide generation and abnormal endothelium-related responses were found to correlate positively with the number of cardiovascular risk factors present [50]. Aortic samples from NOX2 knockout mice failed to respond to hypertensive experiments or to hypotensive challenging as a result of a substantial reduction in superoxide production [51]; interestingly, transgenic mice overexpressing endothelial cell NOX2 exhibited basal activity similar to controls but demonstrated remarkable sensitivity when challenged with angiotensin II [52]. This is an important finding because the involvement of this vasoactive peptide in pregnancy-induced hypertensive disorders has long been recognized [53] and has been interpreted as resulting from enhanced sensitivity [54].

As NOX production of superoxide anions intensifies in smooth muscle cells and human trophoblasts, persistent NF-kB activation ensues [55], which reduces NO bioavailability. This set of conditions promotes local inflammation and further oxidation, both consistently implicated in the pathogenesis of the endothelial dysfunction antedating PE and other disorders at the utero-placental interface [44,54,56,57].

In the current study involving pregnancies that followed a normal course, a validated DHE-based fluorescence method was used as an indicator of NOX activity. Higher placental bed NOX activity related DHE conversion at term was strongly correlated with higher UtA-PI measured at 20–22 weeks (and at term) and also correlated significantly with notch persistence; as only AoI-PI at term was significant, the placental correlations are weaker, emphasizing the value of UtA-PI as previously reported [39,42]. It is uncertain whether fetal changes are independent of placental bed redox modifications or are secondary to these modifications because the foetoplacental unit is reliant on uterine artery perfusion. The finding of a negative correlation between NOX activity at the placental bed (but not at the placenta) and BMI is surprising in view of the general recognition that obesity is associated with oxidative stress [58]. However, this correlation may reflect only a particular local regulation as adipocytes produce a variety of peptides with modulatory abilities, including adiponectin, which was found to down-regulate NOX activity [59,60].

We are convinced that the same mechanisms that enhance placental bed NOX activity related DHE conversion in the identified clusters are able to maintain higher UtA-PI in the same clusters. Therefore, considering the strong correlation between the higher levels of UtA-PI at 20–22 weeks and NOX activity in the uterine tissue at term, it is conceivable that, should UtA-PI become even higher, enhanced NOX activity would increase in a parallel fashion. Eventually, excessive local oxidation would result in abnormally high UtA-PI and unfavourable clinical outcomes; that is, the intensity of the oxidative insult would mark the distinction between functional disturbance and disease.

Although this study does not present placental bed NOX as a disorder biomarker, it provides strong evidence that, at both the uterus and the placenta, NOX is an important intervenient in the redox balance at the human fetal–maternal interface. Further knowledge of its regulation will provide useful insight for the better management of hypertensive disorders of pregnancy.

Study limitations and future research

The longitudinal k-means algorithm also suffers from some drawbacks [34]. (1) There are no formal hypothesis tests to check the validity of the partition. (2) The number of clusters must be known a priori. (3) The algorithm convergence to a global maximum is not assured, and therefore one cannot be sure that the best partition has been found. Another obvious limitation of the statistical analysis in this study was its sample size. A larger sample size would allow for the application of (semi-)parametric models (such as finite mixture models for clustering and *t*-tests for the evaluation of enzymatic activities within the clusters), which are known to be less conservative than non-parametric approaches (4). The intervention of other ROS producers and ROS scavengers was not studied, thus limiting the interpretation of the role of other ROS producers and antioxidant molecules.

Conclusions

This study provides evidence that in normal pregnancies, there is an important involvement of NOX mediated superoxide production, at the fetal/maternal interface. Notably, it was the placental bed that exhibited stronger positive correlation between NOX activity and UtA-PI.

Authors' contributions

G-M. designed the study, performed all Doppler measurements, collected the placenta/placental bed samples, analyzed the data, and wrote the manuscript; E.S. designed the study, coordinated all laboratorial experiments, analyzed the data, and composed the manuscript; A.R.G. performed all statistical analyses; J.P.S. contributed to the critical revision of the manuscript and coordinated the review of clinical cases; A.I.S. and J.A. participated in laboratory experiments; F.M. designed the study and contributed to the critical revision of the manuscript; H.A. designed the study, contributed to supervision, analyzed the data, and wrote the manuscript. All authors contributed to data interpretation and the final version of the manuscript, which all approved.

Conflict of interest

The authors declare no conflicts of interest.

Acknowledgements

We are grateful to the staff of the Department of Obstetrics of Centro Hospitalar do Porto. ARG was partially funded by the European Regional Development Fund through the programme COMPETE and by the Portuguese Government through the FCT - Fundação para a Ciência e a Tecnologia under the project PEst-C/MAT/UI0144/2013. ES was partially funded by the Portuguese Government and the European Union through FCT- Fundação para a Ciência e a Tecnologia, Programa Operacional Potencial Humano/Fundo Social Europeu under the fellowship SFRH/BPD/72536/2010.

Appendix A. Supporting information

Supplementary data associated with this article can be found in the online version at http://dx.doi.org/10.1016/j.jbiomech.2015.03.029.

References

[1] C. Hoffman, H.L. Galan, Assessing the 'at-risk' fetus: Doppler ultrasound, Current Opinion in Obstetrics and Gynecology 21 (2) (2009) 161–166. http://dx.doi.org/10.1097/GCO.0b013e3283292468 19996868.
[2] T. Stampalija, G.M. Gyte, Z. Alfirevic, Utero-placental Doppler ultrasound for improving pregnancy outcome, Cochrane Database of Systematic Reviews 9 (9) (2010) CD008363. http://dx.doi.org/10.1002/14651858.CD008363.pub2 20824875.
[3] O. Gómez, F. Figueras, S. Fernández, M. Bennasar, J.M. Martínez, B. Puerto, E. Gratacós, Reference ranges for uterine artery mean pulsatility index at 11–41 weeks of gestation, Ultrasound in Obstetrics and Gynecology 32 (2) (2008) 128–132. http://dx.doi.org/10.1002/uog.5315 18457355.
[4] G. Acharya, Technical aspects of aortic Isthmus Doppler velocimetry in human fetuses, Ultrasound in Obstetrics and Gynecology 33 (6) (2009) 628–633. http://dx.doi.org/10.1002/uog.6406 19479680.
[5] J. Ruskamp, J.C. Fouron, J. Gosselin, M.J. Raboisson, C. Infante-Rivard, F. Proulx, Reference values for an index of fetal aortic isthmus blood flow during the second half of pregnancy, Ultrasound in Obstetrics and Gynecology 21 (5) (2003) 441–444. http://dx.doi.org/10.1002/uog.105 12768553.
[6] J.C. Fouron, J. Gosselin, M.J. Raboisson, J. Lamoureux, C.A. Tison, C. Fouron, L. Hudon, The relationship between an aortic isthmus blood flow velocity index and the postnatal neurodevelopmental status of fetuses with placental circulatory insufficiency, American Journal of Obstetrics and Gynecology 192 (2) (2005) 497–503. http://dx.doi.org/10.1016/j.ajog.2004.08.026 15695993.
[7] S.E. Sonesson, J.C. Fouron, Doppler velocimetry of the aortic isthmus in human fetuses with abnormal velocity waveforms in the umbilical artery, Ultrasound in Obstetrics and Gynecology 10 (2) (1997) 107–111. http://dx.doi.org/10.1046/j.1469-0705.1997.10020107.x 9286019.
[8] K. Mäkikallio, P. Jouppila, J. Räsänen, Retrograde net blood flow in the aortic isthmus in relation to human fetal arterial and venous circulations, Ultrasound in Obstetrics and Gynecology 19 (2) (2002) 147–152. http://dx.doi.org/10.1046/j.0960-7692.2001.00626.x 11876806.
[9] K. Mäkikallio, P. Jouppila, J. Räsänen, Retrograde aortic isthmus net blood flow and human fetal cardiac function in placental insufficiency, Ultrasound in Obstetrics and Gynecology 22 (4) (2003) 351–357. http://dx.doi.org/10.1002/uog.232 14528469.
[10] G. Rizzo, A. Capponi, M. Vendola, M.E. Pietrolucci, D. Arduini, Relationship between aortic isthmus and ductus venosus velocity waveforms in severe growth restricted fetuses, Prenatal Diagnosis 28 (11) (2008) 1042–1047. http://dx.doi.org/10.1002/pd.2121 18973156.
[11] M. Del Río, J.M. Martínez, F. Figueras, M. Bennasar, A. Olivella, M. Palacio, O. Coll, B. Puerto, E. Gratacós, Doppler assessment of the aortic isthmus and perinatal outcome in preterm fetuses with severe intrauterine growth restriction, Ultrasound in Obstetrics and Gynecology 31 (1) (2008) 41–47. http://dx.doi.org/10.1002/uog.5237 18157796.
[12] K. Mäkikallio, Is it time to add aortic isthmus evaluation to the repertoire of Doppler investigations for placental insufficiency? Ultrasound in Obstetrics and Gynecology 31 (1) (2008) 6–9. http://dx.doi.org/10.1002/uog.5239 18098344.
[13] S. Lin, I. Shimizu, N. Suehara, M. Nakayama, T. Aono, Uterine artery Doppler velocimetry in relation to trophoblast migration into the myometrium of the placental bed, Obstetrics and Gynecology 85 (5 Pt 1) (1995) 760–765. http://dx.doi.org/10.1016/0029-7844(95)00020-R 7724109.
[14] I. Brosens, R. Pijnenborg, L. Vercruysse, R. Romero, The "Great obstetrical syndromes" are associated with disorders of deep placentation, American Journal of Obstetrics and Gynecology 204 (3) (2011) 193–201. http://dx.doi.org/10.1016/j.ajog.2010.08.009 21094932.
[15] C.V. Steer, J. Williams, J. Zaidi, S. Campbell, S.L. Tan, Intra-observer, inter-observer, interultrasound transducer and intercycle variation in colour Doppler assessment of uterine artery impedance, Human Reproduction 10 (2) (1995) 479–481 7769083.
[16] L. Guedes-Martins, J. Saraiva, R. Gaio, F. Macedo, H. Almeida, Uterine artery impedance at very early clinical pregnancy, Prenatal Diagnosis 34 (8) (2014) 719–725. http://dx.doi.org/10.1002/pd.4325 24431243.
[17] L. Guedes-Martins, A. Cunha, J. Saraiva, R. Gaio, F. Macedo, H. Almeida, Internal iliac and uterine arteries Doppler ultrasound in the assessment of normotensive and chronic hypertensive pregnant women, Scientific Reports 4 (2014) 3785. http://dx.doi.org/10.1038/srep03785 24445576.
[18] A.T. Papageorghiou, C.K. Yu, R. Bindra, G. Pandis, K.H. Nicolaides, Fetal Medicine Foundation Second Trimester Screening Group, Multicenter screening for pre-eclampsia and fetal growth restriction by transvaginal uterine artery Doppler at 23 weeks of gestation, Ultrasound in Obstetrics and Gynecology 18 (5) (2001) 441–449. http://dx.doi.org/10.1046/j.0960-7692.2001.00572.x 11844162.

[19] A.T. Papageorghiou, C.K. Yu, I.E. Erasmus, H.S. Cuckle, K.H. Nicolaides, Assessment of risk for the development of pre-eclampsia by maternal characteristics and uterine artery Doppler, BJOG 112 (6) (2005) 703–709. http://dx.doi.org/10.1111/j.1471-0528.2005.00519.x 15924523.

[20] H.J. van den Elzen, T.E. Cohen-Overbeek, D.E. Grobbee, R.W. Quartero, J. W. Wladimiroff, Early uterine artery Doppler velocimetry and the outcome of pregnancy in women aged 35 years and older, Ultrasound in Obstetrics and Gynecology 5 (5) (1995) 328–333. http://dx.doi.org/10.1046/j.1469-0705.1995.05050328.x 7614138.

[21] M.W. Aardema, M.C. Saro, M. Lander, B.T. De Wolf, H. Oosterhof, J. G. Aarnoudse, Second trimester Doppler ultrasound screening of the uterine arteries differentiates between subsequent normal and poor outcomes of hypertensive pregnancy: two different pathophysiological entities? Clinical Science 106 (4) (2004) 377–382. http://dx.doi.org/10.1042/CS20030385 14636154.

[22] G.C. Smith, C.K. Yu, A.T. Papageorghiou, A.M. Cacho, K.H. Nicolaides, Fetal Medicine Foundation Second Trimester Screening Group, Maternal uterine artery Doppler flow velocimetry and the risk of stillbirth, Obstetrics and Gynecology 109 (1) (2007) 144–151. http://dx.doi.org/10.1097/01.AOG.0000248536.94919.e3 17197600.

[23] J.S. Cnossen, R.K. Morris, G. ter Riet, B.W. Mol, J.A. van der Post, A. Coomarasamy, A.H. Zwinderman, S.C. Robson, P.J. Bindels, J. Kleijnen, K. S. Khan, Use of uterine artery Doppler ultrasonography to predict pre-eclampsia and intrauterine growth restriction: a systematic review and bivariable meta-analysis, CMAJ 178 (6) (2008) 701–711. http://dx.doi.org/10.1503/cmaj.070430 18332385.

[24] K. Bedard, K.H. Krause, The NOX family of ROS-generating NADPH oxidases: physiology and pathophysiology, Physiological Reviews 87 (1) (2007) 245–313. http://dx.doi.org/10.1152/physrev.00044.2005 17237347.

[25] J.M. Davis, R.L. Auten, Maturation of the antioxidant system and the effects on preterm birth, Seminars in Fetal and Neonatal Medicine 15 (4) (2010) 191–195. http://dx.doi.org/10.1016/j.siny.2010.04.001 20452845.

[26] T. Cindrova-Davies, H.W. Yung, J. Johns, O. Spasic-Boskovic, S. Korolchuk, E. Jauniaux, G.J. Burton, D.S. Charnock-Jones, Oxidative stress, gene expression, and protein changes induced in the human placenta during labor, American Journal of Pathology 171 (4) (2007) 1168–1179. http://dx.doi.org/10.2353/ajpath.2007.070528 17823277.

[27] G.J. Burton, E. Jauniaux, D.S. Charnock-Jones, The influence of the intrauterine environment on human placental development, International Journal of Development Biology 54 (2–3) (2010) 303–312. http://dx.doi.org/10.1387/ijdb.082764gb 19757391.

[28] G.J. Burton, E. Jauniaux, Oxidative stress, Best Practice and Research: Clinical Obstetrics and Gynaecology 25 (3) (2011) 287–299. http://dx.doi.org/10.1016/j.bpobgyn.2010.10.016 21130690.

[29] H.P. Robinson, Sonar measurement of fetal crown-rump length as means of assessing maturity in first trimester of pregnancy, British Medicine Jounal 4 (5883) (1973) 28–31 4755210.

[30] T. Sousa, D. Pinho, M. Morato, J. Marques-Lopes, E. Fernandes, J. Afonso, S. Oliveira, F. Carvalho, A. Albino-Teixeira, Role of superoxide and hydrogen peroxide in hypertension induced by an antagonist of adenosine receptors, European Journal of Pharmacology 588 (2–3) (2008) 267–276. http://dx.doi.org/10.1016/j.ejphar.2008.04.044 18519134.

[31] X.Y. Yi, V.X. Li, F. Zhang, F. Yi, D.R. Matson, M.T. Jiang, P.L. Li, Characteristics and actions of NAD(P)H oxidase on the sarcoplasmic reticulum of coronary artery smooth muscle, American Journal of Physiology: Heart and Circulatory Physiology 290 (3) (2006) H1136–H1144. http://dx.doi.org/10.1152/ajpheart.00296.2005 16227345.

[32] M.M. Bradford, A rapid and sensitive method for the quantitation of microgram quantities of protein utilizing the principle of protein-dye binding, Analytical Biochemistry 72 (1976) 248–254. http://dx.doi.org/10.1016/0003-2697(76)90527-3 942051.

[33] J.M. Bland, D.G. Altman, Applying the right statistics: analyses of measurement studies, Ultrasound in Obstetrics and Gynecology 22 (1) (2003) 85–93. http://dx.doi.org/10.1002/uog.122 12858311.

[34] C. Genolini, B. Falissard, KmL: k-means for longitudinal data, Computional Statistics 25 (2) (2010) 317–328. http://dx.doi.org/10.1007/s00180-009-0178-4.

[35] U. Maulik, S. Bandyopadhyay, Performance evaluation of some clustering algorithms and validity indices, IEEE Transaction on Pattern Analysis and Machine Intelligence 24 (12) (2002) 1650–1654. http://dx.doi.org/10.1109/TPAMI.2002.1114856.

[36] R. Development Core Team R: A language and environment for statistical computing R Foundation for Statistical Computing, Vienna, Austria, 2010. Available at: http://www.R-project.org/ (accessed 18.06.13).

[37] R. Pijnenborg, L. Vercruysse, I. Brosens, Deep placentation, Best Practice and Research: Clinical Obstetrics and Gynaecology 25 (3) (2011) 273–285. http://dx.doi.org/10.1016/j.bpobgyn.2010.10.009 21212025.

[38] S. Sağol, E. Ozkinay, K. Oztekin, N. Ozdemir, The comparison of uterine artery Doppler velocimetry with the histopathology of the placental bed, Australian and New Zealand Journal of Obstetrics and Gynaecology 39 (3) (1999) 324–329. http://dx.doi.org/10.1111/j.1479-828X.1999.tb03407.x 10554944.

[39] R. Madazli, A. Somunkiran, Z. Calay, S. Ilvan, M.F. Aksu, Histomorphology of the placenta and the placental bed of growth restricted foetuses and correlation with the Doppler velocimetries of the uterine and umbilical arteries, Placenta 24 (5) (2003) 510–516. http://dx.doi.org/10.1053/plac.2002.0945 12744927.

[40] M.M. Kennelly, N. Farah, M.J. Turner, B. Stuart, Aortic Isthmus Doppler velocimetry: role in assessment of preterm fetal growth restriction, Prenatal Diagnosis 30 (5) (2010) 395–401. http://dx.doi.org/10.1002/pd.2474 20232481.

[41] F. Figueras, A. Benavides, M. Del Del Rio, F. Crispi, E. Eixarch, J.M. Martinez, E. Hernandez-Andrade, E. Gratacós, Monitoring of fetuses with intrauterine growth restriction: longitudinal changes in ductus venosus and aortic isthmus flow, Ultrasound in Obstetrics and Gynecology 33 (1) (2009) 39–43. http://dx.doi.org/10.1002/uog.6278 19115231.

[42] M.W. Aardema, H. Oosterhof, A. Timmer, I. van Rooy, J.G. Aarnoudse, Uterine artery Doppler flow and uteroplacental vascular pathology in normal pregnancies and pregnancies complicated by pre-eclampsia and small for gestational age foetuses, Placenta 22 (5) (2001) 405–411. http://dx.doi.org/10.1053/plac.2001.0676 11373150.

[43] T. Warren Liao, Clustering of time series data – a survey, Pattern Recognition 38 (11) (2005) 1857–1874. http://dx.doi.org/10.1016/j.patcog.2005.01.025.

[44] L. Guedes-Martins, L. Matos, A. Soares, E. Silva, H. Almeida, AGEs, contributors to placental bed vascular changes leading to preeclampsia, Free Radical Research 47 (Suppl. 1) (2013) S70–S80. http://dx.doi.org/10.3109/10715762.2013.815347 23796030.

[45] J.D. Lambeth, Nox enzymes, ROS, and chronic disease: an example of antagonistic pleiotropy, Free Radical Biology and Medicine 43 (3) (2007) 332–347. http://dx.doi.org/10.1016/j.freeradbiomed.2007.03.027 17602948.

[46] X.L. Cui, B. Chang, L. Myatt, Expression and distribution of NADPH oxidase isoforms in human myometrium – role in angiotensin II-induced hypertrophy, Biology of Reproduction 82 (2) (2010) 305–312. http://dx.doi.org/10.1095/biolreprod.109.080275 19812300.

[47] R. Lim, R. Acharya, P. Delpachitra, S. Hobson, C.G. Sobey, G.R. Drummond, E. M. Wallace, Activin and NADPH-oxidase in preeclampsia: insights from in vitro and murine studies, American Journal of Obstetrics and Gynecology 212 (1) (2015) 86.e1–86.e12. http://dx.doi.org/10.1016/j.ajog.2014.07.021 25046804.

[48] S.R. Thomas, K. Chen, J.F. Keaney, Hydrogen peroxide activates endothelial nitric-oxide synthase through coordinated phosphorylation and dephosphorylation via a phosphoinositide 3-kinase-dependent signaling pathway, Journal of Biological Chemistry 277 (8) (2002) 6017–6024. http://dx.doi.org/10.1074/jbc.M109107200 11744698.

[49] T.R. Everett, C.C. Lees, Beyond the placental bed: placental and systemic determinants of the uterine artery Doppler waveform, Placenta 33 (11) (2012) 893–901. http://dx.doi.org/10.1016/j.placenta.2012.07.011 22902007.

[50] T.J. Guzik, N.E. West, E. Black, D. McDonald, C. Ratnatunga, R. Pillai, K. M. Channon, Vascular superoxide production by NAD(P)H oxidase: association with endothelial dysfunction and clinical risk factors, Circulation Research 86 (9) (2000) E85–E90 10807876.

[51] O. Jung, J.G. Schreiber, H. Geiger, T. Pedrazzini, R. Busse, R.P. Brandes, gp91phox-containing NADPH oxidase mediates endothelial dysfunction inrenovascular hypertension, Circulation 109 (14) (2004) 1795–1801. http://dx.doi.org/10.1161/01.CIR.0000124223.00113.A4 15037533.

[52] C.E. Murdoch, S.P. Alom-Ruiz, M. Wang, M. Zhang, S. Walker, B. Yu, A. Brewer, A.M. Shah, Role of endothelial Nox2 NADPH oxidase in angiotensin II-induced hypertension and vasomotor dysfunction, Basic Research in Cardiology 106 (4) (2011) 527–538. http://dx.doi.org/10.1007/s00395-011-0179-7 21528437.

[53] N.F. Gant, G.L. Daley, S. Chand, P.J. Whalley, P.C. MacDonald, A study of angiotensin II pressor response throughout primigravid pregnancy, Journal of Clinical Investigation 52 (11) (1973) 2682–2689. http://dx.doi.org/10.1172/JCI107462 4355997.

[54] S. Sankaralingam, I.A. Arenas, M.M. Lalu, S.T. Davidge, Preeclampsia: current understanding of the molecular basis of vascular dysfunction, Expert Reviews in Molecular Medicine 8 (3) (2006) 1–20. http://dx.doi.org/10.1017/S1462399406010465 16438753.

[55] R. Dechend, C. Viedt, D.N. Müller, B. Ugele, R.P. Brandes, G. Wallukat, J.K. Park, J. Janke, P. Barta, J. Theuer, A. Fiebeler, V. Homuth, R. Dietz, H. Haller, J. Kreuzer, F.C. Luft, AT1 receptor agonistic antibodies from preeclamptic patients stimulate NADPH oxidase, Circulation 107 (12) (2003) 1632–1639. http://dx.doi.org/10.1161/01.CIR.0000058200.90059.B1 12668498.

[56] K. Ota, S. Yamagishi, M. Kim, S. Dambaeva, A. Gilman-Sachs, K. Beaman, J. Kwak-Kim, Elevation of soluble form of receptor for advanced glycation end products (sRAGE) in recurrent pregnancy losses (RPL): possible participation of RAGE in RPL, Fertility and Sterility 102 (3) (2014) 782–789. http://dx.doi.org/10.1016/j.fertnstert.2014.06.010 25044082.

[57] L.C. Sánchez-Aranguren, C.E. Prada, C.E. Riaño-Medina, M. Lopez, Endothelial dysfunction and preeclampsia: role of oxidative stress, Frontiers in Physiology 5 (2014) 372. http://dx.doi.org/10.3389/fphys.2014.00372 25346691.

[58] S. Le Lay, G. Simard, M.C. Martinez, R. Andriantsitohaina, Oxidative stress and metabolic pathologies: from an adipocentric point of view, Oxidative Medicine and Cellular Longevity 2014 (2014) 908539. http://dx.doi.org/10.1155/2014/908539 25143800.

[59] F. Jiang, H.K. Lim, M.J. Morris, L. Prior, E. Velkoska, X. Wu, G.J. Dusting, Systemic upregulation of NADPH oxidase in diet-induced obesity in rats, Redox Report 16 (6) (2011) 223–229. http://dx.doi.org/10.1179/174329211X13049558293713 22195989.

[60] Y. Zhang, X.L. Wang, J. Zhao, Y.J. Wang, W.B. Lau, Y.X. Yuan, E.H. Gao, W.J. Koch, X.L. Ma, Adiponectin inhibits oxidative/nitrative stress during myocardial ischemia and reperfusion via PKA signaling, American Journal of Physiology - Endocrinology and Metabolism 305 (12) (2013) E1436–E1443. http://dx.doi.org/10.1152/ajpendo.00445.2013 24129398.

Article 7

Guedes-Martins L, Saraiva J, Felgueiras Ó, Carvalho M, Cerdeira A, Macedo F, Gaio R, Almeida H. Uterine artery impedance during puerperium in normotensive and chronic hypertensive pregnant women. *Arch Gynecol Obstet.* 2015; 291:1237-46.

Arch Gynecol Obstet
DOI 10.1007/s00404-014-3560-6

MATERNAL-FETAL MEDICINE

Uterine artery impedance during puerperium in normotensive and chronic hypertensive pregnant women

Luís Guedes-Martins · Joaquim Saraiva · Óscar Felgueiras · Mariana Carvalho · Ana Cerdeira · Filipe Macedo · Rita Gaio · Henrique Almeida

Received: 23 March 2014 / Accepted: 25 November 2014

Abstract
Purpose The present study compared the Doppler flow pulsatility indices (PI) in the uterine arteries (UtA) during the puerperium between healthy women and those with stage-1 essential hypertension who had uncomplicated pregnancies and delivered by elective caesarean section. The change in the mean arterial pressure (MAP) and body mass index (BMI) over time was also assessed.
Methods A longitudinal and prospective study was performed in singleton pregnancies of 28 normotensive (NT) and 24 hypertensive (HT) women. The UtA-PI was measured immediately before caesarean section (time 0) and at 1 week (time 1) and 4 weeks (time 2) postpartum. The presence or absence of early diastolic notches was recorded. The change in the MAP, BMI, and UtA-PI over time and between the two populations was modelled through multivariate linear regression using the generalised least squares.
Results In both groups, the UtA-PI significantly increased from time 0 to time 1 ($p < 0.05$) and time 2 ($p < 0.05$). Stage-1 hypertension did not change the trend but did increase the UtA-PI magnitude ($p < 0.05$). The presence of uterine artery notching increased over time, from 6 to 98 %, in both groups ($p < 0.001$); however, in the HT group, at time 1, the majority of women exhibited positive notching [92 % (HT) vs 57 % (NT), $p = 0.013$].
Conclusions Chronic stage-1 hypertensive women with normal pregnancy outcomes exhibited a progressively increasing postpartum UtA impedance. This trend also occurred in normotensive women, albeit at a significantly lower magnitude.

L. Guedes-Martins (✉) · H. Almeida
Department of Experimental Biology, Faculty of Medicine, University of Porto, 4200-319 Porto, Portugal
e-mail: luis.guedes.martins@gmail.com

L. Guedes-Martins · J. Saraiva · M. Carvalho
Departamento da Mulher e da Medicina Reprodutiva, Centro Hospitalar do Porto EPE, Largo Prof. Abel Salazar, 4099-001 Porto, Portugal

J. Saraiva
Obstetrics-Gynecology, Private Hospital Trofa, 4785-409 Trofa, Portugal

Ó. Felgueiras · R. Gaio
Department of Mathematics, Faculty of Sciences, University of Porto, Rua do Campo Alegre, 4169-007 Porto, Portugal

Ó. Felgueiras · R. Gaio
CMUP-Centre of Mathematics, University of Porto, Rua do Campo Alegre, 4169-007, Porto, Portugal

A. Cerdeira
Gulbenkian Program for Advanced Medical Education, 1067-001 Lisbon, Portugal

A. Cerdeira
Department of Medicine, Beth Israel Deaconess Medical Center, Harvard Medical School, Boston, MA 02215, USA

F. Macedo
Department of Cardiology, Faculty of Medicine, University of Porto, 4200-319 Porto, Portugal

F. Macedo
Centro Hospitalar S. João, 4200-319 Porto, Portugal

H. Almeida
Obstetrics-Gynecology, Hospital-CUF Porto, 4100 180 Porto, Portugal

Published online: 04 December 2014

Keywords Doppler ultrasound · Uterine artery · Postpartum · Hypertension · Pulsatility index

Introduction

Soon after a pregnancy is established, there is a progressive increase in the blood demand in the pelvic canal to meet the requirements of the growing uterus and foetus. The uterine artery (UtA) in particular undergoes important functional changes that can be assessed using computerised analysis of its blood velocity spectrum measured by Doppler ultrasound. This procedure has expanded quite rapidly in obstetrics recently due to its non-invasive nature and the relative simplicity of currently available devices and techniques. Moreover, the technique enables quantitative measurement of the impedance as the pulsatility (PI) and resistance (RI) indices, which are important for functional categorization of the uterine artery. The PI is considered to describe the shape of the velocity waveform much better than other indices [1].

The UtA impedance has been measured in reproductive-age women before pregnancy [2, 3], during pregnancy [1, 4], and at delivery [5, 6]. In non-pregnant women, the uterine artery flow velocity during systole rapidly rises and falls, and is followed by a notch during early diastole [2]; during the menstrual cycle, the impedance decreases during the luteal phase before increasing as menstruation approached in parallel with the increasing plasma progesterone and oestradiol concentrations, which rise as implantation nears [3, 7].

During pregnancy in healthy women, the uterine artery blood volume increases and is paralleled by a progressive decrease in the blood flow impedance beginning at early gestation [4] and lasting throughout the remaining pregnancy until term [1]. This is thought to result from the impressive structural changes at the placental bed. The placenta-derived trophoblastic cells migrate across the decidua layer to the inner third of the myometrium to reach the maternal spiral arteries, which are the distal branches of the uterine artery; the trophoblasts then invade the vascular walls and replace most of the muscular and endothelial cells [8, 9]. This migration renders the uterine arteries low-impedance/high-capacitance vessels, and the PI decreases. In contrast, a sustained or increased UtA-PI is thought to have prognostic value for the development of uterine disorders such as preeclampsia (PE) [10, 11] and placental abruption [12, 13], and is correlated with adverse perinatal outcomes [14–16].

Upon delivery, the hemodynamic features reverse; the cardiac output and heart rate fall, and in most studies, the uterine artery impedance increases due to a sudden drop in nutritional demand. In fact, increased vascular resistance reportedly begins very early postpartum and progresses thereafter [17–19]; the UtA protodiastolic notch also reappears in tandem in a progressive fashion [19]. In contrast to the wealth of studies performed during pregnancy, the changes in the pelvic circulation puerperium have received much less attention. However, serious pathological conditions can arise during this period including haemorrhage, anaemia, infection, disabling pain, and unexpected PE. Preeclampsia is particularly important because it is first recognised at the postpartum period in approximately 5 % of cases, and its morbidity and mortality may be considerable [20].

Thus, it is important to have a better understanding of the changing pelvic features, circulatory or otherwise, during this postpartum period. Apart from obtaining data from normotensive women, we reasoned that additional information on the uterine artery performance during pregnancy could be provided by a parallel study in women with chronic stable hypertension because hypertension is a prevalent condition and a known risk factor for serious disorders of the pregnancy, including PE [21–23]. Therefore, in the present study, we compared the Doppler flow impedance in the uterine arteries postpartum in healthy, normotensive women to those with stage-1 essential hypertension who had uncomplicated pregnancies and a normal puerperium period. To exclude the expected confounder effect of the delivery method on the postpartum uterine artery impedance behaviour, only women undergoing elective caesarean section were included.

Materials and methods

Subjects

This study was approved by the local ethics committee of Centro Hospitalar do Porto-Unidade Maternidade Júlio Dinis, and all subjects provided informed consent [Ref. 150-13(096-DEFI/122-CES)].

From January 2010 to December 2012, women with singleton pregnancies at term and scheduled for elective caesarean section (due to foetal breech presentation, suspected cephalopelvic disproportion, or previous caesarean section) were recruited and allocated into two groups. The first group included healthy women who had uneventful pregnancies. The second comprised women with a history of chronic arterial hypertension prior to pregnancy. Acceptable medication in both groups was folic acid, vitamin, and iron supplements. Additionally, all hypertensive pregnant women received acetylsalicylic acid (100 mg per day) and methyldopa (500–750 mg divided into two to three doses per day). Oral acetylsalicylic acid was

administered starting at 6–14 weeks of gestation and continued until the day of delivery, according to our institutional protocol for managing chronic hypertensive pregnant women. Before pregnancy, the majority of patients required multiple medications to control their hypertension including thiazide, angiotensin-converting enzyme inhibitor, angiotensin receptor blockers, or calcium channel blockers. After the first appointment, antihypertensive drugs were discontinued, and the blood pressure response was closely monitored. Antihypertensive therapy was reinstituted if persistent diastolic pressures of 95–99 mmHg or a systolic pressure $\geq$150 mmHg was observed at any time during pregnancy.

Gestational age was determined by ultrasonography between 11 and 14 weeks. Biometric data, blood pressure, uterine artery Doppler flow analysis, and the body mass index (BMI) were measured at three time points: immediately before caesarean section (Time 0), and 1 (Time 1) and 4 (Time 2) weeks after delivery. On the day of caesarean section, all women were observed by a senior specialist who reviewed the patient's history and verified the absence of diabetes and other endocrine disorders, immune diseases, renal, structural heart diseases, haematological conditions, and chronic infections. Patients in labour, those with ruptured membranes, those with multiple foetuses, and those receiving β-tocolytic drugs, as well as those who had reported per-operative complications were excluded. Foetal disorders or newborn abnormalities, verified by a neonatologist at birth and 1 month later, were additional criteria for exclusion.

Blood pressure assessment

The blood pressure (BP) was measured immediately before Doppler flow assessment using an automated instrument (GE Healthcare Carescape™ V100 Vital Signs Monitor with DINAMAP Blood Pressure) three consecutive times and averaged. Blood pressure was expressed as the mean arterial pressure (MAP) according to the formula:

$$\text{MAP} = \frac{(2 \times \text{diastolic pressure}) + \text{systolic pressure}}{3}.$$

Doppler flow assessment

The Doppler flow evaluation of right and left UtA was performed at the three time points employing a 4 MHz convex transabdominal probe at baseline (Time 0) and a transvaginal transducer at Times 1 and 2 (GE Healthcare Technologies, Voluson 730 Pro, USA). Nursing mothers were required to abstain from breastfeeding for at least 30 min prior to examination.

For the UtA transabdominal evaluation (Time 0), the probe was placed on the lower abdominal quadrants and angled medially, and colour Doppler imaging was used to localise the UtA as it crossed over the external iliac artery. In all cases, an angle less than 30° was assured before the pulsed Doppler probe was placed over the entire vessel width. Angle correction was then applied, and the signal was updated until three similar consecutive waveforms were observed. The left and right uterine artery pulsatility (UtA-PI) indices were calculated using the device software. For the UtA transvaginal assessment (Times 1 and 2), a sagittal section of the uterus was obtained, and the cervical canal and internal cervical ostium were identified. The transducer was gently tilted from side to side, and colour flow mapping was used to identify each uterine artery alongside the cervix and uterus at the level of the internal ostium. Pulsed wave Doppler was used with the sampling gate set at 2 mm to image the entire vessel and ensure that the angle of insonation was <30°. Finally, the mean UtA-PI of the left and right arteries was calculated (Fig. 1).

The presence or absence of a bilateral early protodiastolic notch in the UtA was noted. A positive notch was defined as a persistent decrease in the blood flow velocity during early diastole below the diastolic peak velocity in at least one UtA Doppler ultrasound spectrum. Absence of the notch was defined by its bilateral absence.

All measurements were made by a single investigator with extensive experience in Doppler ultrasound to avoid inter-observer variability. Intra-observer reliability was estimated from two consecutive readings among the first 40 PI recordings in the UtA (20 transabdominal and 20 transvaginal).

Statistical analysis

Univariate data analysis was performed using the Chi square test or Fisher's test as appropriate to determine independence amongst two factors, the *t* test for the difference in means from two independent populations, and one-way analysis of variance for repeated measurements. Tukey's multiple comparisons test was used to assess statistically significant differences across more than two means in paired populations.

The change in the UtA-PI, MAP, and BMI over time in each group was modelled through multiple linear regression. The generalised least squares with maximum likelihood estimation method was applied to correlated and heteroscedastic errors following a normal distribution. For each dependent variable, the best model was chosen based on the lowest value of the Bayesian Information Criterion (BIC).

For each woman with a hypertensive status *h* (equal to 1 for hypertensive women and 0 otherwise), at continuous time *t* representing the number of weeks after labour, the MAP was modelled by the following equation:

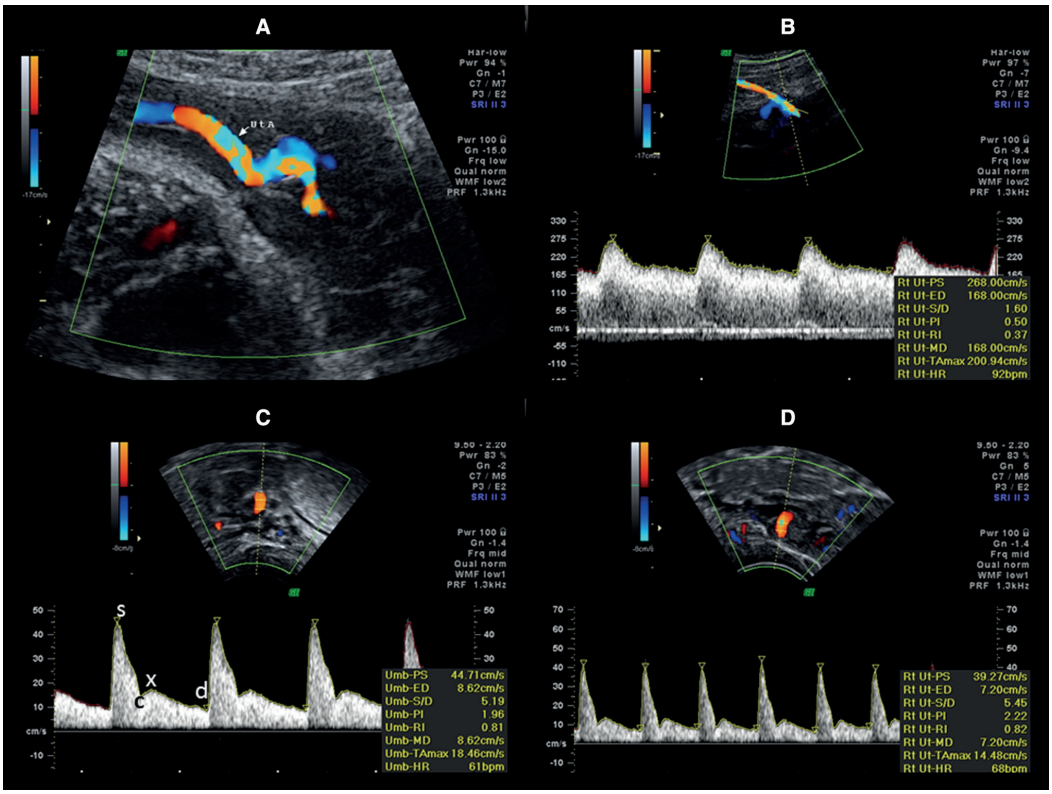

Fig. 1 **a** Uterine artery (UtA) depicted in colour flow map. Typical Doppler shift spectra recorded at time 0 (**b**), 1 week (**c**), and 4 weeks (**d**) after delivery. In **b** waveforms, the velocity gradually decreased from its systolic peak, and a continuous forward flow was observed during diastole. In **c** and **d**, the waveforms show a notch before beginning continuous diastole forward flow. Pulsatility index (PI), the measure of impedance of blood flow distal to the sampling point, was calculated according to the formula: $\mathrm{PI} = \frac{(s-d)}{\mathrm{mean}}$, where s is the peak systolic, d is the minimum end-diastolic, and *mean* is the average maximum Doppler shift frequency over the cardiac cycle. c early diastolic, x maximum diastolic frequency

$$\mathrm{MAP}(h,t) = \beta_0(h) + \beta_1(h)t + \varepsilon. \quad (1)$$

Both the intercept and the time-slope coefficient are linear functions of the hypertensive status, and ε represents the errors of the model. The errors correlation structure had compound symmetry within each hypertensive status. Time was coded as 0, 1, or 4, and was considered a continuous variable to reflect the real time differences between the three evaluation periods.

For BMI, the best fitted model was as follows:

$$\log(\mathrm{BMI}(h,t)) = \beta_0(h) + \beta_2 t + \varepsilon \quad (2)$$

with the BMI logarithm linear in both hypertensive status and time.

The model obtained for the pulsatility index had an identical structure to model (2). However, the errors from model (2) had an identical compound symmetry structure within each individual and different variances depending on the hypertensive status, but the errors correlation structure in the PI model had a compound symmetry within each hypertensive status and different error variances according to the hypertensive status.

The intraclass correlation coefficient (ICC) and 95 % confidence intervals were calculated using a two-way mixed-effects model with absolute agreement. The reliability coefficient, which is the difference value exceeded by only 5 % of measurement pairs on the same subject, was calculated as 1.96 times the standard deviation of the difference between pairs of repeated measurements.

Statistical analyses were performed using the R language and software environment for statistical computation, version 3.0.11 [24]. The significance level was fixed at 0.05.

Results

A total 84 pregnant women at term were initially eligible based on the established inclusion criteria. However, 32 (38.1 %) were later excluded: 7 patients were in early labour; 5 had multiple pregnancies; 4 had diabetes; 3 presented technical difficulties during PI measurement in the uterine/umbilical arteries; 2 had suspected preeclampsia; 8 were lost during follow-up; and 3 were excluded because of puerperium complications (2 had prolonged postpartum haemorrhage and 1 had surgical site infection).

Among the 52 enrolled women, 28 (53.8 %) were normotensive (NT), and 24 (46.2 %) had stage-1 chronic arterial hypertension (HT) (Table 1). The patient ages ranged from 17 to 42 years, and 67 % were less than 35 years. This was the first pregnancy in 65 % of the women. All delivered at term with a mean gestational age at delivery of 39.5 weeks [standard deviation (SD) 0.85]. There were significant differences between the NT and HT groups in parity (nulliparous predominated the HT group) and BMI (higher classes predominated the HT group).

During the puerperium, the presence of uterine artery notching increased over time from 6 to 98 % (Table 2) in both groups ($p < 0.001$). During the first (week 0) and third (week 4) time points, there were no significant differences between the NT and HT groups in the presence of notching; however, in the HT group, the majority of women exhibited positive notching at the second (week 1) time point [92 % (HT) vs 57 % (NT)], and the difference was statistically significant ($p = 0.013$). The mean (SD) of the MAP, BMI, and UtA-PIs at each time point and in each group are shown in Table 3. The crude effect of time on the mean MAP, BMI, and UtA-PIs is shown in Fig. 2. There was an overall decreasing trend in the mean MAP and BMI, and an increasing trend in the mean UtA-PI over time (Fig. 2a, b, and c, respectively).

The reliability coefficients were 0.080 and 0.457 for the transabdominal and transvaginal UtA-PI measurements, respectively. The intraclass correlation coefficient for the intra-observer reliability was 0.976 for the transabdominal (95 % CI 0.933–0.989) and 0.858 for the transvaginal (95 % CI 0.642–0.944) assessments, which is quite high [25].

Multivariate analysis

The net effect of time on the MAP, BMI, and UtA-PI was considered merely indicative; therefore, multivariate analyses were performed by adjusting the effect to potential

Table 1 Demographic characteristics of the study population

	All ($n = 52$)	Normotensive ($n = 28$)	Hypertensive ($n = 24$)	p value[b]
Age (intervals in years)				
17–24	8 (15 %)	3 (11 %)	5 (21 %)	0.359
25–34	27 (52 %)	17 (61 %)	10 (42 %)	
35–42	17 (33 %)	8 (28 %)	9 (37 %)	
Education level (years)				
<7	4 (8 %)	1 (4 %)	3 (12 %)	0.386
7–9	10 (19 %)	4 (14 %)	6 (25 %)	
10–12	23 (44 %)	13 (46 %)	10 (42 %)	
>12	15 (29 %)	10 (36 %)	5 (21 %)	
Smoking				
No	46 (88 %)	25 (89 %)	21 (87 %)	1.000
Yes	6 (12 %)	3 (11 %)	3 (13 %)	
Parity				
0	34 (65 %)	14 (50 %)	20 (83 %)	0.026
≥1	18 (35 %)	14 (50 %)	4 (17 %)	
Body mass index[a] (kg/m^2)				
18–24	19 (37 %)[c]	14 (50 %)	5 (21 %)	0.009
25–29	14 (27 %)[c]	9 (32 %)	5 (21 %)	
30–51	19 (37 %)[c]	5 (18 %)	14 (58 %)	
GA at delivery (weeks ± SD)	39.5 (0.85)	39.5 (0.87)	39.5 (0.85)	0.840
Birth weight at delivery (g), mean (SD)	3,239.4 (405.36)	3,209.5 (432.71)	3,274.4 (377.08)	0.566

BMI body mass index, *GA* gestational age, *SD* standard deviation

[a] BMI: measurement at time 0

[b] Tests homogeneity of proportions between the hypertensive and normotensive populations

[c] The summed relative frequencies in the three categories was 101 % due to rounding

Table 2 Absolute (relative, %) frequencies for positive notching of uterine arteries in normotensive and hypertensive women

Time (weeks)	All ($n = 52$)	p value[a]	Normotensive ($n = 28$)	Hypertensive ($n = 24$)	p value[b]
0	3 (6 %)	<0.001	1 (4 %)	2 (8 %)	0.590
1	38 (73 %)	<0.001	16 (57 %)	22 (92 %)	0.013
4	51 (98 %)	<0.001	27 (96 %)	24 (100 %)	1.000

[a] Tests the equality of population frequencies amongst positive and negative notching

[b] Tests the homogeneity of proportions between the hypertensive and normotensive populations

Table 3 Mean (standard deviation) MAP, BMI, and PI at each time point in the whole sample and stratified by hypertensive status

Weeks	Time points		
	0	1	4
All ($n = 52$)			
MAP	95.692 (13.189)	94.474 (12.486)	90.526 (9.911)
BMI	31.403 (5.488)	30.331 (5.449)	28.788 (5.522)
UtA-PI	0.808 (0.208)	1.301 (0.338)	1.915 (0.383)
Normotensive ($n = 28$)			
MAP	87.048 (9.070)	84.738 (6.868)	84.917 (7.446)
BMI	30.115 (5.759)	29.322 (5.805)	27.263 (5.630)
UtA-PI	0.746 (0.227)	1.134 (0.292)	1.832 (0.438)
Hypertensive ($n = 24$)			
MAP	105.778 (9.594)	105.833 (6.348)	97.069 (8.352)
BMI	32.907 (4.843)	31.507 (4.859)	30.568 (4.927)
UtA-PI	0.879 (0.159)	1.495 (0.283)	2.013 (0.286)

MAP mean arterial pressure, *BMI* body mass index, *UtA-PI* uterine artery pulsatility index

confounders and accommodating the study design. Known confounding variables such as maternal age, BMI, and parity were also considered in the analysis; they were not statistically significant and were not considered in the final model.

MAP and BMI models

Although the mean MAP significantly decreased over time ($p < 0.05$) in the HT group, the time variable failed to have a significant effect in the NT group (Fig. 3a). The corresponding model is described in the "Statistical analysis" section; estimates of the coefficients and respective 95 % confidence intervals are presented in Table 4. The predicted BMI and the 95 % confidence intervals for the NT and HT group over time are shown in Fig. 3b. In both groups, the BMI exhibited a decreasing trend, but there was no significant difference between the NT and HT groups. Estimates of the coefficients and 95 % confidence

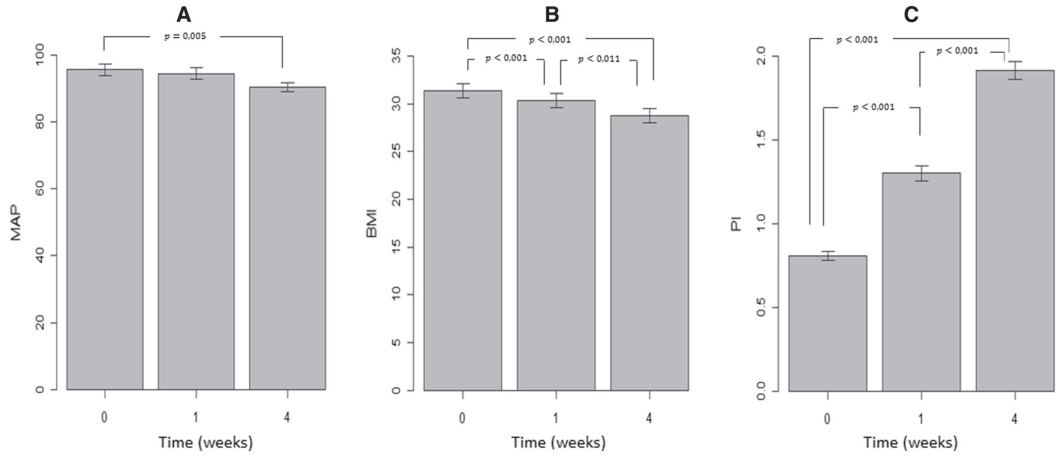

Fig. 2 Mean (±standard deviation) MAP (**a**), BMI (**b**), and UtA-PI (**c**) at each time point in the entire sample. *MAP* mean arterial pressure, *BMI* body mass index, *UtA-PI* uterine artery pulsatility index

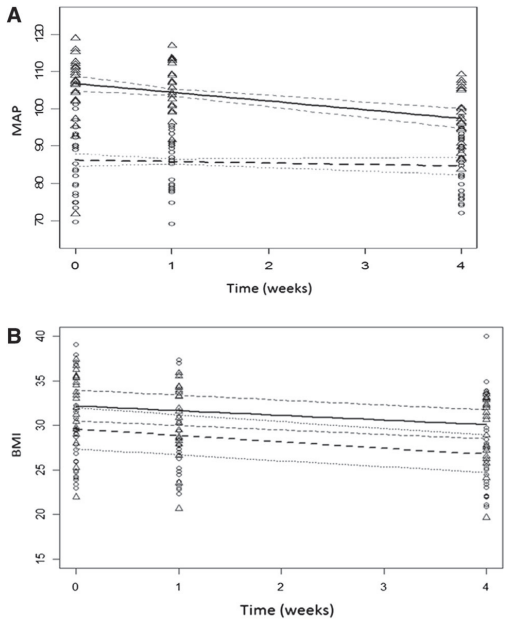

Fig. 3 Predicted mean arterial pressure (**a**) and body mass index (**b**) over time in normotensive (*dashed line*, *circles*) and hypertensive (*solid line*, *triangles*) women. The 95 % confidence intervals for the respective predictions are indicated (*dashed bands*)

Table 4 Estimated coefficients and correlation of the regression model predicting the MAP at different covariates combinations

Covariates	Coefficient	95 % CI
Intercept	86.338*	84.533, 87.922
Hypertension	20.581*	17.989, 23.173
Time	−0.396	−1.413, 0.621
Hypertension × time	−1.953*	−3.449, −0.456

MAP mean arterial pressure, *CI* confidence interval

* $p < 0.05$

intervals for the corresponding model are presented in Table 5.

UtA pulsatility indices

The predicted and observed mean UtA-PI in the NT and HT groups are depicted in Fig. 4. In both groups, the uterine artery impedance showed a significant increase over time ($p < 0.05$). Additionally, the PI in the HT group was significantly higher over time compared with the NT group. The estimated coefficients of the regression model used to predict the PI at the different covariates combinations are presented in Table 6.

Table 5 Estimated coefficients, correlation, and variance parameters of the regression model predicting the BMI at different covariates combinations

Covariates	Coefficient	95 % CI
Intercept	3.387*	3.309, 3.465
Hypertension	0.084	−0.011, 0.179
Time	−0.025*	−0.031, −0.020
Hypertension × time	0.008*	0.001, 0.015
Correlation parameter	0.955	
Variance factor for hypertension	0.640	

BMI body mass index, *CI* confidence interval

* $p < 0.05$

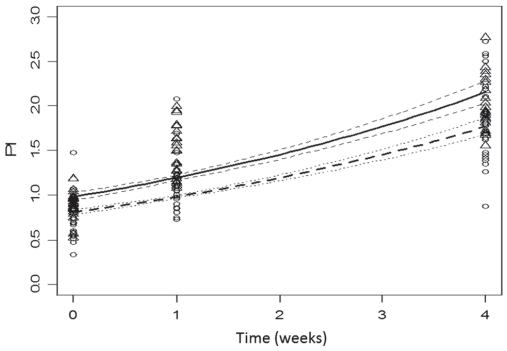

Fig. 4 Predicted mean pulsatility (PI) index of the uterine artery over time in normotensive (*dashed line*, *circles*) and hypertensive (*solid line*, *triangles*) women. The 95 % confidence intervals for the respective predictions are indicated (*dashed bands*)

Table 6 Estimated coefficients, correlation, and variance parameters of the regression model predicting the uterine artery PI at different covariates combinations

Covariates	Coefficient	95 % CI
Intercept	−0.215*	−0.254, −0.293
Hypertension	0.197*	0.177, 0.217
Time	0.197*	0.173, 0.220
Correlation parameter	−0.012	
Variance factor for hypertension	0.821	

PI pulsatility index, *CI* confidence interval

* $p < 0.05$

Discussion

During pregnancy, remarkable circulatory changes occur in the pelvis because the foetus has increased nutritional demands that the uterine circulation must accommodate. As expected, the uterine artery, as the immediate

intervenient in this process, has become an important target in obstetrical Doppler ultrasound studies. Several reports performed at different gestational ages have shown that the uterine artery impedance provides relevant predictive information on serious maternal and foetal complications. As a result, UtA-PI and notch assessment has been recommended for use in daily clinical practice [16]. Although the value of UtA impedance assessment during pregnancy is unquestionable, its postpartum utility is less clear and has received less attention. Yet, the ability to predict certain postpartum pathologies would be immensely useful; therefore, appropriate prognostic tools are needed. Among the potential complications, PE, postpartum haemorrhage, retained placental tissue, and infection are particularly relevant.

After delivery, remarkable structural and functional changes occur in the uterus to re-establish the non-pregnant condition, starting immediately upon placenta delivery and continuing for the following 6–8 weeks. This transition involves the spiral arteries, whose high capacitance properties are no longer necessary; as a result, the lumen is obliterated through thrombosis, endarteritis, and intima thickening [26]. Despite the substantial vascularization that is still present [18], the occlusion increases the local vascular resistance [27, 28]. The immediate cause for these events is the pressure imposed by the brisk postpartum myometrium contraction, but there is evidence that it may also be mediated immunologically because defects in complement expression have been observed in cases of placental site subinvolution [29].

In our investigation, the uterine artery PI was assessed during the recognised period of uterine involution; based on the study design, we are convinced that the changes reflected are quite specific and intrinsic patterns of postpartum involution as variables associated with labour differences were precluded. In this study, we examined the uterine arterial circulation after caesarean section in the absence of labour, which ensured the absence of any confounding effect related to other modes of delivery (spontaneous vaginal, ventouse, or forceps) and labour-related variables such as dystocia, phase latency variability, first stage duration, and myometrial contraction.

In normotensive women, the UtA-PI was significantly increased during the puerperal period. Interestingly, the mean value at the first time point, i.e., immediately before the caesarean section, is quite similar to the previously reported third trimester mean [30]. Although there may be some variability in the specific postpartum period assessed, the observed increase in the vascular resistance is consistent with most studies [17–19]. Few studies report no change [31], likely reflecting design variation.

An important novel finding in the current study concerns the UtA-PI in women with chronic hypertension and uncomplicated pregnancies. Again, the mean PI at the first time point was similar to the previously reported third trimester value in hypertensive women [30], and at the remaining time points, the UtA-PI progressively increased postpartum at a rate similar to that in normotensive women. However, the UtA-PI increases at higher magnitude compared with that in normotensive women. Remarkably, this peri- and postpartum difference has been recognised at other points during pregnancy [30]. Although the cause of this UtA-PI increase in normotensive and hypertensive women is unknown, the decreased concentration of locally active compounds such as oestradiol or progesterone, which decrease substantially after delivery [32], cannot be ignored.

Less clear is the cause of the parallel UtA-PI increase observed in both groups. We suspect that this trend, which was stable and continuous despite the dramatic uterine changes, reflects the steady and robust regulatory mechanisms in the vasculature. The responsible mechanisms may be systemic as those thought to control essential hypertension [33], but they may also reflect local activity, pregnancy-dependent factors, or genetic modulations that collectively allow the UtA to adequately perfuse the uterus irrespective of its pathologic condition. For example, women of Andean ancestry exhibit a three times higher UtA-PI compared with women of European descent, despite living at similar altitudes; however, during pregnancy, the hemodynamic adjustments lead to rather similar UtA-PIs in both [34].

An understanding of the uterine impedance recovery during the puerperium returning to the non-pregnant condition can help show the normal physiology and provide important insights into specific disorders, with PE as the most important one. The morbidity and mortality associated with PE cannot be overlooked, and delivery does not completely eliminate the risk of PE and its complications, which can become apparent when successful treatment has been seemingly achieved [20, 35]. Indeed, PE frequently shows up without any clinical signs or may present with non-specific or mild symptoms [36].

A number of molecules with local and systemic action have been shown to modulate the occurrence of PE including nitric oxide, components of the renin–angiotensin system, and certain growth factors [37], but assessment is cumbersome or clinically unfeasible. During the puerperal period, apart from continued monitoring and reporting of signs and symptoms, a hemodynamic approach, such as uterine artery impedance measurement, could be a useful way to detect impending PE or other conditions. However, additional studies are required to verify the diagnostic or prognostic utility of UtA Doppler ultrasound for specific hypertensive syndromes puerperium.

Study limitations

The present study comprised only uneventful pregnancies with normal neonatal and puerperal outcomes, and cannot be extrapolated to patients with other hypertensive conditions during pregnancy. Additionally, the hypertensive patients were treated from the first trimester onwards with daily low-dose acetylsalicylic acid and methyldopa. However, this regimen was prescribed in all the hypertensive patients, and therefore, this confounder was not isolated in the statistical analysis (the proportions were 100 and 0 %, respectively).

Acknowledgments We thank the staff at the Department of Obstetrics of Centro Hospitalar do Porto.

Conflict of interest The authors declare that they have no conflict of interest.

References

1. Gómez O, Figueras F, Fernández S, Bennasar M, Martínez JM, Puerto B, Gratacós E (2008) Reference ranges for uterine artery mean pulsatility index at 11–41 weeks of gestation. Ultrasound Obstet Gynecol 32:128–132
2. Schulman H, Fleischer A, Farmakides G, Bracero L, Rochelson B, Grunfeld L (1986) Development of uterine artery compliance in pregnancy as detected by Doppler ultrasound. Am J Obstet Gynecol 155:1031–1036
3. Tan SL, Zaidi J, Campbell S, Doyle P, Collins W (1996) Blood flow changes in the ovarian and uterine arteries during the normal menstrual cycle. Am J Obstet Gynecol 175:625–631
4. Guedes-Martins L, Saraiva J, Gaio R, Macedo F, Almeida H (2014) Uterine artery impedance at very early clinical pregnancy. Prenat Diagn 34:719–725
5. Cooley SM, Donnelly JC, Walsh T, MacMahon C, Gillan J, Geary MP (2011) The impact of umbilical and uterine artery Doppler indices on antenatal course, labor and delivery in a low-risk primigravid population. J Perinat Med 39:143–149
6. Fratelli N, Prefumo F, Andrico S, Lorandi A, Recupero D, Tomasoni G, Frusca T (2011) Effects of epidural analgesia on uterine artery Doppler in labour. Br J Anaesth 106:221–224
7. Steer CV, Campbell S, Pampiglione JS, Kingsland CR, Mason BA, Collins WP (1990) Transvaginal colour flow imaging of the uterine arteries during the ovarian and menstrual cycles. Hum Reprod 5:391–395
8. Pijnenborg R, Vercruysse L, Hanssens M (2006) The uterine spiral arteries in human pregnancy: facts and controversies. Placenta 27:939–958
9. Pijnenborg R, Vercruysse L, Brosens I (2011) Deep placentation. Best Pract Res Clin Obstet Gynaecol 25:273–285
10. Harrington K, Goldfrad C, Carpenter RG, Campbell S (1997) Transvaginal uterine and umbilical artery Doppler examination of 12–16 weeks and the subsequent development of pre-eclampsia and intrauterine growth retardation. Ultrasound Obstet Gynecol 9:94–100
11. Papageorghiou AT, Yu CK, Bindra R, Pandis G, Nicolaides KH, Fetal Medicine Foundation Second Trimester Screening Group (2001) Multicenter screening for pre-eclampsia and fetal growth restriction by transvaginal uterine artery Doppler at 23 weeks of gestation. Ultrasound Obstet Gynecol 18:441–449
12. Harrington K, Cooper D, Lees C, Hecher K, Campbell S (1996) Doppler ultrasound of the uterine arteries: the importance of bilateral notching in the prediction of pre-eclampsia, placental abruption or delivery of a small-for-gestational-age baby. Ultrasound Obstet Gynecol 7:182–188
13. Schwarze A, Nelles I, Krapp M, Friedrich M, Schmidt W, Diedrich K, Axt-Fliedner R (2005) Doppler ultrasound of the uterine artery in the prediction of severe complications during low-risk pregnancies. Arch Gynecol Obstet 271:46–52
14. Coleman MA, McCowan LM, North RA (2000) Mid-trimester uterine artery Doppler screening as a predictor of adverse pregnancy outcome in high-risk women. Ultrasound Obstet Gynecol 15:7–12
15. Axt-Fliedner R, Schwarze A, Nelles I, Altgassen C, Friedrich M, Schmidt W, Diedrich K (2005) The value of uterine artery Doppler ultrasound in the prediction of severe complications in a risk population. Arch Gynecol Obstet 271:53–58
16. Cnossen JS, Morris RK, ter Riet G, Mol BW, van der Post JA, Coomarasamy A, Zwinderman AH, Robson SC, Bindels PJ, Kleijnen J, Khan KS (2008) Use of uterine artery Doppler ultrasonography to predict pre-eclampsia and intrauterine growth restriction: a systematic review and bivariable meta-analysis. CMAJ 178:701–711
17. Kirkinen P, Dudenhausen J, Baumann H, Huch A, Huch R (1988) Postpartum blood flow velocity waveforms of the uterine arteries. J Reprod Med 33:745–748
18. Van Schoubroeck D, Van den Bosch T, Scharpe K, Lu C, Van Huffel S, Timmerman D (2004) Prospective evaluation of blood flow in the myometrium and uterine arteries in the puerperium. Ultrasound Obstet Gynecol 23:378–381
19. Mulic-Lutvica A, Eurenius K, Axelsson O (2007) Longitudinal study of Doppler flow resistance indices of the uterine arteries after normal vaginal delivery. Acta Obstet Gynecol Scand 86:1207–1214
20. Matthys LA, Coppage KH, Lambers DS, Barton JR, Sibai BM (2004) Delayed postpartum preeclampsia: an experience of 151 cases. Am J Obstet Gynecol 190:1464–1466
21. Sibai B, Dekker G, Kupferminc M (2005) Pre-eclampsia. Lancet 365:785–799
22. Macdonald-Wallis C, Lawlor DA, Fraser A, May M, Nelson SM, Tilling K (2012) Blood pressure change in normotensive, gestational hypertensive, preeclamptic, and essential hypertensive pregnancies. Hypertension 59:1241–1248
23. Romundstad PR, Magnussen EB, Smith GD, Vatten LJ (2010) Hypertension in pregnancy and later cardiovascular risk: common antecedents? Circulation 122:579–584
24. R Development Core Team (2013) R: a language and environment for statistical computing. R Foundation for Statistical Computing, Vienna. http://www.r-project.org. Accessed 18 Dec 2013
25. Bland JM, Altman DG (2003) Applying the right statistics: analyses of measurement studies. Ultrasound Obstet Gynecol 22:85–93
26. Weydert JA, Benda JA (2006) Subinvolution of the placental site as an anatomic cause of postpartum uterine bleeding: a review. Arch Pathol Lab Med 130:1538–1542
27. Morris R, Sunesara I, Rush L, Anderson B, Blake PG, Darby M, Sawardecker S, Novotny S, Bofill JA, Martin JN Jr (2014) Maternal hemodynamics by thoracic impedance cardiography for normal pregnancy and the postpartum period. Obstet Gynecol 123:318–324
28. Mabie WC, DiSessa TG, Crocker LG, Sibai BM, Arheart KL (1994) A longitudinal study of cardiac output in normal human pregnancy. Am J Obstet Gynecol 170:849–856
29. Andrew A, Bulmer JN, Morrison L, Wells M, Buckley CH (1993) Subinvolution of the uteroplacental arteries: an immunohistochemical study. Int J Gynecol Pathol 12:28–33

30. Guedes-Martins L, Cunha A, Saraiva J, Gaio R, Macedo F, Almeida H (2014) Internal iliac and uterine arteries Doppler ultrasound in the assessment of normotensive and chronic hypertensive pregnant women. Sci Rep 4:3785
31. Nakai Y, Imanaka M, Nishio J, Maeda T, Ozaki A, Sun TT, Ogita S (1997) Uterine blood flow velocity waveforms during early postpartum course following caesarean section. Eur J Obstet Gynecol Reprod Biol 74:121–124
32. Lewis PR, Galvin PM, Short RV (1987) Salivary oestriol and progesterone concentrations in women during late pregnancy, parturition and the puerperium. J Endocrinol 115:177–181
33. Bolívar JJ (2013) Essential hypertension: an approach to its etiology and neurogenic pathophysiology. Int J Hypertens 2013:547809
34. Wilson MJ, Lopez M, Vargas M, Julian C, Tellez W, Rodriguez A, Bigham A, Armaza JF, Niermeyer S, Shriver M, Vargas E, Moore LG (2007) Greater uterine artery blood flow during pregnancy in multigenerational (Andean) than shorter-term (European) high-altitude residents. Am J Physiol Regul Integr Comp Physiol 293:R1313–R1324
35. Sibai BM (2012) Etiology and management of postpartum hypertension-preeclampsia. Am J Obstet Gynecol 206:470–475
36. Al-Safi Z, Imudia AN, Filetti LC, Hobson DT, Bahado-Singh RO, Awonuga AO (2011) Delayed postpartum preeclampsia and eclampsia: demographics, clinical course, and complications. Obstet Gynecol 118:1102–1107
37. Conti E, Zezza L, Ralli E, Caserta D, Musumeci MB, Moscarini M, Autore C, Volpe M (2013) Growth factors in preeclampsia: a vascular disease model. A failed vasodilation and angiogenic challenge from pregnancy onwards? Cytokine Growth Factor Rev 24:411–425

Article 8

Guedes-Martins L, Gaio AR, Saraiva J, Cunha A, Macedo F, Almeida H. Uterine artery impedance during the first eight postpartum weeks. *Sci Rep*. 2015; 5:8786.

SCIENTIFIC REPORTS

OPEN

SUBJECT AREAS:
OUTCOMES RESEARCH
PHYSIOLOGY
DISEASES

Received
3 September 2014

Accepted
4 February 2015

Published
5 March 2015

Correspondence and requests for materials should be addressed to L.G.-M. (luis.guedes.martins@gmail.com)

Uterine artery impedance during the first eight postpartum weeks

L. Guedes-Martins[1,2,3], A. R. Gaio[4,5], J. Saraiva[1,3], A. Cunha[3], F. Macedo[6] & H. Almeida[1,2,7]

[1]Department of Experimental Biology, Faculty of Medicine, University of Porto, 4200-319 Porto, Portugal, [2]IBMC-Instituto de Biologia Molecular e Celular, 4150-180 Porto, Portugal, [3]Hospital Centre of Porto EPE, Department of Women and Reproductive Medicine, Largo Prof. Abel Salazar, 4099-001 Porto, Portugal, [4]Department of Mathematics, Faculty of Sciences, University of Porto, 4169-007 Porto, Portugal, [5]CMUP-Centre of Mathematics, University of Porto, 4169-007 Porto, Portugal, [6]Department of Cardiology, Faculty of Medicine, University of Porto, 4200-319 Porto, Portugal, [7]Obstetrics-Gynecology, Hospital-CUF Porto, 4100-180 Porto, Portugal.

The aim of this study was to construct reference ranges for the uterine artery (UtA) mean pulsatility (PI) and resistance (RI) indices from 1–8 weeks postpartum. A prospective, cross-sectional, and observational study was performed with 320 healthy women from week 1 through week 8 postpartum. UtAs were examined transvaginally using colour and pulsed Doppler imaging, and the means of the right and left values of the PI and RI, as well as the presence or absence of a bilateral protodiastolic notch, were recorded. The 5th, 50th and 95th reference percentile curves for the UtA-PI and UtA-RI were derived using regression models. The adjusted reference intervals uncovered a convergence trend at the week 8 time-point, although impedance was lower at the week 1 time-point in multiparous women compared with primiparous women. The notching prevalence was 22.5% (9/40) at week 1 and 95.0% (38/40) at week 8. The study revealed consistent evidence of a progressive increase of postpartum uterine impedance and provided new average UtA-PI and UtA-RI reference charts for weeks 1 through 8. Multiparity does not change the trend but does impart a lower rate of increase, likely as a consequence of previous vascular structural and functional differences.

Doppler ultrasound has been used to measure the flow resistance indices of the uterine arteries during the menstrual cycle[1,2], pregnancy[3], and labour[4,5]. Throughout the menstrual cycle, a lack of significant uterine artery (UtA) impedance changes[2] or higher UtA impedance early and late in the cycle, compared with reduced levels mid-cycle or in the luteal phase, has been reported[6,7].

The results that accompany the pelvic circulatory changes necessary to adapt the blood supply to the nutritionally demanding developing foetus are more consistent over the course of pregnancy. This unique situation translates into a continuous reduction in uterine artery resistance starting by week 6 of pregnancy[8,9]. This downward trend has been proposed to result from an appropriate trophoblast invasion of the uterine spiral arteries that, when abnormal, correlates with resistive uterine artery behaviour[3,10].

In contrast to the extensive literature available during pregnancy, Doppler research on the uterine artery during the postpartum period is scarce. Nevertheless, puerperal conditions affecting the uterine circulation might occur, and the ability of UtA impedance, as measured by Doppler ultrasound, to predict these conditions would be immensely useful[11–13]. Among the potential complications, preeclampsia, postpartum haemorrhage, retained placental tissue, and infection are particularly relevant.

The absence of reference curves for uterine arteries resistance indices in an uneventful postpartum period has limited the assessment of puerperal conditions, as well as research progression in the area. This is important because in addition to providing relevant knowledge on the return of the local circulation to the previous, non-pregnant state, those reference values could help to more accurately interpret the pathophysiology of the puerperium[13]. This need led us to measure the UtA mean pulsatility (PI) and resistance (RI) indices at 1–8 weeks postpartum in an appropriate selected population to derive normative, weekly based reference ranges.

Results

Figure 1 shows the numbers of postpartum women at each stage of the study. The main characteristics and pregnancy outcomes of the 320 women are shown in Table 1. In 40.3% ($CI_{95\%}$: 34.9–45.9) of the cases, Caesarean section was the mode of delivery; in more than 90% of those cases, the reason for that procedure was prior Caesarean delivery, dystocia, foetal distress, or breech presentation (Table 2). The evaluated postpartum period ranged from 1 to 8 weeks, and the collected data were balanced, with 40 observations made per week.

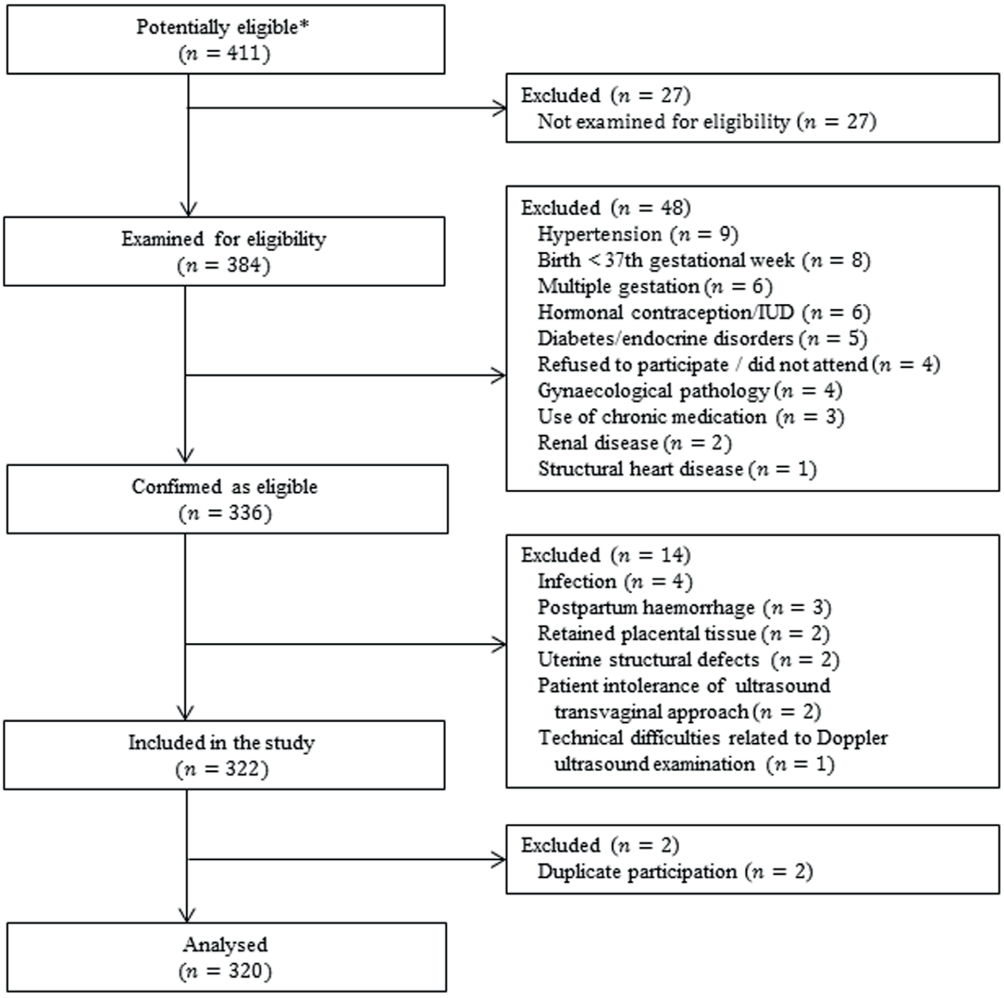

Figure 1 | **Study flowchart: numbers of postpartum women at each stage of the study.** IUD, intrauterine device. * Any postpartum women attended by our clinical investigator during the study protocol were considered to be potentially eligible.

At the time of the Doppler measurements, 30.3% ($CI_{95\%}$: 25.4–35.7) of the mothers were not breastfeeding, 16.6% ($CI_{95\%}$: 12.8–21.2) were smokers, and 23.4% ($CI_{95\%}$: 18.9–28.5) had a BMI greater than or equal to 30 Kg/m^2. The 10^{th} percentile of the sample for birth weight was 2770 g.

Figure 2 shows the different types of uterine artery Doppler shift spectra obtained at different time-points. A gradual increase in the RI and PI were observed from A (week 1) to C (week 8), whereas the diastolic flow became weaker, exhibiting a well-defined protodiastolic notch (Figure 2C).

The prevalence of uterine artery positive notching (defined as at least one notch) was 22.5% (9/40) at week 1 and 95.0% (38/40) at week 8 ($p < 0.001$), as shown in Table 3. Except for week 3, at which the notch incidence was significantly lower in multiparous women ($p < 0.001$), no additional significant, parity-related differences for notching were detected over time.

The reliability coefficient for the UtA-PI was 0.170. The ICC for absolute agreement among the single observer measurements was 0.985, with a 95% CI ranging from 0.982 to 0.988. Similarly, the reliability coefficient for the UtA-RI measurements was 0.042. The ICC for the absolute agreement among the single observer measurements was 0.982, with a 95% CI ranging from 0.978 to 0.986.

The magnitude of the obtained ICC values for the pulsatility and resistance indices allowed for one of the two measurements obtained from each woman to be ignored in the statistical analysis. Because the sonographer only performed one measurement in his/her day-to-day practice, the first measurements were considered.

UtA-PI. The crude effect of the postpartum week progression on the UtA-PI was estimated by a nonlinear model, which was reduced to a quadratic polynomial on the log-transformed variables. The regression model equation and the estimated coefficient values are presented in Table 4A. The likelihood ratio test favoured the model with no correction for error variances. Due to small departures from normality on the left tail, the 4 observations with standardised residuals less than −2.5 were removed. The UtA-PI values of these women corresponded to the lowest values observed at weeks 1, 2, 7 and 8. The predicted regression curve was basically a concave-up

Table 1 | Main characteristics and obstetric data of the 320 women included in the study

		n (%)
Age intervals, in years	18–24	54 (16.9)
	25–34	166 (51.9)
	35–43	100 (31.2)
Age, *years* (mean ± SD*)	30.8 ± 6.50	-
Ethnicity	White	309 (96.6)
	Black	4 (1.2)
	Other	7 (2.2)
Parity	>1	119 (37.2)
Body mass index† (*kg/m²*)	16–24	118 (36.9)
	25–29	127 (39.7)
	30–44	75 (23.4)
Smoking†		53 (16.6)
GA‡ at delivery, *weeks* (median ± IQR**)	40.1 (39.1–40.6)	-
Caesarean section		129 (40.3)
Apgar score at 5′	<7	0 (0)
Birth weight at delivery, *g* (mean ± SD*)	3160.7 (±344.93)	-
Haemoglobin on day 2, *g/dL* (mean ± SD*)	11.1 (±1.05)	-
Breastfeeding†		223 (69.7)

*SD, standard deviation;
**IQR, interquartile range;
†Obtained by the moment of the Doppler flow acquisition;
‡GA, gestational age.

increasing function of the postpartum time, with an increasing rate of softening from the 2nd postpartum week onwards (Figure 3, Table 5).

Adjustment for potential time effect confounders only identified parity as a statistically significant variable; maternal age, BMI, smoking, mode of delivery, infant birth weight, breastfeeding, and haemoglobin on postpartum day 2 did not have significant effects on the UtA resistance indices during the first eight postpartum weeks (Table 4). The resulting model was a cubic polynomial on the log-transformed variables, with significant second-order interaction terms between parity and postpartum time. Model estimates are presented in Table 4B, and the 5th, 50th and 95th percentiles are plotted in Figure 4A. The error variances were allowed to differ depending on the postpartum week. The set of seven observations with standardised residuals less than −2.5 compromised the error normality; therefore, those observations were removed (Figure 4A). As depicted in Figure 4A, multiparous women started the postpartum period by

Table 2 | Indication for Caesarean sections (n = 129) in the study sample

		Caesarean Deliveries (%)*
Primary	Dystocia	26 (20.2)
	Non-reassuring foetal heart rate	17 (13.2)
	Abnormal presentation	15 (11.6)
	Unsuccessful trial of forceps or vacuum	12 (9.3)
Repeat	No VBAC attempt	38 (29.5)
	Failed VBAC	14 (10.8)
	Unsuccessful trial of forceps or vacuum	7 (5.4)

*Data are shown as absolute (relative, %) frequencies; VBAC, vaginal birth after caesarean.

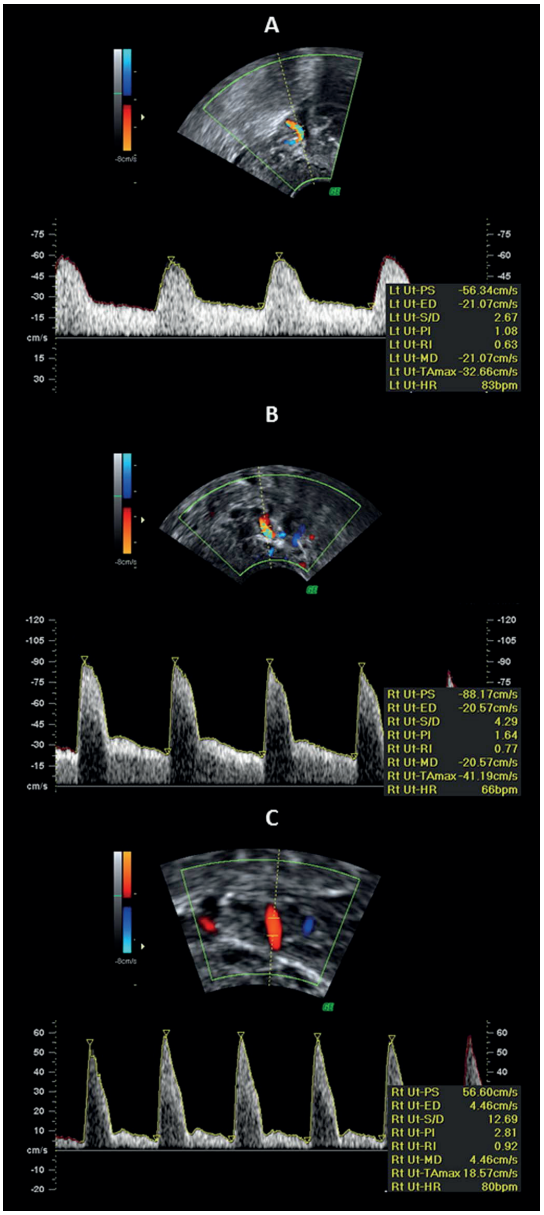

Figure 2 | Doppler shift spectra recorded from the uterine arteries at 1 (A), 4 (B) and 8 (C) weeks postpartum. (A) Waveforms with velocities gradually decreasing from the systolic peak and with continuous forward flow in diastole; (B + C) waveforms with a notch and with continuous forward flow in diastole. The pulsatility index (PI) is used as a measurement of impedance of the flow blood distal to the sampling point and is automatically calculated according to the formula $PI = \frac{(s-d)}{mean}$, where s is the peak, d is the minimum, and the $mean$ is the average maximum Doppler shift frequency over the cardiac cycle. The resistance index (RI) is automatically calculated using the formula $RI = \frac{(s-d)}{s}$, where s is peak systolic, d is end-diastolic, c is early diastolic, and x is maximum diastolic frequency.

Table 3 | Absolute (relative, %) parity frequencies in each group of 40 women examined per week and absolute (relative, %) frequencies for postpartum uterine artery positive notching (at least one notch)

	Parity		Positive Notching				
						Multiparous	
Week	Primiparous	Multiparous	All n (%)	p-value*	Primiparous n (%)	n (%)	p-value†
1	28 (70.0)	12 (30.0)	9 (22.5)	<0.001	8 (28.6)	1 (8.3)	0.233
2	28 (70.0)	12 (30.0)	8 (20.0)		8 (28.6)	0 (0)	0.079
3	26 (65.0)	14 (35.0)	17 (42.5)		16 (61.5)	1 (7.1)	<0.001
4	28 (70.0)	12 (30.0)	31 (77.5)		25 (89.3)	6 (50.0)	0.012
5	24 (60.0)	16 (40.0)	34 (85.0)		21 (87.5)	13 (81.2)	0.668
6	24 (60.0)	16 (40.0)	32 (80.0)		20 (83.3)	12 (75.0)	0.691
7	22 (55.0)	18 (45.0)	35 (87.5)		21 (95.5)	14 (77.8)	0.155
8	21 (52.5)	19 (47.5)	38 (95.0)		20 (95.2)	18 (94.7)	1.000

*p-value from a χ^2-test assessing the value of positive notching frequencies along the postpartum weeks;
†p-value from χ^2-tests assessing the homogeneity of proportions between primiparous and multiparous women (using Bonferroni's correction for multiple comparisons, significance should be taken at the level of 0.006 [0.05/8]).

exhibiting lower UTA-PIs than those predicted for the primiparous women. As time progressed, the predicted values for each group approached one another.

UtA-RI. The crude effect of the postpartum week progression on the UtA-RI was estimated using a quadratic polynomial. The regression model equation and the estimated coefficient values are presented in Table 4A. The likelihood ratio test favoured the model with different variances according to the postpartum week. Due to small departures from normality on the left tail, the 5 observations with standardised residuals less than −2.5 were removed. The UtA-RI values of these women corresponded to the lowest values observed in weeks 5, 6 and 8. The predicted regression curve was a concave-down increasing function, which would theoretically achieve its maximum at 8.6 weeks (Figure 3).

As for the PI, the adjustment for potential time effect confounders only identified parity as a statistically significant variable. The resulting model is presented in Table 4B and is plotted in Figure 4B: it is a quadratic polynomial plotted against postpartum weeks, with different intercept and slope coefficients according to the parity status. Error variances were again allowed to differ with the postpartum week. Six observations with standardised residuals less than −2.5 compromised the error normality and were therefore removed from the model. During the first weeks, the UtA-RI values for multiparous women were significantly lower than those observed for primiparous women (Figure 4, Table 5). However, as time progressed, that effect ceased to be significant, and the predicted values for both groups were no longer significantly different from one another.

Discussion

During the first few weeks after delivery, an important change occurs in the pelvic circulation because the blood requirements of pregnancy are no longer necessary. Exactly how quickly these regional haemodynamic changes return to the non-pregnant state is not well understood. The process involves spiral artery luminal obliteration due to phenomena such as thrombosis, endarteritis and intima thickening[14], which result in increased local vascular resistance[15]. Although this finding may reflect systemic circulatory changes[16,17], an immediate cause for the events is the mechanical pressure imposed by the contracted postpartum myometrium, as well as, possibly, local immunological phenomena[18]. As the structural involution of the uterine artery and distal branches occurs, functional changes can be assessed using a computerised analysis of the blood velocity spectrum obtained with Doppler ultrasound. In our cross-sectional investigation, assessment of the UtA-PI and UtA-RI during the first eight weeks postpartum uncovered a progressive, significant increase in UtA impedance.

Statistics. Our study provides reference ranges of the mean UtA-PI and UtA-RI for each week between 1 and 8 weeks postpartum in an appropriately large sample of healthy, normotensive women. Furthermore, stringent and validated methodological guidelines were employed to construct these reference ranges[19,20]. Although a cross-sectional design was used, we included the same number of observations at each week postpartum for reasons related to clinical practice procedures.

The reliability study of the UtA-PI and UtA-RI measurements was based on the ICC. Because the number of obtained coefficients was greater than 0.7, the authors inferred that the measurements were highly repeatable, with a very low measurement error[19,21].

From the statistical point of view, a variety of strategies for constructing reference intervals and percentile charts have been published[22]: linear regression, if necessary, along with modelling of the residual standard deviation; the LMS curves method, introduced by Cole[23]; the non-parametric HRY method of Healy, Rabash and Young[24]; and, finally, non-parametric quantile regression. In this study, the authors used the linear model, regressing UtA-PI and UtA-RI on polynomial functions of the postpartum time and considering adjustments for potential confounders such as parity, maternal age, BMI, smoking, mode of delivery (vaginal vs Caesarean section), infant birth weight, breast-feeding, and haemoglobin on day 2 postpartum. Because the evaluation of the goodness of fit of the model was very satisfactory, the percentile curves for the UtA-PI and UtA-RI were confidently identified from those linear models.

UtA-PI and UtA-RI reference ranges. Transvaginal assessment of UtA impedance by employing Doppler ultrasound offers several advantages over the transabdominal route[25]. The vessel is easily identified and is located within close proximity, thus yielding clearer waveforms. Additionally, the insonation angle is near 0°, which results in high reproducibility[25,26].

Previous reports addressing postpartum uterine artery impedance reported results with considerable variation in the time-points assessed, the indices employed and the population features, which may underlie the diversity of observations. Although there is a general consensus that within 12–14 weeks postpartum, the uterine artery impedance rises towards the non-pregnant values[13,27–32], the findings are conflicting at earlier days; a marked increase[27–32], no change or even a minor transient reduction in impedance data have all been reported[13,32].

The current cross-sectional study also provides evidence of an increasing trend towards pre-pregnancy impedance values; in addition, it provides more time points, studied on a regular weekly basis, and considerably extended the number of patients. In agreement with a previous longitudinal study[13,33] this study showed that by 8

Table 4 | Estimates of the regression coefficients and corresponding p-values for the PI and RI models during the postpartum period (A), as well as stratified by the parity status (B). The additive effects of potential time confounders are also shown; only the parity status had a statistically significant time-adjusted effect (A)

		Variables	Regression Coefficients	p-values
A*	log (PI)	*Intercept*	0.203	0.000
		log(Week)	−0.023	0.653
		log²(Week)	0.164	0.000
		Multiparous (vs primiparous)	−0.127	0.000
		BMI 25–29 (vs BMI 16–24)	−0.032	0.137
		BMI 30–44 (vs BMI 16–24)	−0.025	0.337
		Age 25–34 (vs age 18–24)	−0.022	0.419
		Age 35–43 (vs age 18–24)	0.001	0.974
		Vaginal (vs Caesarean)	0.036	0.061
		Smoker (vs non-smoker)	0.017	0.506
		Birth weight (g)	0.000	0.991
		Haemoglobin on day 2 (g/dL)	−0.007	0.470
	RI	*Intercept*	0.508	0.000
		Week	0.086	0.000
		Week²	−0.005	0.000
		Multiparous (vs primiparous)	−0.037	0.000
		BMI 25–29 (vs BMI 16–24)	0.002	0.819
		BMI 30–44 (vs BMI 16–24)	0.002	0.873
		Age 25–34 (vs age 18–24)	−0.002	0.860
		Age 35–43 (vs age 18–24)	0.001	0.940
		Vaginal (vs Caesarean)	0.001	0.943
		Smoker (vs non-smoker)	−0.008	0.416
		Birth weight (g)	0.694	0.694
		Haemoglobin on day 2 (g/dL)	0.106	0.106
B†	log (PI)	*Intercept*	0.255	0.000
		Multiparous (vs primiparous)	−0.141	0.001
		log(Week)	−0.229	0.019
		log(Week): Multiparous	−0.209	0.018
		log²(Week)	0.489	0.000
		log²(Week): Multiparous	0.127	0.002
		log³(Week)	−0.115	0.003
	RI	*Intercept*	0.535	0.000
		Multiparous (vs primiparous)	−0.117	0.000
		Week	0.088	0.000
		Week: Multiparous	0.014	0.000
		Week²	−0.006	0.000

*A: The estimated equation for PI was $\mathbb{E}(\log(PI)|w) = \beta_0 + \beta_1 \log(w) + \beta_2 \log^2(w)$ or, equivalently, $\mathbb{E}(PI|w) = Cw^{\beta_1 + \beta_2 \log(w)}$ with $C = e^{\beta_0}$, for any given week w. The estimated equation for RI was $\mathbb{E}(\mathrm{RI}|w) = \beta_0 + \beta_1 w + \beta_2 w^2$.
†B: The estimated equation for PI was $\mathbb{E}(\log(PI)|w,s) = \beta_0(s) + \beta_1(s)\log(w) + \beta_2(s)\log^2(w) + \beta_3 \log^3(w)$ or, equivalently, $\mathbb{E}(PI|w,s) = Cw^{\beta_1(s) + \beta_2(s)\log(w) + \beta_3 \log^2(w)}$ with $C = e^{\beta_0(s)}$, for any given week w and parity status s. The estimated equation for RI was $\mathbb{E}(\mathrm{RI}|w,s) = \beta_0(s) + \beta_1(s) w + \beta_2 w^2$.
The letter $\mathbb{E}$ in the equations denotes the expected value. The primiparous category was taken as the reference class. PI, pulsatility index; RI, resistance index; UtA, uterine artery.

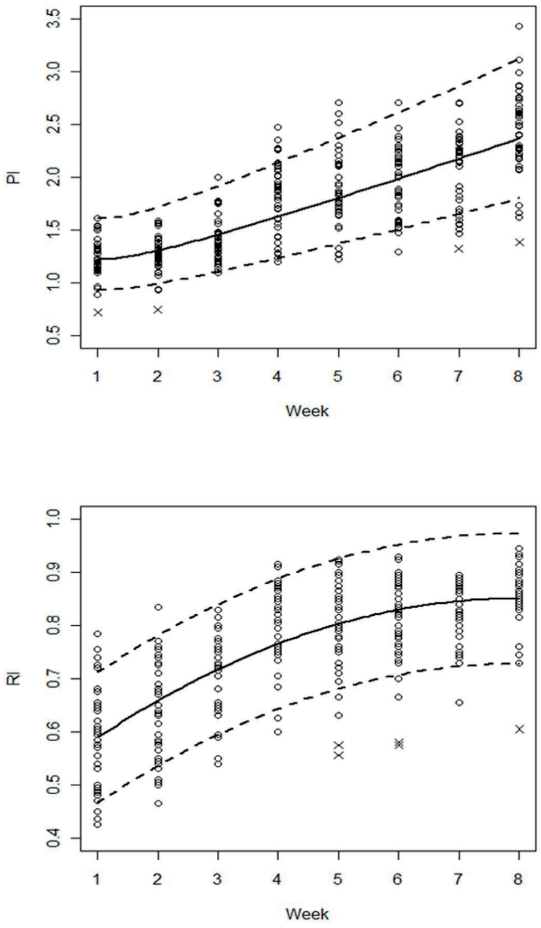

Figure 3 | Sample values and the estimated 5th, 50th and 95th percentile regression curves for the uterine artery pulsatility (PI) and resistance (RI) indices in all women during the first 8 postpartum weeks. Points marked with (x) were removed from the model fitting to improve normality.

weeks postpartum, the regional pelvic circulation had not yet recovered to the non-pregnant state[27], emphasising that the time needed for UtA re-adaptation to the non-pregnant state is more extensive than previously assumed[13,27]. It is possible that longer-term factors acting at the endothelium of the uterine artery or systemically[6,31] take part in the cardiovascular adaptation that results in the normal waveform[30].

Accompanying this trend, the reappearance of the proto-diastolic notch was noticed as early as the second day postpartum[27]. Our study confirms that in the early days after delivery, only a small number of patients will display notching (defined as at least one notch) but, with a gradual increase each week, the presence of this feature approaches 100% of cases, similarly to the findings of a previous report from others[13].

Effect of parity on uterine flow impedance. In our research, maternal age, BMI, smoking, mode of delivery (vaginal vs Caesarean section), infant birth weight, breast-feeding, and haemoglobin on day 2 postpartum did not cause any significant effects on UtA impedance during the first eight weeks postpartum. However, during the same period, UtA impedance was significantly affected by maternal parity, a condition not examined in previous reports and a likely reason for the diversity of results.

In the current study, multiparous women exhibited lower UTA PIs and RIs during the early weeks, which converged to values similar to primiparous RIs and PIs by the eighth week. Presumably, the UtA capacitance properties observed in multiparous women are the result of vascular structural features that remained from the first pregnancy. In fact, although the well-known spiral artery remodelling that occurs during pregnancy[34] reverts upon delivery, not all vessels recover to their pre-pregnancy conditions. Indeed, spiral artery internal elastic lamina duplication or fragmentation was described at the endometrial/myometrial junction of parous women in contrast to nulliparous women[35]. We are convinced that such permanent structural changes endow the spiral arteries with reduced impedance and underlie the parity-related lower UtA-PI and UtA-RI values that we report in the immediate postpartum period.

Table 5 | Predicted percentile values for the uterine artery pulsatility (PI) and resistance (RI) indices according to postpartum week; A - not accounting for parity status; B - stratified by parity status

A						
	PI			RI		
Weeks	5th	50th	95th	5th	50th	95th
1	0.930	1.225	1.613	0.466	0.589	0.711
2	0.990	1.304	1.717	0.536	0.659	0.781
3	1.104	1.454	1.915	0.595	0.718	0.840
4	1.233	1.624	2.139	0.643	0.766	0.889
5	1.368	1.802	2.373	0.681	0.803	0.926
6	1.508	1.986	2.615	0.707	0.830	0.953
7	1.651	2.174	2.864	0.723	0.846	0.968
8	1.797	2.367	3.117	0.728	0.851	0.973
B						
	Primiparous			Multiparous		
Weeks	5th	50th	95th	5th	50th	95th
PI						
1	1.008	1.291	1.653	0.889	1.121	1.413
2	1.047	1.341	1.717	0.849	1.071	1.350
3	1.215	1.556	1.992	0.992	1.251	1.578
4	1.384	1.772	2.269	1.166	1.470	1.853
5	1.534	1.965	2.516	1.343	1.693	2.134
6	1.662	2.128	2.725	1.515	1.910	2.408
7	1.767	2.262	2.897	1.677	2.115	2.666
8	1.850	2.369	3.033	1.829	2.306	2.907
RI						
1	0.495	0.617	0.738	0.417	0.514	0.612
2	0.565	0.686	0.808	0.501	0.598	0.696
3	0.622	0.744	0.865	0.573	0.670	0.768
4	0.668	0.789	0.911	0.632	0.730	0.828
5	0.701	0.823	0.944	0.680	0.778	0.875
6	0.722	0.844	0.966	0.716	0.814	0.911
7	0.732	0.854	0.975	0.740	0.837	0.935
8	0.729	0.851	0.972	0.751	0.849	0.947

External validity, study limitations and future research. As with any study, the choice of an appropriate sample is of great importance. While some published studies used routinely collected data, resulting in the inclusion of multiple observations of some participants, Altman and Chitty[36] advocate specifically collecting data for the purpose of developing reference ranges (sometimes misleadingly called 'normal ranges'), with each participant being included only once. Within this objective, it is important to have as unselected a sample as possible because reference data should relate to 'normal' characteristics[37]. In reality, 'reference intervals' for known sonographic features, either maternal or foetal, are not synonymous with 'normal ranges' for these characteristics[36,37]. This is because in clinical practice, it is extremely difficult (nearly impossible) to obtain a truly unselected population. Our goal was achieved with a methodology that sought an appropriate selected sample, but we did not have a truly unselected population. Therefore, any maternal condition that could potentially affect the uterine artery Doppler was deemed reasonable to be an exclusion criterion. However, our study design may attract criticism for producing supernormal ranges that are less applicable to the general population. For this reason, despite the current inclusion criteria, we did not exclude participants due to complicating factors that developed after recruitment. Nevertheless, no complications occurred in the studied group (patients 'Included in the study') during the first eight postpartum weeks.

As with the introduction of any new technology into clinical practice, it is essential that those conducting Doppler assessment are adequately trained and that their results are subjected to rigorous audit. Although our data were collected by a single, very experienced operator, which could compromise the external validity of his results, Doppler blood flow measurements of the UtA impedance were found to be highly repeatable only when carried out by well-trained operators[25]. Because the usefulness of a screening test depends not only on its predictive ability but also on its reproducibility, future studies are needed to demonstrate the usefulness of these reference ranges, as well as their applicability.

In short, the median 5th and the 95th percentile regression curves of the pulsatility and resistance indices of the uterine artery increase from week 1 to week 8 postpartum. Parity does not change the trend, but primiparous women have higher UtA resistance indices in the earlier postpartum weeks. The UtA impedance reference ranges presented here are likely to be clinically useful in the assessment of postpartum disorders, including retained placental tissue in the uterine cavity, which delays the normal involution of uterine vessels[18,35], infection, postpartum bleeding and enhanced myometrial vascularity[15]. Additional studies are necessary to confirm these findings and to further support the use of postpartum UtA Doppler patterns as a prognostic tool.

Methods

This study was approved by the local ethics committee of the Hospital Centre of Porto, Department of Women's Reproductive Medicine. All of the subjects provided their informed consent (IRB protocol number: 150-13[096-DEFI/122-CES]). The methods were carried out in accordance with the approved guidelines.

From January 2010 to December 2013, a prospective, cross-sectional, observational study was conducted, including 320 healthy women with singleton pregnancies who gave birth between the 37th and 41st gestational week, either vaginally or by Caesarean section. Gestational age was calculated by ultrasonography performed between 11

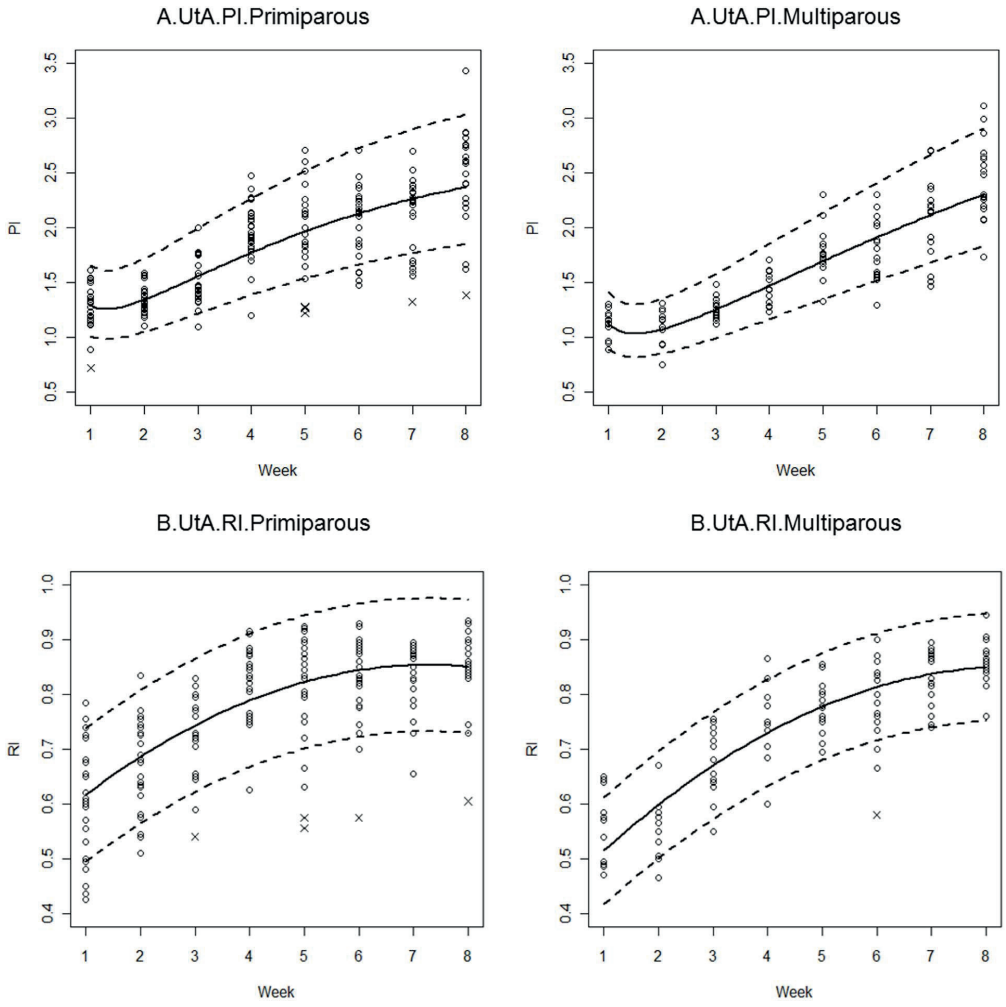

Figure 4 | Sample values and the estimated 5th, 50th and 95th percentile regression curves for the uterine artery (UtA) pulsatility (A) and resistance (B) indices during the first 8 postpartum weeks, stratified by the parity status (left: primiparous; right: multiparous). Points marked with (x) were removed from the model fitting to improve normality. PI, pulsatility index; RI, resistance index.

and 14 weeks, and the participants were consecutively recruited after meeting the eligibility criteria.

Each woman was assessed only once between days 1 and 56 postpartum and was categorised to the respective week to assess a total of 40 women per week. During the postpartum appointments, a senior specialist reviewed the patients' medical histories and verified the absence of hormonal contraception or intrauterine devices, present or past gynaecological pathology (e.g., fibroids, adnexal pathology or prior gynaecologic surgery), hypertension, diabetes and other endocrine disorders, immune diseases, renal and structural heart diseases, haematological conditions (with particular emphasis on postpartum haemorrhage) and acute or chronic infections. Current acceptable medications included vitamin and iron supplements; previous administration of prostaglandin E analogues, low-dose oxytocin regimens, and vaginal misoprostol to induce labour in accordance with ACOG Practice Bulletin N.107 were also acceptable[38].

The medical records included each patient's age, body mass index (BMI), parity, pregnancy outcome, mode of delivery, and haemoglobin level on day 2 postpartum, the child's birth weight and Apgar score, and whether the mother was breast- or formula-feeding.

Prior to uterine artery Doppler evaluation, we conducted a rigorous transvaginal ultrasound to exclude uterine structural defects, retained placental tissue or adnexal pathology. In the first week after delivery, a transabdominal assessment complemented the evaluation to improve the accuracy. In this setting, the presence of fluid and debris in the uterine cavity was considered to be irrelevant[39]. Doppler flow studies were consecutively scheduled until the requirement of 40 measurements per postpartum week was met.

Doppler flow study. UtA Doppler examinations were performed using a Voluson 730 Pro (GE Healthcare Technologies, Milwaukee, WI, USA) with a 5-MHz vaginal probe. Employing a transvaginal transducer (GE Healthcare Probe Type RIC5-9 W, Horizontal Standard EN60601-1), a single experienced operator (LG-M; 6 years of experience in obstetric and gynaecologic ultrasound) made all of the measurements to minimise inter-observer variability. The measurements were made with the women in the lithotomy position and with empty urinary bladders. Smokers and nursing mothers were required to abstain from smoking and breastfeeding for at least 2 h and 30 minutes, respectively, before the procedure.

A sagittal section of the uterus was obtained, and the cervical canal and internal cervical ostium were identified. Subsequently, the transducer was gently tilted from side to side, and then colour flow mapping was used to identify each uterine artery along the side of the cervix and uterus at the level of the internal ostium. Pulsed wave Doppler was used with the sampling gate set at 1–2 mm to cover the entire vessel, and angle correction was used where appropriate to ensure that the angle of insonation was less than 30°. The PI and RI were measured when three similar consecutive waveforms were obtained; then, the mean PI and RI of the left and right arteries were calculated (Figure 2). In general, no more than 1 minute was needed to assess both

arteries. We noted the presence or absence of an early bilateral protodiastolic notch, defined as a persistent decrease in blood flow velocity in early diastole below the diastolic peak velocity.

Intra-observer reliability was obtained from two consecutive readings at the beginning and the end of the scan of the 640 recordings (right UtA 320 + left UtA 320) of resistance and pulsatility indices in the uterine arteries. In the present context, there was only a single observer, who was completely unaware of any of the other results.

Efforts to address potential sources of bias. Any postpartum women attended by our clinical investigator during the study protocol were considered to be potentially eligible. The scheduling of postpartum consultations was randomly made by the hospital secretariat according to the availability of the clinical investigator (AC). Patients were consecutively recruited, and ultrasonographic examinations were scheduled so that a total of 40 women were examined per postpartum week. The selection of the participants was achieved by a single investigator who was unaware of the Doppler measurement results. Finally, the researcher responsible for the Doppler measurements had no access to clinical data that was obtained by the investigator responsible for determining patient eligibility.

Statistical analysis. Sample size calculation basically followed Altman & Ohuma (2013)[40] and Papageorghiou *et al.* (2014)[41]. It was carried out in relation to the precision and accuracy of a single percentile and regression-based limits, as first proposed by Royston (1991)[42] and extended by Bellera & Hanley (2007)[43]. In 1991, Royston[42] provided the following formula for the standard error of a *p*th percentile from the normal distribution:

$$SE_p = SD\sqrt{\frac{1+\frac{1}{2}Z_p^2}{n}} \quad (1)$$

where *SE* is the standard error, *SD* is the standard deviation of the measurements, Z_p is the value of the standard normal distribution corresponding to the *p*th percentile, and *n* is the sample size.

Our aim was to obtain the 5th and the 95th reference percentiles, with $Z_p = 1.645$. A cross-sectional study of 320 individuals, with 40 individuals sampled per week, would then provide

$$SE_p = 0.186\ SD \quad (2)$$

Bearing in mind that the distance between the extreme percentiles is approximately 3.3 SD, the equation above shows that the percentile estimates will be given with great precision.

Bellera & Hanley[43] showed that the above formula is only valid at the mean value of the time covariate. Assuming that the postpartum weeks are uniformly distributed, our sample size would provide a relative margin of error (ratio of the width of the confidence interval for the reference limit to the width of the reference range) of approximately 13%, which also seems to be very reasonable. Nevertheless, as stated by Bellera & Hanley[43], whenever heteroscedasticity of PI values across postpartum time exists, the above formulae should be used as a rough guide for sample size planning.

Intra-class correlation coefficients (ICC) and 95% confidence intervals (CIs) were calculated with a two-way mixed-effects model. The reliability coefficient, which is the difference value that will be exceeded by only 5% of pairs of measurements on the same subject, was calculated as 1.96 times the standard deviation (SD) of the difference between pairs of repeated measurements[19]. The chi-square test or Fisher's test (as appropriate) was used to compare proportions.

Maternal age, BMI, parity status (primiparous vs multiparous), smoking, mode of delivery (vaginal vs Caesarean section), infant birth weight, breastfeeding, and haemoglobin on day 2 postpartum were considered potential time-effect confounders. However, adequate adjustment for these variables identified parity as the only statistically significant confounder.

Population reference intervals for the crude and parity status-adjusted behaviour of PI and RI during the first eight postpartum weeks were derived from regression models[20]. The fitting process utilised generalised least squares, allowing for errors with unequal variances. Only linear models were considered, occasionally with log-transformed variables, and no polynomials of a degree greater than 3 were used. In fact, these curves can exhibit unrealistic features such as waviness or sharp deviations at extreme values of the domain[20]. After removing the outliers (no more than 7 within each model), the error distribution assessment did not compromise normality. The 5th (resp. 95th) percentile curve was then given by the regression predicted curve minus (resp. plus) 1.96 times the residual standard deviation, whereas the 50th percentile curve corresponded to the (mean) regression curve. Whenever possible, model comparisons were based on the likelihood ratio test; otherwise, they were based on the Bayesian information criterion (BIC).

The crude (resp. parity adjusted) effect of the postpartum week progression on the UtA-PI was estimated by a nonlinear model that reduced to a quadratic (resp. cubic) polynomial on the log-transformed variables. The crude (resp. parity adjusted) effect of the postpartum week progression on the UtA-RI was estimated by a quadratic polynomial on the original variables. All of the models, except that of the effect of the crude time on UtA-PI, presented different error variances according to the week being considered.

All of the statistical analyses were performed using the R language and software environment for statistical computation, version 2.12.1[44]. The significance level was fixed at 0.05.

Our research has adhered to the Strengthening the Reporting of Observational studies in Epidemiology (STROBE) guidelines for observational studies, and all recommendations were included in the study.

1. Tan, S. L., Zaidi, J., Campbell, S., Doyle, P. & Collins, W. Blood flow changes in the ovarian and uterine arteries during the normal menstrual cycle. *Am J Obstet Gynecol.* **175**, 625–31 (1996).
2. Ziegler, W. F., Bernstein, I., Badger, G., Leavitt, T. & Cerrero, M. L. Regional hemodynamic adaptation during the menstrual cycle. *Obstet Gynecol.* **94**, 695–9 (1999).
3. Cnossen, J. S. *et al.* Use of uterine artery Doppler ultrasonography to predict pre-eclampsia and intrauterine growth restriction: a systematic review and bivariable meta-analysis. *CMAJ.* **178**, 701–11 (2008).
4. Li, H., Gudmundsson, S. & Olofsson, P. Uterine artery blood flow velocity waveforms during uterine contractions. *Ultrasound Obstet Gynecol.* **22**, 578–85 (2003).
5. Valentin, M., Ducarme, G., Ceccaldi, P. F., Bougeois, B. & Luton, D. Uterine artery, umbilical, and fetal cerebral Doppler velocities after epidural analgesia during labor. *Int J Gynaecol Obstet.* **118**, 145–8 (2012).
6. Steer, C. V. *et al.* Transvaginal colour flow imaging of the uterine arteries during the ovarian and menstrual cycles. *Hum Reprod.* **5**, 391–5 (1990).
7. Sladkevicius, P., Valentin, L. & Marsál, K. Blood flow velocity in the uterine and ovarian arteries during the normal menstrual cycle. *Ultrasound Obstet Gynecol.* **3**, 199–208 (1993).
8. Gómez, O. *et al.* Reference ranges for uterine artery mean pulsatility index at 11–41 weeks of gestation. *Ultrasound Obstet Gynecol.* **32**, 128–32 (2008).
9. Guedes-Martins, L., Saraiva, J., Gaio, R., Macedo, F. & Almeida, H. Uterine artery impedance at very early clinical pregnancy. *Prenat Diagn.* **34**, 719–25 (2014).
10. Prefumo, F., Sebire, N. J. & Thilaganathan, B. Decreased endovascular trophoblast invasion in first trimester pregnancies with high-resistance uterine artery Doppler indices. *Hum Reprod.* **19**, 206–9 (2004).
11. Zalel, Y., Gamzu, R., Lidor, A., Goldenberg, M. & Achiron, R. Color Doppler imaging in the sonohysterographic diagnosis of residual trophoblastic tissue. *J Clin Ultrasound.* **30**, 222–5 (2002).
12. Mulic-Lutvica, A., Eurenius, K. & Axelsson, O. Uterine artery Doppler ultrasound in postpartum women with retained placental tissue. *Acta Obstet Gynecol Scand.* **88**, 724–8 (2009).
13. Mulic-Lutvica, A., Eurenius, K. & Axelsson, O. Longitudinal study of Doppler flow resistance indices of the uterine arteries after normal vaginal delivery. *Acta Obstet Gynecol Scand.* **86**, 1207–14 (2007).
14. Weydert, J. A. & Benda, J. A. Subinvolution of the placental site as an anatomic cause of postpartum uterine bleeding: a review. *Arch Pathol Lab Med.* **130**, 1538–42 (2006).
15. Van Schoubroeck, D. *et al.* Prospective evaluation of blood flow in the myometrium and uterine arteries in the puerperium. *Ultrasound Obstet Gynecol.* **23**, 378–81 (2004).
16. Morris, R. *et al.* Maternal hemodynamics by thoracic impedance cardiography for normal pregnancy and the postpartum period. *Obstet Gynecol.* **123**, 318–24 (2014).
17. Mabie, W. C., DiSessa, T. G., Crocker, L. G., Sibai, B. M. & Arheart, K. L. A longitudinal study of cardiac output in normal human pregnancy. *Am J Obstet Gynecol.* **170**, 849–56 (1994).
18. Andrew, A., Bulmer, J. N., Morrison, L., Wells, M. & Buckley, C. H. Subinvolution of the uteroplacental arteries: an immunohistochemical study. *Int J Gynecol Pathol.* **12**, 28–33 (1993).
19. Bland, J. M. & Altman, D. G. Applying the right statistics: analyses of measurement studies. *Ultrasound Obstet Gynecol.* **22**, 85–93 (2003).
20. Royston, P. & Wright, E. M. How to construct 'normal ranges' for fetal variables. *Ultrasound Obstet Gynecol.* **11**, 30–8 (1998).
21. Walter, S. D., Eliasziw, M. & Donner, A. Sample size and optimal designs for reliability studies. *Stat Med.* **17**, 101–10 (1998).
22. Hynek, M. Approaches for Constructing Age-Related Reference Intervals and Centile Charts for Fetal Size. *Eur J Biomed Inform.* **6**, 43–52 (2010).
23. Cole, T. J. & Green, P. J. Smoothing reference centile curves: the LMS method and penalized likelihood. *Stat Med.* **11**, 1305–19 (1992).
24. Healy, M. J., Rasbash, J. & Yang, M. Distribution-free estimation of age-related centiles. *Ann Hum Biol.* **15**, 17–22 (1988).
25. Papageorghiou, A. T., To, M. S., Yu, C. K. & Nicolaides, K. H. Repeatability of measurement of uterine artery pulsatility index using transvaginal color Doppler. *Ultrasound Obstet Gynecol.* **18**, 456–9 (2001).
26. Jaffa, A. J., Weissman, A., Har-Toov, J., Shoham, Z. & Peyser, R. M. Flow velocity waveforms of the uterine artery in pregnancy: transvaginal versus transabdominal approach. *Gynecol Obstet Invest.* **40**, 80–3 (1995).
27. Tekay, A. & Jouppila, P. A longitudinal Doppler ultrasonographic assessment of the alterations in peripheral vascular resistance of uterine arteries and ultrasonographic findings of the involuting uterus during the puerperium. *Am J Obstet Gynecol.* **168**, 190–8 (1993).

28. Kirkinen, P., Dudenhausen, J., Baumann, H., Huch, A. & Huch, R. Postpartum blood flow velocity waveforms of the uterine arteries. *J Reprod Med* **33**, 745–8 (1988).
29. Baumann, H. *et al.* Blood flow velocity waveforms in large maternal and uterine vessels throughout pregnancy and postpartum: a longitudinal study using Duplex sonography. *Br J Obstet Gynaecol.* **95**, 1282–91 (1988).
30. Long, M. G., Boultbee, J. E., Hanson, M. E. & Begent, R. H. Doppler time velocity waveform studies of the uterine artery and uterus. *Br J Obstet Gynaecol.* **96**, 588–93 (1989).
31. Everett, T. R. & Lees, C. C. Beyond the placental bed: placental and systemic determinants of the uterine artery Doppler waveform. *Placenta* **33**, 893–901 (2012).
32. Nakai, Y. *et al.* Uterine blood flow velocity waveforms during early postpartum course following caesarean section. *Eur J Obstet Gynecol Reprod Biol.* **74**, 121–4 (1997).
33. Diniz, C. P., Araujo-Júnior, E., Lima, M. M., Guazelli, C. A. & Moron, A. F. Ultrasound and Doppler assessment of uterus during puerperium after normal delivery. *J Matern Fetal Neonatal Med.* (2014) [Epub ahead of print].
34. Brosens, J. J., Parker, M. G., McIndoe, A., Pijnenborg, R. & Brosens, I. A. A role for menstruation in preconditioning the uterus for successful pregnancy. *Am J Obstet Gynecol.* **200**, 615.e1–6 (2009).
35. Khong, T. Y., Adema, E. D. & Erwich, J. J. On an anatomical basis for the increase in birth weight in second and subsequent born children. *Placenta.* **24**, 348–53 (2003).
36. Altman, D. G. & Chitty, L. S. Charts of fetal size: 1. Methodology. *Br J Obstet Gynaecol.* **101**, 29–34 (1994).
37. Silverwood, R. J. & Cole, T. J. Statistical methods for constructing gestational age-related reference intervals and centile charts for fetal size. *Ultrasound Obstet Gynecol.* **29**, 6–13 (2007).
38. ACOG Committee on Practice Bulletins -- Obstetrics. ACOG Practice Bulletin No.107: Induction of labor. *Obstet Gynecol.* **114**, 386–97 (2009).
39. Mulic-Lutvica, A., Bekuretsion, M., Bakos, O. & Axelsson, O. Ultrasonic evaluation of the uterus and uterine cavity after normal, vaginal delivery. *Ultrasound Obstet Gynecol.* **18**, 491–8 (2001).
40. Altman, D. G. & Ohuma, E. O. International Fetal and Newborn Growth Consortium for the 21st Century. Statistical considerations for the development of prescriptive fetal and newborn growth standards in the INTERGROWTH-21st Project. *BJOG.* **120 Suppl 2**, 71–6 (2013).
41. Papageorghiou, A. T. *et al.* International Fetal and Newborn Growth Consortium for the 21st Century (INTERGROWTH-21st). International standards for fetal growth based on serial ultrasound measurements: the Fetal Growth Longitudinal Study of the INTERGROWTH-21st Project. *Lancet.* **384**, 869–79 (2014).
42. Royston, P. Constructing time-specific reference ranges. *Stat Med.* **10**, 675–90 (1991).
43. Bellera, C. A. & Hanley, J. A. A method is presented to plan the required sample size when estimating regression-based reference limits. *J Clin Epidemiol.* **60**, 610–5 (2007).
44. R Development Core Team. R: A language and environment for statistical computing. R Foundation for Statistical Computing, Vienna, Austria. http://www.R-project.org/ [12 March 2013] (2010).

Acknowledgments

We are grateful to the staff of the Department of Obstetrics of Centro Hospitalar do Porto. The second author was partially funded by the European Regional Development Fund through the COMPETE program and by the Portuguese Government through the FCT - Fundação para a Ciência e a Tecnologia - under the project PEst-C/MAT/UI0144/2013.

Author contributions

L.G.-M. designed the study, performed all Doppler measurements, analysed the data, and wrote the manuscript. A.R.G. performed all statistical analyses. J.S. contributed to the critical revision of the manuscript. A.C. coordinated the review of clinical cases. F.M. designed the study. H.A. designed the study, analysed the data, and wrote the manuscript. All authors contributed to the data interpretation and the final version of the manuscript, which all approved. All authors read and approved the final manuscript.

Additional information

Competing financial interests: The authors declare no competing financial interests.

How to cite this article: Guedes-Martins, L. *et al.* Uterine artery impedance during the first eight postpartum weeks. *Sci. Rep.* **5**, 8786; DOI:10.1038/srep08786 (2015).

4 . DISCUSSION AND CONCLUSIONS

The UtA is the main blood provider of the uterus in non-pregnant conditions. When pregnancy is established and blood demands increase, UtA adapts to the new condition by straightening its longitudinal shape. In addition, at the placental bed, spiral arteries (the arteriolar tips of UtA successive divisions) become invaded by new, non-maternal, cells that provide structural ground for functional changes. Therefore, the UtA, its divisions as well as its predecessor, the IIA, are likely targets of regulators, aiming at endowing the fetus with the necessary nurture.

The current investigation has focused on the UtA, and its predecessor, in order to obtain functional information along the reproductive life, with emphasis on pregnancy. In the course of this condition, impedance to flow in the UtA decreases (Gómez *et al*., 2008) as a result of the normal placental bed structural changes that convert UtA from a resistance into a capacitance vessel. As opposed, when trophoblast differentiation and spiral artery invasion are defective, upstream resistance increase is found. While normal UtA-PI, and its notch status, shows strong negative predictive value for placental complications of pregnancy, the positive predictive value is poor. This may, at least in part, be accounted for by the influence of non-placental factors related to maternal cardiovascular adaptation (Everett & Lees, 2012). Therefore, it is hypothesized that UtA Doppler waveforms are influenced by systemic factors beyond those of placental origin.

To address the aim number 1, UtA impedance was measured in women at reproductive age before pregnancy (ARTICLE 1), during pregnancy (ARTICLEs 2-4), at delivery (ARTICLE 5,6), and during the puerperium (ARTICLEs 7, 8). In addition (aim number 2), information on artery performance throughout the pregnancy was provided by a parallel study in women with long-term, stable, essential hypertension (RCOG 2010; Romundstad *et al*., 2010; Mustafa *et al.*, 2012; Sibai *et al.*, 2005; Macdonald-Wallis *et al.,* 2012).

UtA impedance through the menstrual cycle. This investigation (ARTICLE 1) revealed a cyclic variation in UtA impedance during the normal menstrual cycle; while the UtA-PI was high during the temporal extremes, it showed a mid-cycle depression, with the minimal values occurring between days 13 and 17 (Figure 6).

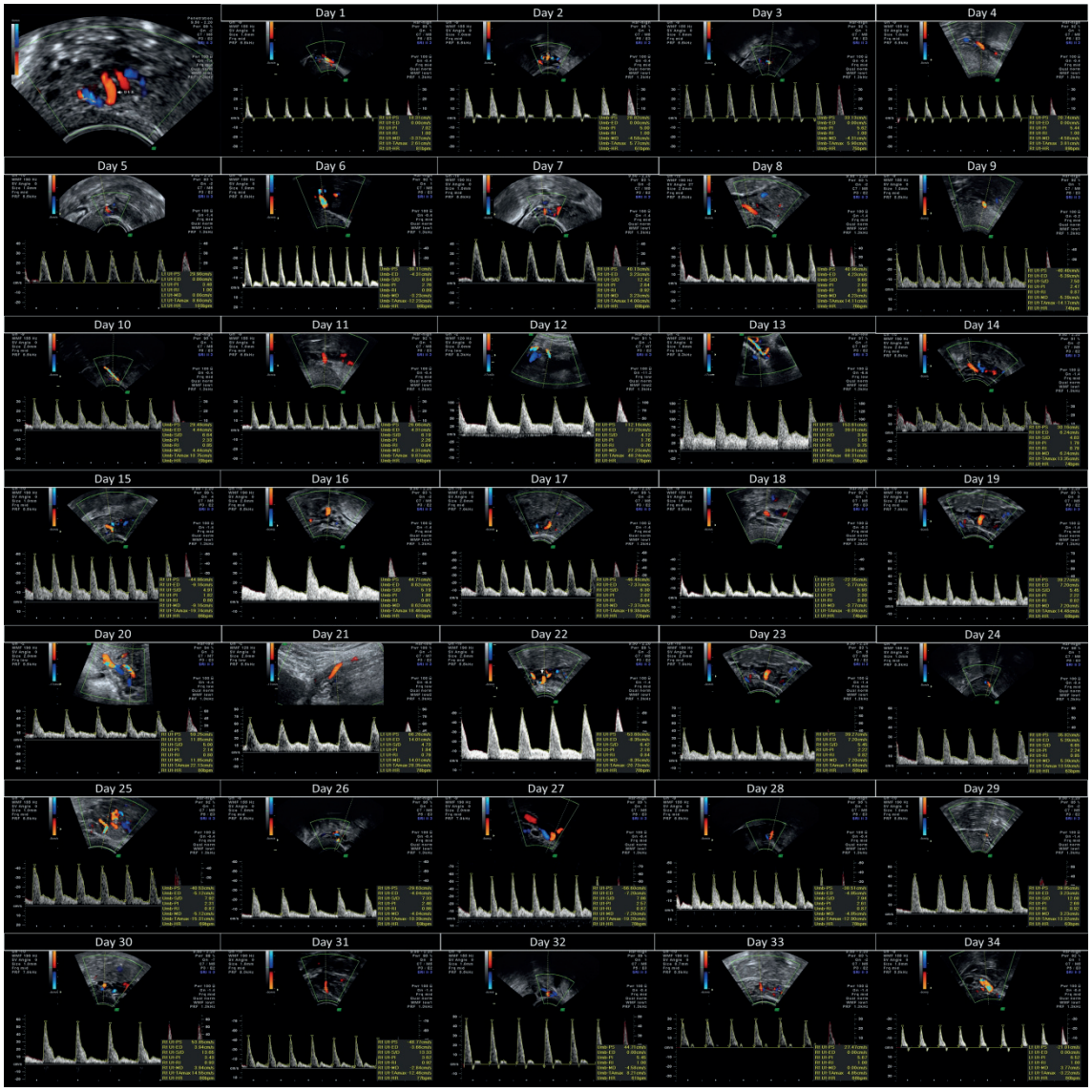

Figure 6. Different types of Doppler shift spectra recorded from UtA during the normal menstrual cycle. The UtA-PI was high during the temporal extremes and showed a mid-cycle depression at a time when implantation may occur. At the temporal extremes of the menstrual cycle, the UtA waveforms were characterized by a scarce or absent diastolic flow.

Moreover, independent assessment of the effects of age and parity also revealed that both were associated with significant UtA impedance decrease at the extremes of the cycle, but not in the mid-cycle, when the uterine cavity lining undergoes significant structural changes. The variations include the median, 5th, and 95th percentiles of the UtA-PI regression curves from the initial to the final third of the menstrual cycle. While the mechanism underlying the variation is uncertain, its reduction was found to correlate with increased plasma progesterone and estradiol (Steer *et al*., 1990). For unknown

reasons, age and parity do not change the trend; instead, they flatten the extremities of the cycle while leaving its middle unaltered, which suggests a local regulation of uterine perfusion in preparation for implantation and pregnancy.

Uterine artery impedance at very early gestational age. The decrement in vascular resistance, starting at a very early gestational age (ARTICLE 2), indicates that the local mechanisms of vascular impedance reduction are in progress well before deep placentation is established. In reality, a reduction in spiral artery PI from 5 weeks onwards (Valentin *et al*., 1996; Makikallio *et al.,* 2004; Mercé *et al.*, 1996) or radial artery RI from 6 weeks onwards (Tamura *et al.,* 2008) were noted.

Such lower impedance continues even in the condition of incomplete miscarriage. In fact, low UtA impedance persistence was associated with a considerable risk (Deeks & Altman, 2004) for uterine curettage 8 weeks after the diagnosis (ARTICLE 3), a time when the spontaneous resolution is unlikely. In the current investigation, in the setting of spontaneous early pregnancy loss, we verified that low UtA-PI at 2 weeks upon medical treatment is able to identify women who will achieve complete resolution, as distinct from those who will not and, thus, should remain under close surveillance. Indeed, the UtA-RI and PI at 2 weeks showed reasonable sensitivity, specificity and positive predictive values for patients requiring dilation and curettage 8 weeks after. In contrast to the UtA-PI sustained decrement, favoring incomplete resolution, local vascular relaxation impairment was associated with complications as complete abortion, intrauterine growth restriction and pre-eclampsia (Aardema *et al*., 2001; Tamura *et al*., 2008).

Therefore, this first group of studies (ARTICLEs 1-3) shows that the UtA impedance decrement is a notable indicator of pregnancy progression or placentar retention, which supports the clinical importance of its assessment and emphasizes the value of local circulatory factors.

Apart from extravillous trophoblasts (EVTs) endovascular colonization, an additional, decidual contribution, appears to exist. In fact, arterial structural modifications similar to normal remodeling were reported in early pregnancies while trophoblast invasion was absent (Craven *et al.,* 1998). Indeed, even when present, only rarely such EVTs were intimately associated with altered vessels (Smith *et al*., 2009) and, actually, the most impressive cellular feature in the decidua was the large quantity

of leukocytes, uterine natural killer cells and macrophages. These cells are important producers of vasoactive, extracellular matrix and angiogenic compounds that are released to the cellular environment and whose role in the spiral artery remodeling process has been firmly recognized (Smith *et al*., 2009; Lash *et al*., 2006; Hazan *et al*., 2010).

The internal iliac artery exhibits peculiar impedance performance compared to the uterine artery. For a better understanding of uterine regional hemodynamic adaptation, a longitudinal collection of PIs and RIs for the IIA and UtA was made in each trimester of uneventful pregnancies (ARTICLE 4). As expected, mean UtA-PI and UtA-RI decreased progressively from the first to the third trimesters in a statistically significant fashion, which is consistent with trophoblast cell invasion. In contrast to the UtA impedance, IIA-PI and IIA-RI revealed a remarkable increase in the same period. As the IIA immediately precedes UtA, such distinct performance is quite interesting. In fact, instead of becoming a capacitance vessel, as UtA, the IIA behaved much like a resistance vessel, where the progressive RI and PI increase is the likely consequence of enhanced blood velocity, previously observed in the common iliac artery (Palmer *et al*., 1992), the immediate IIA predecessor.

These findings indicate that during pregnancy, the maternal circulation adapts to the growing fetus in a way that the low-resistance UtA is rapidly filled by the heightened maternal cardiac output and the heightened IIA flow velocity (ARTICLE 4). Such adaptation is progressive, as evidenced by the trimester-related upward shift of the IIA to UtA proportion, and we are convinced that the shift endows the local circulation with a reserve capacity to meet the continued, growing, fetal needs.

Adaptation is also noticed in another stable hemodynamic condition as in long-term, hypertensive women. These are known to be at risk for developing PE and intrauterine growth retardation but, more commonly, they course with an uneventful pregnancy and deliver a healthy infant, as was verified in all the members of the population we studied. Their UtA and IIA impedances exhibited a performance that parallels the normotensive condition, although PI and RI levels are different (ARTICLE 4). So, in hypertensive women, a high-velocity flow originating from the IIA feeds the large-capacity UtA and placental bed with nutrient- and oxygen-rich blood in a progressive, regular pattern as well. Eventually, such modifications may have started

even before pregnancy, as shown by the first-trimester PI and RI values of both arteries (ARTICLEs 1,2,4).

From this comparison and the elimination of confounding variables, a model emerges indicating that perfusion of the pregnant uterus depends on regulatory mechanisms governing the pelvic circulation; as they sense local needs, they adapt the arterial flow properties immediately upon entering the pelvis and thus ascribes the IIA with a determinant role in uterine perfusion.

One of those influencing mechanisms is the sympathetic tonus. For its assessment, stage-1 chronic hypertensive pregnant women at term, who were undergoing an elective caesarean section under spinal blockade, were investigated (ARTICLE 5). Not unexpectedly, when blockade was induced a statistically significant decrease in mean arterial pressure (MAP) was found in both groups; the reduction, however, was more pronounced in the chronic hypertensive group. This finding was interpreted as reflecting the rapid onset of sympathetic blockade (Tarkkila & Isola, 1992; Carpenter *et al.,* 1992) and the dependence of hypertension on sympathetic innervation. Moreover, although the UtA-PI was significantly higher in the hypertensive group, when spinal blockade was installed, the UtA-PI drop converged to a similar value in both groups (ARTICLE 5). Not only this observation further stressed the role of the sympathetic nervous system in hypertension modulation, it also favored the likelihood of different levels of sympathetic activation in hypertensive patients (Mancia *et al*., 1999; Grassi *et al.,* 2011). Interestingly, despite the pelvic PI drop, no change in umbilical artery PI was found, suggesting that independent circulatory mechanisms are activated in the fetus to prevent adverse effects. Still, we are convinced of their time-dependency, as along the pregnancy distinct fetal aorta PI variation was found when hypertensive and normotensive women where compared (Guedes-Martins *et al*., 2014). Such difference is probably consequent to the activation of a persistent counter resistant compensatory mechanism.

Placental bed NOX activity at term parallels uterine artery impedance. Although spiral artery structural transformation largely determines the UtA impedance decrement, other factors related to maternal vascular and endothelial function at the placental bed also matter. Among these, the involvement of biological oxidation was investigated (ARTICLE 6). It was shown that in pregnancies with normal outcome,

higher placental bed NOX activity at term was strongly correlated with clusters of higher UtA-PI measured at 20-22 weeks and at term, and significantly correlated with UtA notch persistence (ARTICLE 6). The finding contrasted with the fetal aortic PI at term, whose correlations were weaker, and was in agreement with previous reports on UtA-PI (Aardema *et al.,* 2001; Madazli *et al.,* 2003).

The study thus suggests that the same mechanisms that lead to enhanced placental bed NOX activity also maintain higher UtA-PI (ARTICLE 6), making conceivable that should UtA-PI become even higher, enhanced NOX activity would increase in parallel. Eventually, excessive oxidation resulted in abnormally high UtA-PI and unfavorable clinical outcome; that is, the intensity of the oxidative insult would mark the distinction between functional disturbance and disease.

Uterine artery impedance following delivery. Aiming at strengthening the interpretation of the studies discussed, attention was devoted to the effect of placental removal on the UtA impedance behavior. While immediately before delivery the mean value was similar to third-trimester (ARTICLE 4), upon delivery, UtA-PI of normotensive women increased significantly (ARTICLE 7). This finding *per se* was expected, considering the observations on incomplete miscarriage we described (ARTICLE 3), and was consistent with the results of most other studies (Kirkinen *et al.,* 1988; Van Schoubroeck *et al.,* 2004; Mulic-Lutvica *et al.,* 2007).

One important novel finding concerned the UtA-PI in women with chronic hypertension and uncomplicated pregnancies (ARTICLE 7). Again, at the first time-point, i.e., immediately before delivery, mean PI was similar to third-trimester value (ARTICLE 4). However, upon delivery, the UtA-PI of hypertensive women rose at a rate similar to normotensive women, but to reach a comparatively higher magnitude, a difference that had been recognized during pregnancy (ARTICLE 4).

Non-pregnant uterine waveform takes several weeks to return to normal following removal of the placenta. In agreement with a previous longitudinal study (Mulic-Lutvica *et al.,* 2007; Diniz *et al*., 2014), our research showed that, by 8 weeks postpartum, the regional pelvic circulation had not yet recovered to the non-pregnant state (ARTICLE 8), emphasizing that the time needed for UtA re-adaptation to the non-pregnant state is more extensive than previously assumed (Tekay & Jouppila, 1993; Mulic-Lutvica *et al.,* 2007). Additionally, multiparous women exhibited lower UTA-PIs

and RIs during the early weeks of puerperium, which converged to values similar to primiparous RIs and PIs by the eighth week. Presumably, such multiparous women UtA capacitance properties are the result of vascular structural features that remained from the first pregnancy. In fact, although the spiral artery remodeling reverts upon delivery (Brosens *et al.,* 2009), not all vessels do so entirely. Indeed, spiral artery internal elastic lamina duplication or fragmentation was described at the endometrial/myometrial junction of parous women in contrast to nulliparous women (Khong *et al*., 2003). Such permanent structural changes likely endow the spiral arteries with the parity-related reductions in UtA-PI and UtA-RI values that we observed in the postpartum period.

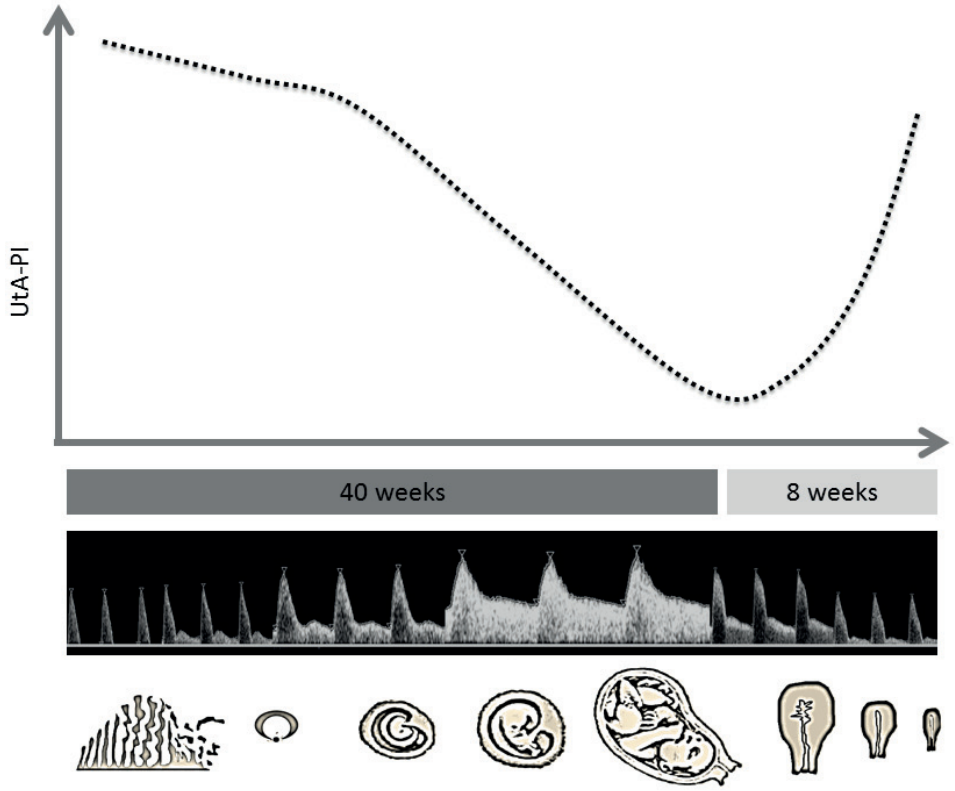

Figure 7. The impedance of the UtA decreases from the first day of menstruation until delivery. At this time, more than 8 weeks are needed to recover the normal impedance value.

To conclude. Due to the impedance changes verified in the course of this study, the UtA is set at the center of the female pelvic circulation. They start at the first menstruation day and, approximately by mid cycle, a PI reduction is noticed. This

downward trend is not disturbed by important modulators of woman´s reproductive biology as her age or parity.

Since early in pregnancy, even before the placentation is established, either the fetal derived trophoblastic invasion or additional maternal originated vasoactive compounds promote UtA caliber modulation and impedance reduction, which provide a progressive, permanent, arrival of blood to the growing *conceptus* along the pregnancy (Figure 7). At the end of pregnancy, and upon delivery, it is clear that UtA waveform takes weeks to return to baseline suggesting that, although spiral artery transformation largely determines UtA impedance, additional factors related to maternal vascular and endothelial function also matter.

The study reveals an unique property related to UtA. We refer to its supplier, the internal iliac artery, derived from the division of the major common iliac artery, itself a division of the aorta. In this setting, the comparison of IIA and UtA hemodynamic properties evidenced a peculiar impedance character. In fact, the IIA hemodynamic parallels the iliac artery and evidences a pregnancy related enhanced resistance, a change, that promotes an enormous influx of blood to be delivered to the succeeding branches as the UtA.

Interestingly, the IIA is the first artery to cross the pelvic brim and enter the pelvis. At this new site, and upon branching into the UtA, it appears to find a different set of regulatory conditions in the case pregnancy ensues. Indeed, the resistance vessel gives way to a capacitance vessel, whose impedance decreases progressively to provide copious blood to the growing fetus, to increase again in the succeeding 8 weeks upon delivery, before returning to the initial levels (Figure 7).

As a whole, the study shows in a compelling way that in important moments for the establishment or course of the human female reproductive function, local tissues organize to facilitate and ensure substantial blood perfusion. We would dare to say, in a sounding way, that such regulation promotes the blood flow into a blood flood. In addition, this study supports the continued efforts to move forward the research on the pelvic maternal circulatory changes. Although UtA remains an artery of major interest, the simplicity by which IIA can be assessed, easier than UtA, and the information that it may provide, suggests that it may complement UtA assessment.

At last, as insights regarding the molecular mechanisms underlying the changes at the placental bed are needed, redox mechanisms were investigated. Although placental bed NOX was not identified as a biomarker disorder, strong evidence was provided that NOX is an intervenient in the redox balance at the human fetal-maternal interface where it acts as an important modulator of uterine vascular resistance.

5 . BIBLIOGRAPHY

Aardema MW, Oosterhof H, Timmer A, van Rooy I, Aarnoudse JG. Uterine artery Doppler flow and uteroplacental vascular pathology in normal pregnancies and pregnancies complicated by pre-eclampsia and small for gestational age fetuses. *Placenta*. 2001; 22:405-11.

Aardema MW, Saro MC, Lander M, De Wolf BT, Oosterhof H, Aarnoudse JG. Second trimester Doppler ultrasound screening of the uterine arteries differentiates between subsequent normal and poor outcomes of hypertensive pregnancy: two different pathophysiological entities? *Clin Sci (Lond)*. 2004; 106:377-82.

Abramowicz JS, Sheiner E. Ultrasound of the placenta: a systematic approach. Part II: functional assessment (Doppler). *Placenta*. 2008; 29:921-9.

Albaiges G, Missfelder-Lobos H, Parra M, Lees C, Cooper D, Nicolaides KH. Comparison of color Doppler uterine artery indices in a population at high risk for adverse outcome at 24 weeks' gestation. *Ultrasound Obstet Gynecol.* 2003; 21:170-3.

Aldrich JE. Basic physics of ultrasound imaging. *Crit Care Med*. 2007; 35: S131-7.

Allen M, Svensson L, Roach M, Hambor J, McNeish J, Gabel CA. Deficiency of the stress kinase p38alpha results in embryonic lethality: characterization of the kinase dependence of stress responses of enzyme-deficient embryonic stem cells. *J Exp Med.* 2000; 191:859-70.

Amador S. Teaching medical physics to general audiences. *Biophys J.* 1994; 66:2217 21.

Amanso AM, Griendling KK. Differential roles of NADPH oxidases in vascular physiology and pathophysiology. *Front Biosci (Schol Ed)*. 2012; 4:1044-64.

American College of Obstetricians and Gynecologists; Task Force on Hypertension in Pregnancy. Hypertension in pregnancy. Report of the American College of Obstetricians and Gynecologists' Task Force on Hypertension in Pregnancy. *Obstet Gynecol*. 2013; 122:1122-31.

Anumba DO, Lincoln K, Robson SC. Predictive value of clinical and laboratory indices at first assessment in women referred with suspected gestational hypertension. *Hypertens Pregnancy*. 2010; 29:163-79.

Arduini D, Rizzo G, Romanini C. Doppler ultrasonography in early pregnancy does not predict adverse pregnancy outcome. *Ultrasound Obstet Gynecol.* 1991; 1:180-5.

Assali NS, Rauramo L, Peltonen T. Measurement of uterine blood flow and uterine metabolism. VIII. Uterine and fetal blood flow and oxygen consumption in early human pregnancy. *Am J Obstet Gynecol.* 1960; 79:86-98.

Babior BM, Lambeth JD, Nauseef W. The neutrophil NADPH oxidase. *Arch Biochem Biophys.* 2002; 397:342-4.

Balasch J, Gratacós E. Delayed childbearing: effects on fertility and the outcome of pregnancy. *Fetal Diagn Ther*. 2011; 29:263-73.

Bánfi B, Maturana A, Jaconi S, Arnaudeau S, Laforge T, Sinha B, Ligeti E, Demaurex N, Krause KH. A mammalian H+ channel generated through alternative splicing of the NADPH oxidase homolog NOH-1. *Science.* 2000; 287:138-42.

Bedard K, Krause KH. The NOX family of ROS-generating NADPH oxidases: physiology and pathophysiology. *Physiol Rev.* 2007; 87:245-313.

Bramham K, Parnell B, Nelson-Piercy C, Seed PT, Poston L, Chappell LC. Chronic hypertension and pregnancy outcomes: systematic review and meta-analysis. *BMJ*. 2014; 348:g2301.

Brosens I, Pijnenborg R, Vercruysse L, Romero R. The "Great Obstetrical Syndromes" are associated with disorders of deep placentation. *Am J Obstet Gynecol.* 2011; 204:193-201.

Brosens JJ, Parker MG, McIndoe A, Pijnenborg R, Brosens IA. A role for menstruation in preconditioning the uterus for successful pregnancy. *Am J Obstet Gynecol*. 2009; 200:615.e1-6.

Burton GJ, Jauniaux E, Charnock-Jones DS. The influence of the intrauterine environment on human placental development. *Int J Dev Biol*. 2010; 54:303-12.

Burton GJ. Oxygen, the Janus gas; its effects on human placental development and function. *J Anat*. 2009; 215:27-35.

Burton GJ, Scioscia M, Rademacher TW. Endometrial secretions: creating a stimulatory microenvironment within the human early placenta and implications for the aetiopathogenesis of preeclampsia. *J Reprod Immunol*. 2011; 89:118-25.

Campbell S, Bewley S, Cohen-Overbeek T. Investigation of the uteroplacental circulation by Doppler ultrasound. *Semin Perinatol*. 1987; 11:362-8.

Campbell S, Diaz-Recasens J, Griffin DR, Cohen-Overbeek TE, Pearce JM, Willson K, Teague MJ. New doppler technique for assessing uteroplacental blood flow. *Lancet.* 1983; 1:675-7.

Capeless EL, Clapp JF. Cardiovascular changes in early phase of pregnancy. *Am J Obstet Gynecol.* 1989; 161:1449-53.

Carpenter RL, Caplan RA, Brown DL, Stephenson C, Wu R. Incidence and risk factors for side effects of spinal anesthesia. *Anesthesiology.* 1992; 76:906-16.

Chapman AB, Abraham WT, Zamudio S, Coffin C, Merouani A, Young D, Johnson A, Osorio F, Goldberg C, Moore LG, Dahms T, Schrier RW. Temporal relationships between hormonal and hemodynamic changes in early human pregnancy. *Kidney Int.*1998; 54:2056-63.

Cnossen JS, Morris RK, ter Riet G, Mol BW, van der Post JA, Coomarasamy A, Zwinderman AH, Robson SC, Bindels PJ, Kleijnen J, Khan KS. Use of uterine artery Doppler ultrasonography to predict pre-eclampsia and intrauterine growth restriction: a systematic review and bivariable meta-analysis. *CMAJ.* 2008; 178:701-11.

Craven CM, Morgan T, Ward K. Decidual spiral artery remodelling begins before cellular interaction with cytotrophoblasts. *Placenta.* 1998; 19:241-52.

Cunningham FG, Leveno KJ, Bloom SL, Spong CY, Dashe JS, Hoffman BL, Casey MB, Sheffield JS. Williams Obstetrics. *Fetal Imagin*g, 24th edition, Mc Graw Hill Education, 2014, pp. 219-221.

Dal J, Vural B, Caliskan E, Ozkan S, Yucesoy I. Power Doppler ultrasound studies of ovarian, uterine, and endometrial blood flow in regularly menstruating women with respect to luteal phase defects. *Fertil Steril*. 2005; 84:224-7.

Davis JM, Auten RL. Maturation of the antioxidant system and the effects on preterm birth. *Semin Fetal Neonatal Med*. 2010; 15:191-5.

Deeks JJ, Altman DG. Diagnostic tests 4: likelihood ratios. *BMJ.* 2004; 329:168 9.

Diniz CP, Araujo Júnior E, Lima MM, Guazelli CA, Moron AF. Ultrasound and Doppler assessment of uterus during puerperium after normal delivery. *J Matern Fetal Neonatal Med.* 2014; 27:1905-11.

Edwards EW, DiPette DJ, Townsend RR, Cohen DL. Top 10 landmark studies in hypertension. *J Am Soc Hypertens*. 2014; 8:437-47.

Evans DH. Colour flow and motion imaging. *Proc Inst Mech Eng H*. 2010; 224:241-53.

Everett TR, Lees CC. Beyond the placental bed: placental and systemic determinants of the uterine artery Doppler waveform. *Placenta*. 2012; 33:893-901.

Flo K, Wilsgaard T, Vårtun A, Acharya G. A longitudinal study of the relationship between maternal cardiac output measured by impedance cardiography and

uterine artery blood flow in the second half of pregnancy. *BJOG*. 2010; 117:837-44.

Frusca T, Soregaroli M, Platto C, Enterri L, Lojacono A, Valcamonico A. Uterine artery velocimetry in patients with gestational hypertension. *Obstet Gynecol*. 2003; 102:136-40.

Gómez O, Figueras F, Fernández S, Bennasar M, Martínez JM, Puerto B, Gratacós E. Reference ranges for uterine artery mean pulsatility index at 11-41 weeks of gestation. *Ultrasound Obstet Gynecol*. 2008; 32:128-32.

Gómez O, Figueras F, Martínez JM, del Río M, Palacio M, Eixarch E, Puerto B, Coll O, Cararach V, Vanrell JA. Sequential changes in uterine artery blood flow pattern between the first and second trimesters of gestation in relation to pregnancy outcome. *Ultrasound Obstet Gynecol.* 2006; 28:802-8.

Gómez O, Martínez JM, Figueras F, Del Río M, Borobio V, Puerto B, Coll O, Cararach V, Vanrell JA. Uterine artery Doppler at 11-14 weeks of gestation to screen for hypertensive disorders and associated complications in an unselected population. *Ultrasound Obstet Gynecol*. 2005; 26:490-4.

Grassi G, Seravalle G, Dell'Oro R, Mancia G. Sympathetic mechanisms, organ damage, and antihypertensive treatment. *Curr Hypertens Rep*. 2011; 13:303-8.

Grummer MA, Sullivan JA, Magness RR, Bird IM. Vascular endothelial growth factor acts through novel, pregnancy-enhanced receptor signalling pathways to stimulate endothelial nitric oxide synthase activity in uterine artery endothelial cells. *Biochem J*. 2009; 417:501-11.

Guedes-Martins L, Cunha A, Saraiva J, Rita-Gaio A, Cerdeira AS, Macedo F, Almeida H. Foetal aortic flow velocity waveforms in healthy and hypertensive pregnant women. *Cardiovasc Ultrasound*. 2014; 12:1.

Guedes-Martins L, Matos L, Soares A, Silva E, Almeida H. AGEs, contributors to placental bed vascular changes leading to preeclampsia. *Free Radic Res.* 2013; S1:70-80.

Hajjar I, Kotchen JM, Kotchen TA. Hypertension: trends in prevalence, incidence, and control. *Annu Rev Public Health*. 2006; 27:465-90.

Harrington K, Carpenter RG, Goldfrad C, Campbell S. Transvaginal Doppler ultrasound of the uteroplacental circulation in the early prediction of pre-eclampsia and intrauterine growth retardation. *Br J Obstet Gynaecol*. 1997; 104:674-81.

Harrington K, Cooper D, Lees C, Hecher K, Campbell S. Doppler ultrasound of the uterine arteries: the importance of bilateral notching in the prediction of pre-eclampsia, placental abruption or delivery of a small for-gestational-age baby. *Ultrasound Obstet Gynecol*. 1996; 7:182-8.

Harrington K, Fayyad A, Thakur V, Aquilina J. The value of uterine artery Doppler in the prediction of uteroplacental complications in multiparous women. *Ultrasound Obstet Gynecol*. 2004; 23:50-5.

Harrington K, Goldfrad C, Carpenter RG, Campbell S. Transvaginal uterine and umbilical artery Doppler examination of 12-16 weeks and the subsequent development of pre-eclampsia and intrauterine growth retardation. *Ultrasound Obstet Gynecol*. 1997; 9:94-100.

Hazan AD, Smith SD, Jones RL, Whittle W, Lye SJ, Dunk CE. Vascular leukocyte interactions: mechanisms of human decidual spiral artery remodeling in vitro. *Am J Pathol*. 2010; 177:1017-30.

Harman D. Aging: a theory based on free radical and radiation chemistry. *J Gerontol*. 1956; 11:298-300.

Hwang J, Ing MH, Salazar A, Lassègue B, Griendling K, Navab M, Sevanian A, Hsiai TK. Pulsatile versus oscillatory shear stress regulates NADPH oxidase subunit expression: implication for native LDL oxidation. *Circ Res*. 2003; 93:1225-32.

Istance D, Theisens H. Ageing OECD societies in Trends shaping education 2008. Centre for Educational Research and Innovation. Organization for Economic Co-Operation and Development, OECD. 2008; 13-20.

Ivanovski M, Damcevski N, Radevska B, Doicev G. Assessment of uterine artery and arcuate artery blood flow by transvaginal color Doppler ultrasound on the day of human chorionic gonadotropin administration as predictors of pregnancy in an in vitro fertilization program. *Akush Ginekol (Sofiia)*. 2012; 51:55-60.

Jauniaux E, Jurkovic D, Campbell S. In vivo investigations of the anatomy and the physiology of early human placental circulations. *Ultrasound Obstet Gynecol.* 1991; 1:435-45.

Jokubkiene L, Sladkevicius P, Rovas L, Valentin L. Assessment of changes in endometrial and subendometrial volume and vascularity during the normal menstrual cycle using three dimensional power Doppler ultrasound. *Ultrasound Obstet Gynecol*. 2006; 27:672-9.

Jurkovic D, Jauniaux E, Kurjak A, Hustin J, Campbell S, Nicolaides KH. Transvaginal color Doppler assessment of the uteroplacental circulation in early pregnancy. *Obstet Gynecol*. 1991; 77:365-9.

Karumanchi SA, Maynard SE, Stillman IE, Epstein FH, Sukhatme VP. Preeclampsia: a renal perspective. *Kidney In*t. 2005; 67:2101-13.

Katz R, Karliner JS, Resnik R. Effects of a natural volume overload state (pregnancy) on left ventricular performance in normal human subjects. *Circulation*. 1978; 58:434-41.

Khong TY, Adema ED, Erwich JJ. On an anatomical basis for the increase in birth weight in second and subsequent born children. *Placenta*. 2003; 24:348-53.

Kirkinen P, Dudenhausen J, Baumann H, Huch A, Huch R. Postpartum blood flow velocity waveforms of the uterine arteries. *J Reprod Med*. 1988; 33:745-8.

Konje JC, Kaufmann P, Bell SC, Taylor DJ. A longitudinal study of quantitative uterine blood flow with the use of color power angiography in appropriate for gestational age pregnancies. *Am J Obstet Gynecol*. 2001; 185:608-13.

Kossoff G. Basic physics and imaging characteristics of ultrasound. *World J Surg*. 2000; 24:134-42.

Kurjak A, Zudenigo D, Predanic M, Kupesic S. Recent advances in the Doppler study of early fetomaternal circulation. *J Perinat Med*. 1993; 21:419-39.

Lain KY, Roberts JM. Contemporary concepts of the pathogenesis and management of preeclampsia. *JAMA*. 2002; 287:3183-6.

Lambeth JD, Kawahara T, Diebold B. Regulation of Nox and Duox enzymatic activity and expression. *Free Radic Biol Med*. 2007; 43:319-31.

Lash GE, Otun HA, Innes BA, Bulmer JN, Searle RF, Robson SC. Low oxygen concentrations inhibit trophoblast cell invasion from early gestation placental explants via alterations in levels of the urokinase plasminogen activator system. *Biol Reprod.* 2006; 74:403-9.

Leow MK. Environmental origins of hypertension: phylogeny, ontogeny and epigenetics. *Hypertens Res*. 2015; 38:299-307.

Li H, Gudnason H, Olofsson P, Dubiel M, Gudmundsson S. Increased uterine artery vascular impedance is related to adverse outcome of pregnancy but is present in only one-third of late third-trimester pre-eclamptic women. *Ultrasound Obstet Gynecol.* 2005; 25:459-63.

Macdonald-Wallis C, Lawlor DA, Fraser A, May M, Nelson SM, Tilling K. Blood pressure change in normotensive, gestational hypertensive, preeclamptic, and essential hypertensive pregnancies. *Hypertension*. 2012; 59:1241-8.

Madazli R, Somunkiran A, Calay Z, Ilvan S, Aksu MF. Histomorphology of the placenta and the placental bed of growth restricted foetuses and correlation with the Doppler velocimetries of the uterine and umbilical arteries. *Placenta*. 2003; 24:510-6.

Mäkikallio K, Jouppila P, Tekay A. First trimester uterine, placental and yolk sac haemodynamics in pre-eclampsia and preterm labour. *Hum Reprod*. 2004 Mar; 19:729-33.

Mancia G, Grassi G, Giannattasio C, Seravalle G. Sympathetic activation in the pathogenesis of hypertension and progression of organ damage. *Hypertension*. 1999; 34:724-8.

Mandala M, Osol G. Physiological remodelling of the maternal uterine circulation during pregnancy. *Basic Clin Pharmacol Toxicol*. 2012; 110:12-8.

Mathews TJ, Hamilton BE. Delayed childbearing: More women are having their first child later in life. NCHS data brief, no 21. Hyattsville, MD. National Center for Health Statistics. 2009; 21:1-8.

Matos L, Stevenson D, Gomes F, Silva-Carvalho JL, Almeida H. Superoxide dismutase expression in human cumulus oophorus cells. *Mol Hum Reprod*. 2009; 15:411-9.

McCarthy AL, Woolfson RG, Raju SK, Poston L. Abnormal endothelial cell function of resistance arteries from women with preeclampsia. *Am J Obstet Gynecol*. 1993; 168:1323-30.

McVeigh ER. Emerging imaging techniques. *Circ Res*. 2006; 98:879-86.

Meler E, Figueras F, Mula R, Crispi F, Benassar M, Gómez O, Gratacós E. Prognostic role of uterine artery Doppler in patients with preeclampsia. *Foetal Diagn Ther*. 2010; 27:8-13.

Mercé LT, Barco MJ, Bau S. Color Doppler sonographic assessment of placental circulation in the first trimester of normal pregnancy. *J Ultrasound Med*. 1996; 15:135-42.

Moon KC, Park JS, Norwitz ER, Kim DI, Oh KJ, Park CW, Jun JK, Syn HC. Expression of extracellular signal-regulated kinase1/2 and p38 mitogen activated protein kinase in the invasive trophoblasts at the human placental bed. *Placenta*. 2008; 29:391-5.

Mudgett JS, Ding J, Guh-Siesel L, Chartrain NA, Yang L, Gopal S, Shen MM. Essential role for p38alpha mitogen-activated protein kinase in placental angiogenesis. *Proc Natl Acad Sci U S A*. 2000; 97:10454-9.

Mulic-Lutvica A, Eurenius K, Axelsson O. Longitudinal study of Doppler flow resistance indices of the uterine arteries after normal vaginal delivery. *Acta Obstet Gynecol Scand.* 2007; 86:1207-14.

Mustafa R, Ahmed S, Gupta A, Venuto RC. A comprehensive review of hypertension in pregnancy. *J Pregnancy*. 2012; 2012:105918.

Myatt L. Review: Reactive oxygen and nitrogen species and functional adaptation of the placenta. *Placenta*. 2010; 31:S66-9.

National Collaborating Centre for Women's and Children's Health (UK). Hypertension in Pregnancy: The Management of Hypertensive Disorders During Pregnancy. London: RCOG Press; 2010.

National Heart, Lung and Blood Institute. Report of the Working Group on Research on Hypertension During Pregnancy. 2001; http://www.nhlbi.nih.gov/resources/hyperten_preg/.

Ochi H, Suginami H, Matsubara K, Taniguchi H, Yano J, Matsuura S. Micro-bead embolization of uterine spiral arteries and changes in uterine arterial flow velocity waveforms in the pregnant ewe. *Ultrasound Obstet Gynecol*. 1995; 6:272-6.

O'Leary DH. Vascular ultrasonography. *Radiol Clin North Am*. 1985; 23:39-56.

Osol G, Mandala M. Maternal Uterine Vascular Remodeling During Pregnancy. *Physiology (Bethesda, Md)*. 2009; 24:58-71.

Oyelese Y, Ananth CV. Placental abruption. *Obstet Gynecol*. 2006; 108:1005-16.

Palmer RM, Ashton DS, Moncada S. Vascular endothelial cells synthesize nitric oxide from L-arginine. *Nature*. 1988; 333:664-6.

Palmer SK, Zamudio S, Coffin C, Parker S, Stamm E, Moore LG. Quantitative estimation of human uterine artery blood flow and pelvic blood flow redistribution in pregnancy. *Obstet Gynecol*. 1992; 80:1000-6.

Papageorghiou AT, Yu CK, Bindra R, Pandis G, Nicolaides KH; Fetal Medicine Foundation Second Trimester Screening Group. Multicenter screening for pre-eclampsia and fetal growth restriction by transvaginal uterine artery Doppler at 23 weeks of gestation. *Ultrasound Obstet Gynecol*. 2001; 18:441-9.

Papageorghiou AT, Yu CK, Erasmus IE, Cuckle HS, Nicolaides KH. Assessment of risk for the development of pre-eclampsia by maternal characteristics and uterine artery Doppler. *BJOG*. 2005; 112:703-9.

Pates JA, Hatab MR, McIntire DD, Cunningham FG, Twickler DM. Determining uterine blood flow in pregnancy with magnetic resonance imaging. *Magn Reson Imaging*. 2010; 28:507-10.

Price DT, Vita JA, Keaney JF Jr. Redox control of vascular nitric oxide bioavailability. *Antioxid Redox Signal*. 2000; 2(4):919-35.

Romundstad PR, Magnussen EB, Smith GD, Vatten LJ. Hypertension in pregnancy and later cardiovascular risk: common antecedents? *Circulation*. 2010; 122:579-84.

Rosenfeld CR, DeSpain K, Word RA, Liu XT. Differential sensitivity to angiotensin II and norepinephrine in human uterine arteries. *J Clin Endocrinol Metab*. 2012; 97:138-47.

Sciscione AC, Hayes EJ; Society for Maternal-Fetal Medicine. Uterine artery Doppler flow studies in obstetric practice. *Am J Obstet Gynecol*. 2009; 201:121-6.

Seely EW, Ecker J. Chronic hypertension in pregnancy. *Circulation*. 2014; 129:1254-61.

Sibai B, Dekker G, Kupferminc M. Pre-eclampsia. *Lancet*. 2005; 365:785-99.

Sibai BM, Stella CL. Diagnosis and management of atypical preeclampsia-eclampsia. *Am J Obstet Gynecol*. 2009; 200:481.e1-7.

Sladkevicius P, Valentin L, Marsál K. Blood flow velocity in the uterine and ovarian arteries during the normal menstrual cycle. *Ultrasound Obstet Gynecol*. 1993; 3:199-208.

Smith GC, Yu CK, Papageorghiou AT, Cacho AM, Nicolaides KH; Fetal Medicine Foundation Second Trimester Screening Group. Maternal uterine artery Doppler flow velocimetry and the risk of stillbirth. *Obstet Gynecol*. 2007; 109:144-51.

Smith SD, Dunk CE, Aplin JD, Harris LK, Jones RL. Evidence for immune cell involvement in decidual spiral arteriole remodeling in early human pregnancy. *Am J Pathol*. 2009; 174:1959-71.

Sprague B, Chesler NC, Magness RR. Shear stress regulation of nitric oxide production in uterine and placental artery endothelial cells: experimental studies and hemodynamic models of shear stresses on endothelial cells. *Int J Dev Biol*. 2010; 54:331-9.

Sprague BJ, Phernetton TM, Magness RR, Chesler NC. The effects of the ovarian cycle and pregnancy on uterine vascular impedance and uterine artery mechanics. *Eur J Obstet Gynecol Reprod Biol*. 2009; 144:S170-8.

Steer CV, Campbell S, Pampiglione JS, Kingsland CR, Mason BA, Collins WP. Transvaginal colour flow imaging of the uterine arteries during the ovarian and menstrual cycles. *Hum Reprod.* 1990; 5:391-5.

Steer CV, Williams J, Zaidi J, Campbell S, Tan SL. Intra-observer, interobserver, interultrasound transducer and intercycle variation in colour Doppler assessment of uterine artery impedance. *Hum Reprod*. 1995; 10:479-81.

Suh YA, Arnold RS, Lassegue B, Shi J, Xu X, Sorescu D, Chung AB, Griendling KK, Lambeth JD. Cell transformation by the superoxide-generating oxidase Mox1. *Nature*. 1999; 401:79-82.

Tamura H, Miwa I, Taniguchi K, Maekawa R, Asada H, Taketani T, Matsuoka A, Yamagata Y, Ishikawa H, Sugino N. Different changes in resistance index between uterine artery and uterine radial artery during early pregnancy. *Hum Reprod*. 2008; 23:285-9.

Tan SL, Zaidi J, Campbell S, Doyle P, Collins W. Blood flow changes in the ovarian and uterine arteries during the normal menstrual cycle. *Am J Obstet Gynecol*. 1996; 175:625-31.

Tarkkila P, Isola J. A regression model for identifying patients at high risk of hypotension, bradycardia and nausea during spinal anesthesia. *Acta Anaesthesiol Scand*. 1992; 36:554-8.

Taylor KJ, Holland S. Doppler US. Part I. Basic principles, instrumentation, and pitfalls. *Radiology*. 1990; 174:297-307.

Tekay A, Jouppila P. A longitudinal Doppler ultrasonographic assessment of the alterations in peripheral vascular resistance of uterine arteries and ultrasonographic findings of the involuting uterus during the puerperium. *Am J Obstet Gynecol*. 1993; 168:190-8.

Trudinger BJ, Giles WB, Cook CM. Uteroplacental blood flow velocity-time waveforms in normal and complicated pregnancy. *Br J Obstet Gynaecol*. 1985; 92:39-45.

Valentin L, Sladkevicius P, Laurini R, Söderberg H, Marsal K. Uteroplacental and luteal circulation in normal first-trimester pregnancies: Doppler ultrasonographic and morphologic study. *Am J Obstet Gynecol*. 1996; 174:768-75.

Valko M, Leibfritz D, Moncol J, Cronin MT, Mazur M, Telser J. Free radicals and antioxidants in normal physiological functions and human disease. *Int J Biochem Cell Biol.* 2007; 39:44-84.

van den Elzen HJ, Cohen-Overbeek TE, Grobbee DE, Quartero RW, Wladimiroff JW. Early uterine artery Doppler velocimetry and the outcome of pregnancy in women aged 35 years and older. *Ultrasound Obstet Gynecol*. 1995; 5:328-33.

van Oppen AC, Stigter RH, Bruinse HW. Cardiac output in normal pregnancy: a critical review. *Obstet Gynecol*. 1996; 87:310-8.

Van Schoubroeck D, Van den Bosch T, Scharpe K, Lu C, Van Huffel S, Timmerman D. Prospective evaluation of blood flow in the myometrium and uterine arteries in the puerperium. *Ultrasound Obstet Gynecol*. 2004; 23:378-81.

Vodstrcil LA, Tare M, Novak J, Dragomir N, Ramirez RJ, Wlodek ME, Conrad KP, Parry LJ. Relaxin mediates uterine artery compliance during pregnancy and increases uterine blood flow. *FASEB J*. 2012; 26:4035-44.

Wang L, Qiao J, Li R, Zhen X, Liu Z. Role of endometrial blood flow assessment with color Doppler energy in predicting pregnancy outcome of IVF-ET cycles. *Reprod Biol Endocrinol*. 2010; 8:122.

Webster RP, Roberts VH, Myatt L. Protein nitration in placenta – functional significance. *Placenta*. 2008; 29:985-94.

Yoganathan AP, Cape EG, Sung HW, Williams FP, Jimoh A. Review of hydrodynamic principles for the cardiologist: applications to the study of blood flow and jets by imaging techniques. *J Am Coll Cardiol*. 1988; 12:1344-53.

Ziegler WF, Bernstein I, Badger G, Leavitt T, Cerrero ML. Regional hemodynamic adaptation during the menstrual cycle. *Obstet Gynecol*. 1999; 94:695-9.

Zou MH, Shi C, Cohen RA. Oxidation of the zinc-thiolate complex and uncoupling of endothelial nitric oxide synthase by peroxynitrite. *J Clin Invest*. 2002; 109:817-26.

U.PORTO
FMUP FACULDADE DE MEDICINA
UNIVERSIDADE DO PORTO

LUÍS GUEDES-MARTINS • 2015

U.PORTO

UNIVERSIDADE DO PORTO